UNIVERSIDADE BEIRA INTERIOR

Characterization of bitter taste receptors expression and function in the human blood-cerebrospinal fluid barrier

Ana Catarina Abreu Duarte

Tese para obtenção do Grau de Doutor em
Biomedicina
(3º ciclo de estudos)

Orientador: Prof. Doutora Cecília Reis Alves dos Santos
Co-orientador: Prof. Doutora Isabel Maria Theriaga Mendes Varanda Gonçalves

Júri:
Prof. Doutora Maria do Rosário Rodrigues de Almeida Martins
Prof. Doutor Pedro Miguel Guerreiro da Costa Guerreiro
Prof. Doutora Maria Eugenia Gallardo Alba
Prof. Doutora Fernanda Cristina Gomes de Sousa Marques

fevereiro de 2021

Dedicatory

To my family and everyone that always supported me.

Acknowledgements

First of all, I would like to thank my supervisor Professor Cecília Santos and my co-supervisor Isabel Gonçalves for all the support, guidance, and knowledge transmitted to me. Also, I would like to thank for their availability, patience and kindness along these years that made possible to reach this day.

Moreover, I would like to acknowledge the Universidade da Beira Interior and the CICS-UBI, for providing the equipment and the facilities required to develop this thesis. Also, I would like to thank the funding from the ICON project (Interdisciplinary Challenges On Neurodegeneration; CENTRO-01-0145-FEDER-000013) and to the PPBI-Portuguese Platform of BioImaging (POCI-01-0145-FEDER-022122).

In addition, I would like to thank to COMPLEXUS group members. During the last years, I had the pleasure to work with outstanding people that support me in many situations. I would like to specially thank Telma for the support and the opportunity to work together, and Joana for all the knowledge transmitted during these years. Of course, I would like to thank my co-workers and friends Margarida Almeida, Raquel Costa, Raquel Brito e Daniela Talhada for accompanying me during this journey.

I would like to thank my family for the continuous support during the last years.

Finally, I would like to thank André for his unconditional love, support, kindness and patience in these challenging years.

Resumo

A presença e a funcionalidade de alguns recetores gustativos de compostos amargos (TR2) foi demonstrada recentemente nas células epiteliais do plexo coróide (PC) de rato. As células do PC formam a barreira sangue-líquido cefalorraquidiano, uma das principais barreiras cerebrais. A presença de TR2 no PC sugere que estes recetores possam estar envolvidos na monitorização da composição química do sangue e do líquido cefalorraquidiano.

As barreiras do cérebro desempenham um papel crucial na proteção do sistema nervoso central (SNC) impedindo o acesso de substâncias nocivas ao cérebro. Consequentemente, muitos fármacos direcionados para o tratamento de patologias do SNC não conseguem ultrapassar estas barreiras. Isto deve-se, em grande parte, à presença de diversos transportadores nas células que constituem estas barreiras, os quais transportam os fármacos para fora das células e, portanto, impedem a sua acumulação nas células alvo.

Diversos compostos amargos, ligandos dos TR2, possuem propriedades anti-tumorais e de neuroprotecção. Contudo, a biodisponibilidade destes compostos é, normalmente, muito baixa o que dificulta a sua aplicação terapêutica. Adicionalmente, sabe-se que estes compostos interagem com transportadores membranares nas células das barreiras do cérebro. Isto sugere que os compostos amargos com potencial terapêutico sejam transportados para fora das células, o que explica a sua baixa biodisponibilidade, mas também que podem regular a ação dos transportadores de membrana o que poderá contribuir para uma maior acumulação intracelular dos compostos. Uma vez que estes compostos amargos são agonistas dos TR2, é possível que estes tenham um papel crucial na regulação da biodisponibilidade desses compostos ao nível do SNC, tal como reportado em alguns órgãos.

Como tal, o trabalho desenvolvido nesta tese de doutoramento teve como principal objetivo a análise da expressão e da função da via de sinalização gustativa do amargo na barreira sangue-líquido cefalorraquidiano humana. Adicionalmente, foi estudado o papel dos TR2 no transporte do composto resveratrol ao nível da barreira sangue-líquido cefalorraquidiano humana.

Na primeira parte do trabalho, foi possível confirmar a expressão de 13 TAS2Rs e das proteínas efetoras da via de transdução de sinal gustativa num modelo humano da barreira sangue-líquido cefalorraquidiano. Além disto, foi também demonstrada a

funcionalidade dos TAS2R14 e 39, em resposta aos compostos quercetina e cloranfenicol, respetivamente.

Na segunda parte do trabalho, analisámos o transporte do composto amargo, resveratrol, num modelo *in vitro* da barreira sangue-líquido cefalorraquidiano humana, e avaliámos a possível envolvência dos TAS2Rs, que ligam o resveratrol, nesse transporte. Deste trabalho concluiu-se que o resveratrol atravessa a barreira sangue-líquido cefalorraquidiano na direção sangue - líquido cefalorraquidiano (basolateral – apical), de forma dependente do TAS2R14. Observámos também que os transportadores de efluxo ABCC1, ABCC4 e ABCG2 presentes nas células epiteliais do CP transportam o resveratrol, e que este aumenta a expressão do ABCG2 e modula a sua função, bem como a do ABCC4, de forma dependente do TAS2R14.

Em suma, os resultados obtidos durante o desenvolvimento deste projeto permitem afirmar que os TAS2Rs são expressos e estão funcionais na barreira sangue-líquido cefalorraquidiano humana, podendo participar na monitorização da composição química dos fluidos que a circundam. Adicionalmente, reforçam o papel crucial que esta barreira desempenha na regulação do transporte de substâncias para o cérebro. No futuro, será importante continuar a explorar o papel de outros TAS2Rs após ativação pelos seus ligandos no cérebro, assim como, na regulação dos mecanismos de transporte e, também de destoxificação existentes na barreira sangue-líquido cefalorraquidiano. Este conhecimento irá certamente contribuir para uma melhoria dos processos terapêuticos utilizados para entrega de fármacos ao SNC.

Palavras-chave

Plexo coróide; recetores gustativos de compostos amargos; farmacorresistência, barreira sangue-líquido cefalorraquidiano, compostos amargos, resveratrol.

Resumo Alargado

A proteção do sistema nervoso central (SNC) quanto à entrada de moléculas potencialmente tóxicas é assegurada principalmente por duas barreiras, a barreira hematoencefálica formada por células endoteliais e, a barreira sangue-líquido cefalorraquidiano formada pelas células epiteliais do plexo coróide (PC). Estas barreiras permitem ainda a remoção de metabolitos endógenos. Apesar de vital, esta vigilância constante limita a entrega de fármacos ao SNC e, portanto, o tratamento de diversas neuropatologias. Este fenómeno é denominado por farmacorresistência e é assegurado, em grande parte, por diversos transportadores de efluxo nas células que compõem as barreiras cerebrais. Dado que muitos dos fármacos utilizados no tratamento de doenças do SNC (doenças neurodegenerativas, tumores cerebrais e outras) são substratos destes transportadores, a sua interação resulta na fraca acumulação intracelular dos fármacos, limitando assim o seu efeito terapêutico. A principal classe de transportadores envolvida neste evento é a família de transportadores ABC (*ATP-binding cassette*). Deste modo, um dos principais desafios da farmacologia moderna é o desenvolvimento de novas terapias que consigam ultrapassar as barreiras do cérebro.

A barreira sangue-líquido cefalorraquidiano é formada pelas células epiteliais do PC. O PC é uma estrutura altamente vascularizada que se encontra nos ventrículos do cérebro. Desempenha variadas funções no SNC entre as quais a produção e secreção do líquido cefalorraquidiano e de barreira, através do estabelecimento da barreira sangue-líquido cefalorraquidiano.

O nosso grupo de investigação, através de um estudo de *microarrays* de cDNA no PC de rato, identificou a expressão de uma vasta gama de recetores quimiossensoriais, tais como, recetores gustativos, do olfato e vomeronasais. Relativamente aos recetores gustativos, é já conhecida a sua presença em diversos tecidos fora da cavidade oral, onde medeiam vários processos incluindo broncodilatação, inflamação, metabolismo, regulação enteroendócrina, imunidade inata e fertilidade masculina. Em particular, os recetores gustativos de compostos amargos (TR2) parecem ter um papel determinante em muitos destes processos. Assim, é possível que os TR2 respondam a alterações na concentração dos seus ligandos nos fluidos do organismo, ditando assim o destino e os efeitos destes compostos. Portanto, ao nível da barreira sangue-líquido cefalorraquidiano os TR2 poderão desempenhar um papel relevante na vigilância química da composição do sangue e do líquido cefalorraquidiano.

Os compostos que ativam os T2Rs, compostos amargos, correspondem a grupos de moléculas muito diversos, podendo ter origem natural ou sintética. A ligação de um composto amargo a um TR2 e a consequente ativação do recetor associada à sensação de paladar amargo, foi pela primeira vez identificada na cavidade oral e, uma vez que muitos dos compostos tóxicos têm o sabor amargo, corresponde a uma reação protetora do organismo para evitar a ingestão de substâncias tóxicas. Contudo, hoje sabe-se que os TR2 são expressos numa vasta gama de tecidos fora da cavidade oral, conhecendo-se também outras funções em diferentes tecidos e órgãos. Um dos principais grupos de compostos amargos são os flavonóides, compostos derivados de plantas e cujas propriedades anti-inflamatórias, antioxidantes e anti-tumorais têm sido extensamente estudadas na última década. Além dos flavonóides existem muitos outros compostos amargos com idêntico potencial terapêutico como é o caso do resveratrol, entre outros. Dadas as suas propriedades intrínsecas, o potencial terapêutico destes compostos tem sido avaliado ao nível das doenças que afetam o SNC e em vários tipos de cancro. Contudo, a biodisponibilidade destes compostos nos tecidos alvo, incluindo o cérebro, é normalmente muito baixa sendo, portanto, um obstáculo para a sua aplicação no tratamento de doenças. Nos últimos anos, vários estudos têm tentado analisar os mecanismos envolvidos na biodisponibilidade destes compostos, mas é ainda um assunto que carece de maior entendimento. No entanto, sabe-se que muitos destes compostos interagem com transportadores ABC, podendo comportar-se como substratos, inibidores ou indutores da sua atividade em vários tecidos, incluindo as barreiras do cérebro e a barreira sangue-tumor. Uma vez que, os TR2 são ativados por compostos amargos, surge a hipótese de que estes recetores possam regular os efeitos biológicos destes compostos nos mais variados tecidos em que se encontram. Aliás, existem evidências deste mecanismo, nomeadamente ao nível do trato gastrointestinal e das vias respiratórias. Assim, para um melhor entendimento sobre os efeitos destes compostos e da extensão do seu potencial terapêutico quer seja no SNC ou noutros tecidos, é essencial analisar o papel dos TR2.

O trabalho desenvolvido nesta tese de doutoramento teve como principal objetivo a análise da expressão e da função da via de sinalização gustativa dos compostos amargos na barreira sangue-líquido cefalorraquidiano, num modelo *in vitro* que mimetiza o PC humano. Foi também alvo de estudo, o papel dos TR2 humanos, TAS2Rs, como moduladores do efeito de ligandos específicos com potencial neuroprotetor na função e na atividade de certos transportadores ABC na barreira sangue-líquido cefalorraquidiano.

No primeiro trabalho apresentado nesta tese confirmámos a presença de TAS2Rs na barreira sangue-líquido cefalorraquidiano humana. Identificámos a presença de 13 transcritos de TAS2Rs e a expressão proteica de 4 TAS2Rs (4, 5, 14 e 39) na linha celular humana de plexo coróide HIBCPP (*human malignant choroid plexus papilloma cell line*). A expressão dos TAS2R4, 5, 14 e 39 foi também analisada e validada em cortes histológicos de PC de homens e de mulheres. Além dos TAS2Rs, a expressão de proteínas efetoras da via de sinalização do paladar foi também analisada nas células HIBCPP, tendo-se confirmado a presença da α-gustaducina (GNAT3), da fosfolipase C Beta 2 (PLCβ2) e do canal 5 de potencial de recetor transitório (TRPM5). Para analisar a funcionalidade da via de sinalização do paladar, realizaram-se estudos de *single cell calcium imaging* nas células HIBCPP. Com estes ensaios, demonstrou-se que as células HIBCPP respondem a vários estímulos amargos, através da ativação dos TAS2Rs. Mais especificamente, o flavonóide quercetina ativou o recetor 14 e o antibiótico cloranfenicol ativou o recetor TAS2R39, verificando-se uma diminuição significativa nos níveis de cálcio intracelular após o silenciamento da expressão destes recetores.

No segundo trabalho apresentado foi avaliado o papel de alguns dos TAS2Rs identificados no transporte de um composto fenólico com alto valor terapêutico, o resveratrol, através da barreira sangue-líquido cefalorraquidiano humana. Inicialmente, foi analisada a capacidade das células HIBCPP responderem ao resveratrol via TAS2R14 e/ou TAS2R39, ligando previamente identificado destes dois recetores. Observou-se que as células HIBCPP respondem ao resveratrol via TAS2R14. Em seguida, através de ensaios de permeação, com culturas de HIBCPP em insertos, modelo *in vitro* que mimetiza a barreira, examinámos o transporte de resveratrol na direção basolateral-apical, simulando a passagem sangue - líquido cefalorraquidiano. Foi possível detetar a presença de resveratrol no lado apical após um período de incubação, demonstrando assim que este composto atravessa a barreira sangue-líquido cefalorraquidiano. Ainda, o silenciamento do TAS2R14, localizado na membrana celular basolateral, reduziu os níveis de resveratrol no lado apical, indicando que a passagem de resveratrol através das células epiteliais do PC é dependente da ativação do TAS2R14. Posto isto, colocou-se a hipótese do TAS2R14 regular a ação de transportadores ABC nas células do PC, influenciando o transporte de resveratrol através destas células. Foram selecionados dois transportadores membranares basolaterais, o ABCC1 e o ABCC4, e um apical, o ABCG2. A utilização de substratos e inibidores específicos destes transportadores permitiu observar que a inibição de cada um destes transportadores afeta o transporte de resveratrol nas células HIBCPP, favorecendo a acumulação intracelular do composto. Assim, todos estes transportadores estão envolvidos no transporte de resveratrol na

barreira sangue-líquido cefalorraquidiano. Relativamente ao efeito do próprio resveratrol na expressão e função destes transportadores obtiveram-se resultados muito interessantes. O resveratrol aumentou a expressão do ABCG2 via TAS2R14, o mesmo não se verificando relativamente aos outros transportadores analisados. Por outro lado, o resveratrol modula a função de ambos os transportadores ABCC4 e ABCG2 de forma dependente da expressão de TAS2R14, induzindo alterações nos níveis intracelulares de substratos específicos.

No seu conjunto, os resultados obtidos nesta tese apoiam a hipótese de que os TAS2Rs presentes na barreira sangue-líquido cefalorraquidiano atuam na vigilância da composição química do sangue e do líquido cefalorraquidiano através da regulação da atividade de transportadores de efluxo. Um dos dados mais relevantes é certamente a confirmação de que o resveratrol consegue passar a barreira sangue-líquido cefalorraquidiano humana, realçando a sua importância na entrega de fármacos ao SNC. No futuro, espera-se que os estudos aqui apresentados sirvam de ponto de partida para muitos outros com enfoque no transporte de outros compostos amargos ao nível da barreira sangue-líquido cefalorraquidiano. Adicionalmente, espera-se que os TR2 recebam a devida atenção como reguladores dos efeitos dos seus ligandos, o que contribuirá certamente para um melhor entendimento dos processos envolvidos na entrega de fármacos ao SNC e, portanto, no desenvolvimento de novas abordagens terapêuticas mais eficazes.

Palavras-chave

Plexo coróide; recetores gustativos de compostos amargos; farmacorresistência, barreira sangue-líquido cefalorraquidiano, compostos amargos, resveratrol.

Abstract

Bitter taste receptors (TR2) expression and functionality was recently reported in the rat choroid plexus (CP). CP epithelial cells establish a major brain barrier, the blood-cerebrospinal fluid barrier (BCSFB). Given their capacity to bind a large array of chemical compounds, we hypothesised that TR2 might be involved in monitoring the composition of blood and cerebrospinal fluid.

Brain barriers play a critical role in the protection of the central nervous system (CNS) by hindering the access of toxic substances to the brain. Consequently, many drugs targeting neurological disorders are impaired to cross these barriers. This is explained through the expression of several membrane transporters in brain barriers cells that efflux drugs, thus impairing drug cell accumulation in the brain.

A wide range of compounds that bind to TR2 show neuroprotective and anti-tumoral properties. However, their low bioavailability in the CNS restrains its therapeutic application. Additionally, bitter compounds might interact with transporters that are also found in brain barriers. Therefore, bitter compounds might be effluxed which explains their low bioavailability but can also regulate the action of these transporters in order to increase their or other drugs' intracellular accumulation. Considering that bitter compounds are TR2 agonists it is possible that TR2 play an important role on the bioactive effects of bitter compounds in the CNS, as reported in other tissues.

The main goal of this doctoral thesis was to analyse the expression and function of the bitter signalling pathway in the human BCSFB. Additionally, the role of human TR2 (TAS2Rs) as modulator of specific neuroactive bitter compounds on ABC transporters function and activity at the BCSFB was also evaluated.

The first research work presented showed the expression of 13 TAS2Rs as well as of downstream effector proteins of the taste signalling pathway in the human BCSFB. Moreover, we demonstrated that TAS2R14 and TAS2R39 are functional in a human cell model of the BCSFB and respond to bitter compounds quercetin and chloramphenicol, respectively.

The second research work evaluated resveratrol transport across the BCSFB and the involvement of TAS2Rs. Results showed that resveratrol is able to cross the BCSFB from blood to cerebrospinal fluid in a dependent manner of TAS2R14 expression at CP epithelial cells. Further, efflux transporters ABCC1, ABCC4 and ABCG2, which are expressed at CP epithelial cells, transport resveratrol. Additionally, resveratrol

upregulated ABCG2 expression and regulated ABCC4 and ABCG2 efflux activity in TAS2R14 dependent way.

In conclusion, the results obtained during this project demonstrate that TAS2Rs are expressed and functional at the human BCSFB and support their participation in the monitorization of chemical composition of the surrounding fluids. Furthermore, the major achievements of this thesis strongly support the role of BCSFB in the regulation of the transport of molecules into the brain. In the future, it is necessary to further exploit the role of other TAS2Rs as mediators of the effects of bitter compounds in the brain, as well as in the regulation of transport and detoxifying systems at the BCSFB. The knowledge hereby created has far-reaching potential for improving the challenging task of delivering therapeutic drugs into the CNS.

Keywords

Choroid plexus; bitter taste receptors, pharmacoresistance, blood-cerebrospinal fluid barrier, *bitter compounds*, resveratrol.

Thesis Overview

This Doctoral thesis is organized in 6 chapters.

The first and second chapters enclose the introductory section and intend to contextualize the putative relevance of the bitter taste signalling pathway in the blood-cerebrospinal fluid barrier. In the first chapter the chemical surveillance at the choroid plexus is discussed, focusing on the bitter taste receptors (TR2). Additionally, the expression and activity of TR2 in other tissues is also analyzed. In the second chapter, the biological relevance of bitter compounds is reviewed in the frame of central nervous system disorders and puts in evidence TR2 as their potential targets.

The third chapter presents the general and specific aims established for the work plan of this doctoral thesis.

The fourth and fifth chapters present the results of the research work developed:

- Research Work 1: Bitter taste receptors profiling in the human blood-cerebrospinal fluid-barrier (Chapter 4);
- Research Work 2: The bitter taste receptor TAS2R14 regulates resveratrol transport across the human blood-cerebrospinal fluid barrier (Chapter 5);

Finally, the sixth chapter contains the concluding remarks highlighting the advances obtained during this research work and discuss the future directions in the chemosurveillance at the brain barriers.

Index

List of Figures

Chapter 1

Chapter 2

Chapter 4

Chapter 5

List of Tables

Chapter 1

Chapter 2

Chapter 4

Chapter 5

Abbreviations

ABC	ATP-binding cassette carrier family
ABCB1	ATP-binding cassette subfamily B member 1
ABCC1	ATP-binding cassette subfamily C member 1
ABCC4	ATP-binding cassette sub-family C member 4
ABCG2	ATP-binding cassette subfamily G member 2
AChE	Acetylcholinesterase
AD	Alzheimer's Disease
ADMA	Asymmetrical dimethylarginine
AHL	Acyl-homoserine lactone
AIF	Apoptosis Inducing Factor
AJ	Adherens junction
Akt	Protein kinase B
AT	Annealing temperature
ATP	Adenosine triphosphate
Aβ	Amyloid beta
BBB	Brain blood barrier
BCSFB	Blood cerebrospinal fluid barrier
BDNF	Brain-derived neurotrophic factor
BP	Base pair
BRCA1	Breast cancer type 1 susceptibility protein
BSA	Bovine serum albumin
BTB	Blood-tumour barrier
BTB	Blood-tumour barrier
CAT	Catalase
Cdk4	Cyclin-dependent kinase 4
Cdk6	Cyclin-dependent kinase 6
Cdk7	Cyclin-dependent kinase 7
cDNA	complementary Deoxyribonucleic acid
ChAT	Choline acetyltransferase
CHOP	C/EBP homologous protein
CJD	Creutzfeldt–Jakob Disease
CNS	Central nervous system
COX-2	Cyclooxygenase-2
CP	Choroid plexus

CPEC	Choroid plexus epithelial cells
CREB	cAMP response element binding
CSF	Cerebrospinal fluid
CYX	Cycloheximide
DAB	Diaminobenzidine
DAG	Diacylglycerol
DB	Denatonium benzoate
DMEM-F12	Dulbecco's Modified Eagle Medium: nutrient mixture F-12
DMPP	1,1-dimethyl-4-phenylpiperazinium iodide
DMSO	Dimethyl sulfoxide
DNA	Deoxyribonucleic acid
ECM	Extracellular matrix
EEC	Enteroendocrine cells
EMT	Epithelial-mesenchymal transition
ERK	Extracellular signal regulated kinase
ERα	Estrogen receptor alpha
EVOM	Epithelial-volt-ohm-meter
EZH2	Enhancer of zeste homolog 2
FBS	Fetal bovine serum
FL-MTX	Fluorescein-methotrexate
FW	Forward
GDNF	Glial cell line-derived neurotrophic factor
GEO	Gene Expression Omnibus
GFAP	Glial fibrillary acidic protein
GLP-1	Glucagon-like peptide-1
GNAT3	G protein subunit alpha transducin 3
Gnb3	G protein subunit beta 3
GPCR	G protein couple receptor
Gper	G protein-coupled estrogen receptor 1
GPX	Glutathione peroxidase
GRx	Glutaredoxin
GSK-3β	Glycogen synthase kinase 3 beta
GST	Glutathione S-transferase
Gαolf	Olfactory G-protein
HBMEC	Human Brain Microvascular Endothelial Cells
HIBCPP	Human choroid plexus papilloma cell line
HIF-1α	Hypoxia-inducible factor 1-alpha

HO-1	Heme oxygenase
HPLC	High-performance liquid chromatography
HSP70	70 kilodalton heat shock proteins
ICC	Immunocytochemistry
IFN-γ	Interferon gamma
IHC	Immunohistochemistry
IL-12	Interleukin 12
IL-1β	Interleukin 1 beta
iNOS	Inducible nitric oxide synthase
Ip3	Inositol 1,4,5-trisphosphate
IP3R3	Type 3 ion channels
ISH	In situ hybridization
IκB-α	Nuclear factor of kappa light polypeptide gene enhancer in B-cells inhibitor, alpha
JNK	c-Jun N-terminal kinase
Kb	Kilobase
KDAC	Lysine deacetylases
Keap1	Kelch-like ECH-associated protein 1
KRB	Krebs Ringer buffer
LAMP 1	Lysosomal-associated membrane protein 1
LC3	Microtubule-associated protein 1A/1B-light chain 3
LDL	Low density lipoprotein
LPS	Lipopolysaccharide
MALAT1	Metastasis Associated Lung Adenocarcinoma Transcript 1
MAPK	Mitogen Activated Protein Kinases
MCA	Middle cerebral artery
MDA	Malondialdehyde
MGMT	O6-alkylguanine DNA alkyltransferase
miR-	microRNA
MMP	Matrix metallopeptidases
MnSOD	Manganese superoxide dismutase
MPTP	1-methyl-4-phenyl-1,2,3,6-tetrahydropyridine
MTT	3-(4,5-dimethylthiazol-2-yl)-2,5-dophenyltetrazolium bromide
NB	Northern blot
NF-κB	Nuclear factor kappa-light-chain-enhancer of activated B cells
NQO-1	NAD(P)H dehydrogenase [quinone] 1
Nrf2	nuclear factor erythroid 2-related factor

NSCLC	Non-small cell lung cancer
PARP	Poly (ADP-ribose) polymerase
PBS	Phosphate saline buffer
PD	Parkinson's Disease
PFA	Paraformaldehyde
PGC-1α	Peroxisome proliferator-activated receptor gamma coactivator 1-alpha
PGE2	Prostaglandin E2
PI3K	Phosphoinositide 3-kinase
PIP2	phosphatidylinositol 4,5-bisphosphate
Plcb2	Phospholipase C-beta 2
PMSF	Phenylmethylsulfonyl Fluoride
PRMT5	Protein arginine N-methyltransferase 5
PROP	6-n-propylthiouracil
PSP	Progressive Supranuclear Palsy
PTC	Phenylthiocarbamide
PTEN	Phosphatase and tensin homolog
PTU	Phenylthiourea
PVDF	Polyvinylidene Difluoride
RAGE	Receptor for advanced glycation endproducts
RANKL	Receptor activator of nuclear factor kappa-B ligand
ROS	Reactive oxygen species
RT	Reverse transcribed
RT	Room temperature
RT-PCR	Reverse Transcriptase Polimerase chain reaction
RT-qPCR	Real time RT-PCR
RV	Reverse
siRNA	Small interfering ribonucleic acid
SLC	Solute carrier family
SOD	Superoxide dismutase
STAT3	Signal transducers and activators of transcription protein 3
TR1	Taste receptor type 1
TR2	Taste receptor type 2
Tas1r1/TAS1R1	Taste receptor type 1 member 1 (rodent/human)
Tas1r2/TAS1R2	Taste receptor type 1 member 2 (rodent/human)
Tas1r3/TAS1R2	Taste receptor type 1 member 3 (rodent/human)
TBS	Tris-buffer saline

TEER	Transepithelial electrical resistance
Tg	Transgenic
TJ	Tight Junction
TLR4	Toll-like receptor 4
TNF-α	Tumor necrosis factor alpha
TR	Taste receptor
TRPM5	Transient receptor potential cation channel, subfamily M, member 5
UGT	UDP glucuronosyltransferase
VEGF	Vascular endothelial growth factor
VEGF-A	Vascular endothelial growth factor A
VEGFR2	Vascular endothelial growth factor receptor 2
Western blot	WB
Wnt2	Wingless-type MMTV integration site family, member 2
x-IAP	X-linked inhibitor of apoptosis protein
XO	Xanthine oxidase
ZO-1	Zonula Occludens 1
ΔΨm	Mitochondrial membrane potential

Chapter 1

Introduction - Part A
The Senses of the Choroid Plexus

Most of this chapter is as in the original publications which I co-authored:

1) Santos C.R.A., **Duarte A.C.**, Quintela T., Tomás J., Albuquerque T., Marques F., Palha J.A., Gonçalves I. (2016) The choroid plexus as a sex hormone target: Functional implications. Frontiers in Neuroendocrinology, DOI: 10.1016/j.yfrne.2016.12.002

2) Santos C.R.A., **Duarte A.C.**, Costa A.R., Tomás J., Quintela T., Gonçalves I. (2019) The senses of the choroid plexus. Progress in Neurobiology, DOI: https://doi.org/10.1016/j.pneurobio.2019.101680

Some alterations to the original publications were introduced to further sustain the aim of the thesis. My major contributions to these publications were: Literature reviewing; Microarray analysis; Writing.

1.1. The choroid plexus

The choroid plexuses (CPs) are highly vascularized structures, located in the ventricular system of the brain. In the lateral ventricles of the mammalian brain, CPs form a sheet-like structure, whereas in the third and fourth ventricles these resemble villus like structures. The CPs are formed by single layers of cuboidal epithelial cells laying on a basement membrane. Below the basement membrane, within the connective tissue, lays a network of fenestrated capillaries, fibroblasts and immune cells (e.g., mast cells, macrophages, granulocytes), and a rich extracellular matrix [1]. The CPs' epithelial cells (CPEC) are connected by tight junctions (TJ), adherens junctions (AD) and desmosomes, forming a sealed barrier that prevents paracellular movement of substances into and out of the brain. CPEC also have numerous microvilli and cilia at the ventricle facing (apical) side, and extensive infoldings at the blood facing (basolateral) side, thus providing a large surface for contact between the epithelium and the cerebrospinal fluid (CSF) and between the epithelium and the stroma interstitial fluid on the other side [2]. In addition, the CPEC apical and basolateral membranes contain a wide range of transporters, channels, pumps and receptors that mediate and set the pace for the exchange of compounds between the periphery and the CSF. These are essential to fulfil the CPs' role as a source of nutrients for the brain, and also for the excretion of molecules originating from the brain metabolism. Several fundamental functions have been attributed to the CPs and have been within the scope of recent reviews. The best known functions of CPs are CSF formation [1], nutrient and hormone supply to the CSF and brain, clearance of deleterious compounds and waste products from brain metabolism [3–5], immune surveillance [6], amyloid beta (Aβ) clearance [7, 8], and neurogenesis [9–11]. Other emerging functions of the CPs are chemical surveillance as depicted from the presence of the taste and olfactory transduction pathways in CPEC [12, 13] and the potential function of the CP as an extra-suprachiasmatic nucleus circadian clock [14] (Figure 1.1.).

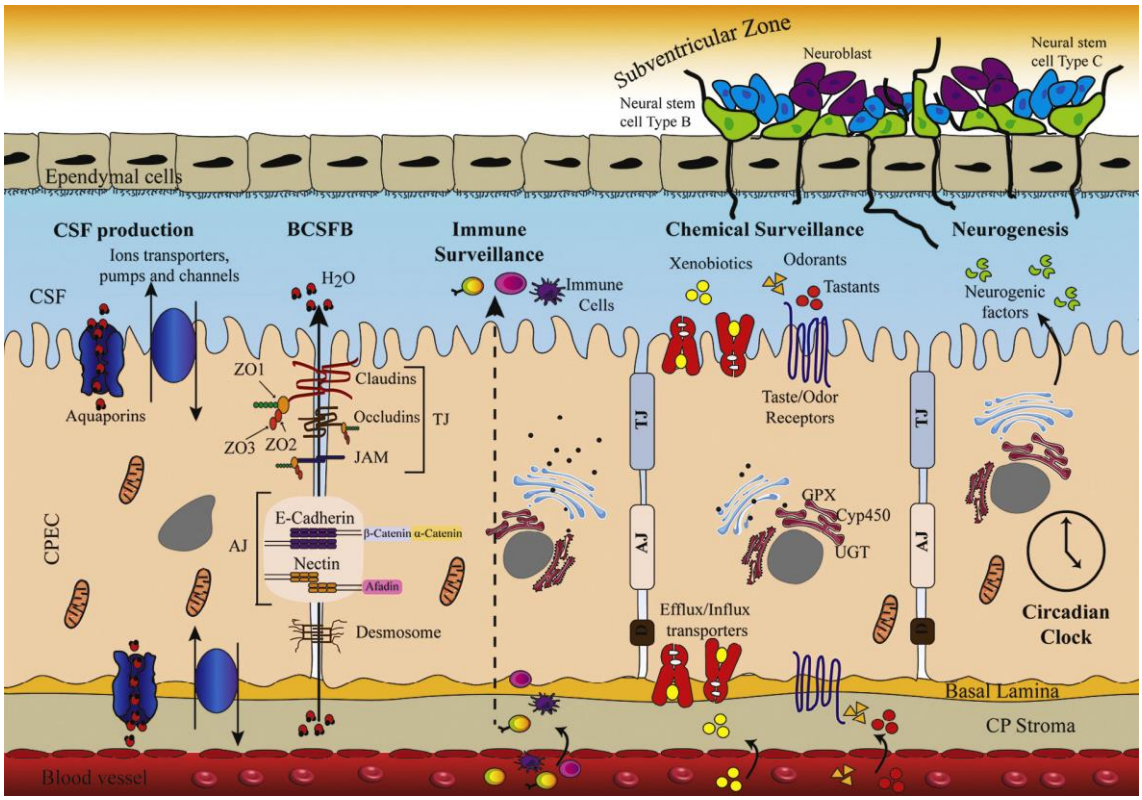

Figure 1. 1. Main biological functions of the choroid plexuses. (CP – choroid plexuses; CSF – cerebrospinal fluid; CPEC – choroid plexuses epithelial cell; TJ – tight junction; AJ – adherens junction; ZO – zonula occludens protein; JAM – junctional adhesion molecules; Cyp450 – cytochrome P450; GPX – glutathione peroxidase; UGT – UDP glucuronosyltransferase).

1.2. Chemical surveillance at the choroid plexus

We identified a wide range of chemosensory receptors transcripts in the rat CPs by cDNA microarrays [15]: 34 taste receptors (TRs), over a 1000 odorant receptor, and 196 vomeronasal receptors. We demonstrated that the olfactory and taste transduction pathways are active in the CPs [12, 13]. ORs and TRs, and some effector components of their signalling pathway were also identified in the cerebral cortex of mice and throughout the human brain [16, 17]. Transcriptome analysis indicate that these systems are also expressed in the human CP (GSE49974) [18], and some of these receptors are also expressed at the blood-brain barrier (BBB) (GSE45171) [19]. Beyond their functions in the perception of odours and flavours, a growing body of evidence show that in non-olfactory and at extra-oral organs, chemosensory receptors are essential for the crosstalk between cells and their niches, and with external cues, responding to their ligands and bringing about downstream responses. Expression of chemosensory receptors in the CPs is a novel and intriguing subject, potentially of high relevance due to its barrier function between the blood and the CSF. Given the large amount and variety of compounds circulating in the blood, CSF and brain interstitial fluid, it is likely that these receptors have crucial functions in the chemosurveillance system of the CNS.

1.2.1. Taste receptors

Taste receptors that bind sweet, umami and bitter compounds are G protein coupled receptors (GPCRs) that generate taste perception upon binding to their ligands. As such, they evaluate the nutrient content of food (sweet and umami receptors) or prevent the ingestion of toxic substances (bitter receptors). Sweet and umami taste receptors were initially described in the oral cavity: taste receptor type 1 (TR1; Tas1r in rodents and TAS1R in humans) that bind sweet and umami compounds, and taste receptor type 2 (TR2; Tas2r in rodents and TAS2R in humans) that detect bitter compounds. The TR1 class form two dimeric receptors, the T1R1/T1R3 that respond to umami (glutamate in humans, or most non-aromatic L-amino acids in rodents) and the T1R2/T1R3 that respond to sweet, and the TR2 class bind bitter compounds [20]. Almost all of the human TAS2R repertoire has now been effectively "deorphanized" [21]. Regarding rodent Tas2r ligands, Lossow et al. identified cognate compounds for 21 of the 34 mouse bitter Tas2r [22], but there is substantial amino acid sequence divergence between homologous human and rodent bitter TRs genes, which may result in functionally distinct receptors [23]. Both TR1 and TR2 utilize the same signalling cascade effectors: ligand binding to TRs results in a conformational change of the receptor and in the activation of a series of signal transducers such as the taste-specific heterotrimeric G-protein gustducin (formed by α-gustducin, Gβ3 and Gγ13 subunits), which activates a specific phospholipase C-beta 2 (PLCB2) to produce IP3 (Figure 1.2.). The IP3 opens the inositol 1,4,5-trisphosphate receptor type 3 ion channels (ITPR3), triggering an increase in intracellular Ca2+ levels which will activate a taste-selective cation channel, the transient receptor potential channel, subfamily M, member 5 (TRPM5), that eventually depolarizes the cell [20, 24].

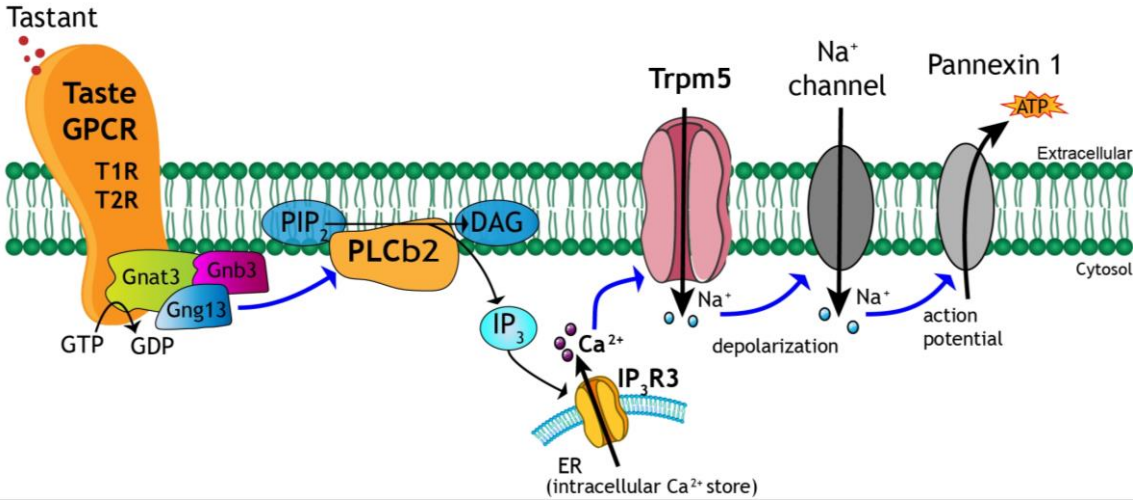

Figure 1. 2. Taste pathway signal transduction. Sweet, umami and bitter stimuli utilize taste receptors, which belong to the superfamily of G protein-coupled receptors (GPCR). Sweet and umami activates taste receptors type 1 (TR1) while bitter activates taste receptors type 2 (TR2). However, the transduction mechanism is identical: the tastant binds to the receptor, resulting in a conformational change and in the activation of a

series of signal transducers such as the taste-specific heterotrimeric G-protein gustaducin (formed by α-gustducin, Gβ3 and Gγ13 subunits), which activates phospholipase C-beta 2 (PLCβ2) to cleave phosphatidylinositol 4,5-bisphosphate (PIP2) into diacylglycerol (DAG) producing inositol 1,4,5-trisphosphate (IP3). The IP3 opens receptor type 3 ion channels (IP3R3), triggering an increase in intracellular Ca2+ levels which will activate the transient receptor potential channel M5 (TRPM5), that eventually depolarizes the cell.

The first identification of taste signaling components outside the oral cavity was the description of α-gustducin and TRs in the brush cells of the stomach and intestine [25]. Later, Zancanaro et al [26] described α-gustducin in the nasal and upper airway tissue, the first time in a tissue outside the digestive tract, suggesting that common transduction mechanisms could be shared by unrelated chemosensory tissues. The discovery of about 35 bitter TRs in rodents (25 in humans) in oral taste bud cells [27] was followed by a large number of studies showing ectopic expression of TRs in distinct organs and tissues [28–30]. It is becoming evident that TR2, are expressed in extra-oral tissues, where they perform functions like bronchodilation, inflammation, metabolism, enteroendocrine regulation, innate immunity and male fertility (Table 1.1.). It is clear, with all these data, that depending on tissue/cell/organ and on the TR2, different effects may occur in response to alterations in the concentrations of their ligands in the body fluids. The physiologic roles of TR2 in health and disease were recently reviewed [29–32] highlighting that TRs might be of therapeutic potential, mainly because of the wide range of known ligands. TR2' ligands are numerous and diverse and can be either endogenous or exogenous ligands, present in body fluids. Natural compounds such as flavonoids or synthetic chemicals such as the anti-psychotic haloperidol are good examples of the diversity of bitter ligands. Moreover, these compounds might be able to activate only one or several TRs. For example, the flavonoid quercetin binds only TAS2R14 [33], however the antibiotic chloramphenicol can bind to seven of the human TAS2R [21].

1.2.1.1. Taste receptors at extra-oral organs

As already mentioned, we identified 34 TRs genes expressed in rat CP by cDNA microarrays [15], but only 50% of them are conserved in humans. Among those, only eight were previously described in other organs, with ligands and/or functions identified and high/medium levels of expression: Tas1r1, Tas1r3, Tas2r135, Tas2r126, Tas2r118, Tas2r139, Tas2r140 and Tas2r121. Tas2r135 and Tas2r126 are two of the few bitter TRs expressed in mouse myometrium [34]. Denatonium and phenanthroline treatment, both Tas2r135 bitter ligands, can completely relax myometrium pre-contracted by different uterotonics. Besides, Tas2r135, Tas2r126 and other Tas2rs have been described along the rodent gastrointestinal tract: stomach (in a total of 9 expressed Tas2r), small intestine (in a total of 7 Tas2r) and large intestine (in a total of 12 expressed Tas2r) [35, 36]. The

expression of TR2 in mouse gut muscle and the contractility responses to bitter ligands, as denatonium benzoate, suggest its modulator role in the gastrointestinal motility with effects on gastric emptying and satiation [36]. Tas2r135 is also expressed in white adipose tissue and pre-adipocytes, where it is implicated in the regulation of metabolism and development of obesity [28]. Tas2r135 and Tas2r126 are also two of the seven bitter TRs identified in rodent heart that are upregulated after nutrient deprivation and starvation. These findings could reflect a potential function of these Tas2r as nutrient sensors in the heart [23]. TAS2R16 (homologous to the rodent Tas2r118) is expressed in human brain tissue: Pyramidal, Purkinje and hippocampal neurons [37]. The only functional study about TAS2R in the CNS was the stimulation of the neuroblastoma cell line SH-SY5Y with salicin or diphenidol, two ligands of TAS2R16, that revealed increased extracellular signal regulated kinase (ERK) and cAMP response element binding (CREB) phosphorylation, promoting neurite outgrowth in these cells. These results show that salicin might modulate neurite outgrowth by bitter TR activation [37]. Salicin from willow bark has been used since a long time ago in China and Europe for the treatment of headache, pain and inflammation. The existence of TAS2R16 in the human CP [18], as well as its homologous in rat CP (Tas2r118), has increased interest because the presence of its natural ligand salicin in the blood and/or CSF may promote neurite outgrowth, and could be used as therapeutic target in the case of CNS injury. Tas2r139, TAS2R39 in humans, was identified in omental, mesenteric and cerebral arteries. The treatment of pre-contracted arteries with Tas2r agonists, chloroquine and quinine, resulted in their relaxation in a concentration-dependent manner [38]. Tas2r139 is also expressed in detrusor smooth muscle and the activation of Tas2r with chloroquine or denatonium benzoate relaxes this muscle and suppresses overactive bladder symptoms [39]. This bitter receptor is also one of the TAS2R expressed in human heart, with the putative function of nutrient sensor in this organ [23]. TAS2R14 (homologous to the rodent Tas2r140) is one of the most studied bitter TRs, identified in several tissues, with different biological functions in varied locations. TAS2R14 is expressed in the ciliated epithelial cells and in the smooth muscle cells of the airways [40, 41]. Anti-inflammatory properties of flavones, in airways, were linked to respiratory epithelial innate immunity through TR2 activation: flavones binding to TAS2R14 elicit nitric oxide production, increasing ciliary beating and mucociliary clearance [41, 42]. Moreover, also in the airways, TR2 agonists evoked increased [Ca2+] intracellular in the smooth muscle cells, relaxation of isolated cells and dilation of airways [43]. Given the need for efficacious bronchodilators for treating lung diseases, this pathway has been exploited for therapy with the thousands of known synthetic and naturally occurring bitter compounds. Besides, transcriptome analysis revealed upregulation of bitter TRs in leucocytes of

severe asthmatics [44]. Tas2r140 (or TAS2R14) was also described in the smooth muscle cells of several arteries: rat mesenteric and cerebral arteries and in human omental arteries. Quinine treatment, both a Tas2r140 and TAS2R14 ligand, relaxed these arteries in a concentration-dependent manner [38]. This TR2 was also identified in human and mouse urogenital tract (detrusor smooth muscle and myometrium). Once again, TAS2R14 activation by chloroquine and other bitter ligands, elicited relaxation of detrusor muscle and myometrium, respectively [34, 39]. An additional location of this TR2 is the human and rodent gastrointestinal tract. TAS2R14 is expressed in the stomach and colon, with putative gastric acid secretion and gastrointestinal motility functions, respectively [35, 36, 45]. TAS2R13 (homologous to the rodent Tas2r121) is expressed in the human frontal cortex [46]. The functions of TR2 in the brains of humans and rodents, including the CP, are yet unknown. It is possible that exogenous ligands of TR2 in the brain are transported through the blood, CSF and the extracellular fluid. Additionally, brain TR2 might be stimulated by endogenous compounds from neighbouring cells, or even from the same cells, thus having a self-stimulating mechanism regulating internal trafficking. The generalized expression of these TR2 lends weight to the idea that these receptors in the brain may sustain physiological roles and, suggests a new scenario in the chemical signalling system of the CNS.

1.3. Conclusions

Placed on the interface between the periphery (blood) and the CNS, the CP is well positioned to sense alterations in the fluids in contact with its apical side (CSF side) and in its basolateral side (blood side) and respond to them accordingly, in order to ensure brain homeostasis. This overwhelming task requires permanent surveillance of the blood and CSF for the presence of noxious compounds, and the assessment of general alterations in the composition of these body fluids. Moreover, it requires a complex detoxification system of the CSF [2] and selective efflux and influx receptors that accurately control molecular trafficking across the blood-cerebrospinal fluid barrier (BCSFB). How these mechanisms are regulated is still a poorly understood subject. The large repertoire of chemosensory receptors in CPs cells, such as TR2, supports the existence of an upstream mechanism to assess the composition of the blood and CSF and to deploy appropriate downstream responses of the cell machinery that allow coping with the chemical alterations sensed. Given the nature of TR2 as GPCRs, ligands can be hydrophilic molecules, and downstream signalling may be either genomic or nongenomic and affect the main intracellular pathways (affecting cell proliferation, migration, chemiotaxis, endocrine responses), as seen in non-gustatory organs. It is thus of utmost importance to elucidate the function of TR2 at the BCSFB as they represent a

promising route for manipulating the entrance, metabolism and the clearance of a large number of chemicals in the brain.

Table 1. 1. Expression of TR2 in extra-oral tissues.

Tissue, cell, organ	TR2	Function	Ligand	Analysis method	Refs
ADIPOSE TISSUE					
Mouse gonadal, subcutaneous and mesenteric white adipose tissue; pre-adipocytes (3T3-F442A)	mTas2r108, 135	Regulation of adipocytes metabolism	DB, quinine	RT-PCR	[47]
AIRWAYS					
Human and mouse solitary chemosensory cells (sinuses)	hTAS2R4, 10, 47	Antimicrobial peptide release	DB	RT-PCR, IHC, ICC	[48–50] [51–53]
	mTas2r108, 119	Detection of irritants and bacterial signals/Changes in respiratory rate/trigger trigeminally-mediated protective airway reflexes	DB, quinine, CYX	IHC, ICC, RT-PCR,	
Human and mouse ciliated epithelial cells (nose and sinuses)	hTAS2R14 (mTas2r140)	Anti-inflammatory effect	DB, flavone	ICC	[41, 54] [55]
	hTAS2R38 (mTas2r138)	Nitric oxide release (bactericide) Mucociliary clearance (↑ciliary beat frequency)	DB, AHL, PTC	IHC, ICC	[56, 57]
Human and mouse ciliated epithelial cells (trachea, bronchi)	hTAS2R1, 3 ,4, 7-10, 13, 14, 16, 38, 43, 46	Mucociliary clearance (↑ciliary beat frequency)	Bitter agonists	Microarray, RT-PCR, IHC	[58]
	mTas2r105,108	Changes in respiratory rate	CYX		[42]
Human and mouse smooth muscle cells (trachea, bronchi)	hTAS2R1, 3, 4, 5, 8, 9, 10, 13, 14, 19, 20, 30, 31, 42, 46, 50	Bronchodilatation	Chloroquinine, quinine, DB	RT-qPCR, ICC	[40, 43, 59]
	mTas2r107	Bronchodilatation	Choloroquinine, quinine, DB	RT-PCR, IHC	[60, 61]
ARTERIES (smooth muscle cells)					
Human pulmonary artery, Guinea pig aorta, mouse aorta	hTAS2R1, 3, 4, 5, 7, 9, 10, 13, 14, 16, 38, 40, 42, 43, 44, 45, 46, 47, 48, 49, 50, 60	Regulation of the vascular tone (vasodilation/ vasoconstriction)	Chloroquine, DB, dextromethorphan, noscapine	RT-qPCR, WB, ICC	[62, 63]

Human omental arteries Rat mesenteric and cerebral arteries	hTAS2R3, 4, 7, 10, 14, 39, 40 rTas2r7, 39, 40, 108, 114, 130, 137, 140	Vasodilation	Chloroquine, quinine	RT-PCR WB, IIC, IHC	[38]
BONE MARROW					
Bone marrow stromal-derived cells	hTAS2R46	Extracellular release of ATP	DB, thujone, nicotine	RT-PCR, IHC, ICC	[64]
BRAIN					
Human brain neurons (Pyramidal, Purkinje, Hippocampal); SH-SY5Y cells	hTAS2R16	Neurite outhgrowth	Salicin, diphenidol	RT-PCR, IHC, ICC, WB	[37]
Human frontal cortex	hTAS2R4, 5, 10, 13, 14, 50	Differential expression in PD, AD, PSP and CJD		Microarray, RT-qPCR	[46, 65]
Rat brainstem, cerebellum, cortex, nucleus accumbens; C6 Glial cells; primary neuronal cells	rTas2r107, 108(hTAS2R4), 138(hTAS2R38) rTas2r1		DB, quinine	RT-PCR, IHC, WB RT-PCR, IHC	[66] [67]
Rat CP	rTas2r109, 144		Salicin	RT-PCR, IHC	[13]
Mouse hypothalamus, brainstem, hippocampus	mTas2r116			RT-qPCR, ISH	[68]
GASTROINTESTINAL TRACT					
Human and mouse stomach:					
Human parietal cells	hTAS2R7, 10, 14, 43, 46	Gastric acid secretion	Bitter agonists	IHC, ICC, RT-qPCR	[45]
Human and mouse smooth muscle cells	hTAS2R3(mTas2r137), 4(mTas2r108),10, mTas2r135	Gastrointestinal motility	DB, Chloroquine	RT-PCR	[36]
HGT-1 cells	hTAS2R1, 3, 4, 5, 7, 9, 10, 13, 14, 16, 19, 20, 30, 31, 38, 39, 40, 41, 42, 43*, 46, 50	*Gastric acid (proton) secretion	Caffeine	RT-PCR, CRISP-Cas9 KO Tas2r43	[45]

Rat and mouse stomach	rTas2r1-3, 5-12, 16, 34, 38 mT2R108, 109, 113, 115, 126, 134, 135, 137, 138(?), 140, 143			RT-PCR	[35, 69, 70]
Mouse small intestine:					
Duodenum, jejunum, ileum	mTas2r108, 119, 126, 135, 137, 138, 143			RT-PCR	[35]
Jejunum and ileum mucosa (Paneth cells)	mTas2r131	Defensive role		IHC, Tg mice	[35]
STC-1 cells (EEC)	mTas2r102, 105, 118, 119, 123, 126, 127, 130, 108*, 134*,138*, 144*	*CCK release GLP-1 release	DB, PTC, PROP, caffeine, nicotine, CYX, FTC, KDT501	RT-qPCR, IHC/WB	[69–73]
Human and rodent colon:		- PYY and GLP-1 release from enteroendocrine L cells -hT2R1,4,38 activation by 6-PTU causes anion secretion in human and rat large intestine -hT2R14 activation by Hoodia gordinii causes CCK secretion in HuTu80 cells -Bitter Gentiana scabra extract stimulates GLP-1 release			
Human and rat mucosa, HuTu80 cells (h EEC), NCI-H716 cells (h EEC)	hTAS2R1(rTas2r1)*, 3, 4(rTas2r16)*, 5, 10, 13, 38(rTas2r26)*, 39, 40, 42-47, 49, 50, 60		PTC, Bombesin, Hoodia gordinii and Gentiana scabra extracts	RT-PCR, IHC, Tg mice	[74–80]
Mouse mucosa	mTas2r108, 113, 117, 119, 125, 126, 131, 135, 137, 138, 140, 143				
Mouse goblet cells	mTas2r131	Gastrointestinal motility	DB, Chloroquine	RT-PCR, Tg mice	[35, 36, 81]
Mouse smooth muscle	mTas2r108, 135, 137				
Caco-2 cells		Modulation of gut efflux membrane transporters	PTC	RT-PCR, WB	[82]
HEART					
Human and rodent heart (cardiomyocytes, fibroblasts, heart tissue)	hTAS2r3-5, 9, 10, 13, 14, 19, 20, 30, 31, 39, 43, 45, 46, 50	Nutrient sensors (?)		RT-qPCR, ISH	[23]

	(r,m)Tas2r108*, 120, 121, 126, 135, 137**, 143	(* and ** activation): ↘ left ventricular pressure and ↗ aortic pressure; nutrient sensors (?)	* sodium thiocyanate ** sodium benzoate	RT-qPCR, ISH	[23, 83]
KERATINOCYTES					
Human epidermal keratinocytes, HaCat cells	hTAS2R1, 38	↗ the expression of differentiation markers	Diphenidol, amarogentin	IHC, ICC, RT-PCR, WB	[84]
LEUCOCYTES					
Human leucocytes	hTAS2r4, 5, 10, 13, 14, 19, 20, 31, 45, 46, 50	↘ the release of several pro-inflammatory cytokines and eicosanoid from leucocytes	Chloroquine, DB	Microarray, RT-qPCR	[44]
	All the 25 hTAS2R (differential mRNA expression in 5 types of blood leucocytes)			RT-qPCR, ICC	[85]
PANCREAS					
Human tumor pancreatic cells, tumor pancreatic derived cell lines (MiaPaCa-2, Su8686, T3M4, HuH7)	hTAS2R38	Pancreatic cancer progression(?)	PTU, AHL-12	WB, IHC, ICC	[86]
PLACENTA					
Human placental tissues	hTAS2R38		Diphenidol, PTC	IHC, ICC	[87]
TESTIS					
Mouse testis	mTas2r105	Male infertility		IHC, RT-PCR, Tg mice, IHC	[88] [89]
	mTas2r105-108, 113, 117, 119, 125, 126	Sperm behavior and fertilization	Caffeine, PTC, PROP, picrotin, salicin, DB	RT-PCR, RT-qPCR, ISH	[90]
Mouse testis, cauda of epididymis, sperm	mTas2r131			Tg mice, RT-PCR, IHC, ISH	[91]

THYMUS					
Murine Thymus	mTas2r131			Tg mice	[91]
	mTas2r105, 108, 131			RT-qPCR, Tg mice	[92]
THYROID					
Human thyroid; NthyOri3-1 cells	hTAS2R4, 10, 38, 42, 43	Regulation of thyroid hormone secretion	Camphor, Chloramphenicol, Colchicine, CYX, DB, PROP	RT-qPCR, IHC, Tg mice	[93]
Mouse thyroid	mTas2r131				
UROGENITAL TRACT					
Human and mouse detrusor smooth muscle	hTAS2R1, 4 ,5, 7-10, 13, 14, 20, 30, 31, 38-40, 45, 50 mTas2r114, 117, 130, 138, 144	Detrusor muscle relaxation	Chloroquine Chloroquine, DB, quinine	RT-qPCR	[39]
Human and mouse myometrium (uterine smooth muscle cells)	hTAS2R4, 5, 10, 13, 14 mTas2r126, 135, 137, 143	Relax contracted myometrium	DB, 1,10-phenanthroline, chloroquine	IHC, RT-qPCR	[34]
Mouse urethral chemosensory cells (brush cells)	mTas2r108	Acetylcholine release (↑bladder detrusor muscle activity)	DB	Tg mice, RT-PCR, IHC	[94]
Mouse kidney	mTas2r108, 119, 135, 137, 138, 140, 143 mTas2r105*, 106, 110, 113, 114, 134, 143	*Maintenance of the structure of the glomerulus and renal tubule		RT-PCR Tg mice, RT-PCR, WB, IHC	[95] [96]

TAS2R-human taste receptors type 2; Tas2r-rodent taste receptor type 2; *-orthologous gene; RT-PCR-Reverse transcriptase PCR; RT-qPCR-Reverse transcriptase real time PCR; IHC-immunohistochemistry; ICC -immunocytochemistry; WB-western blot; ISH-In situ hybridization; Tg-transgenic; NB-northern blot; AHL-acyl-homoserine lactone; DB-Denatonium benzoate; PTC-phenylthiocarbamide; PTU-Phenylthiourea; PROP-6-n-propylthiouracil; CYX-Cycloheximide; DMPP-1,1-dimethyl-4-phenylpiperazinium iodide; EEC-enteroendocrine cells; GLP-1-Glucagon-like peptide-1; PD-Parkinson's Disease; AD-Alzheimer's Disease; PSP- Progressive Supranuclear Palsy; CJD-Creutzfeldt–Jakob Disease; h-human; m-mouse; r-rat.

1.4. References

1. Redzic ZB, Segal MB (2004) The structure of the choroid plexus and the physiology of the choroid plexus epithelium. Adv Drug Deliv Rev 56:1695–1716. https://doi.org/10.1016/j.addr.2004.07.005

2. Ghersi-Egea JF, Mönkkönen KS, Schmitt C, et al (2009) Blood-brain interfaces and cerebral drug bioavailability. Rev Neurol (Paris) 165:1029–1038. https://doi.org/10.1016/j.neurol.2009.09.011

3. Johanson C, Stopa E, Baird A, Sharma H (2011) Traumatic brain injury and recovery mechanisms: Peptide modulation of periventricular neurogenic regions by the choroid plexus-CSF nexus. J Neural Transm 118:115–133. https://doi.org/10.1007/s00702-010-0498-0

4. Richardson SJ, Wijayagunaratne RC, D'Souza DG, et al (2015) Transport of thyroid hormones via the choroid plexus into the brain: the roles of transthyretin and thyroid hormone transmembrane transporters. Front Neurosci 9:66. https://doi.org/10.3389/fnins.2015.00066

5. Spector R, Robert Snodgrass S, Johanson CE (2015) A balanced view of the cerebrospinal fluid composition and functions: Focus on adult humans. Exp Neurol 273:57–68. https://doi.org/10.1016/j.expneurol.2015.07.027

6. Schwartz M, Baruch K (2014) The resolution of neuroinflammation in neurodegeneration: Leukocyte recruitment via the choroid plexus. EMBO J 33:7–22. https://doi.org/10.1002/embj.201386609

7. Pahnke J, Langer O, Krohn M (2014) Alzheimer's and ABC transporters - new opportunities for diagnostics and treatment. Neurobiol Dis 72:54–60. https://doi.org/doi:10.1016/j.nbd.2014.04.001

8. Pascale CL, Miller MC, Chiu C, et al (2011) Amyloid-beta transporter expression at the blood-CSF barrier is age-dependent. Fluids Barriers CNS 8:21. https://doi.org/10.1186/2045-8118-8-21

9. Falcão AM, Marques F, Novais A, et al (2012) The path from the choroid plexus to the subventricular zone: Go with the flow! Front Cell Neurosci 6:1–8. https://doi.org/10.3389/fncel.2012.00034

10. Johansson P a (2014) The choroid plexuses and their impact on developmental neurogenesis. Front Neurosci 8:340. https://doi.org/10.3389/fnins.2014.00340

11. Lun MP, Monuki ES, Lehtinen MK (2015) Development and functions of the choroid plexus-cerebrospinal fluid system. Nat Rev Neurosci 16:445–57. https://doi.org/10.1038/nrn3921

12. Gonçalves I, Hubbard PC, Tomás J, et al (2016) ‘ Smelling ’ the cerebrospinal fluid : olfactory signaling molecules are expressed in and mediate chemosensory signaling from the choroid plexus. FEBS J 283:1748–1766. https://doi.org/10.1111/febs.13700

13. Tomás J, Santos CRA, Quintela T, Gonçalves I (2016) “Tasting” the cerebrospinal fluid: Another function of the choroid plexus? Neuroscience 320:160–171. https://doi.org/10.1016/j.neuroscience.2016.01.057

14. Quintela T, Sousa C, Patriarca FM, et al (2015) Gender associated circadian oscillations of the clock genes in rat choroid plexus. Brain Struct Funct 220:1251–1262. https://doi.org/10.1007/s00429-014-0720-1

15. Quintela T, Goncalves I, Carreto LC, et al (2013) Analysis of the effects of sex hormone background on the rat choroid plexus transcriptome by cDNA microarrays. PLoS One 8:e60199. https://doi.org/10.1371/journal.pone.0060199

16. Ferrer I, Garcia-Esparcia P, Carmona M, et al (2016) Olfactory Receptors in Non-Chemosensory Organs: The Nervous System in Health and Disease. Front Aging Neurosci 8:163. https://doi.org/10.3389/fnagi.2016.00163

17. Otaki JM, Yamamoto H, Firestein S (2004) Odorant Receptor Expression in the Mouse Cerebral Cortex. J Neurobiol 58:315–327. https://doi.org/10.1002/neu.10272

18. Janssen SF, Van Der Spek SJF, Ten Brink JB, et al (2013) Gene expression and functional annotation of the human and mouse choroid plexus epithelium. PLoS One 8:. https://doi.org/10.1371/journal.pone.0083345

19. Cecchelli R, Aday S, Sevin E, et al (2014) A stable and reproducible human blood-brain barrier model derived from hematopoietic stem cells. PLoS One 9:. https://doi.org/10.1371/journal.pone.0099733

20. Chandrashekar J, Hoon MA, Ryba NJ, Zuker CS (2006) The receptors and cells for mammalian taste. Nature 444:288–294. https://doi.org/10.1038/nature05401

21. Meyerhof W, Batram C, Kuhn C, et al (2009) The molecular receptive ranges of human TAS2R bitter taste receptors. Chem Senses 35:157–170. https://doi.org/10.1093/chemse/bjp092

22. Lossow K, Hübner S, Roudnitzky N, et al (2016) Comprehensive analysis of mouse bitter taste receptors reveals different molecular receptive ranges for orthologous receptors in mice and humans. J Biol Chem 291:15358–15377. https://doi.org/10.1074/jbc.M116.718544

23. Foster SR, Porrello ER, Purdue B, et al (2013) Expression, regulation and putative nutrient-sensing function of taste GPCRs in the heart. PLoS One 8:e64579. https://doi.org/10.1371/journal.pone.0064579

24. Chaudhari N, Roper SD (2010) The cell biology of taste. J Cell Biol 190:285–296.

https://doi.org/10.1083/jcb.201003144

25. Höfer D, Püschel B, Drenckhahn D (1996) Taste receptor-like cells in the rat gut identified by expression of α-gustducin. Proc Natl Acad Sci U S A 93:6631–6634. https://doi.org/10.1073/pnas.93.13.6631

26. Zancanaro C, Caretta CM, Merigo F, et al (1999) A-Gustducin Expression in the Vomeronasal Organ of the Mouse. Eur J Neurosci 11:4473–4475. https://doi.org/10.1046/j.1460-9568.1999.00912.x

27. Adler E, Hoon MA, Mueller KL, et al (2000) A novel family of mammalian taste receptors. Cell 100:693–702. https://doi.org/10.1016/S0092-8674(00)80705-9

28. Avau B, Depoortere I (2016) The bitter truth about bitter taste receptors: Beyond sensing bitter in the oral cavity. Acta Physiol 216:407–420. https://doi.org/10.1111/apha.12621

29. Dalesio NM, Barreto Ortiz SF, Pluznick JL, Berkowitz DE (2018) Olfactory, Taste, and Photo Sensory Receptors in Non-sensory Organs: It Just Makes Sense. Front Physiol 9:1673–1691. https://doi.org/10.3389/fphys.2018.01673

30. Lee SJ, Depoortere I, Hatt H (2019) Therapeutic potential of ectopic olfactory and taste receptors. Nat Rev Drug Discov 18:116–138. https://doi.org/10.1038/s41573-018-0002-3

31. Lu P, Zhang C-H, Lifshitz LM, ZhuGe R (2017) Extraoral bitter taste receptors in health and disease. J Gen Physiol 149:

32. Shaik FA, Singh N, Arakawa M, et al (2016) Bitter taste receptors: Extraoral roles in pathophysiology. Int J Biochem Cell Biol. https://doi.org/10.1016/j.biocel.2016.03.011

33. Levit A, Nowak S, Peters M, et al (2014) The bitter pill : clinical drugs that activate the human bitter taste receptor TAS2R14. FASEB J 27:1181–1197. https://doi.org/10.1096/fj.13-242594

34. Zheng K, Lu P, Delpapa E, et al (2017) Bitter taste receptors as targets for tocolytics in preterm labor therapy. FASEB J 31:4037–4052. https://doi.org/10.1096/fj.201601323RR

35. Prandi S, Voigt A, Meyerhof W, Behrens M (2018) Expression profiling of Tas2r genes reveals a complex pattern along the mouse GI tract and the presence of Tas2r131 in a subset of intestinal Paneth cells. Cell Mol Life Sci 75:49–65. https://doi.org/10.1007/s00018-017-2621-y

36. Avau B, Rotondo A, Thijs T, et al (2015) Targeting extra-oral bitter taste receptors modulates gastrointestinal motility with effects on satiation. Sci Rep 5:15985. https://doi.org/10.1038/srep15985

37. Wölfle U, Haarhaus B, Kersten A, et al (2015) Salicin from willow bark can modulate neurite outgrowth in human neuroblastoma SH-SY5Y cells. Phyther Res 29:1494–1500. https://doi.org/10.1002/ptr.5400

38. Chen J-G, Ping N-N, Liang D, et al (2017) The expression of bitter taste receptors in mesenteric, cerebral and omental arteries. Life Sci 170:16–24. https://doi.org/10.1016/j.lfs.2016.11.010

39. Zhai K, Yang Z, Zhu X, et al (2016) Activation of bitter taste receptors (tas2rs) relaxes detrusor smooth muscle and suppresses overactive bladder symptoms. Oncotarget 7:21156–21167

40. Robinett KS, Koziol-White CJ, Akoluk A, et al (2014) Bitter Taste Receptor Function in Asthmatic and Nonasthmatic Human Airway Smooth Muscle Cells. Am J Respir Cell Mol Biol 50:678–683. https://doi.org/10.1165/rcmb.2013-0439RC

41. Hariri BM, McMahon DB, Chen B, et al (2017) Flavones modulate respiratory epithelial innate immunity: Anti-inflammatory effects and activation of the T2R14 receptor. J Biol Chem 292:8484–8497. https://doi.org/10.1074/jbc.M116.771949

42. Krasteva G, Canning BJ, Hartmann P, et al (2011) Cholinergic chemosensory cells in the trachea regulate breathing. Proc Natl Acad Sci 108:9478–9483. https://doi.org/10.1073/pnas.1019418108

43. Deshpande DA, Wang WC, McIlmoyle EL, et al (2010) Bitter taste receptors on airway smooth muscle bronchodilate by localized calcium signaling and reverse obstruction. Nat Med 16:1299–1304. https://doi.org/10.1038/nm.2237

44. Orsmark-Pietras C, James A, Konradsen JR, et al (2013) Transcriptome analysis reveals upregulation of bitter taste receptors in severe asthmatics. Eur Respir J 42:65–78. https://doi.org/10.1183/09031936.00077712

45. Liszt KI, Ley JP, Lieder B, et al (2017) Caffeine induces gastric acid secretion via bitter taste signaling in gastric parietal cells. Proc Natl Acad Sci U S A 114:E6260–E6269. https://doi.org/10.1073/pnas.1703728114

46. Garcia-Esparcia P, Schlüter A, Carmona M, et al (2013) Functional genomics reveals dysregulation of cortical olfactory receptors in Parkinson disease: novel putative chemoreceptors in the human brain. J Neuropathol Exp Neurol 72:524–39. https://doi.org/10.1097/NEN.0b013e318294fd76

47. Avau B, Bauters D, Steensels S, et al (2015) The Gustatory Signaling Pathway and Bitter Taste Receptors Affect the Development of Obesity and Adipocyte Metabolism in Mice. PLoS One 10:e0145538. https://doi.org/10.1371/journal.pone.0145538

48. Braun T, Mack B, Kramer MF (2011) Solitary chemosensory cells in the respiratory and vomeronasal epithelium of the human nose: a pilot study. Rhinology 49:507–12. https://doi.org/10.4193/Rhino11.121

49. Barham HP, Cooper SE, Anderson CB, et al (2013) Solitary chemosensory cells and bitter

taste receptor signaling in human sinonasal mucosa. Int Forum Allergy Rhinol 3:450–7. https://doi.org/10.1002/alr.21149

50. Lee RJ, Kofonow JM, Rosen PL, et al (2014) Bitter and sweet taste receptors regulate human upper respiratory innate immunity. J Clin Invest 124:1393–1405. https://doi.org/10.1172/JCI72094

51. Tizzano M, Gulbransen BD, Vandenbeuch A, et al (2010) Nasal chemosensory cells use bitter taste signaling to detect irritants and bacterial signals. Proc Natl Acad Sci U S A 107:3210–5. https://doi.org/10.1073/pnas.0911934107

52. Tizzano M, Cristofoletti M, Sbarbati A, Finger TE (2011) Expression of taste receptors in Solitary Chemosensory Cells of rodent airways. BMC Pulm Med 11:1–12. https://doi.org/10.1186/1471-2466-11-3

53. Finger TE, Böttger B, Hansen A, et al (2003) Solitary chemoreceptor cells in the nasal cavity serve as sentinels of respiration. Proc Natl Acad Sci U S A 100:8981–6. https://doi.org/10.1073/pnas.1531172100

54. Lee RJ, Chen B, Redding KM, et al (2014) Mouse nasal epithelial innate immune responses to *Pseudomonas aeruginosa* quorum-sensing molecules require taste signaling components. Innate Immun 20:606–617. https://doi.org/10.1177/1753425913503386

55. Lee RJ, Xiong G, Kofonow JM, et al (2012) T2R38 taste receptor polymorphisms underlie susceptibility to upper respiratory infection. J Clin Invest 122:4145–4159. https://doi.org/10.1172/JCI64240

56. Lee RJ, Cohen NA (2015) Taste receptors in innate immunity. Cell Mol Life Sci 72:217–236. https://doi.org/10.1007/s00018-014-1736-7

57. Lee RJ, Cohen NA (2015) Role of the bitter taste receptor T2R38 in upper respiratory infection and chronic rhinosinusitis. Curr Opin Allergy Clin Immunol 15:14–20. https://doi.org/10.1097/ACI.0000000000000120

58. Shah AS, Yehuda BS, Moninger TO, et al (2009) Motile cilia of human airway epithelia are chemosensory. Science (80-) 325:1131–1134. https://doi.org/10.1126/science.1173869

59. Camoretti-Mercado B, Pauer SH, Yong HM, et al (2015) Pleiotropic Effects of Bitter Taste Receptors on [Ca2+]i Mobilization, Hyperpolarization, and Relaxation of Human Airway Smooth Muscle Cells. PLoS One 10:e0131582. https://doi.org/10.1371/journal.pone.0131582

60. Zhang C-H, Lifshitz LM, Uy KF, et al (2013) The Cellular and Molecular Basis of Bitter Tastant-Induced Bronchodilation. PLoS Biol 11:e1001501. https://doi.org/10.1371/journal.pbio.1001501

61. Tan X, Sanderson MJ (2014) Bitter tasting compounds dilate airways by inhibiting

airway smooth muscle calcium oscillations and calcium sensitivity. Br J Pharmacol 171:646–62. https://doi.org/10.1111/bph.12460

62. Upadhyaya JD, Singh N, Sikarwar AS, et al (2014) Dextromethorphan Mediated Bitter Taste Receptor Activation in the Pulmonary Circuit Causes Vasoconstriction. PLoS One 9:e110373. https://doi.org/10.1371/journal.pone.0110373

63. Manson ML, Säfholm J, Al-Ameri M, et al (2014) Bitter taste receptor agonists mediate relaxation of human and rodent vascular smooth muscle. Eur J Pharmacol 740:302–311. https://doi.org/10.1016/j.ejphar.2014.07.005

64. Lund TC, Kobs AJ, Kramer A, et al (2013) Bone Marrow Stromal and Vascular Smooth Muscle Cells Have Chemosensory Capacity via Bitter Taste Receptor Expression. PLoS One 8:e58945. https://doi.org/10.1371/journal.pone.0058945

65. Ansoleaga B, Garcia-Esparcia P, Llorens F, et al (2013) Dysregulation of brain olfactory and taste receptors in AD, PSP and CJD, and AD-related model. Neuroscience 248:369–382. https://doi.org/10.1016/j.neuroscience.2013.06.034

66. Singh N, Vrontakis M, Parkinson F, Chelikani P (2011) Functional bitter taste receptors are expressed in brain cells. Biochem Biophys Res Commun 406:146–151. https://doi.org/10.1016/j.bbrc.2011.02.016S0006-291X(11)00199-9 [pii]

67. Dehkordi O, Rose JE, Fatemi M, et al (2012) Neuronal expression of bitter taste receptors and downstream signaling molecules in the rat brainstem. Brain Res 1475:1–10. https://doi.org/10.1016/j.brainres.2012.07.038

68. Herrera Moro Chao D, Argmann C, Van Eijk M, et al (2016) Impact of obesity on taste receptor expression in extra-oral tissues: emphasis on hypothalamus and brainstem. Sci Rep 6:29094. https://doi.org/10.1038/srep29094

69. Wu SV, Rozengurt N, Yang M, et al (2002) Expression of bitter taste receptors of the T2R family in the gastrointestinal tract and enteroendocrine STC-1 cells. Proc Natl Acad Sci U S A 99:2392–7. https://doi.org/10.1073/pnas.042617699

70. Wu SV, Chen MC, Rozengurt E (2005) Genomic organization, expression, and function of bitter taste receptors (T2R) in mouse and rat. Physiol Genomics 22:693–702. https://doi.org/10.1152/physiolgenomics.00030.2005

71. Chen MC, Wu S, Reeve J, Rozengurt E (2006) Bitter stimuli induce Ca2+ signaling and CCK release in enteroendocrine STC-1 cells: role of L-type voltage-sensitive Ca2+ channels. AJP Cell Physiol 291:C726–C739. https://doi.org/10.1152/ajpcell.00003.2006

72. Jeon T-I, Zhu B, Larson JL, Osborne TF (2008) SREBP-2 regulates gut peptide secretion through intestinal bitter taste receptor signaling in mice. J Clin Invest 118:3693–700. https://doi.org/10.1172/JCI36461

73. Kok BP, Galmozzi A, Littlejohn NK, et al (2018) Intestinal bitter taste receptor activation alters hormone secretion and imparts metabolic benefits. Mol Metab 16:76–87. https://doi.org/10.1016/j.molmet.2018.07.013

74. Rozengurt E (2006) Taste receptors in the gastrointestinal tract. I. Bitter taste receptors and alpha-gustducin in the mammalian gut. Am J Physiol Gastrointest Liver Physiol 291:G171–G177. https://doi.org/10.1152/ajpgi.00073.2006

75. Rozengurt N, Wu SV, Chen MC, et al (2006) Colocalization of the alpha-subunit of gustducin with PYY and GLP-1 in L cells of human colon. Am J Physiol Gastrointest Liver Physiol 291:G792-802. https://doi.org/10.1152/ajpgi.00074.2006

76. Jang H-J, Kokrashvili Z, Theodorakis MJ, et al (2007) Gut-expressed gustducin and taste receptors regulate secretion of glucagon-like peptide-1. Proc Natl Acad Sci 104:15069–15074. https://doi.org/10.1073/pnas.0706890104

77. Lim W, Miller R, Park J, Park S (2014) Consumer sensory analysis of high flavonoid transgenic tomatoes. J Food Sci 79:S1212-7. https://doi.org/10.1111/1750-3841.12478

78. Kaji I, Karaki S, Fukami Y, et al (2009) Secretory effects of a luminal bitter tastant and expressions of bitter taste receptors, T2Rs, in the human and rat large intestine. Am J Physiol Gastrointest Liver Physiol 296:G971-81. https://doi.org/10.1152/ajpgi.90514.2008

79. Le Nevé B, Foltz M, Daniel H, Gouka R (2010) The steroid glycoside H.g.-12 from Hoodia gordonii activates the human bitter receptor TAS2R14 and induces CCK release from HuTu-80 cells. Am J Physiol Liver Physiol 299:G1368–G1375. https://doi.org/10.1152/ajpgi.00135.2010

80. Suh H-W, Lee K-B, Kim K-S, et al (2015) A bitter herbal medicine Gentiana scabra root extract stimulates glucagon-like peptide-1 secretion and regulates blood glucose in db/db mouse. J Ethnopharmacol 172:219–226. https://doi.org/10.1016/j.jep.2015.06.042

81. Prandi S, Bromke M, Hübner S, et al (2013) A subset of mouse colonic goblet cells expresses the bitter taste receptor Tas2r131. PLoS One 8:e82820. https://doi.org/10.1371/journal.pone.0082820

82. Jeon T-I, Seo Y-K, Osborne TF (2011) Gut bitter taste receptor signalling induces ABCB1 through a mechanism involving CCK. Biochem J 438:33–37. https://doi.org/10.1042/bj20110009

83. Foster SR, Blank K, See Hoe LE, et al (2014) Bitter taste receptor agonists elicit G-protein-dependent negative inotropy in the murine heart. FASEB J 28:4497–508. https://doi.org/10.1096/fj.14-256305

84. Wölfle U, Elsholz FA, Kersten A, et al (2015) Expression and functional activity of the bitter taste receptors TAS2R1 and TAS2R38 in human keratinocytes. Skin Pharmacol Physiol

28:137–46. https://doi.org/10.1159/000367631

85. Malki A, Fiedler J, Fricke K, et al (2015) Class I odorant receptors, TAS1R and TAS2R taste receptors, are markers for subpopulations of circulating leukocytes. J Leukoc Biol 97:533–545. https://doi.org/10.1189/jlb.2a0714-331rr

86. Gaida MM, Mayer C, Dapunt U, et al (2016) Expression of the bitter receptor T2R38 in pancreatic cancer: localization in lipid droplets and activation by a bacteria-derived quorum-sensing molecule. Oncotarget 7:12623–12632. https://doi.org/10.18632/oncotarget.7206

87. Wölfle U, Elsholz F, Kersten A, et al (2016) Expression and Functional Activity of the Human Bitter Taste Receptor TAS2R38 in Human Placental Tissues and JEG-3 Cells. Molecules 21:306. https://doi.org/10.3390/molecules21030306

88. Li F, Zhou M (2012) Depletion of bitter taste transduction leads to massive spermatid loss in transgenic mice. Mol Hum Reprod 18:289–297. https://doi.org/10.1093/molehr/gas005

89. Li F (2013) Taste perception: from the tongue to the testis. Mol Hum Reprod 19:349–360. https://doi.org/10.1093/molehr/gat009gat009 [pii]

90. Xu J, Cao J, Iguchi N, et al (2013) Functional characterization of bitter-taste receptors expressed in mammalian testis. Mol Hum Reprod 19:17–28. https://doi.org/10.1093/molehr/gas040

91. Voigt A, Hübner S, Lossow K, et al (2012) Genetic labeling of Tas1r1 and Tas2r131 taste receptor cells in mice. Chem Senses 37:897–911. https://doi.org/10.1093/chemse/bjs082

92. Soultanova A, Voigt A, Chubanov V, et al (2015) Cholinergic chemosensory cells of the thymic medulla express the bitter receptor Tas2r131. Int Immunopharmacol 29:143–147. https://doi.org/10.1016/j.intimp.2015.06.005

93. Clark AA, Dotson CD, Elson AET, et al (2015) TAS2R bitter taste receptors regulate thyroid function. FASEB J 29:164–172. https://doi.org/10.1096/fj.14-262246

94. Deckmann K, Filipski K, Krasteva-Christ G, et al (2014) Bitter triggers acetylcholine release from polymodal urethral chemosensory cells and bladder reflexes. Proc Natl Acad Sci U S A 111:8287–92. https://doi.org/10.1073/pnas.1402436111

95. Rajkumar P, Aisenberg WH, Acres OW, et al (2014) Identification and Characterization of Novel Renal Sensory Receptors. PLoS One 9:e111053. https://doi.org/10.1371/journal.pone.0111053

96. Liu X, Gu F, Jiang L, et al (2015) Expression of bitter taste receptor Tas2r105 in mouse kidney. Biochem Biophys Res Commun 458:733–738. https://doi.org/10.1016/j.bbrc.2015.01.089

Chapter 2

Introduction - Part B
Bitter receptors as mediators of the action of therapeutic bitter compounds

This chapter will be submitted for publication as a review article:
Duarte A.C., Costa A.R., Gonçalves I., Santos C.R.A. (2020), Bitter receptors as mediators of the action of therapeutic bitter compounds.

2.1. Introduction

Brain diseases are a major healthcare problem worldwide. The incidence of neuronal and neurodegenerative disorders including AD and PD as well as stroke is increasing along with the progressive aging of the population, despite many efforts to present valuable and permanent solutions in their prevention and treatment. Despite the great advances on the understanding of their pathophysiological mechanisms, effective therapies for CNS disorders such as neurodegenerative diseases (e.g. AD and PD), ischemic stroke or brain cancer (e.g. gliomas) are scarce. The complexity of these disorders partly justifies the failure of most therapies. On the other hand, the existence of brain barriers that hinder the drugs' access to the brain also plays an important role in limiting the efficacy of different therapies. There are two main brain barriers: the BBB formed by brain capillary endothelial cells, astrocytes' end-feet, pericytes, and neurons; and the BCSFB corresponding to CP epithelial cells, localized at the brain ventricles [1]. These barriers are constituted by tight junctions that limit the passage of molecules through the paracellular route, and by several membrane cell transporters that influx or efflux molecules, including nutrients, waste metabolites, toxins, xenobiotics, and small peptides (Fig. 2.1). Regarding brain drug delivery, ATP- binding cassette (ABC) transporters play a critical role at brain-barriers and are responsible for the efflux of many drugs out of the brain. Together, the BBB and the BCSFB regulate the molecular exchanges between the periphery and the CNS to maintain its homeostasis [2]. Additionally, when treating brain cancer and brain metastasis (such as non–small cell lung cancer (NSCLC), breast cancer, and melanoma), another interface must be considered: the blood-tumor barrier (BTB) [3]. This barrier is formed by brain tumor capillaries and although distinct from BBB, also display numerous efflux transporters that contribute to the chemoresistance phenomenon observed in the treatment of brain cancers or brain metastasis derived from primary tumors outside the CNS [4] (Figure 2.1).

Currently, drug delivery to the brain constitutes one of the main challenges in pharmacology, since many drugs fail to reach their therapeutic targets. Therefore, it is important to exploit the effects of new molecules in the CNS and evaluate their potential to reverse disease-associated cellular mechanisms as well as in counteracting the action of efflux mechanisms at blood-brain barriers and BTB.

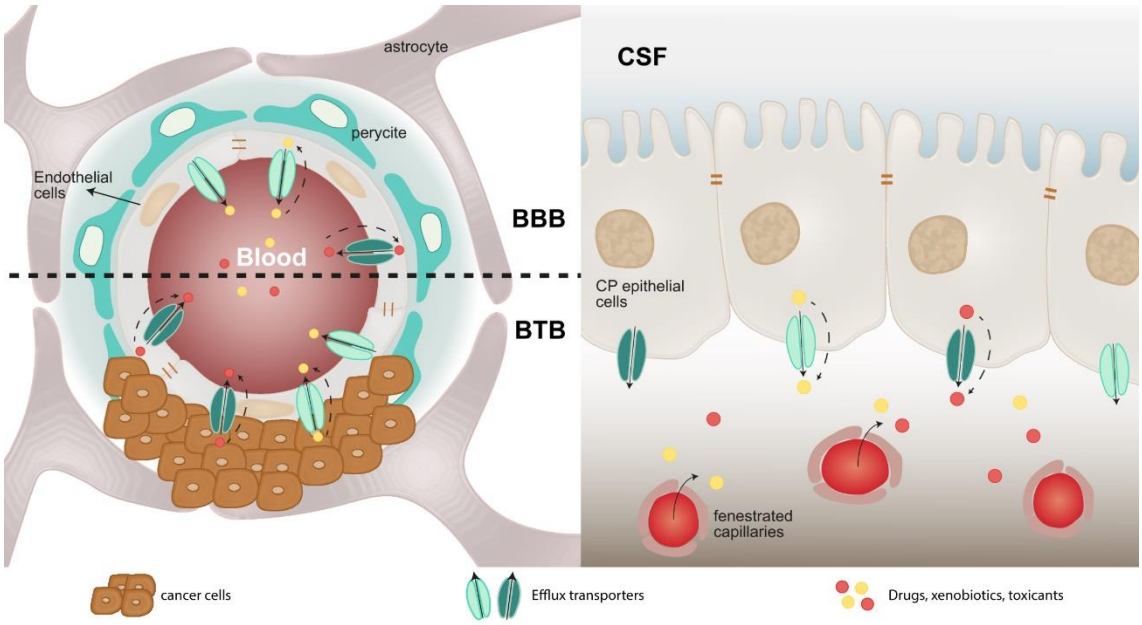

Figure 2. 1. Brain drug delivery is restrained by efflux mechanisms present at brain barriers and BTB. Brain endothelial cells and CP epithelial cells establish the main brain barriers, the BBB and the BCSFB, respectively. Brain endothelial cells surrounding brain tumors or metastasis display particular features that enhance tumor's chemoresistance and are designated BTB. Both endothelial, CP epithelial and cancer cells express multiple transporters that efflux drugs and other molecules impacting the treatment of many CNS disorders. BBB – blood-brain barrier; BTB – blood-tumor barrier; CP – choroid plexus.

2.2. Many therapeutic compounds taste bitter

Interestingly, 30% of bitter compounds of the BitterDB database [5] are also found in the DrugBank, and 66% of approved drugs are predicted to be bitter [6]. These data reinforce the therapeutic potential of bitter compounds.

Bitter molecules are chemically diverse, can be natural or synthetic, and include hydroxyl fatty acids, fatty acids, peptides, amino acids, amines, amides, azacycloalkanes, N-heterocyclic compounds, ureas, thioureas, carbamides, esters, lactones, carbonyl compounds, phenols, crown ethers, terpenoids, secoiridoids, alkaloids, glycosides, flavonoids, steroids, halogenated or acetylated sugars, and metal ions [7] (Figure 2.2). Although structurally diverse, bitter compounds are abundantly found as phenolic compounds or polyphenols, that can be subdivided in two major categories: flavonoids and nonflavonoids. Polyphenols belong to a vast group of plant-derived organic compounds, including fruits, vegetables, seeds, leaves, and roots, that have been associated to the prevention of chronic diseases [8]. Flavonoids can be further classified into six groups (flavones, isoflavones, flavanones, flavonols, flavanols and anthocyanidins), based on their chemical structure [8, 9] (Figure 2.2.). Flavones, such as apigenin and luteolin, are the most basic structure of flavonoids and are mostly found in herbs and spices. Isoflavones, also known as phytoestrogens, are present in soybeans,

soy derivates and herbs, and includes daidzein and genistein. Flavonols, such as quercetin and kaempferol, are the most abundant flavonoids in fruits and vegetables and present high antioxidant activity. Flavanones are less abundant flavonoids and are mainly found in citrus fruits such as naringenin. In turn, flavanols are the most abundant flavonoids in nature and can be found in several plant-based products as green tea, cocoa, cereals, vegetables and fruits. Major flavanols are epicatechin, epigallocatechin gallate and procyanidin C2. Anthocyanidins, such as cyanidin, can be found in berry-type fruits and other coloured fruits and vegetables [8, 9]. A major nonflavonoid compound is the stilbene trans-resveratrol, mainly found in the skin of red wine grapes, but also in other grapes and berries, peanuts, and pistachio (Figure 2.2.). Besides polyphenols, bitter compounds can also be found in other natural classes such as alkaloids (e.g. caffeine, papaverine, and noscapine), terpenoids (e.g. curcubitacins), saponins (e.g. amarogentin), amino acids, and peptides [10]. There is also a great variety of synthetic bitter compounds, and many of these are used in therapeutics. This is the case of the antimalaria drug chloroquine, the immunosuppressive agent azathioprine, the antibiotic dapsone or the antipsychotic haloperidol [11]. Table 2.1. summarizes the classes and sources of some of the most studied bitter compounds that present potential application in the treatment of brain disorders.

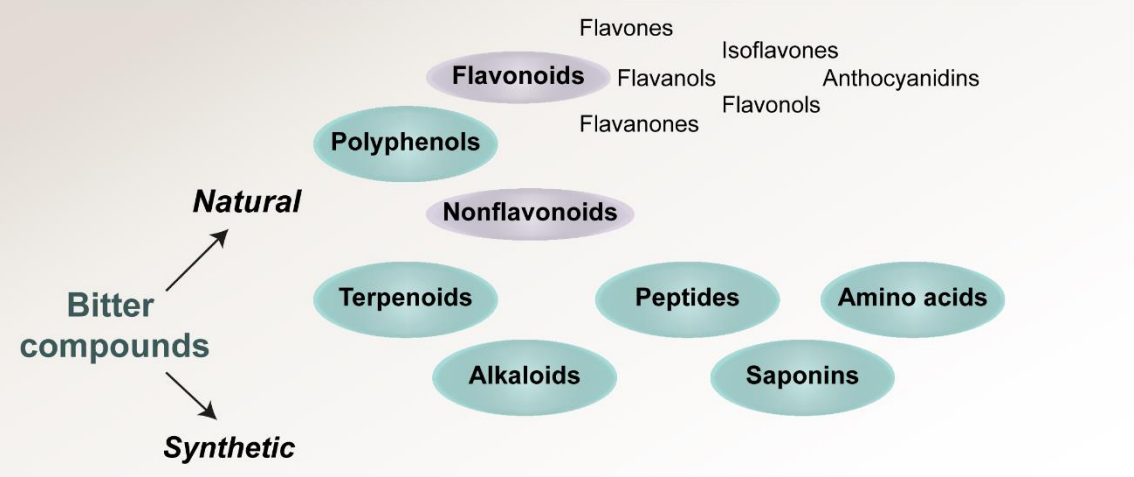

Figure 2. 2. Classes of bitter compounds. Bitter compounds can be divided in natural and synthetic. Additionally, natural bitter compounds comprise several families namely, polyphenols, terpenoids, alkaloids, peptides, saponins and amino acids.

Table 2. 1. Bitter ligands, sources and cognate TR2.

Bitter ligand	**Class**	**Sources**	**TR2**	**Refs**
Arborescin	Guaianolide sesquiterpene lactone	Artemisia gorgonum (Asteraceae)	1, 4, 10, 14, 43, 46	[12]
Azathioprine	Thiopurine	Synthetic	4, 10, 14, 46	[14]
Brucine	Alkaloid	Dried seed of Strychnosnux-vomica L. Loganiaceae	4, 46	[10]
Dapsone	Sulfone	Synthetic	4, 10, 40	[15]
Epicatechin	Flavanol	Woody plants, green tea	4, 5, 39	[16]
Epigallocatechin gallate	Flavan	Green and black tea	14, 39	
Eriodictyol	Flavanone	Eriodictyon californicum	14, 39	[17]
Genistein	Isoflavone	Soy derivates	14, 39	[18]
Haloperidol	Butyrophenone	Synthetic	10, 14	[19]
Liquiritigenin	Flavanone	Radix glycyrrhiza	14, 39	[20] [13]
Luteolin	Flavone	Vegetables and fruits	14, 39	[21]
Naringenin	Flavonone	Vegetables, citrus fruits, nuts, coffee and tea	14, 39	[22]
Noscapine	Phthalide-isoquinoline alkaloid	Papaver somniferum	14	[23]
Papaverine	Isoquinoline alkaloid	Papaver somniferum L	7, 10, 14	[24]
Parthenolide	Sesquiterpene lactone	Tanacetum parthenium	1, 4, 8, 10, 14, 44, 46	[25]
Procyanidin C2	Proanthocyanidin	Apple, cocoa, grapes, and berries	5	[8]
Quercetin	Flavonol	Fruits, vegetables, spices, herbs and cereal grains	14	[26]
Resveratrol	Polyphenol, stilbene	Grapes, berries, peanuts and red wine	14, 39	[27]
Kaempferol	Flavonol	Seeds, leaves, fruits, flowers, and vegetables	14, 39	[28]

2.3. Therapeutic effects of bitter compounds

2.3.1. Neuroprotection

The typical hallmarks observed in these CNS diseases include increased oxidative stress and inflammation, protein misfolding, and cell death [29, 30]. Thus, therapeutic approaches based on drugs that can prevent and/or reverse these events present a great therapeutic potential. Interestingly, there are several bitter compounds with neuroactive effects by modulating multiple molecular targets, as already demonstrated *in vitro* and *in vivo* (Table 2.2.).

In AD, Aβ deposition and consequent plaque formation in the brain is correlated with increased oxidative stress, cell death, and cognitive decline. Notably, many bitter compounds have shown to counteract these events (Table 2.2.). Epigallocatechin gallate, genistein, naringenin, quercetin and resveratrol contributed to the degradation of Aβ and hyperphosphorylation of tau proteins in several studies [31–37]. Moreover, several reports showed the ability of bitter compounds to ameliorate cognitive impairment and improve the behavioural performance in mice and rat disease models [31, 33–36, 38–41]. Furthermore, these compounds can also mediate a decrease in cell apoptosis (inhibiting caspase-3 activation and reducing Bax/Bcl-2 ratio) [32, 39, 42, 43], inflammation [44, 45], and oxidative stress by regulating the expression and activity of inflammatory markers (TNF-α, IL-1β, iNOS) and antioxidant enzymes (SOD, GSH, catalase (CAT)) [43, 45]. Similarly, in PD, other bitter compounds showed beneficial effects; epigallocatechin gallate improved behavioural deficits, reduced oxidative stress, and increased dopamine levels in a mouse model of PD [46]; naringenin administration *in vivo* also reduced oxidative stress, inflammation, and cell apoptosis [47, 48].

Stroke or cerebral ischemia causes a lesion and a reduction in the blood flow, triggering multiple correlated events such as energy failure, loss of cell-ion homeostasis, acidosis, increased intracellular calcium levels, excitotoxicity, oxidative stress, BBB disruption, and activation of glial cells [49]. Flavonoids such as epigallocatechin gallate, eriodictyol, and kaempferol as well as nonflavonoid resveratrol decreased infarct volume in stroke models [50–56]. Moreover, dapsone, an antibiotic usually used in leprosy and dermatological disorders [15], also decreased the damaged area and improved the neurological deficits [57]. Additionally, this compound downregulated the expression of the nuclear factor erythroid 2-related factor (Nrf2) in neurons and glial cells leading to decreased oxidative stress. Since stroke compromises oxygen and blood supply, angiogenesis is a critical process for recovery. Interestingly, both epigallocatechin gallate [50] and resveratrol [58] induced angiogenesis in the damaged area.

Table 2. 2. Neuroprotective effects of bitter compounds.

Bitter agonist	Biological activity	Experimental model	Ref
Dapsone	Promoted functional recovery: ↑ neurological deficits; ↑ Fractional anisotropy values; ↓ Tissue damage; ↓ Nrf2 expression in neurons and glial cells; ↓ Oxidative stress.	Wistar Han cerebral ischemia rat model (MCA occlusion)	[57]
	Protected brain microvascular integrity; ↓ Body weight; ↓ Serum oxLDL; ↑ ZO-1 and occludin expression. ↑ LC-3 II.	C57BL/6J High Fat Diet mouse model	[59]
	Inhibited LDL oxidation; ↑ ZO-1, occludin, claudin-5; ↓ Intracellular oxLDL; Attenuated lysosome dysfunction; Activated autophagy; Reversed LAMP1 aggregation in cytoplasm; ↓ ZO-1 destruction.	Brain capillaries HBMEC	
	Attenuated spatial learning and memory impairment; Inhibited autophagy: ↑ LC3B-II/LC3B-I and Beclin 1, and ↓ p62.	Sprague Dawley rats treated with propofol	[60]
Epigallocatechin gallate	Ameliorated cognitive impairment; ↓ Aβ plaques formation.	Sprague–Dawley cognitive impairment rat model	[31]
	Prevented Aβ1-42-induced toxicity; ↑ Cell viability and ↓ cell apoptosis; ↓ Endoplasmatic reticulum stress-induced cytotoxicity: GRP78, CHOP, cleaved-caspase-12.	SH-SY5Y (Aβ1-42-induced neuronal apoptosis)	[32]
	↓ neuronal apoptosis: ↓ cleaved-caspase-3; Downregulated ER stress associated-proteins: GRP78, CHOP, and cleaved-caspase-12.	APP/PS1 transgenic mice model	
	↓ Neprilysin expression via ERK and PI3K activation; ↑ Neprilysin release into extracellular space; ↑ Aβ degradation.	Rat cortical astrocytes	[61]
	Improved behavioural deficits; ↓ Oxidative stress; ↑ Dopamine levels; Regulated iron-proteins expression: ↑ ferroportin.	C57 mouse model of Parkinson Disease (MPTP-induced)	[61]

Improved neurological function; ↓ infarct volume; Promoted angiogenesis: ↑ nº of Ki67/CD31-positive vessels, Nrf2, VEGF, and VEGFR2 expression; ↓ Oxidative stress: ↓ GRP78, CHOP, cleaved-caspase-12.	C57BL/6 cerebral ischemia mouse model (MCA occlusion)	[50]
Prevented mitochondrial impairment of complex I and ATP synthase (complex V) activities; ↑ Cell proliferation; Restored mitochondrial biogenesis: ↑ PGC-1α, nuclear respiratory factor 1 (NRF-1) and mitochondrial transcription factor A (T-FAM); Activated AMPK: ↑ p-AMPK/AMPK ratio.	Ts65Dn mice neural progenitor cells (Down syndrome model)	[62]
↓ Lipid accumulation; ↓ Inflammation: TNF-α, IL-6, and IL-1β; ↓ Microglial activation; ↓ Phosphorylation of JAK2 and STAT3.	BV-2	[63]
↓ Body weight, lipid deposition, and epididymal adipocytes sizes; ↓ Inflammation: TNF-α, IL-6, and IL-1β; ↓ Phosphorylation of JAK2 and STAT3.	C57BL/6J High Fat Diet mouse model	
↑ NEP activity in blood, cortex and hippocampus; Improved memory; ↑ Nº of dendritic spines in the hippocampal CA1 area.	Wistar Han prenatal hypoxia rat model	[64]
Ameliorated obesity and ↓ lipid deposition; Enhanced Brown adipose tissue thermogenesis; ↓ Inflammation: TNF-α, IL-6, and IL-1β; ↓ p-NF-κB and p-STAT3; ↓ Microglial activation.	C57BL/6J High Fat Diet mouse model	[65]
Ameliorated the corticosterone-induced neuronal injuries (nuclear shrinkage, pyknosis fragmentation, and appearance of apoptotic bodies); ↑ Cell viability; ↑ ERK1/2 and PI3K/AKT phosphorylation; ↑ PGC-1α; ↑ ATP production.	Rat primary hippocampal neurons (corticosterone-induced neurotoxicity)	[66]
Improved behavioural performance; Restored glucocorticoid, dopamine and serotonin plasma levels; ↑ PKCα and ERK1/2 expression and phosphorylation; ↑ ATP production.	Wistar Han psychological stress rat model	[67]
↑ Cell viability; ↓ LDH release; ↓ ROS levels and MDA expression; ↓ Cell apoptosis: ↓ Bax and ↑ Bcl-2;	HBMEC (ADMA-induced injury)	[68]

	↓ pERK1/2 and p-38.		
	↑ Cell survival; ↓ Cell apoptosis (↓ activated caspase-3); ↑ Nº type-2b/3 cells and immature neurons.	Balb/C mice	[69]
	Induced neuronal differentiation; ↑ pAkt in hippocampus.	Adherent hippocampal neural precursor cells	
Eriodictyol	Attenuated $A\beta_{25-35}$ cytotoxicity; ↓ JNK/p38 signaling pathway activation; ↑ Nrf2 protein levels leading to ARE pathway activation	Primary cultures of cortical neurons	[70]
	Prevented neuronal death; ↓ Infarct area; Improved neurological and memory; ↓ TNF-α, iNOS and GFAP expression.	Cerebral ischemia mice model	[51]
	Prevented memory and neuronal damage; ↓ $A\beta_{1-42}$ formation; Suppressed AChE and ↑ ChAT activity; Suppressed LPS-induced glial overactivation; Inhibited NF-κB and MAPK pathways.	C57BL/6J mice - LPS induced inflammation	[71]
Genistein	Activated autophagy; Contributed to complete degradation of Aβ and hyperphosphorylated tau protein; Corrected AD associated behaviour.	AD rat model	[33]
	Attenuate spatial recognition, discrimination, and memory deficits; ↓ MDA (malondialdehyde); ↑ SOD and CAT activity and GSH levels; ↓ AChE activity; ↓ IL-6, NF-κB p65, TLR4, TNFα, COX2, iNOS, GFAP; ↑ Nrf2.	LPS-induced cognitive deficits Wistar rats	[72]
Liquiritigenin	Improved behavioral performance; Inhibited AChE and thiobarbituric acid reactive substance activities in the hippocampus; ↑ BDNF protein level, ERK phosphorylation and CREB in the hippocampus.	Scopolamine-induced cognitive deficits CD-1 mice	[20]
Luteolin	Improved spatial learning and memory; ↑ CA1 pyramidal layer thickness.	Streptozotocin-induced AD rat model	[38]
	Improved locomotor function; ↑ Neuron survival; ↓ Cell apoptosis; Suppressed oxidative stress (↓ MDA and XO, ↑ SOD and GSH-Px); Suppressed inflammatory response (↓TNF-α, IL-1β, and IL-18); ↑ Nrf2 levels and ↓ nod-like receptor pyrin domain containing 3 protein expression.	Spinal cord injury rat model	[73]

	Restored cell viability; ↓ ROS levels; Prevented cell apoptosis (↑ Ser112 phosphorylation of Bad and ↓ pro-caspase 3 cleavage); ↑ HO-1 protein expression; Induced MAPKs activation (ERK, p38, JNK, Akt).	Primary cultured rat cortical cells (H_2O_2 induced-oxidative stress)	[74]
Naringenin	↓ Cell apoptosis; ↓ Caspase-3; ↑ PI3K/AKT and estrogen receptor.	PC12 (Aβ25-35-induced AD)	[42]
	↑ Spatial learning and memory; ↓ Aβ plaques and Tau hyper-phosphorylation.	Cortical neurons (Aβ1-42 and Aβ25-35 induced AD)	[34]
	↓ MDA; ↓ Cell apoptosis; ↑ Estrogen receptor; ↑ Spatial memory and cognition.	Wistar rats (Aβ25-35-induced AD)	[39]
	↑ GRx and CAT; ↓ Lipid peroxidation and iNOS; ↓ Nuclear pigmentation and cytoplasmic vacuolation.	C57BL/6 mice (PD model, MPTP-induced)	[47]
	↓ α-synuclein; ↑ Dopamine transporter, DOPAC, HVA and TH; ↓ TNFα and IL-1β; ↑ SOD.	C57BL/6 mice (PD model, MPTP-induced)	[48]
	↓ ROS and MDA; ↑ SOD, GSH; ↓ Caspase-3, Bax and ↑ Bcl-2, AMP, ADP, ATP, ANT, Nrf2, HO-1 and NQO1.	Neurons (hypoxia-induced ischemic stroke)	[43]
	↓ Th1, Th9, Th17; ↑ Treg; ↓ T-bet, PU.1, and RORγt.	C57BL/6 mice ((MOG)35-55-induced EAE)	[75]
	↓ IFNγ, STAT1, STAT3, STAT4, IL-6; ↑ gp-130; ↓ Foxp3.	C57BL/6 mice (EAE induced by anti-CD3/CD28)	[76]
	↓ T cells proliferation, IFN-γ, IL-17A, TNF-α and IL-6; Blocked T cells at G0/G1 phase; ↑ P27; ↓ Retinoblastoma protein phosphorylation, IL-2, CD25 and STAT5.	Mouse T cells (EAE induced by anti-CD3/CD28 and (MOG)35-55	[77]
	↓ TLR4, NF-κB, TNF-α, COX2 and iNOS; ↑ Nrf2, SOD, CAT, and GSH; ↓ MDA and AChE; ↓ GFAP; ↑ Spatial recognition memory, discrimination ratio and retention and recall capability.	Albino Wistar rats (cognitive deficit LPS-induced)	[78]

	↑ SIRT1; ↓ NF-κB; ↑ Serotonin, noradrenaline, dopamine and TH.	Sprague-Dawley rats (cognitive deficit age-induced)	[79]
	↓ Bad, caspase-3 and Bax; ↑ Bcl-2, Bcl-xL; ↓ TUNEL; ↑ PI3K/Akt; ↓ PTEN, NF-κB, TNF-α, IL -6 and IL-1β; Improved of cognitive dysfunction.	Sprague-Dawley rats (cognitive deficit isoflurane-induced)	[80]
	↓ iNOS and COX-2; ↑SOCS3, AMPKα and PKCδ.	BV2 (LPS-induced neuroinflammation)	[81]
	↓JNK, ERK, p38, MAPK, TNF-α, IL-1β; ↑ Arg-1 and IL-10.	BV2 (LPS-induced neuroinflammation)	[82]
	↑ BDNF and GDNF; ↑ Nrf2; ↑ Dopaminergic neurons survival.	Primary rat midbrain neuron-glia co-cultures	[83]
	↑ Mitochondrial complex I- IV activities; ↓ Lesions /10kb; ↑ GSH and GST; ↓ MDA and protein carbonyl; ↑ Spatial and recognition memory.	Swiss Albino mice	[84]
Papaverine	↓ TNF-α and IL-1β by cAMP/PKA signaling pathway; ↓ pMEK and pERK;	Retina primary microglia-LPS-induced microglial activation	[85]
	↓ IL1β and TNFα expression; Modulated phenotype alterations: ↓ Il1rn, Socs3, Nos2 and Ptgs2 transcription, ↑ Arg1 and Mrc1 transcription; ↓ p-IKK expression and inhibited the nuclear translocation of P65.	BV2- LPS-induced microglial activation	[24]
Quercetin	Reversed β-amyloidosis and tauopathy; ↓ Astrogliosis and microgliosis; Enhanced memory and learning.	3Tg-AD mouse model	[35]
	↓ eIF2a phosphorylation and ATF4 expression through GADD34 induction in the brain; Improved memory in aged mice and delayed memory deterioration at the early stage of AD.	APP23 mice with human APP751 complementary DNA with a Swedish double mutation on the C57BL/6 genetic background	[40]
	↓ Neuronal cell apoptosis; ↑ Bcl-2, Bcl-xL and survivin, and ↓ cleaved caspase-3; ↓ ROS; Upregulated pBad and pAKT.	Sprague Dawley rats (Brain Ischemic Injury model, four-vessel occlusion -induced)	[86]
	Enhanced docosahexaenoic acid antioxidant and anti-inflammatory effects: ↓ NO and ROS production;	BV2 (LPS-induced neuroinflammation)	[87]

	↑ Nrf2 and HO-1 expression; ↓ TNFα expression; ↓ Phospho-cytosolic phospholipase A2 and lipid peroxidation product 4-hydroxynonenal.		
	Antidepressant activity by inhibiting NMDA receptors; ↑ NO synthesis and antioxidant activity.	Female Swiss Albino mice (Olfactory bulbectomy)	[88]
	↓ Total cholesterol and HDL decrease; ↓ ROS and MDA level; Ameliorated cognitive impairment by modulating PI3 K/AKT/Nrf2 pathway and activating CREB pathway.	Male Chinese Kunming mice (High fat diet induced-neurotoxicity)	[89]
	Attenuated ROS mediated oxidative stress and mitochondrial DNA oxidation; ↑ MnSOD activity; Prevented cytochrome-c translocation; ↑ Bcl-2 and ↓ Bax, p53 and caspase-3; ↓ DNA damage.	Male albino rats (Aluminium induced-neurotoxicity)	[90]
Resveratrol	Improved memory and cognitive function; ↓ Anxiety; ↓ Aβ and p-tau pathology in the hippocampus (↑ NEP and ↓ BACE1); ↑ AMPK and activated SIRT1 pathway.	3xTg-AD mouse model	[36]
	Improved learning and memory functions; ↑ AMPK and PGC-1; ↓ NF-κB / IL-1β / NLRP3 in hippocampus and prefrontal cortex.	Mouse model of AD (induced-$A\beta_{1-42}$)	[41]
	↓ MMP9 and ↑ IL-4 and FGF-2 in CSF; ↑ MMP10 and ↓ IL-12P40, IL12P70 and RANTES in plasma; ↓ Aβ40 in plasma and in CSF.	People with mild or moderate AD	[37]
	Preserved BBB integrity; ↓ MMP-9 in CSF.	People with mild or moderate AD	[91]
	↓ Cell death: ↓ caspase-3; Promoted mitophagy: ↑ Nº of acidic vesicular organelle, LC3-II/LC3-I ratio, Parkin and Beclin-1 expression, and LC3 and TOMM20 co-localization; ↓ Neuronal oxidative damage; ↑ ΔΨm, ATP, T-SOD and CAT levels.	PC12 ($A\beta_{1-42}$ -induced neurotoxicity)	[92]
	Reverted $A\beta_{1-42}$ -induced neurotoxicity via AMPK signaling: ↑ Cell viability; ↓ Inflammation: ↓ TNF-α, IL-1β, iNOS and COX-2; ↓ Inhibitory kappa B kinases (IKKα and IKKβ); ↓ NF-κB expression and nuclear translocation; ↓ Oxidative stress: ↑ SOD-1, NRF2, Gpx1, CAT, GSH and HO-1.	Human neuronal stem cells ($A\beta_{1-42}$ -induced neurotoxicity)	[45]
	Improved memory function;	ICR mice model of AD ($A\beta_{1-42}$ -injected)	[44]

↓ PDE4A5, 4B1 and 4D3 expression; ↑ BDNF, pCREB, PKA; ↑ BCl-2 and ↓ Bax; ↓ IL-1β and IL-6.		
Improved locomotor activity, muscle strength and coordination; ↓ Haematoma volume and damage area; Via adenosine A1 receptor?	Sprague–Dawley rat stroke model (collagenase-induced intracerebral haemorrhage)	[53]
↑ Cell viability and ↓ Caspase-3 and -9 activity via AMPK signaling; ↑ AMPK and p-AMPK; ↑ Bcl-2 and CREB; Restored mitochondrial activity; ↑ PGC1α, NRF-1 and Tfam.	SH-SY5Y (OGD stroke model)	[93]
Attenuated neurological deficits and cerebral edema; ↓ Neuronal death; ↓ Haematoma volume; ↓ IL-1β.	CD1 mice stroke model (collagenase-induced intracerebral haemorrhage)	[54]
↓ Activated NLRP3 inflammasome, caspase-1, IL-1β and IL-18; ↓ Cerebral infarct volume and brain water content; Improved neurological scores.	Sprague-Dawley rat (MCAO- induced cerebral ischemic)	[55]
↓ Neuronal deficits and infarct volume; ↑ p-AMPK and SIRT1; ↓ PDEs and ↑ ATP and cAMP.	Sprague–Dawley rats (MCAO- induced cerebral ischemic)	[56]
Enhanced angiogenesis and neurogenesis (post-acute treatment); ↑ GDNF and VEGF.	C57BL6 mice (MCAO- induced cerebral ischemic)	[58]
Attenuated cognitive impairment; ↓ Inflammation: ↓ TNF-α, IL-6 and ↑ IL-4 and -10; Modulated PPARγ/NF-κB signaling: ↑ PPARγ and p65, ↓ p-p65 and p-IKBα; ↑ $GABA_AR$, NMDAR1, BNDF, TrKB and CaMKII, and ↓ p-CaMKII;	C57/BL6J mice cognitive impairment model (chemotherapy-induced)	[94]
↓ Cell apoptosis; ↓ Inflammation: ↓ IL-1β, CCL2 and CCL3; Modulated several miRNAs expression targeting pathways related to the pathophysiology of bacterial meningitis (e.g. FOXO and Thyroid hormone signaling pathways).	Infant Wistar Han rat model of pneumococcal meningitis	[95]
Prevented learning and memory deficits; ↓ PPARγ and ↑ p16 expression in hippocampus.	C57BL/6J mice (High fat diet induced-cognitive deficits)	[96]
↑ Cell viability; ↑ ERK1/2 activation.	SH-SY5Y (dopamine induced cell death)	[97]
Inhibited age-dependent motor function decline; ↑ ERK1/2 activation.	C57BL/6 mice (dopamine induced cell death)	

	↓ REST expression via SIRT1 and c-Jun signaling; ↓ Neuronal death.	SH-SY5Y and rat cortical neurons (PCB-95-induced neurotoxicity)	[98]
Kaempferol	↓ Cerebral infarct volume and neurological score; ↓ Brain injury and cell apoptosis; ↓ Inflammation: ↓ TNF-α, IL-6 and IL-1β in serum and brain; ↓ Oxidative stress: ↑ SOD and GSH, and ↓ MDA in serum and brain; Upregulated pAkt and Nrf-2; Downregulated p-GSK-3b, NF-kB and p-NF-kB.	Sprague-Dawley cerebral ischemia rat model (MCA occlusion)	[52]
	Improved short and long –term memory; ↓ Inflammation: ↓ TNF-α, IL-6 and NF-κB p65; ↓ Cell apoptosis: ↓ p53, PARP1 and FOXO-2, and ↑ Bcl-2; ↓ Oxidative stress: ↑ MnSOD and GSH; ↑ SIRT1 nuclear activity and levels and inhibited PARP1.	Wistar Han rats ($CdCl_2$-induced neurotoxicity model)	[99]
	↓ Neuronal damage; ↓ Iba-1 expression; ↓ Inflammation: ↓ IL- 1β, IL-6, TNF-α, MCP-1, COX-2 and iNOS; Protected BBB integrity: ↑ occludin-1, claudin-1 and CX43; ↓ HMGB1 level; Suppressed TLR4/MyD88 inflammatory pathway.	BALB/c mice LPS-induced neuroinflammation	[100]
	↓ Neuronal death in the CA3 region of hippocampus; Improved spatial learning and memory; ↓ Oxidative stress in hippocampus: ↑ GPx, CAT and SOD; ↑ Trkβ and GluA2 expression.	Sprague-Dawley hypoxia rat model	[101]
	↑ Trkβ expression; ↓ pE47; ↓ cell neurodegeneration.	Primary hippocampal cell cultures	
	Improved striatal neuron injury; ↑ TH and PSD95 levels in striatum; ↓ Inflammation: ↓ TNF-α, IL-6, IL-1β, MCP-1, ICAM-1 and COX-2; Protected BBB integrity; Suppressed HMGB1/TLR4 inflammatory pathway activation.	BALB/c mice LPS-induced neuroinflammation	[102]

2.3.2. Anti-cancer effects

Despite cancer in general present several hurdles for current therapies to enhance life expectancy of patients, brain cancer is probably the most challenging due to its unique anatomy and physiology. Brain tumor's therapy usually comprises radiotherapy, chemotherapy and surgery. However, chemoresistance often limits the entrance of drugs into the brain and depending on the tumor localization, surgery might not be an option [103]. Gliomas are the most common malignant primary brain tumors and comprise astrocytomas, oligodendrogliomas, and ependymomas (reviewed in [104]). Glioblastoma, an astrocytoma of grade IV, is the most prevalent and aggressive primary brain tumor and is associated with a poor prognosis and low life expectancy (reviewed in [104]). Besides primary brain tumors, brain metastasis with outer-CNS origin, such as lung, breast and colorectal cancers, melanoma or renal cell carcinoma contribute for the higher mortality associated to brain cancer [103]. Therefore, strategies for increasing survival rates and to develop more efficient therapies require a further understanding of the effects of potential therapeutic agents to counteract molecular and cellular events observed in cancer cells. These include abnormal cell proliferation, deregulation of apoptotic pathways, upregulation of inflammatory cytokines, mitochondrial dysfunction, increased angiogenesis and dysregulation of extracellular matrix dynamics. In the last years, a growing body of evidence show that many bitter compounds display anti-tumoral activity in brain cancer as well as in systemic cancer either *in vitro* and in *in vivo* models (Table 2.3).

Like in neuroprotection, the flavonoids family is among the more studied regarding anti-cancer effects, but it is not the only one. Actually, many other compounds such as the immunosuppressive azathioprine, the alkaloids brucine, noscapine and papaverine, the sulfone dapsone and the lactone parthenolide showed anti-proliferative, anti-invasiveness, pro-apoptotic, anti-angiogenic and anti-metastasis effects in different types of cancer (Table 2.3). In particular, parthenolide has been the focus of many studies showing anti-tumoral effects in various systemic cancers that metastise to the brain, such as colorectal [105, 106] and lung cancers [107–109] (Table 3.). Additionally, parthenolide effects comprises the induction of apoptosis through cell cycle arrest and/or by increasing expression of p53 and activating caspase-3, -9 and PARP (Poly (ADP-ribose) polymerase) and downregulating anti-apoptotic proteins including Bcl-2 and Bcl-xL [107, 109–113]. Moreover, parthenolide inhibited angiogenesis [107, 108] and epithelial-mesenchymal transition (EMT) [108, 109, 114] processes, thus suppressing cancer cells growth, proliferation, and invasiveness abilities. Similarly, several flavonoids are among the most promising anti-cancer compounds. Anti-tumoral effects of these have been

reported in several types of cancer including glioblastoma. Grube and colleagues showed that epigallocatechin gallate, at achievable CNS concentrations, induced cell stress in primary glioblastoma cells, activating autophagic cellular response through increasing ROS levels [115]. Moreover, combination of epigallocatechin gallate and temozolomide sensitized glioblastoma cells to temozolomide effects resulting in decreased cell viability. In another study, epigallocatechin gallate inhibited O6-methylguanine (O6-meG) DNA-methyltransferase (MGMT) expression via WNT/β-catenin pathway which reversed the resistance to temozolomide of GBM-XD and T98G cells [116]. Conversely, in non-tumor glial cells, epigallocatechin gallate enhanced MGMT expression, showing specific anti-tumoral effect. More recently, human U251 glioblastoma cells treated with epigallocatechin gallate showed increased cell senescence related to telomerase activity inhibition [117]. Other flavonoid, luteolin inhibited EGF-induced glioblastoma U87 and U252 cells proliferation and induced apoptosis by arresting cell cycle at S and G2/M phases and increasing cleaved caspase-3 and PARP [118]. Moreover, luteolin inhibited the phosphorylation of proteins that participate in Akt and MAPK pathways. Quercetin and sodium butyrate combination was tested in rat C6 and human T98G glioblastoma cells. This combination had a synergetic effect in inhibiting protective autophagy by downregulating Beclin-1 and LC3B II, thus inducing cell apoptosis [119]. Although, genistein, kaempferol and naringenin effects in glioblastoma were not analysed, these are very interesting flavonoids in the frame of glioblastoma considering their anti-tumoral properties already reported in other types of cancer (Table 2.3). On the other hand, resveratrol has been extensively analysed in different cancers including glioblastoma (Table 2.3). A recent study showed *in vitro* and *in vivo* that resveratrol reverses TGF-β1 induced EMT via Smad signaling, upregulating E-cadherin and downregulating N-cadherin, vimentin, β-catenin, Twistl1, Snail and Slug. Moreover, resveratrol inhibited cell migration, invasion and stem-cell like properties of glioblastoma cells [120].

Table 2. 3. Anti-tumoral activity of bitter compounds.

Bitter agonist	Biological activity	Experimental model	Ref
Azathioprine	↓ Proliferation of resistant cancer cells.	A2780 and A2780-cisplatin-resistant	[121]
	Autophagy activation; ↑ Cell apoptosis; ↓ ΔΨm; ↑ ROS production.	HT29 and HCT116	[122]
	↓ Vav1-dependent invasive cell migration and matrix degradation; ↓ Rac and Cdc42 signaling; ↓ Metastasis.	Pancreatic cancer cell lines Xenograft and genetic mouse models of pancreatic cancer	[123]
Brucine	↓ Cell proliferation, migration and invasion; ↑ Cell apoptosis; ↓ Angiogenesis and vasculogenic mimicry tube formation; F-actin cytoskeleton and microtubule structure disruption; Downregulation of EPHA1, MMP-9, MMP-2.	MDA-MB-231	[124]
	↓ Cell growth and ↑ cell apoptosis; Activated Wnt/β-catenin signaling pathway.	SW480, DLD1 and LoVo	[125]
	↓ Tumor volume and weight.	DLD1-bearing nude mice	
	↓ Tumor incidence; Restoration of biochemical markers levels.	Rat model of chemically induced mammary carcinogenesis	[125]
	↓ Cell proliferation, migration and colony formation; ↑ Cell apoptosis; ↓ MMP2, MMP3 and MMP expression; Inhibited Wnt/β-catenin signaling pathway.	LoVo	[126]
	↓ Tumor growth.	Male immune-deficient BABL/C nude mice	
	↓ Cell migration, invasion, adhesion; ↑ E-cadherin and β-catenin; ↓ Vimentin and fibronectin; ↓ MMP-2 and MMP-9.	MDA-MB-231 and Hs578-T	[127]
	↓ RANKL-induced migration of MDA-MB-231 cells; ↓ TRAP (tartrate resistant acid phosphatase) activity; ↓ Osteoclastogenesis of RAW264.7 cells; ↓ RANKL-induced bone resorption; ↓ RANKL-induced TGF-β1, NF-κB and Hes1 expression; ↓ RANKL-induced Notch1 and Jagged1 protein levels.	RANKL-induced osteoclastogenesis model (co-cultures of r MDA-MB-231 and RAW264.7)	[128]

	↑ OPG/RANKL expression ratio; ↓ Differentiation and bone resorption function of osteoclasts; Expression and secretion of OPG and RANKL regulation in osteoblast cells.	Breast cancer bone metastasis model (co-culture of MDA-MB-231 and MC3T3-E1 cells)	[128]
	↓ Cell viability; ↓ Anchorage-independent growth; ↓ Cell migration.	MCF-7	[128]
	↓ BCL-2 and COX-2 expression; ↑ BAX expression; ↓ Cell survival rate; ↓ Growth of xenograft tumors.	U251 human glioma cell Nude mice tumor xenograft model	[129]
Dapsone	↑ Anti-proliferative activity; ↓ Anchorage-independent growth; ↓ Clonogenic survival; ↓ Cell migration; ↑ Anti-glioma activity against different pro-neoplastic features.	Primary cultured glioma cells	[130]
Epicatechin	↓ Cell viability and ↑ cell apoptosis; Induced cell cycle arrest; MMP dissipation; Inhibited FASN enzymes expression; ↓ Fatty acid levels; ↑ ROS production.	HepG2	[131]
Epigallocatechin gallate	↓ Cell growth; Induced cell cycle arrest in G2/M phase; ↑ Cell apoptosis via the mitochondrial pathway; ↓ Cell migration, invasion, and adhesion; ↓ MMP-2/9 activity; Inhibited the activation of lipid raft-associated EGFR; Prevented EGFR dimerization and activation; Inhibited MEK/ERK1/2 and PI3K/AKT signaling pathways activation; ↓ Proteins involved cell survival regulation.	Caco-2, HCT-116, SW-480, HT-29, and LoVo	[132]
	Improved serum liver markers including ALT, AST, and total bilirubin; ↓ Tumor formation; ↓ Expression of genes associated with high cancer risk; Inhibited fibrosis progression; Inactivated of hepatic stellate cells; Induced senescence-associated secretory phenotype.	Male Wistar rats with induced hepatocellular carcinoma	[133]

Inhibition of tumor sphere formation; Inhibition of ALDH1A1 and SNAI2 (Slug) expression; AXL receptor tyrosine kinase highly expression.	Cancer stem cells (H1299-sdCSCs) obtained from tumor spheres of H1299 human lung cancer cells	[134]
DNA damage; ↑ Phosphorylation of γ-H2AX histone and micronuclei; ↑ Telomere-shortening-induced senescence; ↑ Telomere-independent genotoxicity.	U251	[117]
↓ Cell growth, migration and invasion; "Cadherin switch" prevention; ↓ Expression level of TCF8/ZEB1, β-Catenin, and Vimentin; Inhibited Akt pathway; Suppressed IGFR phosphorylation; Induced Akt degradation.	Panc-1, MIA PaCa-2, BxPC-3, HPAF-II, CFPAC-1, and Su.86.86	[135]
↓ Cell viability; Induced cell cycle arrest in G1 phase; ↑ Caspase-3 and -7 activity; ↑ Cell apoptosis.	HSC-3 (oral squamous cell carcinoma) cells	[136]
↓ Tumor size; ↓ Proliferation: ↓ Ki-67 expression.	Mice tumor xenografts	
↓ Cell viability and ↑ cell apoptosis; Induced cell cycle arrest in G2/M phase; ↑ PARP, pro-caspase-3 and pro-caspase-9 protein levels.	MCF-7	[137]
Tumor growth suppression; Downregulation of proteins associated with apoptosis; ↓ Proliferation: ↓ Ki-67 expression.	Female CB-17 severe combined immunodeficient mice	
Suppressed EMT, invasion and migration; Inhibited TGF-β1-induced expression of EMT markers (↓ E-cadherin and ↑ vimentin); Blocked Smad2/3 phosphorylation and Smad4 translocation.	8505C	[138]
Radiosensitized cells through miR-34a/Sirt1/p53 signaling pathway; ↑ Cell apoptosis: ↓Bcl-2 and ↑ Bax and caspase-3 expression.	H22	[139]
Inhibited tumorspheres; ↓ Stem cell markers; ↓ Proliferation-associated proteins expression; ↑ Cell apoptosis.	Bladder cancer stem cells	[140]
↑ Cell apoptosis; DNA damage; ↓ GRP78 expression; Activated NF-κB; ↓ ABCB1 gene expression and blocked drug efflux; ↑ Caspase-3 and PARP activation and Bad, and ↓ Bcl-2.	HCT-116 and DLD1	[141]

↓ Cell viability and proliferation; Anticarcinogenic effect.	MCF-7 and MDA-MB-23	[142]
Inhibited PGE2 and EP1-selective agonist induced migration; ↑ Bax/Bcl-2; ↓ Cell viability.	HepG2	[143]
↓ Cell growth; ↑ Cell apoptosis: ↑ caspase -3, -8 and -9 activation; Induced autophagy; Regulated several apoptosis-related genes; Induced mitochondrial depolarization; Modulated autophagy-related proteins Beclin1, ATG5 and LC3B levels; Inhibited glycolytic enzymes (HK, PFK, LDH and PK) activities and mRNA levels; ↓ HIF1α and GLUT1 expression.	4T1	[144]
↓ Tumor weight; ↓ Glucose and lactic acid levels; ↓ VEGF expression.	Balb/c mice injected subcutaneously with 4T1 cells	
↓ Cell proliferation and survival; ↑ Cell apoptosis (NB4 cells); Induced cell cycle arrest in G0/G1 phase; ↑ ATM, HMGA2, pATM levels, and SA-β-galactosidase staining; Cellular senescence; Beneficial epigenetic modulation.	NB4 and K562	[145]
↓ MGMT mRNA and protein expression; Reversed TMZ resistance via the WNT/β-catenin pathway; Prevented β-catenin translocation into the nucleus; ↓ TCF1 and LEF1 transcription factors.	GBM-XD and T98G (MGMT-positive GBM)	[116]
↑ MGMT expression.	GliaX	
↓ Cell growth; Induced cell cycle arrest at G1 and G2 phases; ↓ Cyclin E and D1; ↑ p21.	HCT116	[146]
↑ Accumulation of autophagic vacuoles; ↑ ROS production; Sensitized cells to temozolomide.	Primary human GBM cell culture	[115]
↓ Cell proliferation and ↑ cell apoptosis; ↓ p-PI3K and p-Akt.	H1299	[147]
↓ Cell proliferation and ↑ cell apoptosis; ↑ Bcl-2 and, ↓ BAX, BAK1 and cytochrome C.	U266	[148]
↓ Cell proliferation and ↑ cell apoptosis; ↑ Caspase-3 positive cells;	Jurkat cells	[149]

↑ Fas expression.		
↑ Chromosomal instability; ↑ Cell apoptosis; Inhibited of cell division.	COLO205	[150]
↓ Cell viability and cell apoptosis; Induced cell cycle arrest; MMP dissipation; Inhibited FASN enzymes expression; ↓ Fatty acid levels; ↑ ROS production.	HepG2	[131]
↓ Solid tumors; Inhibited carcinogenesis; ↓ Nº of precancerous lesions; ↓ Tumor load; Histological progression delay.	Colon carcinogenesis mouse model	[151]
↑ Cell death and ↓ Cell viability; ↑ ROS production; Induced cell cycle arrest; Induced autophagy;	Primary effusion lymphoma cells	[152]
↓ ΔΨm; ↑ ROS production; Changes in nuclear morphology; ↓ Cell viability; ↓ Phosphorylation of several proteins involved in cell proliferation and survival.	A-431 and SK-BR-3	[153]
↓ Cell proliferation, invasion and migration; Induced cell cycle arrest in G0/G1 phase.	RKO	[154]
↓ Cell viability and invasion; ↑ Cell apoptosis; ↑ TFPI-2 expression.	T24	[155]
Inhibited cell growth; ↑ Cell apoptosis: ↓ Bcl-2, and ↑ Bax and Caspase-3 protein expression; ↓ ABCG2 expression and ↑ adriamycin uptake.	Eca109 and Ec9706	[156]
↓ Cell viability; ↓ β-catenin, pAkt and cyclin D1; Inactivated β-catenin signaling pathway;	MDA-MB-231	[157]
↑ PTEN, Caspase-3 and -9; ↓ Akt; ↑ Bax/Bcl-2 ratio; ↓ hTERT.	T47D	[158]
Inhibited spheroid formation;	Colorectal cancer stem cells	[159]

	↓ Cell proliferation and ↑ cell apoptosis; ↓ Wnt/β-catenin pathway activation.		
	↓ ERα protein levels; ↓ Cell viability.	T-47D	[160]
	↓ Cell proliferation and ↑ cell apoptosis; ↓ EGFR expression; ↓ Erk 1/2 and Mek phosphorylation; ↓ Bcl-2 and ↑ Bax; Inhibited P90 RSK mRNA expression.	SACC-83	[161]
	↓ Cell proliferation, migration and invasion; ↑ Cell apoptosis: ↑ activated caspases-3, -8 and -9, Bax, and PARP, and ↓ Bcl-2.	SW780	[162]
	↓ Tumor volume and weight; ↓ NF-κB and MMP-9 mRNA and protein expression.	Mice bearing SW780 tumors	
	↓ Tumor cells activity; Inhibited tumorsphere formation; ↓ Cancer stem cells markers; ↓ Cell proliferation and ↑ cell apoptosis; ↓ Wnt/β-catenin activation.	A549 and H1299	[163]
	↑ Cell apoptosis; Suppressed β-catenin signaling;	Head and neck cancer patients	[164]
	↓ mRNA and transcriptional activity of β-catenin in p53 wild-type KB cells; Enhanced β-catenin ubiquitination and proteasomal degradation.	KB and FaDu	
	↓ Cell proliferation and ↑ cell apoptosis; ↓ p-β-catenin (Ser552), p-GSK3β(S9) and β-catenin target genes; ↓ Tumor growth in vivo;	SGC-7901	[165]
	↓ Cell proliferation and growth; ↑ pERK1/2 p-p38.	BeWo, JEG-3, and JAR	[166]
	↓ Cell proliferation and ↑ cell apoptosis; Induced autophagy; ↑ Caspase -3 and -9 activity; ↑ Bax, cleaved caspase-3 and -9, Atg5, Atg7, Atg12, Beclin-1, and LC3B-II; ↓ Bcl-2, pAKT (Ser473) and pSTAT3 (Tyr705); ↓ ABCB1 mRNA and protein.	CAR (cisplatin-resistant oral cancer cells)	[167]
	↑ pERK1/2, pJNK1/2 and p38α, p38γ and p38δ, and pAkt levels; Inhibited Akt, ERK1/2 or alternative p38MAPK activity.	HT-29	[168]
Genistein	Induced cell morphological changes; ↓ Total viable cells; Induced G2/M phase arrest and cell apoptosis; ↑ ROS and Ca2+ production; ↓ ΔΨm levels;	HL-60	[18]

	↑ IRE-1α, Calpain 1, GRP78, GADD153, caspase-3, -4, -7 and -9, ATF-6α, Bax and PARP-cleavage; ↓ Bcl-2 and Bid.		
	↓ Tumor weight; ↑ ATF-6α, GRP78, Bax, Bad, and Bak.	BALB/c nu/nu mice	
	Induced cell cycle arrest in G2/M phase; ↓ Cyclin A and B1; ↑ p21WAF1/CIP1 and Cdk; Induced cell apoptosis: ↑ Caspases -3, -8 and -9, and PARP activation, cytosolic release of cytochrome c, and ↑ Bax/Bcl-2 ratio; ↓ Mitochondria integrity; Inactivated PI3K/Akt signaling pathway; ↑ ROS accumulation.	T24	[169]
	↓ Tumor incidence; ↓ Nº and size of tumors; ↓ MDA, NF-κB and Bcl-2 expression; ↑ Nrf2, HO-1 and Bax expression; ↓ mTOR pathway (↓ mTOR, p70S6K1, and 4E-BP1 phosphorylation).	Laying hens ovarian cancer model	[170]
	↓ Cell viability; Inhibited EGFR and AKT activation; Altered MAPK pathway (↓ p-p38, ↑ p-ERK1/2); ↓ IL-6; Induced iNOS; ↓ p-ERα (Ser118) ERβ protein and ERα mRNA levels.	HuCCA-1 and RMCCA-1	[171]
	Inhibited cell growth; ↑ Cell apoptosis: ↑ caspase-3/9 activation; Activated miR-27a expression levels; ↓ MET protein expression;	A549	[172]
	↓ CIP2A and E2F1; ↓ Cell growth and ↑ cell apoptosis;	MCF-7-C3 and T47D	[173]
	↓ Cell proliferation and ↑ cell apoptosis; ↓ Akt, SGK1 and miR-95 mRNA expression; ↓ pAkt.	HCT-116	[174]
	↓ Tumor growth.	Mouse xenograft tumor	
Haloperidol	Inversely associated with gastric cancer risk.	Gastric cancer patients	[175]
	↑ Erastin- and sorafenib-induced cell death; ↑ S1R protein; ↑ Oxidative stress; ↑ Cellular levels of Fe2+ (ferroptosis – cell death); ↑ GSH and lipid peroxidation.	HepG2 and Huh-7	[176]

	↓ Cell proliferation; ↑ Endoplasmic reticulum stress; ↑ Cell Apoptosis.	Pancreatic ductal adenocarcinoma samples	[177]
	↓ Cell migration; ↓ Final tumor size and metastasis.	Mice orthotopic xenograft tumors	
Kaempferol	↓ Cell proliferation and ↑ cell apoptosis; ↓ DHT-induced androgen receptors activation; ↓ Downstream targets of androgen receptors (PSA, TMPRSS2, and TMEPA1); ↓ PSA protein levels; ↓ Androgen receptor protein expression and nuclear accumulation; Suppressed vasculogenic mimicry of PC-3 cells.	LNCaP and PC-3	[178]
	↓ IQGAP3 expression ↓ Cell proliferation and ↑ cell apoptosis; ↓ p-ERK1/2 and Bcl2, and ↑ Bax.	ZR-75-30 and BT474	[179]
	↓ Cell proliferation; Induced cell cycle arrest in G2/M phases; Induced cell apoptosis and DNA damage; ↑ Expression levels of γH2AX, cleaved caspase -3 and -9, and p-ATM.	MDA-MB-231	[180]
	Induced selective cytotoxicity; ↓ ΔΨm; Mitochondrial swelling; Induced cell apoptosis and ROS production; ↑ Release of cytochrome c, ↑ caspase-3 activation.	DEN- and 2-AAF-induced hepatocellular carcinoma in rats	[181]
	Induced cell cycle arrest in G2/M phase; Stimulated the extrinsic apoptosis via death receptors/FADD/Caspase-8 pathway; ↑ p53.	A2780/CP70	[182]
	↓ Cell viability; ↑ SubG1 population; ↓ Akt, BCL2, ABCB1, and ABCC1 genes; ↑ Cell apoptosis; ↑ Caspase-3 protein and mRNA; ↑ Bax/Bcl-2 ratio; Inhibited multidrug resistance.	HL-60 and NB4	[183]
	↓ Cell migration and invasion; ↓ RhoA expression and Rac1 activation; Blocked PKC/MAPK/activator protein-1AP-1 cascade; ↓ MMPs expression and activity.	MDA-MB-231 and MDA-MB-453	[184]
	↓ Cell viability Inhibited telomerase and PI3K/AKT signaling pathway;	HeLa	[185]

	Induced cell apoptosis via p53 and Bax/Bcl-2.		
	↑ Cell apoptosis; ↑ DR4, DR5, CHOP, JNK, ERK1/2, p38; ↑ Caspase-3, -8, -9 and Bax; ↓ Bcl-xL, Bcl-2, survivin, XIAP and c-FLIP.	OVCAR-3 and SKOV-3	[186]
	Promoted DNA methylation; ↓ DNMT3B levels; Promoted Ub proteasome degradation.	Nude mice bearing bladder cancer	[187]
	↓ Cell proliferation and clonal formation; Induced cell cycle arrest in G0/G1 phase; Inhibited tumor glycolysis; ↑ Cell apoptosis: ↑ Bax, caspase-3 and ↓ Bcl-2.	KYSE150 and Eca109	[188]
	Induced morphological changes: smaller nuclei with chromatin condensation and perinuclear apoptotic bodies; ↓ Cell growth; ↑ Cell apoptosis: ↑ PARP cleavage and ↓ Bcl-2.	MCF-7	[189]
	↓ Cell viability and ↑ cell apoptosis; ↑ LDH activity; ↑ GRP78, GRP94, PERK, IRE1α, partial ATF6 cleavage, caspase-4, CHOP and cleaved caspase-3.	HepG2	[190]
	↓ Bcl-2 and ↑ Bax, Fas, cleaved caspase-3, -8, -9, and PARP; ↓ pAKT, TIMP2 and MMP2.	HCCC9810 and QBC939	[191]
	↓ Volume of subcutaneous xenograft.	Xenograft model	
	↓ Nº and volume of metastasis foci; ↓ Ki-67-positive cells.	Lung metastasis model	
	↓ Cell viability and ↑ cell apoptosis; ↓ Migratory activity; Inhibited EGFR related Src, ERK1/2, and AKT pathways.	Miapaca-2, Panc-1, and SNU-213	[192]
	Inhibited TGF-β1-induced EMT; Inhibited cell migration; ↑ E-cadherin; Suppressed mesenchymal markers; ↑ TGF-β1-mediated matrix MMP-2 activity.	A549	[193]
	↓ Cell growth and viability; Inhibited DNA repair protein expression; ↑ DNA damage and condensation; ↓ Protein expression associated with DNA repair system: p-ATM, p-ATR, 14-3-3σ, DNA-PK, MGMT, p53 and MDC1; ↑ p-p53 and p-H2AX.	HL-60	[194]
Luteolin	↓ S100A7 expression by supressing Src/Stat3 signaling;	A431-III	[195]

↓ p-Src, p-Stat3 and p-S100A7; ↓ Cell migration and invasion; ↑ E-cadherin and ↓Twist;		
↓ Cell proliferation; Induced cell cycle arrest in S and G2/M phases; ↓ pAkt, p-mTOR, p-p70S6K and p-MAPK; ↑ Cell apoptosis: ↑ caspase and PARP cleavages, and ↓ Bcl-xL.	U87 and U251	[118]
↓ RPS19 expression; Blocked Akt/mTOR/c-Myc signaling pathway.	A431-III	[196]
↓ Cell proliferation, migration, invasion and adhesion; Inhibited tube-forming potential; Suppressed EMT (↑ E-cadherin, ↓ N-cadherin and vimentin); ↓ p-Akt, HIF-1α, VEGF-A, p-VEGFR-2, MMP-2, and MMP-9 protein levels.	A375 and B16-F10	[197]
Induced PARP cleavage and nuclear fragmentation; ↑ Fas and FasL expression; ↑ Caspases-8 and -3 activation; ↑ Histone H3 acetylation; Activated the c-Jun signaling pathway.	HL-60	[198]
↓ Cell viability; Induced cell cycle arrest in G0/G1 phases; ↑ Cell apoptosis: ↑ caspase-8 and ↓ Bcl-2; ↑ Nº of intracellular autophagosomes; Promoted LC3B-I conversion to LC3B-II; ↑ Beclin 1 expression.	SMMC-7721	[199]
↑ Cell apoptosis: ↑ caspase-3 and -9, cytochrome c and Bax/Bcl-2 ratio; Suppressed PI3K (↓ p-PI3K, p-AKT and p-mTOR) and MAPK (↓ p-ERK1/2) pathways; ↑ Dual-specifcity phosphatases 1, 2, 4 and 5 and ↓ chemokine C-X-C motif ligand 16.	BGC-823	[200]
Inhibited STAT6 phosphorylation; ↓ IL-4 enhanced secretion of CCL2; ↓ IL-4 enhanced migration of monocytes; ↓ Migration of Lewis lung carcinoma cells in a CCL2-dependent manner.	RAW 264.7	[201]
↓ Cell viability and ↑ cell apoptosis; ↓ ΔΨm levels; ↓ SREBP1 and SREBP2 mRNA and SREBP1 protein expression; Inhibited PI3K/AKT/mTOR/SREBP cascade.	JAR and JEG-3	[202]
↓ Cell proliferation; ↑ Cell apoptosis (↑ activated caspase-3 and -9, ↓ Bcl-2/Bax ratio); ↑ pERK, pMEK, pAkt; ↓ Cell migration and EMT (↑ E-cadherin and ↓ N-cadherin) through MEK-ERK pathway.	A549	[203]
↓ Cell proliferation and ↑ cell apoptosis;	Hs578T, MDA-MB-231 and MCF-7	[204]

	Induced cell cycle arrest at S and G2/M phases in Hs578T and MDA-MB-231 cells, and at S phase in MCF-7 cells; ↓ Cyclin B and D1; ↑ FOXO3a expression through PI3K and PKB/Akt inhibition; ↑ FOXO3a target genes: p21 and p27; ↑ Activated PARP and cytochrome c.		
	↓ Cell viability, migration and invasion; ↓ Tube formation; Inhibited Notch signalling: ↓ Notch-1, Hes-1, Hey, VEGF, Cyclin D1 and MMP expression; Regulated miRNAs associated with tumor suppression: ↑ miR-34a, miR-181a, miR-139-5p, miR-224 and miR-246 and ↓ miR-155.	MDA-MB-231 and MCF-7	[205]
Naringenin	Induced cell cycle arrest in G0/G1 and G2/M phase; ↑ p53; ↑Cell apoptosis: nuclei damage, ↑ Bax/Bcl-2 ratio, cytochrome C release, ↑ caspase-3 activation.	HepG2	[206]
	↓ Cell growth and ↑ Cell death.; ↑ pAMPK; ↓ Cyclin D1.	E0771	[207]
	Delayed tumor growth.	OVX C57BL/6 mice injected with E0771 cells	[208]
	↓ Cell proliferation and migration; ↑ Cell apoptosis and ROS production; ↓ ΔΨm and ↑ Bax/Bcl-2 ratio (PC3 cells); ↓ ERK1/2, P70S6K, S6, and P38 phosphorylation (PC3 cells); ↓ ERK1/2, P53, P38, and JNK phosphorylation (LNCaP cells); ↑ pAkt.	PC3 and LNCaP	
	↑ Cell apoptosis; ↓ Prdx-1 (peroxiredoxin-1) expression; ↑ ROS levels; ↑ ASK1 (apoptosis signal-regulation kinase 1), JNK, p38 and p53 expression.	SNU-213	[209]
	↓ TGF-β1 secretion and intracellular accumulation; Inhibited TGF-β1 transport from the trans-Golgi network; ↓ PKC activity.	Balb/c mice inoculated with breast carcinoma T1-Luc2 cells	[210]
	↓ Cell proliferation; ↓ Lipid peroxidation, TNF-α, IL-6 and IL-1β; ↑ SOD, CAT, GPx, GR, GST; ↓ CYP1A1, PCNA and NF-κB expression.	Swiss albino mice (benzo(a)pyrene (B[a]P)-induced lung carcinogenesis)	[211]
	Inhibited HER2 (human epidermal growth factor receptor-2)-TK (Tyrosine Kinase) activity; ↓ Cell proliferation;	SKBR3 and MDA-MB-231	[212]

	↑ Cell apoptosis: ↓ ΔΨm, ↑ condensed cromatin, and ↑ activated caspase-3 and -8.		
	Inhibited cell growth by arresting cell cycle at S and G2/M phases; ↑ Cell apoptosis; ↓ Cdk4, Cdk6, Cdk7, Bcl2, x-IAP and c-IAP-2 expression; ↑ p18, p19, p21, caspase-3, -7, -8 and -9, Bak, AIF and Bax expression; ↓ PI3K, pAkt, pIκBα and NFκBp65; Enhanced the sensitivity of cancer cells to DNA-acting drugs.	SW1116 and SW837, HTB26 and HTB132	[213]
Noscapine	↓ Cell viability; ↑ Cell apoptosis: ↓ Bcl-xL expression and ↑ caspase-3 activation (dependent of TAS2R14 expression).	SKOV3	[214]
	↓ Cell viability (dependent of TAS2R14 expression).	Du145 and PC3	
	↓ Cell proliferation; Enhanced cisplatin effects: ↓ Cell proliferation and arrest cell cycle at G2/M phase; ↑ Cell apoptosis (↓ XIAP, survivin and NF-kB, ↑ caspase-3 expression).	SKOV3/DDP	[215]
	Enhanced cisplatin effects: ↓ Tumor growth; ↑ Cell apoptosis: ↓ XIAP, survivin and NF-kB, and ↑ caspase-3 expression.	Nude mice SKOV3/DDP-xenografted tumor	
Papaverine	Inhibited RAGE-dependent nuclear factor κ-B activation; ↓ Cell proliferation, migration and invasion by suppressing RAGE.	HT1080	[216]
Parthenolide	Inhibited deubiquitinating enzyme ubiquitin-specific peptidase 7; Inhibited Wnt signalling, partly by destabilizing β-catenin; ↓ Cell proliferation and ↑ cell apoptosis.	HCT116, SW480, SW620, Caco-2 and HT-29 (colorectal carcinoma) and HEK293T cells	[105]
	Attenuated TGF-β1-induced elongated, fibroblast-like shape changing in cells; Inhibited TGF-β1-induced cell migration and invasion; ↓ β-catenin, Vimentin, Snail, and Slug, and ↑ E-cadherin.	HT-29 and SW480	[114]
	Attenuated H_2O_2-induced growth inhibition and morphological changes; ↓ ROS; Protected cells from H_2O_2-induced apoptosis; Suppressed ↓ ΔΨm; Restored autophagy flux and mitophagy; Inhibited mitochondrial marker protein TIM23 degradation; ↑ LC3-II expression; ↓ Mitochondria DNA; Prevented H_2O_2-induced lysosomes damage.	C2C12 myoblasts	[217]
	↓ Cell growth; ↓ RANKL stimulated osteoclast formation; ↓ Adhesion and spreading of osteoclast precursors and survival of mature osteoclasts;	LNCaP, PC3, DU145, Mat-Ly-Lu and RM1-BT, and C4-2B4	[218]

Inhibit NFκB activation.		
↓ Cell viability and migration, and ↑ cell apoptosis; ↑ Autophagocytic proteins LC3-II and beclin-1; Inhibited mTOR/PI3K/AKT; Inhibited the growth of the mouse xenograft tumors.	MDA-T32	[219]
Inhibited lung cancer cells ↓ Proliferation stimulating effect of nicotine; ↑ Cell apoptosis; VEGF-inhibiting effects ↓ Bcl-2, and ↑ E2F1, P53, GADD45, Bax, BIM, and caspase-3, -7,- 8, -9; Activation of P53- dependent apoptosis;	A549 and H526	[107]
Prevented tumor formation; ↓ Severity of histopathological changes; Restored detoxification enzymes, lipid peroxidation, and antioxidants ↓ p53 and Bcl-2, and ↑ Bax.	DMBA-induced hamster buccal pouch carcinogenesis	[110]
↑ Cell apoptosis; Induced cell cycle arrest in G1 phase; ↑ Bax, p53, cleaved caspase-3 and -9, and ↓ Bcl-2 and Bcl-xL; ↓ Cyclin D1; ↑ Cyclin-dependent kinase inhibitor 1 expression; Inhibited STAT3 activation; ↓ Cell migration and invasion.	SGC-7901/DDP	[111]
Suppressed Elongation factor1-α and vimentin.	MCF7	[220]
↓ Nrf2 expression; ↓ CAT, MnSOD, HSP70 and Bcl-2 levels; ↑ ROS; Chemoresistance prevention.	MDA-MB231	[106]
Inhibited HIF-1α activity; ↓ Angiogenesis by preventing NF-κB activation; ↓ Protein levels associated with glucose metabolism, angiogenesis, development and survival that are regulated by HIF-1α; Protected the morphological change from EMT state; Inhibited MMP activity; ↓ Cell motility involved in the regulation of the hypoxia-induced EMT markers;	HT-29, DLD-1 and HCT116	[108]
↓ CRC xenograft growth; Regulated NF-κB, HIF-1α and EMT specific marker.	Nude mouse tumor xenograft model	
↓ Cell viability and ↑ cell apoptosis; ↓ Cell proliferation and invasion; Suppressed cell response via targeting on B-Raf and inhibiting MAPK/Erk pathway; ↓ Protein and mRNA expression of c-Myc;	GLC-82	[221]

	Inhibited STAT3 activity.		
	↓ Cell proliferation and ↑ cell apoptosis; Prevented cell migration and invasion; Suppressed migration/invasion-related protein expression: E-cadherin, β-catenin, vimentin, Snail, COX-2, MMP-2, MMP-9; ↓ Bcl-2 and Bcl-xL and ↑ activated caspase-3.	SW620	[109]
	↓ Cell growth and ↑ cell apoptosis; ↑ Autophagy; ↑ p62/SQSTM1, Beclin 1, and LC3II.	Panc-1 and BxPC3	[109]
	Mitochondrial-mediated apoptosis and autophagy; ↑ Caspase-3 activation, Bax, Beclin-1, ATG5 and ATG3; ↓ Bcl-2 and mTOR; Inhibited PI3K and Akt; Activated PTEN; ↑ ROS production and ↓ ΔΨm.	HeLa	[112]
	↑ Autophagy and mitophagy; ↑ PINK1 and Parkin translocation to mitochondria; ↑ Autophagy proteins; ↑ ROS.	Saos-2 and MG-63	[222]
	↑ Cytotoxicity; Nuclear disruption and DNA fragmentation; ↑ Cell apoptosis; Induced cell cycle arrest;	A375	[223]
	Attenuated ubiquitinated Nemo. ↑ IκB-α expression; ↓ p65 levels in nucleus; ↓ NF-κB activity; ↓ Cell proliferation and ↑ cell apoptosis; Induced cell cycle arrest; ↓ Levels of ubiquitinated TRAF6 and total proteins.	RPMI 8226	[113]
	↑ Cell apoptosis: ↑ nuclear fragmentation, caspase- 3, -8 and PARP cleavage, Bim; Induced cytosolic Bim translocation into the mitochondria; Induction of DR5 protein expression.	MC-3 and HN22	[224]
	Tumor size and volume shrinking; ↑ Cell apoptosis by increasing Bim and death receptor 5.	Nude mouse tumor xenografts	
Procyanidin trimer (C1 and C2)	↓ Cell viability and ↑ cell apoptosis; ↑ DNA damage and cell cycle arrest; ↑ Bax, caspase-3 and -9, and ↓ Bcl-2.	MDA-MB-231 and MCF-7	[225]

	↓ Cell viability.	Caco-2, HCT15, HT29, HCT116, SW480 and LoVo	[226]
	Anticancer efficacy by inducing G1 arrest and autophagy; ↓ Akt/mammalian target of the (mTOR) pathway; ↑ ERK1/2 pathway.	A459 and H460	[227]
Quercetin	↓ Tumor incidence and volume; Suppressed DNA damage and induced DNA repair; ↓ ROS levels; ↓ Lipid and protein peroxidation (↓ MDA and protein carbonyl); ↑ CAT, SOD, GPx, GR, and GST expression and activity; ↑ NQO-1 and HO-1 expression. Modulated NRF2/Keap1 signaling (↑ NRF2 and ↓ Keap1).	Wistar Han colorectal cancer model (dimethylhydrazine-induced)	[228]
	↓ Cell proliferation, migration and invasion by ↓ MALAT1; ↑ Cell apoptosis: ↑ Bax/Bcl-2.	PC-3	[229]
	Inhibited tumor growth, EMT process and PI3K/Akt signaling pathway via ↓ MALAT1: ↓ Tumor weight and volume; ↓ Ki67 expression; ↑ E-cadherin and ↓ N-cadherin; ↓ pAkt.	PC-3 xenograft mice model	
	↓ Cell viability; ↑ Cell apoptosis: ↓ Bcl-2 and Bcl-xL, ↑ caspase-3, -9, Bid, Bad, Bax and cytochrome c.	PA-1	[230]
	↓ S100A7 expression through Src/Stat3 signaling; ↓ p-Src, p-Stat3 and p-S100A7; ↓ Cell migration and invasion; ↑ E-cadherin and ↓Twist;	A431-III	[195]
	Enhanced sodium butyrate effects: Inhibited autophagy and ↓ Beclin-1 and LC3B II expression; ↑ Cell apoptosis: morphological alterations (membrane blebbing, nuclear fragmentation and chromatin condensation), ↓ Bcl-2, survivin, PARP and ↑ Bax and caspase-3.	Rat C6 and human T98G	[119]
	↓ Cell viability and proliferation; ↑ Cell apoptosis: chromatin condensation, ↑ Bax, pJNK, p-p38 and pERK1/2, cleaved PARP and ↓ Bcl-2.	A375SM	[231]
	↓ Tumor volume; ↑ Apoptosis; ↑ pJNK and p-p38.	A375SM melanoma tumor xenograft	
	Enhanced cisplatin effects: ↑ Cell apoptosis by down-regulating NF-κB; ↓ pAkt and pIKKβ, NF-κB and xIAP. ↓ PARP and ↑ Caspase-8 and -9 activation.	Tca-8113 and SCC-15	[232]

Enhanced cisplatin effects: ↓ Tumor weight and growth.	Tca-8113 xenograft mice model	
↓ Cell viability; ↓ Cell adhesion, invasion and migration; ↓ MMP-2 and -9, ↑ and -2; ↓ PTHR1 mRNA expression.	U2OS and Saos^{-2}	[233]
↓ Cell proliferation and stem cells spheroid formation; Inhibited PI3K/Akt and MAPK/ERK pathways.	Prostate CSCs, PC3 and LNCap	[234]
↓ Cell proliferation and ↑ cell apoptosis; Induced cell cycle arrest at G1 phase; Inhibited CSCs proliferation, clone formation, and mammosphere generation through PI3K/Akt/mTOR signaling; ↓ m-TOR, p-m-TOR, PI3K, p-PI3K, Akt, p-Akt, ERα, CyclinD1 and Bcl-2 and ↑ Bax.	MCF-7 and breast cancer stem cells ($CD44^+/CD24^-$)	[235]
Inhibited tumor growth and metastatic ability of CSCs.	$CD44^+/CD24^-$ CSCs xenograft mice model	
↓ IL-18 secretion; ↓ AIM2 and pro-caspase-1 expression; ↓ p-JAK2 and p-STAT1; Inhibited nuclear translocation of p-STAT1.	IFN-γ-primed human keratinocytes treated with poly (dA:dT)	[236]
↓ Cell proliferation, migration and invasion; ↓ MMP-2, MMP-9 and VEGF expression; Inhibited glycolysis, ↓ glucose uptake and lactic acid production; Induced autophagy via Akt-mTOR.	MCF-7 and MDA-MB-231	[237]
↓ Tumor growth and metastasis; ↓ VEGF; Inhibited glycolysis; Induced autophagy by inhibiting p-Akt/Akt.	MCF-7 xenograft mice model	
↓ RPS19 expression; Blocked Akt/mTOR/c-Myc signaling pathway.	A431-III	[196]
↓ Cell proliferation; Induced cell cycle arrest at G0/G1 phase; ↓ CDK2 and CDK4, ↑ p16 and p21 expression; ↑ Cell apoptosis: condensed cromatin and nuclear fragmentation, ↑ PARP cleavage, caspase-3 and -9; Induced autophagy: ↑ light chain 3-II, ↓ p62 expression and ↑ acidic vesicular organelles.	HL-60	[238]
↓ Tumor volume; ↑ Cell apoptosis: ↑ PARP cleavage.	HL-60 xenograft mice model	
↓ Cell proliferation; Alleviated side effects of chemotherapeutic drug SN-38 through GSK-3β/β-catenin signaling.	AGS	[239]
Enhanced irinotecan chemotherapeutic effects: ↓ Tumor size;	AGS xenograft mice model	

Inhibited angiogenesis: ↓ VEGF-R2 and VEGF-A in tumor tissue; ↓ % of Tie2-expressing monocytes; ↓ COX-2 and restored E-cadherin expression; ↓ Twist and integrin β6 expression.		
↓ Cell migration and invasion; ↓ HIF-1α, VEGF, MMP2, and MMP9 mRNA and protein expression levels (HOS cells).	HOS and MG63	[240]
↓ Metastatic lung tumor formation and growth.	HOS-osteosarcoma lung metastasis mice model	[241]
Inhibited cell proliferation, migration and invasion; ↑ Cell apoptosis; Inhibited angiogenesis: ↓ VEGF-R.	Y79	
↓ Cell proliferation, migration and invasion; Inhibited EMT: ↑ E-cadherin, ↓ N-cadherin, Vimentin, Zeb1, Twist, Slug, and Snail; ↓ MMP-2 and -7 secretion; ↓ p-STAT3; Reversed IL-6-induced EMT, invasion, and migration.	PANC-1 and PATU-8988	[242]
↓ Cell proliferation and clonogenic survival; Induced cell cycle arrest at G0/G1 phase; ↑ Cell apoptosis: ↑ PARP cleavage, caspase-3 and -8; ↓ pJAK1, pSTAT3, VEGF expression and STAT3-dependent luciferase reporter gene activity; Inhibited MMP-9 secretion and ↓ nuclear translocation of STAT3.	HER2-overexpressing BT-474	[243]
Induced cell toxicity.	CEM, K562, Nalm6, T47D and EAC	[244]
Induced cell cycle arrest at S phase; ↑ Cell apoptosis: ↑ p53, p-p53, MCL1 cleavage, ↓ Bcl-2 and BCL-xL, and ↑ BAX, caspase-3, -9 and PARP cleavage.	Nalm6	
↓ Tumor volume and ↑ mice lifespan; ↓ Cell proliferation: ↓ Ki-67 positive cells; ↑ Cell apoptosis: ↑ p53 and p-p53.	EAC xenograft mice model	
↓ Cell viability; ↑ Cell apoptosis: morphological changes, ↑ Annexin V-positive cells;	CT26 and MC38	[245]
↑ Cell apoptosis via MAPK pathway; ↑ Caspase-3, -9 and PARP cleavage, ↓ Bcl-2 and Bcl-xL; ↑ pERK, pJNK and p-p38; ↓ Cell migration and invasion: ↓ MMP2 and MMP9 activity and ↑ TIMP-1 and TIMP-2 mRNA; ↑ E-cadherin and ↓ N-cadherin, β-catenin and Snail expression.	CT26	
Anti-metastatic effect: ↓ number of tumor nodules and lung weight.	CT26-colorectal lung metastasis mice model	
↓ Cell proliferation and ↑ cell apoptosis; Induced cell cycle arrest at sub-G1 phase; ↑ ROS levels and ↓ ΔΨm; ↓ pAkt, p-P70S6K and pS6, ↑p-p38, p-JNK, p-ERK1/2, and p-P90RSK; Enhanced anti-proliferative effects of cisplatin and paclitaxel.	JAR and JEG3	[246]

	↓ Cell proliferation and migration and ↑ cell apoptosis; Induced cell cycle arrest at G2/M phase; Inhibition of Akt/mTOR pathway: ↓ pAkt, p-P70S6K and 4E-BP1, ↑ MAPK activity;	MDA-MB-231 and MDA-MB-435	[247]
	↓ Tumor growth.	GFP-MDA-MB-231 xenograft mice model	
	↑ CB1-R expression; ↓ Cell proliferation and migration, and ↑ cell apoptosis via CB1-R; Induced cell cycle arrest at S phase; Inhibited PI3K/Akt/mTOR pathway: ↓ GSK3β, PI3K, Akt, S6, 4EBP1, and STAT3 phosphorylation; ↑ β-catenin and induced JNK/JUN pathway.	Caco2 and DLD-1	[248]
	↓ Cell proliferation and ↑ cell apoptosis; Induced cell cycle arrest at G1 phase; ↓ Cyclin D1, p21, Twist and p-p38MAPK expression.	MCF-7	[249]
	↑ Cell apoptosis: ↑ caspase-3, -8, -9 activation, PARP cleavage, Bax, Bak and cytochrome C release, and ↓ Bcl-xL; Induced cell cycle arrest at G0/G1 phase; ↑ ROS levels and ↓ ΔΨm; ↑ pERK.	HL-60	[250]
	↓ Tumor volume; ↑ ROS levels; ↓ Cell proliferation: ↓ Ki67 positive cells; ↑ Cell apoptosis: ↑ PARP and caspase-3 cleavage; ↑ pERK.	HL-60 xenograft mice model	
Resveratrol	Inhibited neoplastic transformation; ↑ Mitochondrial content; ↑ Citrate synthase; ↑ SIRT1 enzyme activity; Prevented ↓ ΔΨm, ATP levels and ↑ mitochondrial superoxide generation and ROS.	Bhas42 (benzo[a]pyrene-induced bioenergetic dysfunction)	[251]
	↓ Cell viability and proliferation; Induced TRAF6 lysosomal degradation; Inhibited NF-κB pathway; Suppressed EMT: ↑ E-cadherin and ↓ vimentin and slug.	DU145 and PC3	[252]
	Modulated epigenetic factors; ↑ BRCA1, p53 and p21 expression; ↓ Methyltransferases PRMT5 and EZH2 expression; ↓ KDAC activity and KDAC1, 2 and 3 expression; ↑ KAT2A and KAT3B expression; ↑ Activating histone marks: H3K9ac and H3K27ac and ↓ repressive histone marks: H4R3me2s and H3K27me3.	MCF-7 and MDA-MB-231	[253]

Induced premature senescence; ↑ p21 and p53; ↑ Rad9; ↓ Cell proliferation, migration and invasion; Supressed EMT: ↑ E-cadherin and γ-catenin, ↓ N-cadherin and vimentin; ↓ Slug.	MCF-7 and A549	[254]
↓ Cell proliferation and colony formation; ↓ EZH2 expression by inhibiting ERK1/2 pathway.	MCF-7 and T47D	[255]
Inhibited cell growth under hypoxic conditions; Cell cycle arrest at G0/G1 phase; Prevented HIF-1α stabilization; ↓ Glucose uptake.	PC-3	[256]
↓ Cell viability and induces cell apoptosis; ↑ ATP2A3 expression; ↓ HDAC activity and HDAC2 expression; ↑ Histone H3 acetylation and histone mark H3K27Ac enrichment; ↑ HAT activity; ↓ DNMT activity; ↓ Methyl-CpG binding proteins (MeCP2 and MBD2).	MCF-7 and MDA-MB-231	[257]
↓ Cell viability; ↑ SET7/9 expression; ↑ p53, cell apoptosis (↑ cleaved caspase-3 and PARP) via SET7/9.	HCT116, CO115 and SW48	[258]
↓ Cell migration; Reversed TGF-β1 induced EMT through PI3K/Akt and Smad signaling: ↓ MMP-2 and -9, Fibronectin, α-SMA, p-PI3K, p-AKT, Smad2, Smad3, p-Smad2, p-Smad3, vimentin, Snail1, and Slug and ↑ E-cadherin.	MDA231	[259]
↓ Tumor weight and growth; ↓ Lung metastasis.	MDA231 xenograft mice model	
Reversed TGF-β1 induced EMT via Smad signaling: ↑ E-cadherin and ↓ N-cadherin, vimentin, β-catenin, Twistl1, Snail and Slug; ↓ Cell migration and invasion; ↓ MMP-2 and -9; Suppressed stem cell-like properties: ↓ Bmi1 and Sox2; ↓ pSmad 2 and 3.	LN18 and U87	[120]
Reversed TGF-β1 induced EMT: ↓ N-cadherin, Vimentin, and pSmad2 and 3.	U87 xenograft mice model	
↓ Cell proliferation; Induced cell cycle arrest at S phase; ↑ Cell apoptosis; Induced changes in cell cycle related genes.	4T1	[260]
Induced chemosensitivity;	MCF-7-ADR	[261]

↓ Cell viability and ↑ cell apoptosis; ↑ miR-122-5p and ↓ miR-542-3p; ↓ Bcl-2, CDK2, CDK4 and CDK6 levels; Induced cell cycle arrest at G1 phase.		
↓ Neuroglobin levels by impairing E2/ERα pathway; ↓ pAkt; Enhanced paclitaxel apoptotic effects (↑ PARP-1 cleavage).	MCF-7 and T47D	[262]
↓ Cell growth and colony formation; ↑ ROS; ↓ NAF-1 expression through Nrf2 pathways: ↑ Nrf2 expression and Nrf2 nuclear translocation; ↑ Cell apoptosis: ↑ Bax and ↓ Bcl-2; Enhanced gemcitabine effects: ↑ cell apoptosis and ↓ cell growth by inhibiting NAF-1.	Panc-1 and Mia paca-2	[263]
Enhanced 5-flurouracil effects: ↓ Cell growth and proliferation and ↑ cell apoptosis; Induced cell cycle arrest at S phase; Supressed EMT: ↓ vimentin and Slug; ↓ Cell stemness (↓ CD51); Inhibited Akt and STAT3 activation; ↑ Anti-telomerase activity by inhibiting STAT3 binding to hTERT.	DLD1 and HCT116	[264]
↓ Cell proliferation and ↑ cell apoptosis; Inhibited Wnt signaling pathway: ↓ β-catenin, c-myc and cyclin D1 expression.	MGC-803	[265]
↓ Cell proliferation; ↑ Cell apoptosis: ↓ ΔΨm, ↑ Bax/Bcl-2 ratio, Fas, Fas-L cleaved caspase-3 and -8; Induced autophagy: ↑ microtubule-associated protein 1 light chain 3-II levels, nº of autophagosomes and Atg5, Beclin-1 and P62 expression; Inhibited PI3-Akt and activated LKB1-AMPKmTOR pathway.	HL-60	[266]
↑ ZFP36 expression and target genes (CCND1, MYC and VEGFA); ↓ DNMT1 and ↑ ZFP36 promoter demethylation; ↓ Cell proliferation and migration.	A549	[267]
Enhanced rapamycin effects: ↓ Cell viability by inhibiting mTORC1 and mTORC2 signaling pathways; ↓ Cyclin D1 and pRb levels; ↑ Activated caspase-3 and PARP.	MM1.S	[268]
↑ DUSP1 expression; Inhibited NF-κB pathway; ↓ COX-2; Sensitizes cells to cisplatin pro-apoptotic effects.	DU145 and PC3	[269]
↓ Cell proliferation, migration and invasion; ↓ Cyclin D1, c-Myc, MMP-2 and MMP-9; ↓ Sox2, Bmi-1, pAkt and pSTAT3.	MDA-MB-231, MCF-7-CAF-CM	[270]

Suppressed stemness properties and ↓ self-renewal signaling molecules expression.		
↓ Cell stemness and self-renewal ability; ↓ Sox2, Bmi-1, pAkt and pSTAT3. ↓ $CD44^{high}/CD24^{low}$ cell population;	MCF-7 – CAF-CM	
Sensitized cells to gemcitabine; Inhibited lipid synthesis (↓ FASN and SREBP1); Rescued stemness induced by gemcitabine by inhibiting SREBP1.	MiaPaCa-2 and PC-1	[271]
↓ Cell viability; Induced cell cycle arrest at S phase; ↑ Cell apoptosis: ↑ Bax, cleaved caspase-3 and -8, and ↓ Bcl-2; Suppressed NF-κB signaling (↓ p65).	SGC-7901	[272]
↓ Cell proliferation; Inhibited H_2O_2 induced cell activation, invasion, migration and glycolysis; ↓ miR-21 and ↑ PTEN.	Human pancreatic stellate cells and Panc-1	[273]
Enhanced TMZ effects: ↓ Cell proliferation and growth; ↑ Cell apoptosis: ↑ Cleaved caspase-3 and Bax, and ↓ XIAP and Bcl-2; Inhibited Wnt signaling pathway: ↓ Wnt2, MGMT and β-catenin, ↑ GSK-3β.	T98G and U138	[274]
Enhanced TMZ effects: ↓ Tumor volume and growth; Inhibited Wnt signaling pathway: ↓ Wnt2, MGMT and β-catenin, ↑ GSK-3β; ↑ Cell apoptosis.	T98G xenograft mice model	
↓ Cell proliferation; Induced cell apoptosis: ↑ caspase-3 and -9, Bax, p53 and ↓ Bcl-2, Bcl-xL; ↓ Cyclin B1.	HeLa	[275]
Inhibited norepinephrine cell invasion and EMT induction: ↑ E-cadherin expression, ↓ Slug; ↓ hTERT by ↓ pSrc and HIF-1α.	SKOV-3 and PA-1	[276]
Arrested cell cycle at G0/G1 phase; ↓ p-GSK3β, cyclin D1, p-PTEN, p-PI3K and p-PKB/Akt.	MGC803	[277]
↓ POK erythroid ontogenic factor the expression and activity.	U87MG, T98G and U251	[278]
↓ Cell proliferation, migration and invasion TGF-β-induced; ↑ E-cadherin, ↓ vimentin, MMP-2, MMP-9, Slug and Snail expression; Inhibited TGF-β1/Smads signaling pathway activation.	LoVo	[279]
Inhibited metastatic ability: ↓ nº of lung metastasis.	GFP-LoVo xenograft mice model	
↓ Tumor weight; Inhibited invasive ability: ↓ nº of metastatic lesions in lung and liver.	LoVo-orthotopic transplantation tumor	
↓ ABCB1 mRNA and protein expression via AMPK activation; ↓ ABCB1 efflux activity; ↓ pIkBα and NF-kB activity.	HCT116/L-oxaliplatin	[280]
↑ Cell apoptosis: ↑ PARP-1 cleavage, chromatin condensation and p53 activation;	HCT-116	[281]

Activated Ataxia Telangiectasia Mutated kinase.		
↓ Cell proliferation; Enhanced 5-Fluorouracil effects by ↓ cell invasion; ↑ Claudin-2 and E-cadherin, ↓ vimentin and Slug; ↓ NF-kB nuclear translocation and activation, and ↓ MMP-9 and caspase-3; Inhibited pIkBα and degradation.	HCT116, SW480	[282]
Improved cytotoxic effects of herceptin: ↓ Bcl-xL expression; ↓ HER-2 receptor (T47D cells).	MCF-7 and T47D	[283]
↓ Glucose uptake; ↑ Cell apoptosis; Inhibited plasma membrane GLUT1 localization by inhibiting Akt activity.	PA-1, OVCAR3, MDAH2774 and SKOV3	[284]
Suppressed EMT: ↑ E-cadherin, ↓ Gli-1, Snail and N-cadherin; Inhibited hedgehog signaling pathway; ↓ Cell proliferation, migration and invasion.	SGC-7901	[285]
↑ Cell apoptosis; ↑ H2AX phosphorylation by regulating MAPK activity; Induced JNK and p38, and blocked ERK.	K562	[286]
↓ Cell proliferation; ↑ Cell apoptosis: ↑ cytochrome c release and Bax, ↓ ΔΨm and Bcl-2; Enhanced anti-tumor effects of cisplatin: ↓ cell proliferation, ↑ cell apoptosis.	H838 and H520	[287]
Enhanced erlotinib effects: ↑ cell viability, colony formation and ↑ cell apoptosis. ↑ ROS; ↓ Survivin and Mcl-1; ↑ p53, PUMA, γH2AX, activated PARP and caspase-3; Suppressed AKT/mTOR/S6 kinase pathway.	H460, A549, PC-9 and H1975	[288]
Combined with rapamycin: Prevented Akt upregulation and autophagy; Inhibited mTORC1 signaling; Inhibited cell growth and induced cell apoptosis (↓ survivin expression, ↑ PARP cleavage).	MCF7 and MDAMB-231	[289]

2.4. Bitter compounds modulate ABC transporters expression and activity

Membrane cell transport and detoxification systems play critical roles in CNS homeostasis. For this reason, altered expression of ABC transporters has also been linked with brain diseases. Besides, a variety of ABC family members are expressed in the BBB, BCSFB and BTB resulting in the efflux of several compounds out of the brain, including chemotherapeutic drugs and other therapies for neurological diseases. The most studied ABC transporters are: ABCB1 (ATP-binding cassette subfamily B member 1), ABCC family members or multidrug-associated proteins (MPRs) and ABCG2 (ATP-binding cassette subfamily G member 2) [290]. In the last years, a large number of studies demonstrated that several bitter compounds, such as flavonoids, interact with ABC transporters (reviewed in [291]). In some cases, these compounds are substrates of one or more ABC transporter which limit their cellular uptake and the therapeutic effect. In addition, some bitter compounds can also act as inhibitors of ABC transporters which might contribute to increase brain drug bioavailability or even their bioavailability [291]. In this section, we present the current knowledge about the interaction of some bitter compounds, flavonoids and non-flavonoids, with ABC transporters.

Flavonoids present an outstanding potential for CNS disorders treatment, but their low bioavailability can limit their health beneficial effects. Therefore, it is essential to understand their bioavailability in the CNS and the mechanisms involved in their transport across biological barriers. Thus, most studies concerning flavonoids transport focus on the role of specific ABC transporters using in vitro models of the intestine, liver and kidney, due to the relevance of these for drug absorption, metabolism and excretion or elimination, respectively. Additionally, studies in cancer cell lines have been carried out elucidating the role of flavonoids on ABC transporters expression and function.

In MGC-803 cells, genistein downregulated ABCC1, ABCC5 and ABCG2 expression [292], while in HepG2 upregulated ABCB1 and ABCC2 [293]. In MCF-7 cells genistein induced ABCC1 and ABCG2 expression, but only ABCC1 in MDA-MB-231 cells. Moreover, MCF-7 cells showed an increase in doxorubicin and mitoxantrone efflux and resistance, dependent on ABCG2 activity [294]. After 3-days genistein administration in Wistar Han rats, hepatic ABCB1 expression increased as well as the biliary excretion of rhodamine-123 and digoxin, both well-known ABCB1 substrates [295]. Yang et al described that the permeability of several flavonoids in a BBB rat model: genistein presented the highest apparent permeability level and quercetin the lowest [296]. Interestingly, verapamil, an ABCB1 inhibitor, increased quercetin flux across this barrier,

indicating that quercetin is a substrate of ABCB1 in rat brain endothelial cells. In Caco-2 cells, liquiritigenin upregulated ABCB1, ABCC2 and ABCG2 expression. In addition, the efflux of rhodamine 123 was enhanced in these cells indicating that liquiritigenin also increased ABCB1 activity [297]. Moreover, ABCC4 and ABCG2 might play an important role in the disposal and elimination of liquiritigenin metabolites after sulfonation [298]. Unlikely many compounds, noscapine is able to cross the BBB [299]. A recent study demonstrated that noscapine and some derivates increased Calcein AM accumulation in NCI/AdrRES cells by directly interacting with ABCB1, inhibiting its function [300]. Quercetin has been widely related with ABC transporters acting as inhibitor, substrate or both (reviewed in [291]). Importantly, quercetin downregulated and inhibited ABCG2 function, in an in vitro rat BCSFB model, Z310 cells, increasing Hoechst 33342 cellular accumulation [301]. Moreover, the quercetin inhibitory effect was even greater than the Ko143 result, a specific ABCG2 inhibitor. Another study about the effects of quercetin on ABCG2 in two porcine BBB in vitro models [302], revealed that quercetin induced ABCG2 expression in PBMEC/C1-2 and primary brain microvascular endothelial cells, decreasing Hoechst 33342 accumulation. Therefore, ABCG2 modulation by quercetin is tissue/cell dependent. Furthermore, it is important to notice that ABCG2 localizes in the apical and luminal sides of the BCSFB and BBB, respectively [303, 304], meaning that in the BCSFB, ABCG2 faces the CSF, while in the BBB, ABCG2 faces the bloodstream. Therefore, in the BBB this transporter seems to limit the access of molecules to the brain, but in the BCSFB it might contribute for the entrance of molecules in the CNS after cell uptake. Despite the relevant data regarding quercetin effects on ABCG2 expression and function at the brain barriers, the transport of quercetin across these has not been explored, yet. Previous studies showed that kaempferol is both an ABCG2 substrate and inhibitor, and an ABCB1 substrate [305]. In MDCK/ABCG2 cells, kaempferol inhibited quercetin efflux by ABCG2, increasing quercetin transport from apical to basolateral side [305]. Therefore, kaempferol and quercetin co-administration might improve quercetin bioavailability. Additionally, bidirectional transport assays with kaempferol showed that its transport in MDCK/ABCG2 cells predominantly occurs from the apical to the basolateral side. Moreover, in the presence of GF120918, an ABCG2 inhibitor, kaempferol cell accumulation increased showing that it is also a substrate of ABCG2. Conversely, kaempferol is not a substrate of ABCC2 in MDCK/ABCC2 cells. In MCF-7/ADR cells kaempferol intracellular levels increased in the presence of an ABCB1 inhibitor, thus showing that it is a substrate of this transporter [305].

Despite the individual ability of flavonoids to interact with ABC transporters, some reports indicate that a combined administration of flavonoids can enhance their

bioavailability [306, 307]. In Caco-2 cells, combination of quercetin and apigenin, but not naringenin, increased the permeability of cells to these compounds and decreased their extracellular concentration probably by reducing their metabolism or increasing cellular uptake. Moreover, quercetin and apigenin acted synergistically to downregulate ABCB1, ABCC2, ABCC3 and ABCG2 and to inhibit ABCB1 ATPase activity [307]. Blackberry extract, containing epicatechin, kaempferol and quercetin metabolites among other phenolic compounds, altered transport and metabolizing systems in Caco-2 cells [306]. Pre-treatment of Caco-2 cells monolayers with blackberry extracts decreased apical to basolateral transport of epicatechin, quercetin-3-O-glucoside and kaempferol-7-O-glucoside. Moreover, blackberry extracts modulated gene expression of Phase II metabolizing enzymes and ABC and SLC (Solute carrier family) transporters which might explain the changes observed in flavonoids transport. Gene expression of SLC7A9, SLC28A1, SLC38A5 decreased and SLC7A11 increased in the apical side, while ABCA1, ABCC5 and SLC7A8 decreased in the basolateral side of Caco-2 cells.

Resveratrol is one of the most studied phytochemicals showing to have neuroprotective and anti-tumoral properties. However, resveratrol presents low bioavailability in targeted cell/tissues which limits its application on CNS therapeutics. Given the potential of resveratrol, its interaction with ABC transporters has been analysed. Resveratrol is transported by ABCC2 and ABCG2 in the intestine [308–310] and in the kidney [311]. Moreover, resveratrol is a substrate of ABCG2 [312] and modulates ABC transporters expression and function [313] in a tissue-dependent way. In rat kidney, resveratrol upregulated ABCG2 [311], but in Caco-2 cells downregulated ABCB1, ABCC1, ABCG2 [314] and ABCC2 [303, 315]. Regarding the bioavailability of resveratrol in the CNS, some reports indicate that resveratrol must cross brain barriers since it is detectable at low levels in rodents [316] and human [317] brains after systemic administration.

2.5. Bitter compounds are chemosensitizers

Some bitter compounds can modulate ABC transporters function which are often responsible for the drug resistance observed in CNS diseases, including brain cancer. Therefore, many studies have been focused on exploring if these compounds can overcome pharmacoresistance or sensitize cancer cells to chemotherapeutic drugs (reviewed in [318]).

Recently, the ability of various flavonoids to overcome ABCB1-mediated pharmacoresistance to antiepileptic drugs was tested in MDCK/ABCB1 cells [319]. Among others, quercetin, kaempferol and epigallocatechin gallate increased rhodamine 123 cellular accumulation probably by inhibiting ABCB1 function, while apigenin,

epicatechin and fisetin induced ABCB1 activity. Moreover, the flavonoids that inhibited ABCB1 also promoted the cellular accumulation of certain antiepileptic drugs such as phenytoin, carbamazepine and licarbazepine and their active metabolites in MDCK/ABCB1 cells. Therefore, coadministration of these flavonoids with already used antiepileptic drugs can be a novel approach to improve the therapy of epilepsy. In MDCK/ABCG2 cells, quercetin and kaempferol inhibited the chemotherapeutic desatinib efflux by ABCG2 resulting in increased cellular accumulation of desatinib [320]. However, no effects were observed in ABCB1 function. In doxorubicin resistant human breast cancer MCF-7 cells, quercetin enhanced the antitumor activities of doxorubicin, paclitaxel, and vincristine by inducing cell apoptosis or arresting cell cycle at G2/M phase. Moreover, quercetin alone or in combination to each chemotherapeutic drug downregulated ABCB1 expression. In accordance, quercetin increased doxorubicin accumulation in cells [321]. Further studies showed that quercetin enhanced apoptotic effects of doxorubicin and not only decreased ABCB1 expression but also downregulated ABCC1 and ABCG2 in breast cancer cells (MCF-7 and MDA-231 cells) [321]. Conversely, these effects were not observed in non-tumoral MCF-10A mammary cells and myocardial AC16 cells. Similarly, in multidrug resistant cell line BEL/5-FU, a human hepatocellular carcinoma model, quercetin sensitize cells to chemotherapeutic drugs 5-FU, mitomycin C and doxorubicin and downregulated ABCB1, ABCC1 and ABCC2 expression. The efflux pump activity of these transporters was inhibited as demonstrated by the increase of rhodamine-123 and doxorubicin intracellular accumulation after quercetin exposure. In addition, Chen and colleagues showed that ABCB1, ABCC1 and ABCC2 inhibition by quercetin was dependent on the FZD7 through the Wnt/β-catenin pathway [322]. Resveratrol can also sensitize cancer cells to chemotherapeutic drugs such as paclitaxel [262], gemcitabine [263, 271], 5-flurouracil [264, 282], rapamycin [268, 289], cisplatin [269], and temozolomide [274].

Considering these findings, the use of some bitter compounds as co-adjuvant therapy might contribute for improving the outcome of current therapies either by promoting drug accumulation on target cells, or by enhancing the therapeutic action of conventional drugs.

2.6. TAS2Rs mediate the effects of bitter compounds

In humans, 25 bitter taste receptors (TAS2Rs) recognize hundreds of bitter compounds that in the oral cavity originate the bitter sense perception [323, 324]. Usually, the receptor-ligand interaction triggers an aversive response that acts as a warning to avoid the ingestion of poisonous aliments due to the toxic profile of many bitter compounds

[325]. However, this concept is not straightforward since many bitter molecules have beneficial health properties [9, 326].

The role of TR2 as modulators of the effects of bitter compounds is poorly discussed in the literature. Although TR2 expression has been reported in many tissues such as airways, gastrointestinal tract, kidney, testis and CP [327, 328], their functional relevance is still a matter of debate, despite the increasing evidence supporting their role in mediating the action of bitter compounds.

In the airways, TAS2R14 mediated flavones anti-inflammatory activity and induced cytokine secretion [329]. Another compound, artesunate improved bronchodilatation in a mice model of asthma showing to be a potential candidate in the treatment of this pathology [330]. Interestingly, in lung macrophages LPS-treatment induced the expression of TAS2R7 and 38 [331]. Moreover, in LPS-stimulated macrophages, two promiscuous bitter compounds quinine and denatonium benzoate supressed the inflammatory response by decreasing TNF-α, CCL3 and CXCL8 levels. More specific ligands, such as dapsone, colchicine, strychnine, and chloroquine also demonstrated to inhibit LPS-induced pro-inflammatory cytokines release, as well as erythromycin, phenanthroline, ofloxacin, carisoprodol, specific ligands of TAS2R10, 5, 9 and 14, respectively. Another study suggests that TAS2R signalling participate in innate immune responses [331]. In primary macrophages, TAS2Rs activation was observed in the presence of several bitter compounds including bacterial TAS2Rs agonists. Moreover, it was demonstrated that TAS2Rs activation by bacterial-derived agonists such as 3-oxo-dodecanoyl-homoserine lactone, flufenamic acid, or *Pseudomonas* quinolone signal, induces phagocytosis in macrophages. Anti-cancer properties of bitter compounds might also be regulated by TAS2Rs. In ovarian cancer cells, noscapine induced cell apoptosis via TAS2R14 [214]. In neuroblastoma cells, TAS2Rs overexpression induced neurite elongation, decreased the expression of cancer stem cells markers (DLK1, CD133, Notch1, and Sox2) and inhibited self-renewal characteristics. In vivo, overexpression of TAS2R8 and TAS2R10 reduced tumor incidence and volume, and downregulated MMP-2 and P-selectin expression. Moreover, TAS2R8 and TAS2R10 over-expression inhibited cell migration and invasion, and MMP expression and activity suggesting that these receptors have an important role in suppressing metastatic potential of neuroblastoma cells [332]. Recently, Singh and colleagues, analysed the expression and function of TAS2R4 and TAS2R14 in breast cancer cells [333]. The authors found that TAS2R4 levels decrease but TAS2R14 increase in breast cancer tissue in comparison to non-cancerous controls. In addition, activation of TAS2R4 and TAS2R14 by quinine and apigenin, respectively, attenuated MDA-MB-231 proliferation and induced early-apoptosis.

However, the same was not observed in non-metastatic MCF-10A cells. Moreover, quinine via TAS2R4 and apigenin via TAS2R14 decreased MDA-MB-231 cells migration and MMP-9 secretion.

Despite a growing body of evidence shows that bitter taste signalling in extra-oral organs respond to internal and external stimuli and participate in several biological processes, the knowledge about TR2 functions is still scarce. Furthermore, the role of TR2 in transport and detoxification systems is even less understood. Jeon and colleagues showed that TAS2R38 activation by phenylthiocarbamide in Caco-2 cells upregulates ABCB1 expression and increases its activity [334]. Although these data support that TR2 signalling is directly involved in the regulation of transport mechanisms, we are far from completely understanding this relation. Therefore, overcoming this gap will contribute to improve the bioavailability of certain therapeutic drugs to the CNS and thus, the treatment of several brain disorders.

2.7. Conclusion

In recent years, a great number of bitter compounds that are able to bind TR2 have shown bioactive effects in several CNS diseases and different types of cancer models. Therefore, bitter compounds are promising candidates in the therapy of CNS disorders. However, their low bioavailability in the CNS and the lack of knowledge about how these molecules cross the blood-brain interfaces restrains their therapeutic application.

On the other hand, some bitter compounds might modulate the transport and detox systems of other molecules, contributing to more efficient drug delivery to the brain. Importantly, several reports indicate a critical role of TR2 in mediating the biological actions of bitter compounds, suggesting that TR2 might also regulate their neuroprotective and anti-tumoral activities (Figure 2.3.). However, if and how TR2 regulate the transport of bitter compounds across BBB, BCSFB and BTB or to what extent TR2 are the actual targets of their bitter ligands and elicit the therapeutic effects attributed to many of these bitter compounds in the CNS still needs clarification.

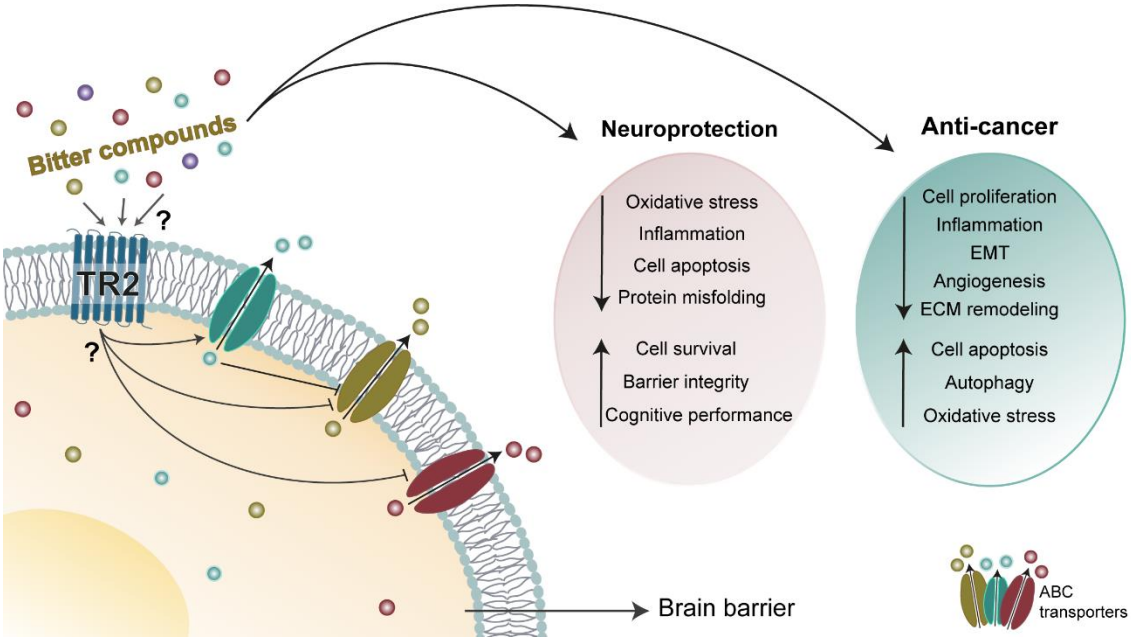

Figure 2. 3. Effects of bitter compounds and role of TR2 as mediators of their actions in the CNS. Binding of bitter compounds to TAS2Rs at the brain barriers might play a critical role in the regulation of membrane ABC transporters function and, thus contribute for the accumulation of bitter compounds in brain cells. Moreover, TR2 activation might mediate bitter compounds neuroprotective and anti-cancer activity. TAS2Rs – bitter taste receptors; ABC – ATP-binding cassette; EMT – epithelial-mesenchymal transition; ECM – extracellular matrix.

2.8. References

1. Boer AG de, Gaillard PJ (2007) Drug targeting to the brain. Annu Rev Pharmacol Toxicol 323–355. https://doi.org/10.1146/annurev.pharmtox.47.120505.105237

2. Gomez-Zepeda D, Taghi M, Scherrmann JM, et al (2020) ABC transporters at the blood–brain interfaces, their study models, and drug delivery implications in gliomas. Pharmaceutics 12:20. https://doi.org/10.3390/pharmaceutics12010020

3. Chamberlain MC, Baik CS, Gadi VK, et al (2017) Systemic therapy of brain metastases: Non-small cell lung cancer, breast cancer, and melanoma. Neuro Oncol 19:i1–i24. https://doi.org/10.1093/neuonc/now197

4. Van Tellingen O, Yetkin-Arik B, De Gooijer MC, et al (2015) Overcoming the blood-brain tumor barrier for effective glioblastoma treatment. Drug Resist Updat 19:1–12. https://doi.org/10.1016/j.drup.2015.02.002

5. Dagan-Wiener A, Di Pizio A, Nissim I, et al (2019) Bitterdb: Taste ligands and receptors database in 2019. Nucleic Acids Res 47:D1179–D1185. https://doi.org/10.1093/nar/gky974

6. Dagan-Wiener A, Nissim I, Ben Abu N, et al (2017) Bitter or not? BitterPredict, a tool for predicting taste from chemical structure. Sci Rep 7:1–13. https://doi.org/10.1038/s41598-017-12359-7

7. Meyerhof W, Batram C, Kuhn C, et al (2009) The molecular receptive ranges of human TAS2R bitter taste receptors. Chem Senses 35:157–170.

https://doi.org/10.1093/chemse/bjp092

8. de la Rosa LA, Moreno-Escamilla JO, Rodrigo-García J, Alvarez-Parrilla E (2018) Phenolic compounds. 253-271 Elsevier Inc. https://doi.org/10.1016/B978-0-12-813278-4.00012-9

9. Ballard CR, Maróstica MR (2018) Health Benefits of Flavonoids. 185-201 Elsevier Inc. https://doi.org/10.1016/B978-0-12-814774-0.00010-4

10. Izawa K, Amino Y, Kohmura M, et al (2010) 4.16 Human–Environment Interactions – Taste. 631-671 Elsevier Ltd.

11. Clark AA, Liggett SB, Munger SD (2012) Extraoral bitter taste receptors as mediators of off-target drug effects. FASEB J 26:4827–4831. https://doi.org/10.1096/fj.12-215087

12. Martins A, Mignon R, Bastos M, et al (2014) In vitro antitumoral activity of compounds isolated from Artemisia gorgonum Webb. Phyther Res 28:1329–1334. https://doi.org/10.1002/ptr.5133

13. Jaggupilli A, Howard R, Upadhyaya JD, et al (2016) Bitter taste receptors: Novel insights into the biochemistry and pharmacology. Int J Biochem Cell Biol 77:184–196. https://doi.org/10.1016/j.biocel.2016.03.005

14. Adam L, Phulukdaree A, Soma P (2018) Effective long-term solution to therapeutic remission in Inflammatory Bowel Disease: Role of Azathioprine. Biomed Pharmacother 100:8–14. https://doi.org/10.1016/j.biopha.2018.01.152

15. Molinelli E, Paolinelli M, Campanati A, et al (2019) Metabolic, pharmacokinetic, and toxicological issues surrounding dapsone. Expert Opin Drug Metab Toxicol 15:367–379. https://doi.org/10.1080/17425255.2019.1600670

16. Khan N, Mukhtar H (2019) Tea polyphenols in promotion of human health. Nutrients 11:39–54. https://doi.org/10.3390/nu11010039

17. Liu K, Cho YY, Yao K, et al (2011) Eriodictyol inhibits RSK2-ATF1 signaling and suppresses EGF-induced neoplastic cell transformation. J Biol Chem 286:2057–2066. https://doi.org/10.1074/jbc.M110.147306

18. Hsiao YC, Peng SF, Lai KC, et al (2019) Genistein induces apoptosis in vitro and has antitumor activity against human leukemia HL-60 cancer cell xenograft growth in vivo. Environ Toxicol 34:443–456. https://doi.org/10.1002/tox.22698

19. Tyler MW, Zaldivar-Diez J, Haggarty SJ (2017) Classics in Chemical Neuroscience: Haloperidol. ACS Chem Neurosci 8:444–453. https://doi.org/10.1021/acschemneuro.7b00018

20. Ko YH, Kwon SH, Lee SY, Jang CG (2017) Liquiritigenin ameliorates memory and cognitive impairment through cholinergic and BDNF pathways in the mouse hippocampus. Arch Pharm Res 40:1209–1217. https://doi.org/10.1007/s12272-017-0954-6

21. Manzoor MF, Ahmad N, Ahmed Z, et al (2019) Novel extraction techniques and pharmaceutical activities of luteolin and its derivatives. J Food Biochem 43:1–19.

https://doi.org/10.1111/jfbc.12974

22. Nouri Z, Fakhri S, El-Senduny FF, et al (2019) On the neuroprotective effects of naringenin: Pharmacological targets, signaling pathways, molecular mechanisms, and clinical perspective. Biomolecules 9:1–27. https://doi.org/10.3390/biom9110690

23. Altinoz MA, Topcu G, Hacimuftuoglu A, et al (2019) Noscapine, a Non-addictive Opioid and Microtubule-Inhibitor in Potential Treatment of Glioblastoma. Neurochem Res 44:1796–1806. https://doi.org/10.1007/s11064-019-02837-x

24. Dang Y, Mu Y, Wang K, et al (2016) Papaverine inhibits lipopolysaccharide-induced microglial activation by suppressing NF-kB signaling pathway. Drug Des Devel Ther 10:851–859. https://doi.org/10.2147/DDDT.S97380

25. Freund RRA, Gobrecht P, Fischer D, Arndt HD (2020) Advances in chemistry and bioactivity of parthenolide. Nat Prod Rep 37:541–565. https://doi.org/10.1039/c9np00049f

26. Suganthy N, Devi KP, Nabavi SF, et al (2016) Bioactive effects of quercetin in the central nervous system: Focusing on the mechanisms of actions. Biomed Pharmacother 84:892–908. https://doi.org/10.1016/j.biopha.2016.10.011

27. Rauf A, Imran M, Butt MS, et al (2018) Resveratrol as an anti-cancer agent: A review. Crit Rev Food Sci Nutr 58:1428–1447. https://doi.org/10.1080/10408398.2016.1263597

28. Imran M, Salehi B, Sharifi-rad J, et al (2019) Kaempferol : A Key Emphasis to Its. 1–16

29. Mattson MP, Arumugam T V. (2018) Hallmarks of Brain Aging: Adaptive and Pathological Modification by Metabolic States. Cell Metab 27:1176–1199. https://doi.org/doi:10.1016/j.cmet.2018.05.011

30. Hipp MS, Kasturi P, Hartl FU (2019) The proteostasis network and its decline in ageing. Nat Rev Mol Cell Biol 20:421–435. https://doi.org/10.1038/s41580-019-0101-y

31. Wei B bin, Liu M yan, Zhong X, et al (2019) Increased BBB permeability contributes to EGCG-caused cognitive function improvement in natural aging rats: pharmacokinetic and distribution analyses. Acta Pharmacol Sin 40:1490–1500. https://doi.org/10.1038/s41401-019-0243-7

32. Du K, Liu M, Zhong X, et al (2018) Epigallocatechin Gallate Reduces Amyloid β-Induced Neurotoxicity via Inhibiting Endoplasmic Reticulum Stress-Mediated Apoptosis. Mol Nutr Food Res 62:1–35. https://doi.org/10.1002/mnfr.201700890

33. Pierzynowska K, Podlacha M, Gaffke L, et al (2019) Autophagy-dependent mechanism of genistein-mediated elimination of behavioral and biochemical defects in the rat model of sporadic Alzheimer's disease. Neuropharmacology 148:332–346. https://doi.org/10.1016/j.neuropharm.2019.01.030

34. Yang Z, Kuboyama T, Tohda C (2017) A systematic strategy for discovering a therapeutic drug for Alzheimer's disease and its target molecule. Front Pharmacol 8:1–13. https://doi.org/10.3389/fphar.2017.00340

35. Maria SA, Ignacio MJ, Jose R-P, et al (2016) The flavonoid quercetin ameliorates

Alzheimer's disease pathology and protects cognitive and emotional function in aged triple transgenic Alzheimer's disease model mice. Neuropharmacology 93:134–145. https://doi.org/10.1016/j.neuropharm.2015.01.027.The

36. Corpas R, Griñán-Ferré C, Rodríguez-Farré E, et al (2019) Resveratrol Induces Brain Resilience Against Alzheimer Neurodegeneration Through Proteostasis Enhancement. Mol Neurobiol 56:1502–1516. https://doi.org/10.1007/s12035-018-1157-y

37. Moussa C, Hebron M, Huang X, et al (2017) Resveratrol regulates neuro-inflammation and induces adaptive immunity in Alzheimer's disease. J Neuroinflammation 14:1–10. https://doi.org/10.1186/s12974-016-0779-0

38. Wang H, Wang H, Cheng H, Che Z (2016) Ameliorating effect of luteolin on memory impairment in an Alzheimer's disease model. Mol Med Rep 13:4215–4220. https://doi.org/10.3892/mmr.2016.5052

39. Ghofrani S, Joghataei MT, Mohseni S, et al (2015) Naringenin improves learning and memory in an Alzheimer's disease rat model: Insights into the underlying mechanisms. Eur J Pharmacol 764:195–201. https://doi.org/10.1016/j.ejphar.2015.07.001

40. Hayakawa M, Itoh M, Ohta K, et al (2015) Quercetin reduces eIF2α phosphorylation by GADD34 induction. Neurobiol Aging 36:2509–2518. https://doi.org/10.1016/j.neurobiolaging.2015.05.006

41. Qi Y, Shang L, Liao Z, et al (2019) Intracerebroventricular injection of resveratrol ameliorated Aβ-induced learning and cognitive decline in mice. Metab Brain Dis 34:257–266. https://doi.org/10.1007/s11011-018-0348-6

42. Zhang N, Hu Z, Zhang Z, et al (2018) Protective Role Of Naringenin Against Aβ25-35-Caused Damage via ER and PI3K/Akt-Mediated Pathways. Cell Mol Neurobiol 38:549–557. https://doi.org/10.1007/s10571-017-0519-8

43. Wang K, Chen Z, Huang L, et al (2017) Naringenin reduces oxidative stress and improves mitochondrial dysfunction via activation of the Nrf2/ARE signaling pathway in neurons. Int J Mol Med 40:1582–1590. https://doi.org/10.3892/ijmm.2017.3134

44. Wang G, Chen L, Pan X, et al (2016) The effect of resveratrol on beta amyloid-induced memory impairment involves inhibition of phosphodiesterase-4 related signaling. Oncotarget 7:17380–17392. https://doi.org/10.18632/oncotarget.8041

45. Chiang MC, Nicol CJ, Cheng YC (2018) Resveratrol activation of AMPK-dependent pathways is neuroprotective in human neural stem cells against amyloid-beta-induced inflammation and oxidative stress. Neurochem Int 115:1–10. https://doi.org/10.1016/j.neuint.2017.10.002

46. Xu Q, Langley M, Kanthasamy AG, Reddy MB (2017) Epigallocatechin Gallate Has a Neurorescue Effect in a Mouse Model of Parkinson Disease. J Nutr 147:1926–1931. https://doi.org/10.3945/jn.117.255034

47. Sugumar M, Sevanan M, Sekar S (2019) Neuroprotective effect of naringenin against

MPTP-induced oxidative stress. Int J Neurosci 129:534–539. https://doi.org/10.1080/00207454.2018.1545772

48. Mani S, Sekar S, Barathidasan R, et al (2018) Naringenin Decreases α-Synuclein Expression and Neuroinflammation in MPTP-Induced Parkinson's Disease Model in Mice. Neurotox Res 33:656–670. https://doi.org/10.1007/s12640-018-9869-3

49. Woodruff TM, Thundyil J, Tang SC, et al (2011) Pathophysiology, treatment, and animal and cellular models of human ischemic stroke. Mol Neurodegener 6:11. https://doi.org/10.1186/1750-1326-6-11

50. Bai Q, Lyu Z, Pan Z, et al (2017) Epigallocatechin-3-gallate promotes angiogenesis via up-regulation of Nfr2 signaling pathway in a mouse model of ischemic stroke. Behav Brain Res 321:79–86. https://doi.org/10.1016/j.bbr.2016.12.037

51. Ferreira E de O, Fernandes MYSD, Lima NMR de, et al (2016) Neuroinflammatory response to experimental stroke is inhibited by eriodictyol. Behav Brain Res 312:321–332. https://doi.org/10.1016/j.bbr.2016.06.046

52. Wang J, Mao J, Wang R, et al (2020) Kaempferol Protects Against Cerebral Ischemia Reperfusion Injury Through Intervening Oxidative and Inflammatory Stress Induced Apoptosis. Front Pharmacol 11:1–12. https://doi.org/10.3389/fphar.2020.00424

53. Aziz N, Iezhitsa I, Agarwal R, et al (2020) Neuroprotection by trans-resveratrol against collagenase-induced neurological and neurobehavioural deficits in rats involves adenosine A1 receptors. Neurol Res 42:189–208. https://doi.org/10.1080/01616412.2020.1716470

54. Bonsack F, Alleyne CH, Sukumari-Ramesh S (2017) Resveratrol attenuates neurodegeneration and improves neurological outcomes after intracerebral hemorrhage in mice. Front Cell Neurosci 11:1–9. https://doi.org/10.3389/fncel.2017.00228

55. He Q, Li Z, Wang Y, et al (2017) Resveratrol alleviates cerebral ischemia/reperfusion injury in rats by inhibiting NLRP3 inflammasome activation through Sirt1-dependent autophagy induction. Int Immunopharmacol 50:208–215. https://doi.org/10.1016/j.intimp.2017.06.029

56. Wan D, Zhou Y, Wang K, et al (2016) Resveratrol provides neuroprotection by inhibiting phosphodiesterases and regulating the cAMP/AMPK/SIRT1 pathway after stroke in rats. Brain Res Bull 121:255–262. https://doi.org/10.1016/j.brainresbull.2016.02.011

57. Diaz-Ruiz A, Roldan-Valadez E, Ortiz-Plata A, et al (2016) Dapsone improves functional deficit and diminishes brain damage evaluated by 3-Tesla magnetic resonance image after transient cerebral ischemia and reperfusion in rats. Brain Res 1646:384–392. https://doi.org/10.1016/j.brainres.2016.06.023

58. Hermann DM, Zechariah A, Kaltwasser B, et al (2015) Sustained neurological recovery induced by resveratrol is associated with angioneurogenesis rather than neuroprotection after focal cerebral ischemia. Neurobiol Dis 83:16–25. https://doi.org/10.1016/j.nbd.2015.08.018

59. Zhan R, Zhao M, Zhou T, et al (2018) Dapsone protects brain microvascular integrity from high-fat diet induced LDL oxidation. Cell Death Dis 9:. https://doi.org/10.1038/s41419-018-0739-y

60. Yang N, Li L, Li Z, et al (2017) Protective effect of dapsone on cognitive impairment induced by propofol involves hippocampal autophagy. Neurosci Lett 649:85–92. https://doi.org/10.1016/j.neulet.2017.04.019

61. Yamamoto N, Shibata M, Ishikuro R, et al (2017) Epigallocatechin gallate induces extracellular degradation of amyloid β-protein by increasing neprilysin secretion from astrocytes through activation of ERK and PI3K pathways. Neuroscience 362:70–78. https://doi.org/10.1016/j.neuroscience.2017.08.030

62. Valenti D, de Bari L, de Rasmo D, et al (2016) The polyphenols resveratrol and epigallocatechin-3-gallate restore the severe impairment of mitochondria in hippocampal progenitor cells from a Down syndrome mouse model. Biochim Biophys Acta - Mol Basis Dis 1862:1093–1104. https://doi.org/10.1016/j.bbadis.2016.03.003

63. Mao L, Hochstetter D, Yao L, et al (2019) Green tea polyphenol (–)-epigallocatechin gallate (EGCG) attenuates neuroinflammation in palmitic acid-stimulated BV-2 microglia and high-fat diet-induced obese mice. Int J Mol Sci 20:. https://doi.org/10.3390/ijms20205081

64. Zhuravin IA, Dubrovskaya NM, Vasilev DS, et al (2019) Regulation of Neprilysin Activity and Cognitive Functions in Rats After Prenatal Hypoxia. Neurochem Res 44:1387–1398. https://doi.org/10.1007/s11064-019-02796-3

65. Zhou J, Mao L, Xu P, Wang Y (2018) Effects of (–)-epigallocatechin gallate (EGCG) on energy expenditure and microglia-mediated hypothalamic inflammation in mice fed a high-fat diet. Nutrients 10:1–13. https://doi.org/10.3390/nu10111681

66. Zhao X, Li R, Jin H, et al (2018) Epigallocatechin-3-gallate confers protection against corticosterone-induced neuron injuries via restoring extracellular signal-regulated kinase 1/2 and phosphatidylinositol-3 kinase/protein kinase B signaling pathways. PLoS One 13:1–17. https://doi.org/10.1371/journal.pone.0192083

67. Zhao1 X, Liu F, Jin H, et al (2018) Involvement of PKCα and ERK1/2 signaling pathways in EGCG's protection against stress-induced neural injuries in Wistar rats. Neuroscience 346:226–237. https://doi.org/https://doi.org/10.1016/j.neuroscience.2017.01.025.

68. Li J, Zhang Z, Lv L, et al (2016) (–)-Epigallocatechin Gallate Inhibits Asymmetric Dimethylarginine-Induced Injury in Human Brain Microvascular Endothelial Cells. Neurochem Res 41:1868–1876. https://doi.org/10.1007/s11064-016-1898-9

69. Ortiz-López L, Márquez-Valadez B, Gómez-Sánchez A, et al (2016) Green tea compound epigallo-catechin-3-gallate (EGCG) increases neuronal survival in adult hippocampal neurogenesis in vivo and in vitro. Neuroscience 322:208–220. https://doi.org/10.1016/j.neuroscience.2016.02.040

70. Jing X, Shi H, Zhu X, et al (2015) Eriodictyol Attenuates β-Amyloid 25–35 Peptide-Induced Oxidative Cell Death in Primary Cultured Neurons by Activation of Nrf2. Neurochem Res 40:1463–1471. https://doi.org/10.1007/s11064-015-1616-z

71. He P, Yan S, Zheng J, et al (2018) Eriodictyol Attenuates LPS-Induced Neuroinflammation, Amyloidogenesis, and Cognitive Impairments via the Inhibition of NF-κB in Male C57BL/6J Mice and BV2 Microglial Cells. J Agric Food Chem 66:10205–10214. https://doi.org/10.1021/acs.jafc.8b03731

72. Mirahmadi SMS, Shahmohammadi A, Rousta AM, et al (2017) Soy isoflavone genistein attenuates lipopolysaccharide-induced cognitive impairments in the rat via exerting anti-oxidative and anti-inflammatory effects. Cytokine 104:151–159. https://doi.org/10.1016/j.cyto.2017.10.008

73. Fu J, Sun H, Zhang Y, et al (2018) Neuroprotective Effects of Luteolin Against Spinal Cord Ischemia-Reperfusion Injury by Attenuation of Oxidative Stress, Inflammation, and Apoptosis. J Med Food 21:13–20. https://doi.org/10.1089/jmf.2017.4021

74. Kim S, Chin YW, Cho J (2017) Protection of cultured cortical neurons by luteolin against oxidative damage through inhibition of apoptosis and induction of heme oxygenase-1. Biol Pharm Bull 40:256–265. https://doi.org/10.1248/bpb.b16-00579

75. Wang J, Qi Y, Niu X, et al (2018) Dietary naringenin supplementation attenuates experimental autoimmune encephalomyelitis by modulating autoimmune inflammatory responses in mice. J Nutr Biochem 54:130–139. https://doi.org/10.1016/j.jnutbio.2017.12.004

76. Wang J, Niu X, Wu C, Wu D (2018) Naringenin modifies the development of lineage-specific effector CD4+ T cells. Front Immunol 9:1–12. https://doi.org/10.3389/fimmu.2018.02267

77. Niu X, Wu C, Li M, et al (2018) Naringenin is an inhibitor of T cell effector functions. J Nutr Biochem 58:71–79. https://doi.org/10.1016/j.jnutbio.2018.04.008

78. Khajevand-Khazaei MR, Ziaee P, Motevalizadeh SA, et al (2018) Naringenin ameliorates learning and memory impairment following systemic lipopolysaccharide challenge in the rat. Eur J Pharmacol 826:114–122. https://doi.org/10.1016/j.ejphar.2018.03.001

79. Sarubbo F, Ramis MR, Kienzer C, et al (2018) Chronic Silymarin, Quercetin and Naringenin Treatments Increase Monoamines Synthesis and Hippocampal Sirt1 Levels Improving Cognition in Aged Rats. J Neuroimmune Pharmacol 13:24–38. https://doi.org/10.1007/s11481-017-9759-0

80. Hua FZ, Ying J, Zhang J, et al (2016) Naringenin pre-treatment inhibits neuroapoptosis and ameliorates cognitive impairment in rats exposed to isoflurane anesthesia by regulating the PI3/Akt/PTEN signalling pathway and suppressing NF-B-mediated inflammation. Int J Mol Med 38:1271–1280. https://doi.org/10.3892/ijmm.2016.2715

81. Wu LH, Lin C, Lin HY, et al (2016) Naringenin Suppresses Neuroinflammatory

Responses Through Inducing Suppressor of Cytokine Signaling 3 Expression. Mol Neurobiol 53:1080–1091. https://doi.org/10.1007/s12035-014-9042-9

82. Zhang B, Wei YZ, Wang GQ, et al (2019) Targeting MAPK pathways by naringenin modulates microglia M1/M2 polarization in lipopolysaccharide-stimulated cultures. Front Cell Neurosci 12:1–11. https://doi.org/10.3389/fncel.2018.00531

83. Wang GQ, Zhang B, He XM, et al (2019) Naringenin targets on astroglial Nrf2 to support dopaminergic neurons. Pharmacol Res 139:452–459. https://doi.org/10.1016/j.phrs.2018.11.043

84. Sumathi T, Christinal J (2016) Neuroprotective Effect of Portulaca oleraceae Ethanolic Extract Ameliorates Methylmercury Induced Cognitive Dysfunction and Oxidative Stress in Cerebellum and Cortex of Rat Brain. Biol Trace Elem Res 172:155–165. https://doi.org/10.1007/s12011-015-0546-6

85. Zhou T, Zhu Y (2019) Cascade Signals of Papaverine Inhibiting LPS-Induced Retinal Microglial Activation. J Mol Neurosci 111–119. https://doi.org/10.1007/s12031-019-01289-w

86. Lei X, Chao H, Zhang Z, et al (2015) Neuroprotective effects of quercetin in a mouse model of brain ischemic/reperfusion injury via anti-apoptotic mechanisms based on the Akt pathway. Mol Med Rep 12:3688–3696. https://doi.org/10.3892/mmr.2015.3857

87. Sun GY, Li R, Yang B, et al (2019) Quercetin potentiates docosahexaenoic acid to suppress lipopolysaccharide-induced oxidative/inflammatory responses, alter lipid peroxidation products, and enhance the adaptive stress pathways in BV-2 microglial cells. Int J Mol Sci 24:1131-1148:. https://doi.org/10.3390/ijms20040932

88. Holzmann I, Da Silva LM, Corrêa Da Silva JA, et al (2015) Antidepressant-like effect of quercetin in bulbectomized mice and involvement of the antioxidant defenses, and the glutamatergic and oxidonitrergic pathways. Pharmacol Biochem Behav 136:55–63. https://doi.org/10.1016/j.pbb.2015.07.003

89. Xia SF, Xie ZX, Qiao Y, et al (2015) Differential effects of quercetin on hippocampus-dependent learning and memory in mice fed with different diets related with oxidative stress. Physiol Behav 138:325–331. https://doi.org/10.1016/j.physbeh.2014.09.008

90. Sharma DR, Wani WY, Sunkaria A, et al (2016) Quercetin attenuates neuronal death against aluminum-induced neurodegeneration in the rat hippocampus. Neuroscience 324:163–176. https://doi.org/10.1016/j.neuroscience.2016.02.055

91. Christine Sawda, Moussa C, Turner RS (2018) Resveratrol for Alzheimer's disease. Ann N Y Acad Sci 1403:142–149. https://doi.org/doi:10.1111/nyas.13431

92. Wang H, Jiang T, Li W, et al (2018) Resveratrol attenuates oxidative damage through activating mitophagy in an in vitro model of Alzheimer's disease. Toxicol Lett 282:100–108. https://doi.org/10.1016/j.toxlet.2017.10.021

93. Lin CH, Nicol CJB, Cheng YC, et al (2020) Neuroprotective effects of resveratrol against

oxygen glucose deprivation induced mitochondrial dysfunction by activation of AMPK in SH-SY5Y cells with 3D gelatin scaffold. Brain Res 1726:146492. https://doi.org/10.1016/j.brainres.2019.146492

94. Shi DD, Dong CM, Ho LC, et al (2018) Resveratrol, a natural polyphenol, prevents chemotherapy-induced cognitive impairment: Involvement of cytokine modulation and neuroprotection. Neurobiol Dis 114:164–173. https://doi.org/10.1016/j.nbd.2018.03.006

95. de Queiroz KB, dos Santos Fontes Pereira T, Araújo MSS, et al (2018) Resveratrol Acts Anti-Inflammatory and Neuroprotective in an Infant Rat Model of Pneumococcal Meningitis by Modulating the Hippocampal miRNome. Mol Neurobiol 55:8869–8884. https://doi.org/10.1007/s12035-018-1037-5

96. Xu BL, Zhang H, Ma LN, et al (2018) Resveratrol prevents high-calorie diet-induced learning and memory dysfunction in juvenile C57BL/6J mice. Neurol Res 40:709–715. https://doi.org/10.1080/01616412.2018.1471118

97. Allen EN, Potdar S, Tapias V, et al (2019) Resveratrol and pinostilbene confer neuroprotection against aging-related deficits through an ERK1/2 dependent-mechanism. J Nutr Biochem 54:77–86. https://doi.org/10.1016/j.jnutbio.2017.10.015

98. Guida N, Laudati G, Anzilotti S, et al (2015) Resveratrol via sirtuin-1 downregulates RE1-silencing transcription factor (REST) expression preventing PCB-95-induced neuronal cell death. Toxicol Appl Pharmacol 288:387–398. https://doi.org/10.1016/j.taap.2015.08.010

99. El-kott AF, Abd-Lateif AEKM, Khalifa HS, et al (2020) Kaempferol protects against cadmium chloride-induced hippocampal damage and memory deficits by activation of silent information regulator 1 and inhibition of poly (ADP-Ribose) polymerase-1. Sci Total Environ 728:1–13. https://doi.org/10.1016/j.scitotenv.2020.138832

100. Cheng X, Yang YL, Yang H, et al (2018) Kaempferol alleviates LPS-induced neuroinflammation and BBB dysfunction in mice via inhibiting HMGB1 release and down-regulating TLR4/MyD88 pathway. Int Immunopharmacol 56:29–35. https://doi.org/10.1016/j.intimp.2018.01.002

101. Das D, Biswal S, Barhwal KK, et al (2018) Kaempferol Inhibits Extra-synaptic NMDAR-Mediated Downregulation of TRkβ in Rat Hippocampus During Hypoxia. IBRO

102. Yang YL, Cheng X, Li WH, et al (2019) Kaempferol attenuates LPS-induced striatum injury in mice involving anti-neuroinflammation, maintaining BBB integrity, and down-regulating the HMGB1/TLR4 pathway. Int J Mol Sci 20:. https://doi.org/10.3390/ijms20030491

103. Achrol AS, Rennert RC, Anders C, et al (2019) Brain metastases. Nat Rev Dis Prim 5:. https://doi.org/10.1038/s41572-018-0055-y

104. Lapointe S, Perry A, Butowski NA (2018) Primary brain tumours in adults. Lancet 392:432–446. https://doi.org/10.1016/S0140-6736(18)30990-5

105. Li X, Kong L, Yang Q, et al (2020) Parthenolide inhibits ubiquitin-specific peptidase 7

(USP7), Wnt signaling, and colorectal cancer cell growth. J Biol Chem 295:3576–3589. https://doi.org/10.1074/jbc.RA119.011396

106. Carlisi D, De Blasio A, Drago-Ferrante R, et al (2017) Parthenolide prevents resistance of MDA-MB231 cells to doxorubicin and mitoxantrone: the role of Nrf2. Cell Death Discov 3:1–12. https://doi.org/10.1038/cddiscovery.2017.78

107. Talib WH, Al Kury LT (2018) Parthenolide inhibits tumor-promoting effects of nicotine in lung cancer by inducing P53 - dependent apoptosis and inhibiting VEGF expression. Biomed Pharmacother 107:1488–1495. https://doi.org/10.1016/j.biopha.2018.08.139

108. Kim SL, Park YR, Lee ST, Kim SW (2017) Parthenolide suppresses hypoxia-inducible factor-1α signaling and hypoxia induced epithelial-mesenchymal transition in colorectal cancer. Int J Oncol 51:1809–1820. https://doi.org/10.3892/ijo.2017.4166

109. Liu YC, Kim SL, Park YR, et al (2017) Parthenolide promotes apoptotic cell death and inhibits the migration and invasion of SW620 cells. Intest Res 15:174–181. https://doi.org/10.5217/ir.2017.15.2.174

110. Baskaran N, Selvam GS, Yuvaraj S, Abhishek A (2018) Parthenolide attenuates 7,12-dimethylbenz[a]anthracene induced hamster buccal pouch carcinogenesis. Mol Cell Biochem 440:11–22. https://doi.org/10.1007/s11010-017-3151-5

111. Li H, Lu H, Lv M, et al (2018) Parthenolide facilitates apoptosis and reverses drug-resistance of human gastric carcinoma cells by inhibiting the STAT3 signaling pathway. Oncol Lett 15:3572–3579. https://doi.org/10.3892/ol.2018.7739

112. Jeyamohan S, Moorthy RK, Kannan MK, Arockiam AJV (2016) Parthenolide induces apoptosis and autophagy through the suppression of PI3K/Akt signaling pathway in cervical cancer. Biotechnol Lett 38:1251–1260. https://doi.org/10.1007/s10529-016-2102-7

113. Kong F cong, Zhang J qiong, Zeng C, et al (2015) Inhibitory effects of parthenolide on the activity of NF-κB in multiple myeloma via targeting TRAF6. J Huazhong Univ Sci Technol - Med Sci 35:343–349. https://doi.org/10.1007/s11596-015-1435-0

114. Zhu SM, Park YR, Seo SY, et al (2019) Parthenolide inhibits transforming growth factor β1-induced epithelial-mesenchymal transition in colorectal cancer cells. Intest Res 17:527–536. https://doi.org/10.5217/IR.2019.00031

115. Grube S, Ewald C, Kögler C, et al (2018) Achievable Central Nervous System Concentrations of the Green Tea Catechin EGCG Induce Stress in Glioblastoma Cells in Vitro. Nutr Cancer 70:1145–1158. https://doi.org/10.1080/01635581.2018.1495239

116. Xie CR, You CG, Zhang N, et al (2018) Epigallocatechin Gallate Preferentially Inhibits O 6 -Methylguanine DNA-Methyltransferase Expression in Glioblastoma Cells Rather than in Nontumor Glial Cells. Nutr Cancer 70:1339–1347. https://doi.org/10.1080/01635581.2018.1539189

117. Udroiu I, Marinaccio J, Sgura A (2019) Epigallocatechin-3-gallate induces telomere

shortening and clastogenic damage in glioblastoma cells. Environ Mol Mutagen 60:683–692. https://doi.org/10.1002/em.22295

118. Anson DM, Wilcox RM, Huseman ED, et al (2018) Luteolin Decreases Epidermal Growth Factor Receptor-Mediated Cell Proliferation and Induces Apoptosis in Glioblastoma Cell Lines. Basic Clin Pharmacol Toxicol 123:678–686. https://doi.org/10.1111/bcpt.13077

119. Taylor MA, Khathayer F, Ray SK (2019) Quercetin and Sodium Butyrate Synergistically Increase Apoptosis in Rat C6 and Human T98G Glioblastoma Cells Through Inhibition of Autophagy. Neurochem Res 44:1715–1725. https://doi.org/10.1007/s11064-019-02802-8

120. Song Y, Chen Y, Li Y, et al (2019) Resveratrol Suppresses Epithelial-Mesenchymal Transition in GBM by Regulating Smad-Dependent Signaling. Biomed Res Int 2019:. https://doi.org/10.1155/2019/1321973

121. Motamedian E, Taheri E, Bagheri F (2017) Proliferation inhibition of cisplatin-resistant ovarian cancer cells using drugs screened by integrating a metabolic model and transcriptomic data. Cell Prolif 50:1–8. https://doi.org/10.1111/cpr.12370

122. Chaabane W, Appell ML (2016) Interconnections between apoptotic and autophagic pathways during thiopurine-induced toxicity in cancer cells: The role of reactive oxygen species. Oncotarget 7:75616–75634. https://doi.org/10.18632/oncotarget.12313

123. Werfel TA, Elion DL, Rahman B, et al (2019) Treatment-induced tumor cell apoptosis and secondary necrosis drive tumor progression in the residual tumor microenvironment through MERTK and IDO1. Cancer Res 79:171–182. https://doi.org/10.1158/0008-5472.CAN-18-1106

124. Xu MR, Wei PF, Suo MZ, et al (2019) Brucine Suppresses Vasculogenic Mimicry in Human Triple-Negative Breast Cancer Cell Line MDA-MB-231. Biomed Res Int 2019:. https://doi.org/10.1155/2019/6543230

125. Ren H, Zhao J, Fan D, et al (2019) Alkaloids from nux vomica suppresses colon cancer cell growth through Wnt/β-catenin signaling pathway. Phyther Res 33:1570–1578. https://doi.org/10.1002/ptr.6347

126. Shi X, Zhu M, Kang Y, et al (2018) Wnt/β-catenin signaling pathway is involved in regulating the migration by an effective natural compound brucine in LoVo cells. Phytomedicine 46:85–92. https://doi.org/10.1016/j.phymed.2018.04.019

127. Li M, Li P, Zhang M, Ma F (2018) Brucine suppresses breast cancer metastasis via inhibiting epithelial mesenchymal transition and matrix metalloproteinases expressions. Chin J Integr Med 24:40–46. https://doi.org/10.1007/s11655-017-2805-1

128. Hu K fei, Kong X ying, Zhong M cun, et al (2017) Brucine inhibits bone metastasis of breast cancer cells by suppressing Jagged1/Notch1 signaling pathways. Chin J Integr Med 23:110–116. https://doi.org/10.1007/s11655-016-2647-2

129. Ruijun W, Wenbin M, Yumin W, et al (2015) Inhibition of glioblastoma cell growth in vitro and in vivo by brucine, a component of Chinese medicine. Oncol Res 22:275–281.

https://doi.org/10.3727/096504015X14344177566282

130. Karpel-Massler G, Kast RE, Siegelin MD, et al (2017) Anti-glioma Activity of Dapsone and Its Enhancement by Synthetic Chemical Modification. Neurochem Res 42:3382–3389. https://doi.org/10.1007/s11064-017-2378-6

131. Khiewkamrop P, Phunsomboon P, Richert L, et al (2018) Epistructured catechins, EGCG and EC facilitate apoptosis induction through targeting de novo lipogenesis pathway in HepG2 cells. Cancer Cell Int 18:1–13. https://doi.org/10.1186/s12935-018-0539-6

132. Zhu W, Li MC, Wang FR, et al (2020) The inhibitory effect of ECG and EGCG dimeric procyanidins on colorectal cancer cells growth is associated with their actions at lipid rafts and the inhibition of the epidermal growth factor receptor signaling. Biochem Pharmacol 175:113923. https://doi.org/10.1016/j.bcp.2020.113923

133. Sojoodi M, Wei L, Erstad DJ, et al (2020) Epigallocatechin Gallate Induces Hepatic Stellate Cell Senescence and Attenuates Development of Hepatocellular Carcinoma. Cancer Prev Res (Phila) 13:497–508. https://doi.org/10.1158/1940-6207.CAPR-19-0383

134. Namiki K, Wongsirisin P, Yokoyama S, et al (2020) (−)-Epigallocatechin gallate inhibits stemness and tumourigenicity stimulated by AXL receptor tyrosine kinase in human lung cancer cells. Sci Rep 10:1–11. https://doi.org/10.1038/s41598-020-59281-z

135. Wei R, Cortez Penso NE, Hackman RM, et al (2019) Epigallocatechin-3-gallate (Egcg) suppresses pancreatic cancer cell growth, invasion, and migration partly through the inhibition of akt pathway and epithelial–mesenchymal transition: Enhanced efficacy when combined with gemcitabine. Nutrients 11:. https://doi.org/10.3390/nu11081856

136. Yoshimura H, Yoshida H, Matsuda S, et al (2019) The therapeutic potential of epigallocatechin-3-gallate against human oral squamous cell carcinoma through inhibition of cell proliferation and induction of apoptosis: In vitro and in vivo murine xenograft study. Mol Med Rep 20:1139–1148. https://doi.org/10.3892/mmr.2019.10331

137. Zan L, Chen Q, Zhang L, Li X (2019) Epigallocatechin gallate (EGCG) suppresses growth and tumorigenicity in breast cancer cells by downregulation of miR-25. Bioengineered 10:374–382. https://doi.org/10.1080/21655979.2019.1657327

138. Li T, Zhao N, Lu J, et al (2019) Epigallocatechin gallate (EGCG) suppresses epithelial-Mesenchymal transition (EMT) and invasion in anaplastic thyroid carcinoma cells through blocking of TGF-β1/Smad signaling pathways. Bioengineered 10:282–291. https://doi.org/10.1080/21655979.2019.1632669

139. Kang Q, Zhang X, Cao N, et al (2019) EGCG enhances cancer cells sensitivity under 60Coγ radiation based on miR-34a/Sirt1/p53. Food Chem Toxicol 133:110807. https://doi.org/10.1016/j.fct.2019.110807

140. Sun X, Song J, Li E, et al (2019) (-)-Epigallocatechin-3-gallate inhibits bladder cancer stem cells via suppression of sonic hedgehog pathway. Oncol Rep 42:425–435. https://doi.org/10.3892/or.2019.7170

141. La X, Zhang L, Li Z, et al (2019) (-)-Epigallocatechin Gallate (EGCG) Enhances the Sensitivity of Colorectal Cancer Cells to 5-FU by Inhibiting GRP78/NF-κB/miR-155-5p/MDR1 Pathway. J Agric Food Chem 67:2510–2518. https://doi.org/10.1021/acs.jafc.8b06665

142. Schröder L, Marahrens P, Koch JG, et al (2019) Effects of green tea, matcha tea and their components epigallocatechin gallate and quercetin on MCF-7 and MDA-MB-231 breast carcinoma cells. Oncol Rep 41:387–396. https://doi.org/10.3892/or.2018.6789

143. Yang H, Wang M, Sun H, et al (2019) Synergetic Effect of EP1 Receptor Antagonist and (-)-Epigallocatechin-3-gallate in Hepatocellular Carcinoma. Pharmacology 104:267–275. https://doi.org/10.1159/000502076

144. Wei R, Mao L, Xu P, et al (2018) Suppressing glucose metabolism with epigallocatechin-3-gallate (EGCG) reduces breast cancer cell growth in preclinical models. Food Funct 9:5682–5696. https://doi.org/10.1039/c8fo01397g

145. Vitkeviciene A, Baksiene S, Borutinskaite V, Navakauskiene R (2018) Epigallocatechin-3-gallate and BIX-01294 have different impact on epigenetics and senescence modulation in acute and chronic myeloid leukemia cells. Eur J Pharmacol 838:32–40. https://doi.org/10.1016/j.ejphar.2018.09.005

146. Ding YP, Gao ZL, Chen BC, et al (2018) The Effect of Different Treatments of (–)-Epigallocatechin-3-Gallate on Colorectal Carcinoma Cell Lines. Nutr Cancer 70:1126–1136. https://doi.org/10.1080/01635581.2018.1497671

147. Gu JJ, Qiao KS, Sun P, et al (2018) Study of EGCG induced apoptosis in lung cancer cells by inhibiting PI3K/Akt signaling pathway. Eur Rev Med Pharmacol Sci 22:4557–4563. https://doi.org/10.26355/eurrev_201807_15511

148. Zhou CG, Hui LM, Luo JM (2018) Epigallocatechin gallate inhibits the proliferation and induces apoptosis of multiple myeloma cells via inactivating EZH2. Eur Rev Med Pharmacol Sci 22:2093–2098. https://doi.org/10.26355/eurrev-201804-14742

149. Ghasemi-Pirbaluti M, Pourgheysari B, Shirzad H, et al (2018) The Inhibitory Effect of Epigallocatechin Gallate on the Viability of T Lymphoblastic Leukemia Cells is Associated with Increase of Caspase-3 Level and Fas Expression. Indian J Hematol Blood Transfus 34:253–260. https://doi.org/10.1007/s12288-017-0854-4

150. Ni J, Guo X, Wang H, et al (2018) Differences in the effects of egcg on chromosomal stability and cell growth between normal and colon cancer cells. Molecules 23:. https://doi.org/10.3390/molecules23040788

151. Wang X, Ye T, Chen WJ, et al (2017) Structural shift of gut microbiota during chemopreventive effects of epigallocatechin gallate on colorectal carcinogenesis in mice. World J Gastroenterol 23:8128–8139. https://doi.org/10.3748/wjg.v23.i46.8128

152. Tsai CY, Chen CY, Chiou YH, et al (2018) Epigallocatechin-3-gallate suppresses human herpesvirus 8 replication and induces ROS leading to apoptosis and autophagy in primary

effusion lymphoma cells. Int J Mol Sci 19:. https://doi.org/10.3390/ijms19010016

153. Filippi A, Picot T, Aanei CM, et al (2018) Epigallocatechin-3-O-gallate alleviates the malignant phenotype in A-431 epidermoid and SK-BR-3 breast cancer cell lines. Int J Food Sci Nutr 69:584–597. https://doi.org/10.1080/09637486.2017.1401980

154. Ying L, Yan F, Williams BR, et al (2016) (-)-Epigallocatechin-3-gallate and EZH2 inhibitor GSK343 have similar inhibitory effects and mechanisms of action on colorectal cancer cells. Clin Exp Pharmacol Physiol 38:42–49. https://doi.org/https://doi.org/10.1111/1440-1681.12854

155. Feng C, Ho Y, Sun C, et al (2017) Epigallocatechin gallate inhibits the growth and promotes the apoptosis of bladder cancer cells. Exp Ther Med 14:3513–3518. https://doi.org/10.3892/etm.2017.4981

156. Liu L, Ju Y, Wang J, Zhou R (2017) Epigallocatechin-3-gallate promotes apoptosis and reversal of multidrug resistance in esophageal cancer cells. Pathol Res Pract 213:1242–1250. https://doi.org/10.1016/j.prp.2017.09.006

157. Hong OY, Noh EM, Jang HY, et al (2017) Epigallocatechin gallate inhibits the growth of MDA-MB-231 breast cancer cells via inactivation of the β-Catenin signaling pathway. Oncol Lett 14:441–446. https://doi.org/10.3892/ol.2017.6108

158. Moradzadeh M, Hosseini A, Erfanian S, Rezaei H (2017) Epigallocatechin-3-gallate promotes apoptosis in human breast cancer T47D cells through down-regulation of PI3K/AKT and Telomerase. Pharmacol Reports 69:924–928. https://doi.org/10.1016/j.pharep.2017.04.008

159. Chen Y, Wang XQ, Zhang Q, et al (2017) (-)-Epigallocatechin-3-gallate inhibits colorectal cancer stem cells by suppressing Wnt/β-catenin pathway. Nutrients 9:1–11. https://doi.org/10.3390/nu9060572

160. Hallman K, Aleck K, Quigley M, et al (2017) The regulation of steroid receptors by epigallocatechin-3-gallate in breast cancer cells. Breast Cancer Targets Ther 9:365–373. https://doi.org/10.2147/BCTT.S131334

161. Lee YH, Song GG (2017) Epigallocatechin gallate inhibits the growth of salivary adenoid cystic carcinoma cells via the EGFR/Erk signal transduction pathway and the mitochondria apoptosis pathway. Neoplasma 64:563–570. https://doi.org/10.4149/neo

162. Luo KW, Wei Chen, Lung WY, et al (2017) EGCG inhibited bladder cancer SW780 cell proliferation and migration both in vitro and in vivo via down-regulation of NF-κB and MMP-9. J Nutr Biochem 41:56–64. https://doi.org/10.1016/j.jnutbio.2016.12.004

163. Xie C, Li X, Geng S, et al (2017) Wnt/β-catenin pathway mediates (–)-Epigallocatechin-3-gallate (EGCG) inhibition of lung cancer stem cells. Biochem Biophys Res Commun 482:15–21. https://doi.org/10.1016/j.bbrc.2016.11.038

164. Shin YS, Kang SU, Park JK, et al (2016) Anti-cancer effect of (-)-epigallocatechin-3-gallate (EGCG) in head and neck cancer through repression of transactivation and enhanced

degradation of β-catenin. Phytomedicine 23:1344–1355. https://doi.org/10.1016/j.phymed.2016.07.005

165. Yang C, Du W, Yang D (2016) Inhibition of green tea polyphenol EGCG((–)-epigallocatechin-3-gallate) on the proliferation of gastric cancer cells by suppressing canonical wnt/β-catenin signalling pathway. Int J Food Sci Nutr 67:818–827. https://doi.org/10.1080/09637486.2016.1198892

166. Shih LJ, Lin YR, Lin CK, et al (2016) Green tea (-)-epigallocatechin gallate induced growth inhibition of human placental choriocarcinoma cells. Placenta 41:1–9. https://doi.org/10.1016/j.placenta.2016.02.017

167. Yuan C-H, Horng C-T, Lee C-F, et al (2016) Epigallocatechin Gallate Sensitizes Cisplatin- Resistant Oral Cancer CAR Cell Apoptosis and Autophagy Through Stimulating AKT/STAT3 Pathway and Suppressing Multidrug Resistance 1 Signaling. Environ Toxicol 32:845–855. https://doi.org/https://doi.org/10.1002/tox.22284

168. Cerezo-Guisado MI, Zur R, Lorenzo MJ, et al (2015) Implication of Akt, ERK1/2 and alternative p38MAPK signalling pathways in human colon cancer cell apoptosis induced by green tea EGCG. Food Chem Toxicol 84:125–132. https://doi.org/10.1016/j.fct.2015.08.017

169. Park C, Cha HJ, Lee H, et al (2019) Induction of G2/M cell cycle arrest and apoptosis by genistein in human bladder cancer T24 cells through inhibition of the ROS-dependent PI3k/Akt signal transduction pathway. Antioxidants 8:1–14. https://doi.org/10.3390/antiox8090327

170. Sahin K, Yenice E, Bilir B, et al (2019) Genistein prevents development of spontaneous ovarian cancer and inhibits tumor growth in hen model. Cancer Prev Res 12:135–145. https://doi.org/10.1158/1940-6207.CAPR-17-0289

171. Tanjak P, Thiantanawat A, Watcharasit P, Satayavivad J (2018) Genistein reduces the activation of AKT and EGFR, and the production of IL6 in cholangiocarcinoma cells involving estrogen and estrogen receptors. Int J Oncol 53:177–188. https://doi.org/10.3892/ijo.2018.4375

172. Yang Y, Zang A, Jia Y, et al (2016) Genistein inhibits A549 human lung cancer cell proliferation via miR-27a and MET signaling. Oncol Lett 12:2189–2193. https://doi.org/10.3892/ol.2016.4817

173. Zhao QX, Zhao M, Parris AB, et al (2016) Genistein targets the cancerous inhibitor of PP2A to induce growth inhibition and apoptosis in breast cancer cells. Int J Oncol 49:1203–1210. https://doi.org/10.3892/ijo.2016.3588

174. Qin J, Chen JX, Zhu Z, Teng JA (2015) Genistein inhibits human colorectal cancer growth and suppresses MiR-95, Akt and SGK1. Cell Physiol Biochem 35:2069–2077. https://doi.org/10.1159/000374013

175. Hsieh YH, Chan HL, Lin CF, et al (2019) Antipsychotic use is inversely associated with gastric cancer risk: A nationwide population-based nested case-control study. Cancer Med

8:4484–4496. https://doi.org/10.1002/cam4.2329
176. Bai T, Wang S, Zhao Y, et al (2017) Haloperidol, a sigma receptor 1 antagonist, promotes ferroptosis in hepatocellular carcinoma cells. Biochem Biophys Res Commun 491:919–925. https://doi.org/10.1016/j.bbrc.2017.07.136
177. Jandaghi P, Najafabadi HS, Bauer AS, et al (2016) Expression of DRD2 Is Increased in Human Pancreatic Ductal Adenocarcinoma and Inhibitors Slow Tumor Growth in Mice. Gastroenterology 151:1218–1231. https://doi.org/10.1053/j.gastro.2016.08.040
178. Da J, Xu M, Wang Y, et al (2019) Kaempferol promotes apoptosis while inhibiting cell proliferation via androgen-dependent pathway and suppressing vasculogenic mimicry and invasion in prostate cancer. Anal Cell Pathol 2019:. https://doi.org/10.1155/2019/1907698
179. Hu G, Liu H, Wang M, Peng W (2019) IQ motif containing GTPase-activating protein 3 (IQGAP3) inhibits kaempferol-induced apoptosis in breast cancer cells by extracellular signal-regulated kinases 1/2 (ERK1/2) signaling activation. Med Sci Monit 25:7666–7674. https://doi.org/10.12659/MSM.915642
180. Zhu L, Xue L (2019) Kaempferol suppresses proliferation and induces cell cycle arrest, apoptosis, and DNA damage in breast cancer cells. Oncol Res 27:629–634. https://doi.org/10.3727/096504018X15228018559434
181. Seydi E, Salimi A, Rasekh HR, et al (2018) Selective Cytotoxicity of Luteolin and Kaempferol on Cancerous Hepatocytes Obtained from Rat Model of Hepatocellular Carcinoma: Involvement of ROS-Mediated Mitochondrial Targeting. Nutr Cancer 70:594–604. https://doi.org/10.1080/01635581.2018.1460679
182. Gao Y, Yin J, Rankin GO, Chen YC (2018) Kaempferol induces G2/M cell cycle arrest via checkpoint kinase 2 and promotes apoptosis via death receptors in human ovarian carcinoma A2780/CP70 Cells. Molecules 23:. https://doi.org/10.3390/molecules23051095
183. Moradzadeh M, Tabarraei A, Sadeghnia HR, et al (2018) Kaempferol increases apoptosis in human acute promyelocytic leukemia cells and inhibits multidrug resistance genes. J Cell Biochem 119:2288–2297. https://doi.org/10.1002/jcb.26391
184. Li S, Yan T, Deng R, et al (2017) Low dose of kaempferol suppresses the migration and invasion of triple-negative breast cancer cells by downregulating the activities of RhoA and Rac1. Onco Targets Ther 10:4809–4819. https://doi.org/10.2147/OTT.S140886
185. Kashafi E, Moradzadeh M, Mohamadkhani A, Erfanian S (2017) Kaempferol increases apoptosis in human cervical cancer HeLa cells via PI3K/AKT and telomerase pathways. Biomed Pharmacother 89:573–577. https://doi.org/10.1016/j.biopha.2017.02.061
186. Zhao Y, Tian B, Wang Y, Ding H (2017) Kaempferol sensitizes human ovarian cancer cells-OVCAR-3 and SKOV-3 to tumor necrosis factor-related apoptosis-inducing ligand (TRAIL)-induced apoptosis via JNK/ERK-CHOP pathway and up-regulation of death receptors 4 and 5. Med Sci Monit 23:5096–5105. https://doi.org/10.12659/MSM.903552
187. Qiu W, Lin J, Zhu Y, et al (2017) Kaempferol modulates DNA methylation and

downregulates DNMT3B in bladder cancer. Cell Physiol Biochem 41:1325–1335. https://doi.org/10.1159/000464435

188. Yao S, Wang X, Li C, et al (2016) Kaempferol inhibits cell proliferation and glycolysis in esophagus squamous cell carcinoma via targeting EGFR signaling pathway. Tumor Biol 37:10247–10256. https://doi.org/10.1007/s13277-016-4912-6

189. Yi X, Zuo J, Tan C, et al (2016) Kaempferol, a flavonoid compound from gynura medica induced apoptosis and growth inhibition in MCF-7 breast cancer cell. African J Tradit Complement Altern Med 13:210–215. https://doi.org/10.21010/ajtcam.v13i4.27

190. Guo H, Ren F, Zhang L, et al (2016) Kaempferol induces apoptosis in HepG2 cells via activation of the endoplasmic reticulum stress pathway. Mol Med Rep 13:2791–2800. https://doi.org/10.3892/mmr.2016.4845

191. Qin Y, Cui W, Yang X, Tong B (2015) Kaempferol inhibits the growth and metastasis of cholangiocarcinoma in vitro and in vivo. Acta Biochim Biophys Sin (Shanghai) 48:238–245. https://doi.org/10.1093/abbs/gmv133

192. Lee J, Kim JH (2016) Kaempferol inhibits pancreatic cancer cell growth and migration through the blockade of EGFR-related pathway in vitro. PLoS One 11:1–14. https://doi.org/10.1371/journal.pone.0155264

193. Jo E, Park SJ, Choi YS, et al (2015) Kaempferol Suppresses Transforming Growth Factor-β1-Induced Epithelial-to-Mesenchymal Transition and Migration of A549 Lung Cancer Cells by Inhibiting Akt1-Mediated Phosphorylation of Smad3 at Threonine-179. Neoplasia 17:525–537. https://doi.org/10.1016/j.neo.2015.06.004

194. Wu LY, Lu HF, Chou YC, et al (2015) Kaempferol induces DNA damage and inhibits DNA repair associated protein expressions in human promyelocytic leukemia HL-60 cells. Am J Chin Med 43:365–382. https://doi.org/10.1142/S0192415X1550024X

195. Fan JJ, Hsu WH, Lee KH, et al (2019) Dietary flavonoids luteolin and quercetin inhibit migration and invasion of squamous carcinoma through reduction of src/stat3/s100a7 signaling. Antioxidants 8:. https://doi.org/10.3390/antiox8110557

196. Chen KC, Hsu WH, Ho JY, et al (2018) Flavonoids Luteolin and Quercetin Inhibit RPS19 and contributes to metastasis of cancer cells through c-Myc reduction. J Food Drug Anal 26:1180–1191. https://doi.org/10.1016/j.jfda.2018.01.012

197. Li C, Wang Q, Shen S, et al (2019) HIF-1α/VEGF signaling-mediated epithelial–mesenchymal transition and angiogenesis is critically involved in anti-metastasis effect of luteolin in melanoma cells. Phyther Res 33:798–807. https://doi.org/10.1002/ptr.6273

198. Wang SW, Chen YR, Chow JM, et al (2018) Stimulation of Fas/FasL-mediated apoptosis by luteolin through enhancement of histone H3 acetylation and c-Jun activation in HL-60 leukemia cells. Mol Carcinog 57:866–877. https://doi.org/10.1002/mc.22807

199. Cao Z, Zhang H, Cai X, et al (2018) Luteolin Promotes Cell Apoptosis by Inducing Autophagy in Hepatocellular Carcinoma. Cell Physiol Biochem 43:1803–1812.

https://doi.org/10.1159/000484066

200. Lu X, Li Y, Li X, Aisa HA (2017) Luteolin induces apoptosis in vitro through suppressing the MAPK and PI3K signaling pathways in gastric cancer. Oncol Lett 14:1993–2000. https://doi.org/10.3892/ol.2017.6380

201. Choi HJ, Choi HJ, Chung TW, Ha KT (2016) Luteolin inhibits recruitment of monocytes and migration of Lewis lung carcinoma cells by suppressing chemokine (C-C motif) ligand 2 expression in tumor-associated macrophage. Biochem Biophys Res Commun 470:101–106. https://doi.org/10.1016/j.bbrc.2016.01.002

202. Lim W, Yang C, Bazer FW, Song G (2016) Luteolin Inhibits Proliferation and Induces Apoptosis of Human Placental Choriocarcinoma Cells by Blocking the PI3K/AKT Pathway and Regulating Sterol Regulatory Element Binding Protein Activity. Biol Reprod 95:82–82. https://doi.org/10.1095/biolreprod.116.141556

203. Meng G, Chai K, Li X, et al (2016) Luteolin exerts pro-apoptotic effect and anti-migration effects on A549 lung adenocarcinoma cells through the activation of MEK/ERK signaling pathway. Chem Biol Interact 257:26–34. https://doi.org/10.1016/j.cbi.2016.07.028

204. Lin CH, Chang CY, Lee KR, et al (2015) Flavones inhibit breast cancer proliferation through the Akt/FOXO3a signaling pathway. BMC Cancer 15:1–12. https://doi.org/10.1186/s12885-015-1965-7

205. Sun DW, Zhang H Da, Mao L, et al (2015) Luteolin Inhibits Breast Cancer Development and Progression in Vitro and in Vivo by Suppressing Notch Signaling and Regulating MiRNAs. Cell Physiol Biochem 37:1693–1711. https://doi.org/10.1159/000438535

206. Hernández-Aquino E, Muriel P (2018) Beneficial effects of naringenin in liver diseases: Molecular mechanisms. World J Gastroenterol 24:1679–1707. https://doi.org/10.3748/wjg.v24.i16.1679

207. Ke JY, Banh T, Hsiao YH, et al (2017) Citrus flavonoid naringenin reduces mammary tumor cell viability, adipose mass, and adipose inflammation in obese ovariectomized mice. Mol Nutr Food Res 61:1–26. https://doi.org/10.1002/mnfr.201600934

208. Lim W, Park S, Bazer FW, Song G (2017) Naringenin-Induced Apoptotic Cell Death in Prostate Cancer Cells Is Mediated via the PI3K/AKT and MAPK Signaling Pathways. J Cell Biochem 118:1118–1131. https://doi.org/10.1002/jcb.25729

209. Park HJ, Choi YJ, Lee JH, Nam MJ (2017) Naringenin causes ASK1-induced apoptosis via reactive oxygen species in human pancreatic cancer cells. Food Chem Toxicol 99:1–8. https://doi.org/10.1016/j.fct.2016.11.008

210. Zhang F, Dong W, Zeng W, et al (2016) Naringenin prevents TGF-β1 secretion from breast cancer and suppresses pulmonary metastasis by inhibiting PKC activation. Breast Cancer Res 18:1–16. https://doi.org/10.1186/S13058-016-0698-0

211. Bodduluru LN, Kasala ER, Madhana RM, et al (2016) Naringenin ameliorates

inflammation and cell proliferation in benzo(a)pyrene induced pulmonary carcinogenesis by modulating CYP1A1, NFκB and PCNA expression. Int Immunopharmacol 30:102–110. https://doi.org/10.1016/j.intimp.2015.11.036

212. Chandrika BB, Steephan M, Kumar TRS, et al (2016) Hesperetin and Naringenin sensitize HER2 positive cancer cells to death by serving as HER2 Tyrosine Kinase inhibitors. Life Sci 160:47–56. https://doi.org/10.1016/j.lfs.2016.07.007

213. Abaza MSI, Orabi KY, Al-Quattan E, Al-Attiyah RJ (2015) Growth inhibitory and chemo-sensitization effects of naringenin, a natural flavanone purified from Thymus vulgaris, on human breast and colorectal cancer. Cancer Cell Int 15:1–19. https://doi.org/10.1186/s12935-015-0194-0

214. Martin LTP, Nachtigal MW, Selman T, et al (2019) Bitter taste receptors are expressed in human epithelial ovarian and prostate cancers cells and noscapine stimulation impacts cell survival. Mol Cell Biochem 454:203–214. https://doi.org/10.1007/s11010-018-3464-z

215. Shen W, Liang B, Yin J, et al (2015) Noscapine Increases the Sensitivity of Drug-Resistant Ovarian Cancer Cell Line SKOV3/DDP to Cisplatin by Regulating Cell Cycle and Activating Apoptotic Pathways. Cell Biochem Biophys 72:203–213. https://doi.org/10.1007/s12013-014-0438-y

216. El-Far AHAM, Munesue S, Harashima A, et al (2018) In vitro anticancer effects of a RAGE inhibitor discovered using a structure-based drug design system. Oncol Lett 15:4627–4634. https://doi.org/10.3892/ol.2018.7902

217. Ren Y, Li Y, Lv J, et al (2019) Parthenolide regulates oxidative stress-induced mitophagy and suppresses apoptosis through p53 signaling pathway in C2C12 myoblasts. J Cell Biochem 120:15695–15708. https://doi.org/10.1002/jcb.28839

218. Marino S, Bishop RT, Carrasco G, et al (2019) Pharmacological Inhibition of NFκB Reduces Prostate Cancer Related Osteoclastogenesis In Vitro and Osteolysis Ex Vivo. Calcif Tissue Int 105:193–204. https://doi.org/10.1007/s00223-019-00538-9

219. Li C, Zhou Y, Cai Y, et al (2019) Parthenolide inhibits the proliferation of MDA-T32 papillary thyroid carcinoma cells in vitro and in mouse tumor xenografts and activates autophagy and apoptosis by downregulation of the mammalian target of rapamycin (mTOR)/PI3K/AKT signaling pathway. Med Sci Monit 25:5054–5061. https://doi.org/10.12659/MSM.915387

220. Jafari N, Nazeri S, Enferadi ST (2018) Parthenolide reduces metastasis by inhibition of vimentin expression and induces apoptosis by suppression elongation factor α – 1 expression. Phytomedicine 41:67–73. https://doi.org/10.1016/j.phymed.2018.01.022

221. Lin M, Bi H, Yan Y, et al (2017) Parthenolide suppresses non-small cell lung cancer GLC-82 cells growth via B-Raf/MAPK/Erk pathway. Oncotarget 8:23436–23447. https://doi.org/10.18632/oncotarget.15584

222. Yang C, Yang QO, Kong QJ, et al (2016) Parthenolide Induces Reactive Oxygen

Species-Mediated Autophagic Cell Death in Human Osteosarcoma Cells. Cell Physiol Biochem 40:146–154. https://doi.org/10.1159/000452532

223. C. George V, R.N. Kumar D, A. Kumar R (2016) Relative In Vitro Potentials of Parthenolide to Induce Apoptosis and Cell Cycle Arrest in Skin Cancer Cells. Curr Drug Discov Technol 13:34–40. https://doi.org/10.2174/1570163813666160224124029

224. Yu HJ, Jung JY, Jeong JH, et al (2015) Induction of apoptosis by parthenolide in human oral cancer cell lines and tumor xenografts. Oral Oncol 51:602–609. https://doi.org/10.1016/j.oraloncology.2015.03.003

225. Koteswari LL, Kumari S, Kumar AB, Malla RR (2018) A comparative anticancer study on procyanidin C1 against receptor positive and receptor negative breast cancer. Nat Prod Res 0:1–8. https://doi.org/10.1080/14786419.2018.1557173

226. Choy YY, Fraga M, Mackenzie GG, et al (2016) The PI3K/Akt pathway is involved in procyanidin-mediated suppression of human colorectal cancer cell growth. Mol Carcinog 55:2196–2209. https://doi.org/10.1002/mc.22461

227. Way T Der, Tsai SJ, Wang CM, et al (2015) Cinnamtannin D1 from Rhododendron formosanum Induces Autophagy via the Inhibition of Akt/mTOR and Activation of ERK1/2 in Non-Small-Cell Lung Carcinoma Cells. J Agric Food Chem 63:10407–10417. https://doi.org/10.1021/acs.jafc.5b04375

228. Darband SG, Sadighparvar S, Yousefi B, et al (2020) Quercetin attenuated oxidative DNA damage through NRF2 signaling pathway in rats with DMH induced colon carcinogenesis. Life Sci 117584. https://doi.org/10.1016/j.lfs.2020.117584

229. Lu X, Chen D, Yang F, Xing N (2020) Quercetin inhibits epithelial-to-mesenchymal transition (EMT) process and promotes apoptosis in prostate cancer via downregulating lncRNA MALAT1. Cancer Manag Res 12:1741–1750. https://doi.org/10.2147/CMAR.S241093

230. Teekaraman D, Elayapillai SP, Viswanathan MP, Jagadeesan A (2019) Quercetin inhibits human metastatic ovarian cancer cell growth and modulates components of the intrinsic apoptotic pathway in PA-1 cell line. Chem Biol Interact 300:91–100. https://doi.org/10.1016/j.cbi.2019.01.008

231. Kim SH, Yoo ES, Woo JS, et al (2019) Antitumor and apoptotic effects of quercetin on human melanoma cells involving JNK/P38 MAPK signaling activation. Eur J Pharmacol 860:172568. https://doi.org/10.1016/j.ejphar.2019.172568

232. Li X, Guo S, Xiong XK, et al (2019) Combination of quercetin and cisplatin enhances apoptosis in OSCC cells by downregulating xIAP through the NF-kB pathway. J Cancer 10:4509–4521. https://doi.org/10.7150/jca.31045

233. Li S, Pei Y, Wang W, et al (2019) Quercetin suppresses the proliferation and metastasis of metastatic osteosarcoma cells by inhibiting parathyroid hormone receptor 1. Biomed Pharmacother 114:108839. https://doi.org/10.1016/j.biopha.2019.108839

234. Erdogan S, Turkekul K, Dibirdik I, et al (2018) Midkine downregulation increases the efficacy of quercetin on prostate cancer stem cell survival and migration through PI3K/AKT and MAPK/ERK pathway. Biomed Pharmacother 107:793–805. https://doi.org/10.1016/j.biopha.2018.08.061

235. Li X, Zhou N, Wang J, et al (2018) Quercetin suppresses breast cancer stem cells (CD44+/CD24−) by inhibiting the PI3K/Akt/mTOR-signaling pathway. Life Sci 196:56–62. https://doi.org/10.1016/j.lfs.2018.01.014

236. Lee KM, Kang JH, Yun M, Lee SB (2018) Quercetin inhibits the poly(dA:dT)-induced secretion of IL-18 via down-regulation of the expressions of AIM2 and pro-caspase-1 by inhibiting the JAK2/STAT1 pathway in IFN-γ-primed human keratinocytes. Biochem Biophys Res Commun 503:116–122. https://doi.org/10.1016/j.bbrc.2018.05.191

237. Jia L, Huang S, Yin X, et al (2018) Quercetin suppresses the mobility of breast cancer by suppressing glycolysis through Akt-mTOR pathway mediated autophagy induction. Life Sci 208:123–130. https://doi.org/10.1016/j.lfs.2018.07.027

238. Chang JL, Chow JM, Chang JH, et al (2017) Quercetin simultaneously induces G0/G1-phase arrest and caspase-mediated crosstalk between apoptosis and autophagy in human leukemia HL-60 cells. Environ Toxicol 32:1857–1868. https://doi.org/10.1002/tox.22408

239. Lei CS, Hou YC, Pai MH, et al (2018) Effects of quercetin combined with anticancer drugs on metastasis-associated factors of gastric cancer cells: in vitro and in vivo studies. J Nutr Biochem 51:105–113. https://doi.org/10.1016/j.jnutbio.2017.09.011

240. Lan H, Hong W, Fan P, et al (2017) Quercetin Inhibits Cell Migration and Invasion in Human Osteosarcoma Cells. Cell Physiol Biochem 43:553–567. https://doi.org/10.1159/000480528

241. Song W, Zhao X, Xu J, Zhang H (2017) Quercetin inhibits angiogenesis–mediated human retinoblastoma growth by targeting vascular endothelial growth factor receptor. Oncol Lett 14:3343–3348. https://doi.org/10.3892/ol.2017.6623

242. Yu D, Ye T, Xiang Y, et al (2017) Quercetin inhibits epithelial-mesenchymal transition, decreases invasiveness and metastasis, and reverses IL-6 induced epithelial-mesenchymal transition, expression of MMP by inhibiting STAT3 signaling in pancreatic cancer cells. Onco Targets Ther 10:4719–4729. https://doi.org/10.2147/OTT.S136840

243. Seo HS, Ku JM, Choi HS, et al (2016) Quercetin induces caspase-dependent extrinsic apoptosis through inhibition of signal transducer and activator of transcription 3 signaling in HER2-overexpressing BT-474 breast cancer cells. Oncol Rep 36:31–42. https://doi.org/10.3892/or.2016.4786

244. Srivastava S, Somasagara RR, Hegde M, et al (2016) Quercetin, a natural flavonoid interacts with DNA, arrests cell cycle and causes tumor regression by activating mitochondrial pathway of apoptosis. Sci Rep 6:1–13. https://doi.org/10.1038/srep24049

245. Kee JY, Han YH, Kim DS, et al (2016) Inhibitory effect of quercetin on colorectal lung

metastasis through inducing apoptosis, and suppression of metastatic ability. Phytomedicine 23:1680–1690. https://doi.org/10.1016/j.phymed.2016.09.011

246. Lim W, Yang C, Park S, et al (2017) Inhibitory Effects of Quercetin on Progression of Human Choriocarcinoma Cells Are Mediated Through PI3K/AKT and MAPK Signal Transduction Cascades. J Cell Physiol 232:1428–1440. https://doi.org/10.1002/jcp.25637

247. Rivera AR, Castillo-Pichardo L, Gerena Y, Dharmawardhane S (2016) Anti-breast cancer potential of quercetin via the AkT/AMPK/mammalian target of rapamycin (mTOR) signaling cascade. PLoS One 11:1–20. https://doi.org/10.1371/journal.pone.0157251

248. Refolo MG, D'Alessandro R, Malerba N, et al (2015) Anti Proliferative and Pro Apoptotic Effects of Flavonoid Quercetin Are Mediated by CB1 Receptor in Human Colon Cancer Cell Lines. J Cell Physiol 230:2973–2980. https://doi.org/10.1002/jcp.25026

249. Ranganathan S, Halagowder D, Sivasithambaram ND (2015) Quercetin suppresses twist to induce apoptosis in MCF-7 breast cancer cells. PLoS One 10:1–21. https://doi.org/10.1371/journal.pone.0141370

250. Lee WJ, Hsiao M, Chang JL, et al (2015) Quercetin induces mitochondrial-derived apoptosis via reactive oxygen species-mediated ERK activation in HL-60 leukemia cells and xenograft. Arch Toxicol 89:1103–1117. https://doi.org/10.1007/s00204-014-1300-0

251. Omidian K, Rafiei H, Bandy B (2020) Increased mitochondrial content and function by resveratrol and select flavonoids protects against benzo[a]pyrene-induced bioenergetic dysfunction and ROS generation in a cell model of neoplastic transformation. Free Radic Biol Med. https://doi.org/10.1016/j.freeradbiomed.2020.01.021

252. Khusbu FY, Zhou X, Roy M, et al (2020) Resveratrol induces depletion of TRAF6 and suppresses prostate cancer cell proliferation and migration. Int J Biochem Cell Biol 118:105644. https://doi.org/10.1016/j.biocel.2019.105644

253. Chatterjee B, Ghosh K, Kanade SR (2019) Resveratrol modulates epigenetic regulators of promoter histone methylation and acetylation that restores BRCA1, p53, p21CIP1 in human breast cancer cell lines. BioFactors 45:818–829. https://doi.org/10.1002/biof.1544

254. Chen KY, Chen CC, Chang YC, Chang MC (2019) Resveratrol induced premature senescence and inhibited epithelial-mesenchymal transition of cancer cells via induction of tumor suppressor Rad9. PLoS One 14:1–17. https://doi.org/10.1371/journal.pone.0219317

255. Hu C, Liu Y, Teng M, et al (2019) Resveratrol inhibits the proliferation of estrogen receptor-positive breast cancer cells by suppressing EZH2 through the modulation of ERK1/2 signaling. Cell Biol Toxicol 35:445–456. https://doi.org/10.1007/s10565-019-09471-x

256. Fonseca J, Moradi F, Maddalena LA, et al (2019) Resveratrol integrates metabolic and growth effects in PC3 prostate cancer cells-involvement of prolyl hydroxylase and hypoxia inducible factor-1. Oncol Lett 17:697–705. https://doi.org/10.3892/ol.2018.9526

257. Izquierdo-Torres E, Hernández-Oliveras A, Meneses-Morales I, et al (2019)

Resveratrol up-regulates ATP2A3 gene expression in breast cancer cell lines through epigenetic mechanisms. Int J Biochem Cell Biol 113:37–47. https://doi.org/10.1016/j.biocel.2019.05.020

258. Liu Z, Wu X, Lv J, et al (2019) Resveratrol induces p53 in colorectal cancer through SET7/9. Oncol Lett 17:3783–3789. https://doi.org/10.3892/ol.2019.10034

259. Sun Y, Zhou QM, Lu YY, et al (2019) Resveratrol inhibits the migration and metastasis of MDA-MB-231 human breast cancer by reversing TGF-β1-induced epithelial-mesenchymal transition. Molecules 24:1–16. https://doi.org/10.3390/molecules24061131

260. Wu H, Chen L, Zhu F, et al (2019) The cytotoxicity effect of resveratrol: Cell cycle arrest and induced apoptosis of breast cancer 4T1 cells. Toxins (Basel) 11:1–20. https://doi.org/10.3390/toxins11120731

261. Zhang W, Jiang H, Chen Y, Ren F (2019) Resveratrol chemosensitizes adriamycin-resistant breast cancer cells by modulating miR-122-5p. J Cell Biochem 120:16283–16292. https://doi.org/10.1002/jcb.28910

262. Cipolletti M, Montalesi E, Nuzzo MT, et al (2019) Potentiation of paclitaxel effect by resveratrol in human breast cancer cells by counteracting the 17β-estradiol/estrogen receptor α/neuroglobin pathway. J Cell Physiol 234:3147–3157. https://doi.org/10.1002/jcp.27309

263. Cheng L, Yan B, Chen K, et al (2018) Resveratrol-induced downregulation of NAF-1 enhances the sensitivity of pancreatic cancer cells to gemcitabine via the ROS/Nrf2 signaling pathways. Oxid Med Cell Longev 2018:. https://doi.org/10.1155/2018/9482018

264. Chung SS, Dutta P, Austin D, et al (2018) Combination of resveratrol and 5-flurouracil enhanced antitelomerase activity and apoptosis by inhibiting STAT3 and Akt signaling pathways in human colorectal cancer cells. Oncotarget 9:32943–32957. https://doi.org/10.18632/oncotarget.25993

265. Dai H, Deng HB, Wang YH, Guo JJ (2018) Resveratrol inhibits the growth of gastric cancer via the wnt/β-catenin pathway. Oncol Lett 16:1579–1583. https://doi.org/10.3892/ol.2018.8772

266. Fan Y, Chiu JF, Liu J, et al (2018) Resveratrol induces autophagy-dependent apoptosis in HL-60 cells. BMC Cancer 18:1–10. https://doi.org/10.1186/s12885-018-4504-5

267. Fudhaili A, Yoon NA, Kang S, et al (2019) Resveratrol epigenetically regulates the expression of zinc finger protein 36 in non-small cell lung cancer cell lines. Oncol Rep 41:1377–1386. https://doi.org/10.3892/or.2018.6898

268. Jin HG, Wu GZ, Wu GH, Bao YG (2018) Combining the mammalian target of rapamycin inhibitor, rapamycin, with resveratrol has a synergistic effect in multiple myeloma. Oncol Lett 15:6257–6264. https://doi.org/10.3892/ol.2018.8178

269. Martínez-Martínez D, Soto A, Gil-Araujo B, et al (2019) Resveratrol promotes apoptosis through the induction of dual specificity phosphatase 1 and sensitizes prostate cancer cells to cisplatin. Food Chem Toxicol 124:273–279.

https://doi.org/10.1016/j.fct.2018.12.014

270. Suh J, Kim DH, Surh YJ (2018) Resveratrol suppresses migration, invasion and stemness of human breast cancer cells by interfering with tumor-stromal cross-talk. Arch Biochem Biophys 643:62–71. https://doi.org/10.1016/j.abb.2018.02.011

271. Zhou C, Qian W, Ma J, et al (2019) Resveratrol enhances the chemotherapeutic response and reverses the stemness induced by gemcitabine in pancreatic cancer cells via targeting SREBP1. Cell Prolif 52:1–12. https://doi.org/10.1111/cpr.12514

272. Wu X, Xu Y, Zhu B, et al (2018) Resveratrol induces apoptosis in SGC-7901 gastric cancer cells. Oncol Lett 16:2949–2956. https://doi.org/10.3892/ol.2018.9045

273. Yan B, Cheng L, Jiang Z, et al (2018) Resveratrol Inhibits ROS-Promoted Activation and Glycolysis of Pancreatic Stellate Cells via Suppression of miR-21. Oxid Med Cell Longev 2018:1346958. https://doi.org/10.1155/2018/1346958

274. Yang HC, Wang JY, Bu XY, et al (2019) Resveratrol restores sensitivity of glioma cells to temozolamide through inhibiting the activation of Wnt signaling pathway. J Cell Physiol 234:6783–6800. https://doi.org/10.1002/jcp.27409

275. Li L, Qiu RL, Lin Y, et al (2018) Resveratrol suppresses human cervical carcinoma cell proliferation and elevates apoptosis via the mitochondrial and p53 signaling pathways. Oncol Lett 15:9845–9851. https://doi.org/10.3892/ol.2018.8571

276. Kim SH, Cho KH, Kim YN, et al (2016) Resveratrol attenuates norepinephrine-induced ovarian cancer invasiveness through downregulating hTERT expression. Arch Pharm Res 39:240–248. https://doi.org/10.1007/s12272-015-0666-8

277. Jing X, Cheng W, Wang S, et al (2016) Resveratrol induces cell cycle arrest in human gastric cancer MGC803 cells via the PTEN-regulated PI3K/Akt signaling pathway. Oncol Rep 35:472–478. https://doi.org/10.3892/or.2015.4384

278. Yang Y, Cui J, Xue F, et al (2016) Resveratrol Represses Pokemon Expression in Human Glioma Cells. Mol Neurobiol 53:1266–1278. https://doi.org/10.1007/s12035-014-9081-2

279. Ji Q, Liu X, Han Z, et al (2015) Resveratrol suppresses epithelial-to-mesenchymal transition in colorectal cancer through TGF-β1/Smads signaling pathway mediated Snail/E-cadherin expression. BMC Cancer 15:1–12. https://doi.org/10.1186/s12885-015-1119-y

280. Wang Z, Zhang L, Ni Z, et al (2015) Resveratrol induces AMPK-dependent MDR1 inhibition in colorectal cancer HCT116/L-OHP cells by preventing activation of NF-κB signaling and suppressing cAMP-responsive element transcriptional activity. Tumor Biol 36:9499–9510. https://doi.org/10.1007/s13277-015-3636-3

281. Demoulin B, Hermant M, Castrogiovanni C, et al (2015) Resveratrol induces DNA damage in colon cancer cells by poisoning topoisomerase II and activates the ATM kinase to trigger p53-dependent apoptosis. Toxicol Vitr 29:1156–1165. https://doi.org/10.1016/j.tiv.2015.04.015

282. Buhrmann C, Shayan P, Kraehe P, et al (2015) Resveratrol induces chemosensitization to 5-fluorouracil through up-regulation of intercellular junctions, Epithelial-to-mesenchymal transition and apoptosis in colorectal cancer. Biochem Pharmacol 98:51–68. https://doi.org/10.1016/j.bcp.2015.08.105

283. Abdel-Latif GA, Al-Abd AM, Tadros MG, et al (2015) The chemomodulatory effects of resveratrol and didox on herceptin cytotoxicity in breast cancer cell lines. Sci Rep 5:1–13. https://doi.org/10.1038/srep12054

284. Gwak H, Haegeman G, Tsang BK, Song YS (2015) Cancer-specific interruption of glucose metabolism by resveratrol is mediated through inhibition of Akt/GLUT1 axis in ovarian cancer cells. Mol Carcinog 54:1529–1540. https://doi.org/10.1002/mc.22227

285. Gao Q, Yuan Y, Gan H, Peng Q (2015) Resveratrol inhibits the hedgehog signaling pathway and epithelial-mesenchymal transition and suppresses gastric cancer invasion and metastasis. Oncol Lett 9:2381–2387. https://doi.org/10.3892/ol.2015.2988

286. Wu XP, Xiong M, Xu CS, et al (2015) Resveratrol induces apoptosis of human chronic myelogenous leukemia cells in vitro through p38 and JNK-regulated H2AX phosphorylation. Acta Pharmacol Sin 36:353–361. https://doi.org/10.1038/aps.2014.132

287. Ma L, Li W, Wang R, et al (2015) Resveratrol enhanced anticancer effects of cisplatin on non-small cell lung cancer cell lines by inducing mitochondrial dysfunction and cell apoptosis. Int J Oncol 47:1460–1468. https://doi.org/10.3892/ijo.2015.3124

288. Nie P, Hu W, Zhang T, et al (2015) Synergistic induction of erlotinib-mediated apoptosis by resveratrol in human non-small-cell lung cancer cells by down-regulating survivin and up-regulating PUMA. Cell Physiol Biochem 35:2255–2271. https://doi.org/10.1159/000374030

289. Alayev A, Berger SM, Kramer MY, et al (2015) The Combination of Rapamycin and Resveratrol Blocks Autophagy and Induces Apoptosis in Breast Cancer Cells. J Cell Biochem 116:450–457. https://doi.org/doi:10.1002/jcb.24997

290. Gil-Martins E, Barbosa DJ, Silva V, et al (2020) Dysfunction of ABC transporters at the blood-brain barrier: Role in neurological disorders. Pharmacol Ther 107554. https://doi.org/10.1016/j.pharmthera.2020.107554

291. Li Y, Revalde J, Paxton JW (2017) The effects of dietary and herbal phytochemicals on drug transporters. Adv Drug Deliv Rev 116:45–62. https://doi.org/10.1016/j.addr.2016.09.004

292. Huang W, Wan C, Luo Q, et al (2014) Genistein-inhibited cancer stem cell-like properties and reduced chemoresistance of gastric cancer. Int J Mol Sci 15:3432–3443. https://doi.org/10.3390/ijms15033432

293. Rigalli JP, Ciriaci N, Arias A, et al (2015) Regulation of multidrug resistance proteins by genistein in a hepatocarcinoma cell line: Impact on sorafenib cytotoxicity. PLoS One 10:1–19. https://doi.org/10.1371/journal.pone.0119502

294. Rigalli JP, Tocchetti GN, Arana MR, et al (2016) The phytoestrogen genistein enhances multidrug resistance in breast cancer cell lines by translational regulation of ABC transporters. Cancer Lett 376:165–172. https://doi.org/10.1016/j.canlet.2016.03.040

295. Semeniuk M, Ceré LI, Ciriaci N, et al (2020) Regulation of hepatic P-gp expression and activity by genistein in rats. Arch Toxicol 94:1625–1635. https://doi.org/10.1007/s00204-020-02708-3

296. Yang Y, Bai L, Li X, et al (2014) Transport of active flavonoids, based on cytotoxicity and lipophilicity: An evaluation using the blood-brain barrier cell and Caco-2 cell models. Toxicol Vitr 28:388–396. https://doi.org/10.1016/j.tiv.2013.12.002

297. He Y, Ci X, Xie Y, et al (2019) Potential detoxification effect of active ingredients in liquorice by upregulating efflux transporter. Phytomedicine 56:175–182. https://doi.org/10.1016/j.phymed.2018.10.033

298. Liu T, Zhang X, Zhang Y, et al (2018) Sulfation disposition of liquiritigenin in SULT1A3 overexpressing HEK293 cells: The role of breast cancer resistance protein (BCRP) and multidrug resistance-associated protein 4 (MRP4) in sulfate efflux of liquiritigenin. Eur J Pharm Sci 124:228–239. https://doi.org/10.1016/j.ejps.2018.08.041

299. Landen JW, Hau V, Wang M, et al (2004) Noscapine crosses the blood-brain barrier and inhibits glioblastoma growth. Clin Cancer Res 10:5187–5201. https://doi.org/10.1158/1078-0432.CCR-04-0360

300. Muthiah D, Henshaw GK, DeBono AJ, et al (2019) Overcoming P-glycoprotein–mediated drug resistance with noscapine derivatives S. Drug Metab Dispos 47:164–172. https://doi.org/10.1124/dmd.118.083188

301. Kaur M, Badhan RKS (2015) Phytoestrogens modulate breast cancer resistance protein expression and function at the blood-cerebrospinal fluid barrier. J Pharm Pharm Sci 18:132–154. https://doi.org/10.18433/j3p31k

302. Kaur M, Badhan RKS (2017) Phytochemical mediated-modulation of the expression and transporter function of breast cancer resistance protein at the blood-brain barrier: An in-vitro study. Brain Res 1654:9–23. https://doi.org/10.1016/j.brainres.2016.10.020

303. Basseville A, Hall MD, Chau CH, et al (2016) The ABCG2 Multidrug Transporter. In: A. G (ed) ABC Transporters - 40 Years on. Springer, Cham, pp 195–226

304. Halwachs S, Lakoma C, Schafer I, et al (2011) The Antiepileptic Drugs Phenobarbital and Carbamazepine Reduce Transport of Methotrexate in Rat Choroid Plexus by Down-Regulation of the Reduced Folate Carrier. Mol Pharmacol 80:621–629. https://doi.org/10.1124/mol.111.072421

305. An G, Gallegos J, Morris ME (2011) The bioflavonoid kaempferol is an Abcg2 substrate and inhibits Abcg2-mediated quercetin efflux. Drug Metab Dispos 39:426–432. https://doi.org/10.1124/dmd.110.035212

306. Redan BW, Albaugh GP, Charron CS, et al (2017) Adaptation in Caco-2 Human

Intestinal Cell Differentiation and Phenolic Transport with Chronic Exposure to Blackberry (Rubus sp.) Extract. J Agric Food Chem 65:2694–2701. https://doi.org/10.1021/acs.jafc.7b00027

307. Ravisankar S, Agah S, Kim H, et al (2019) Combined cereal and pulse flavonoids show enhanced bioavailability by downregulating phase II metabolism and ABC membrane transporter function in Caco-2 model. Food Chem 279:88–97. https://doi.org/10.1016/j.foodchem.2018.12.006

308. El-Readi MZ, Eid SY, Abdelghany AA, et al (2019) Resveratrol mediated cancer cell apoptosis, and modulation of multidrug resistance proteins and metabolic enzymes. Phytomedicine 55:269–281. https://doi.org/10.1016/j.phymed.2018.06.046

309. Jia Y, Liu Z, Huo X, et al (2015) Enhancement effect of resveratrol on the intestinal absorption of bestatin by regulating PEPT1, MDR1 and MRP2 in vivo and in vitro. Int J Pharm 495:588–598. https://doi.org/10.1016/j.ijpharm.2015.09.042

310. Jia Y, Liu Z, Wang C, et al (2016) P-gp, MRP2 and OAT1/OAT3 mediate the drug-drug interaction between resveratrol and methotrexate. Toxicol Appl Pharmacol 306:27–35. https://doi.org/10.1016/j.taap.2016.06.030

311. Huang F, Wu XN, Chen J, et al (2014) Resveratrol reverses multidrug resistance in human breast cancer doxorubicin-resistant cells. Exp Ther Med 7:1611–1616. https://doi.org/10.3892/etm.2014.1662

312. Han Y-S, Bastianetto S, Dumont Y, Quirion R (2006) Specific Plasma Membrane Binding Sites for Polyphenols, Including Resveratrol, in the Rat Brain. J Pharmacol Exp Ther 318:238–245. https://doi.org/10.1124/jpet.106.102319

313. Cooray HC, Janvilisri T, Van Veen HW, et al (2004) Interaction of the breast cancer resistance protein with plant polyphenols. Biochem Biophys Res Commun 317:269–275. https://doi.org/10.1016/j.bbrc.2004.03.040

314. Zhang R, Lu M, Zhang Z, et al (2016) Resveratrol reverses P-glycoprotein-mediated multidrug resistance of U2OS/ADR cells by suppressing the activation of the NF-κB and p38 MAPK signaling pathways. Oncol Lett 12:4147–4154. https://doi.org/10.3892/ol.2016.5136

315. Cooray HC, Blackmore CG, Maskell L, Barrand MA (2002) Localisation of breast cancer resistance protein in microvessel endothelium of human brain. Neuroreport 13:2059–2063. https://doi.org/10.1097/00001756-200211150-00014

316. Wang Q, Xu J, Rottinghaus GE, et al (2002) Resveratrol protects against global cerebral ischemic injury in gerbils. Brain Res 958:439–447. https://doi.org/10.1016/s0006-8993(02)03543-6

317. Turner RS, Thomas RG, Craft S, et al (2015) A randomized, double-blind, placebo-controlled trial of resveratrol for Alzheimer disease. Neurology 85:1383–1391. https://doi.org/10.1212/wnl.0000000000002035

318. de Oliveira Júnior RG, Christiane Adrielly AF, da Silva Almeida JRG, et al (2018)

Sensitization of tumor cells to chemotherapy by natural products: A systematic review of preclinical data and molecular mechanisms. Fitoterapia 129:383–400. https://doi.org/10.1016/j.fitote.2018.02.025

319. Ferreira A, Rodrigues M, Fortuna A, et al (2018) Flavonoid compounds as reversing agents of the P-glycoprotein-mediated multidrug resistance: An in vitro evaluation with focus on antiepileptic drugs. Food Res Int 103:110–120. https://doi.org/10.1016/j.foodres.2017.10.010

320. Fleisher B, Unum J, Shao J, An G (2015) Ingredients in fruit juices interact with dasatinib through inhibition of BCRP: A new mechanism of beverage-drug interaction. J Pharm Sci 104:266–275. https://doi.org/10.1002/jps.24289

321. Li S, Zhao Q, Wang B, et al (2018) Quercetin reversed MDR in breast cancer cells through down-regulating P-gp expression and eliminating cancer stem cells mediated by YB-1 nuclear translocation. Phyther Res 32:1530–1536. https://doi.org/10.1002/ptr.6081

322. Chen Z, Huang C, Ma T, et al (2018) Reversal effect of quercetin on multidrug resistance via FZD7/β-catenin pathway in hepatocellular carcinoma cells. Phytomedicine 43:37–45. https://doi.org/10.1016/j.phymed.2018.03.040

323. Adler E, Hoon MA, Mueller KL, et al (2000) A novel family of mammalian taste receptors. Cell 100:693–702. https://doi.org/10.1016/S0092-8674(00)80705-9

324. Chandrashekar J, Mueller KL, Hoon MA, et al (2000) T2Rs function as bitter taste receptors. Cell 100:703–711. https://doi.org/10.1016/s0092-8674(00)80706-0

325. Chandrashekar J, Hoon MA, Ryba NJP, Zuker CS (2006) The receptors and cells for mammalian taste. Nature 444:288–294. https://doi.org/10.1038/nature05401

326. Panche AN, Diwan AD, Chandra SR (2016) Flavonoids: An overview. J Nutr Sci 5:. https://doi.org/10.1017/jns.2016.41

327. Dalesio NM, Barreto Ortiz SF, Pluznick JL, Berkowitz DE (2018) Olfactory, Taste, and Photo Sensory Receptors in Non-sensory Organs: It Just Makes Sense. Front Physiol 9:1673–1691. https://doi.org/10.3389/fphys.2018.01673

328. Lee SJ, Depoortere I, Hatt H (2019) Therapeutic potential of ectopic olfactory and taste receptors. Nat Rev Drug Discov 18:116–138. https://doi.org/10.1038/s41573-018-0002-3

329. Hariri BM, McMahon DB, Chen B, et al (2017) Flavones modulate respiratory epithelial innate immunity: Anti-inflammatory effects and activation of the T2R14 receptor. J Biol Chem 292:8484–8497. https://doi.org/10.1074/jbc.M116.771949

330. Wang Y, Wang A, Zhang M, et al (2019) Artesunate attenuates airway resistance in vivo and relaxes airway smooth muscle cells in vitro via bitter taste receptor-dependent calcium signalling. Exp Physiol 104:231–243. https://doi.org/10.1113/EP086824

331. Grassin-Delyle S, Salvator H, Mantov N, et al (2019) Bitter Taste Receptors (TAS2Rs) in Human Lung Macrophages: Receptor Expression and Inhibitory Effects of TAS2R Agonists. Front Physiol 10:1–13. https://doi.org/10.3389/fphys.2019.01267

332. Seo Y, Kim YS, Lee KE, et al (2017) Anti-cancer stemness and anti-invasive activity of bitter taste receptors, TAS2R8 and TAS2R10, in human neuroblastoma cells. PLoS One 12:1–20. https://doi.org/10.1371/journal.pone.0176851

333. Singh N, Shaik FA, Myal Y, Chelikani P (2020) Chemosensory bitter taste receptors T2R4 and T2R14 activation attenuates proliferation and migration of breast cancer cells. Mol Cell Biochem 465:199–214. https://doi.org/10.1007/s11010-019-03679-5

334. Jeon T Il, Seo YK, Osborne TF (2011) Gut bitter taste receptor signalling induces ABCB1 through a mechanism involving CCK. Biochem J 438:33–37. https://doi.org/10.1042/BJ20110009

Chapter 3

Global Aims

3. Global Aims

The brain barriers are important gatekeepers of the CNS. However, these structures hinder the access of many drugs to the CNS compromising the treatment of brain diseases. Among the drugs with therapeutic potential for brain diseases are several bitter compounds. However, data about the transport of these compounds across the brain barriers and its accumulation in brain cells is still scarce.

One major brain barrier is the BCSFB established by CP epithelial cells that display transport and detox systems that largely contribute for drug resistance. Therefore, understanding the mechanisms involved in the chemical surveillance of blood and CSF and unveiling possible modulators of these systems is crucial to overcome pharmacoresistance. Recently, we discovered that the bitter taste signalling pathway is expressed and functional in rat CP raising some questions that we intended to answer. Therefore, the main goal of this doctoral thesis was to characterize the bitter taste signalling pathway in the human BCSFB.

The specific aims of this thesis were:

- Confirm and identify which bitter taste receptors (TAS2Rs) are expressed in the human BCSFB;
- Analyze the functionality of TAS2Rs expressed in the human BCSFB;
- Evaluate the role of TAS2Rs in the transport of bitter ligands across the human BCSFB.

Chapter 4

Research Work 1

Bitter taste receptors profiling in the human blood-cerebrospinal fluid-barrier

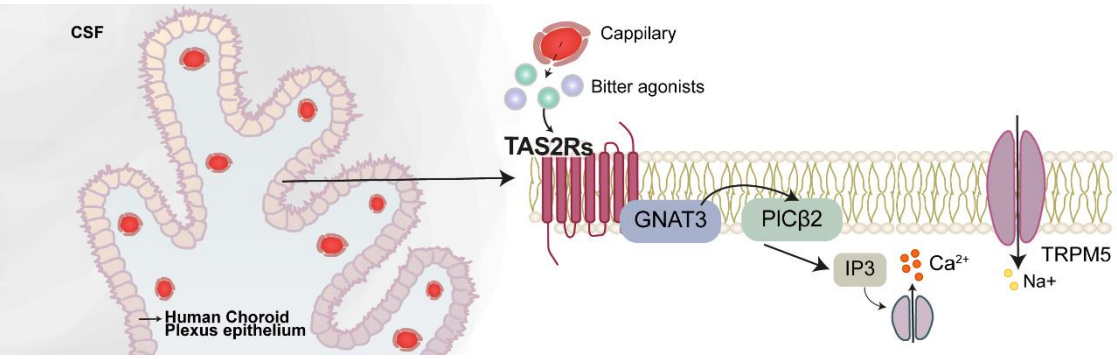

This chapter corresponds to the original research article:

Duarte AC, Santos J, Costa AR, Ferreira CL, Tomás J, Quintela T, Ishikawa H, Schwerk C, Schroten H, Ferrer I, Carro E, Gonçalves I, Santos CRA (2020). Bitter taste receptors profiling in the human blood-cerebrospinal fluid-barrier, Biochemical Pharmacology, https://doi.org/10.1016/j.bcp.2020.113954

4.1. Abstract

The choroid plexus (CP) epithelial cells establish an important blood-brain interface, the blood-cerebrospinal fluid barrier (BCSFB), which constitutes a complementary gateway to the blood-brain-barrier for the entrance of several molecules into the central nervous system (CNS). However, the mechanisms that operate at the BCSFB to regulate the molecular traffic are still poorly understood. The taste signalling machinery, present in many extra-oral tissues, is involved in the chemical sensing of the composition of body fluids. We have identified this pathway in rat CP and hypothesised that it could also be present in the human BCSFB. In this study, we characterised the bitter taste receptors (TAS2Rs) expression profiling in human CP by combining data retrieved from available databases of the human CP transcriptome with its expression analysis in a human CP cell line and IHC of human CP sections from men and women. TAS2R4, 5, 14 and 39 expression was confirmed in human CP tissue by IHC and in HIBCPP cells by RT-PCR, immunofluorescence and Western blot. Moreover, the presence of downstream effector proteins GNAT3, PLCβ2 and TRPM5 was also detected in HIBCPP cells. Then, we demonstrated that HIBCPP cells respond to chloramphenicol via TAS2R39 and to quercetin via TAS2R14. Our findings support an active role of TAS2Rs at the human BCSFB, as surveyors of the bloodstream and CSF compositions. These findings open new avenues for studies on the uptake of relevant compounds for targeted therapies of the CNS.

Keywords: Choroid plexus; blood-cerebrospinal fluid barrier; taste signalling; bitter taste receptors

4.1. Introduction

The CPs, located in the ventricular system of the brain, are formed by single layers of cuboidal epithelial cells laying on a basement membrane. Bellow the basement membrane, within the connective tissue, lays a network of fenestrated capillaries, fibroblasts and immune cells imbedded in a rich extracellular matrix [1]. Several functions have been attributed to the CPs such as CSF formation, biosynthesis of proteins and hormones, clearance of harmful substances from the CSF, immune surveillance, neurogenesis, regulation of the circadian rhythm and chemical surveillance [2]. Notably, CP epithelial cells form a physical barrier between the blood and the CSF, the blood-CSF barrier (BCSFB). Due to the presence of tight junctions that connect the CP epithelial cells, the BCSFB extensively prevents paracellular transport between blood and CSF fluids, thus playing a critical role to ensure the homeostatic balance in the brain environment [3]. Additionally, molecular traffic regulation at the BCSFB is ensured by several influx and efflux transporters and detoxifying enzymes that are present in CP epithelial cells [3].

One of the challenges of modern pharmacology is to understand why many anticancer and other brain targeting drugs fail to reach the CNS at relevant therapeutic concentrations. This occurs mainly because these drugs, independently of their lipophilicity, are effluxed by transporters, such as ATP-binding cassette (ABC) transporters, preventing them from entering the brain circulation [4]. Although the BBB has been the focus of most research on the drug flux to the brain, in the last years, the BCSFB started to be widely studied since it displays a complex and effective detoxifying system and is an additional gateway to the brain [4–6]. Nonetheless, data regarding the regulation of these mechanisms at the BCSFB are still scarce. The presence of taste and olfactory transduction pathways was previously described in the rat CP epithelial cells [7,8] adding potential new players to the chemosensory machinery of the CP. Ultimately, their function may be related to the activation of downstream pathways such as those involved in drug transport and metabolism, as seen in other organs [9,10].

Taste receptors belong to the G-protein coupled receptors family that includes: type 1 taste receptors (TR1) and type 2 taste receptors (TR2). Three different TR1 subunits dimerize to recognize sweet (T1R2+T1R3) or umami (T1R1+T1R3) compounds [11,12]. On the other hand, humans recognize bitter compounds through 25 bitter taste receptors (TAS2Rs) [13,14]. In the mouth, TR1 or TR2s activation are similar and include the activation of the GNAT3, that activates PLCβ2 and induces the production of IP3 which triggers an increase in intracellular calcium levels. In turn, calcium elevation activates

the TRPM5 causing cell depolarization [15,16]. Currently it is well recognized that taste receptors are not restrained to the oral cavity. Instead, they are also expressed in many other organs [17,18]. The expression of taste receptors has been reported in the airways, gut, heart, thyroid and in the CNS [17] and in mouse [19] and rat CP [7]. The function of taste receptors in taste bud cells as sensors of the composition of food and beverages is well understood. However, in extra-oral tissues, studies on their function are still scarce and differ between the organs/tissues/cells analyzed [17,18,20]. However, there is already evidence that TAS2Rs mediate biological functions in response to internal and external chemical stimuli. For example, in the airways, TAS2Rs activation by flavones was related to enhanced anti-inflammatory responses and increased cytokine secretion [21], while artesunate improved bronchodilation [22]. In human neuroblastoma cells TAS2Rs activation mediated an increase in apoptosis and a decrease in cell survival and invasion [23]. Other biological functions, regulated by TAS2R activation include thyroid activity [24], gastrointestinal function [9], spermatogenesis [25] and innate immunity [26]. Bitter taste receptor agonists are numerous and structurally diverse: ions, peptides, alkaloids, polyphenols and glucosinolates [27,28]. Notably, some drugs with therapeutic applications bind and activate TAS2Rs, such as chloroquine (antimalarial), dextromethorphan (antitussive) or haloperidol (antipsycothic) [20]. Moreover, these compounds might be able to activate only a single or multiple TAS2Rs [27,28].

We have previously shown that the taste signalling pathway is present and functional in the rat CP [7]. Thus, we hypothesized that the taste transduction machinery, including TAS2Rs, could also be present in the human BCSFB, acting as chemosensors of the blood and CSF composition. Therefore, we investigated the presence and functionality of TAS2Rs in the human BCSFB. The expression of several bitter receptors was confirmed in human CP samples and in the human CP cell line HIBCPP that is a validated model of the BCSFB [29,30]. Bitter receptors TAS2R4, TAS2R5, TAS2R14 and TAS2R39 were found in both human CP and in HIBCPP cells. Moreover, among the receptors analyzed, TAS2R14, that binds several bitter agonists, presented higher protein levels. In summary, in the present work we were able to show both mRNA and protein expression of key components of the bitter taste signalling pathway in human CP epithelial cells. Additionally, calcium functional assays showed a specific activation of TAS2R14 and TAS2R39, in HIBCPP cells, by bitter quercetin and chloramphenicol stimulus, respectively.

4.2. Materials and Methods

4.2.1. Materials

Bitter compounds chloramphenicol, haloperidol and quercetin were purchased from Sigma-Aldrich (Merck, Portugal), and 3-(4,5-dimethylthiazol-2-yl)-2,5-diphenyltetrazolium bromide (MTT) from Gerbu Biotechnik GmbH (Germany). The primary antibodies, previously validated, rabbit -GNAT3 (sc-395) and -PLCβ2 (sc-206) were obtained from Santa Cruz Biotechnology (USA); rabbit TRPM5 (AB104566) from Abcam (UK); rabbit - TAS2R4 (RRID AB_2201090; OSR00153W), -TAS2R5 (RRID AB_2287162; OSR00154W), -TAS2R10 (RRID AB_2556259; PA5-39708), -TAS2R14 (RRID AB_2556261; PA5-39710), -TAS2R39 (RRID AB_2556262; PA5-39711) from Fisher Thermo Scientific; and mouse β-actin (A1978) from Sigma-Aldrich (Merck, Portugal). Secondary antibodies goat anti-rabbit HRP-conjugated (sc-2004) and goat anti-mouse HRP-conjugated (sc-2005) were purchased from Santa Cruz Biotechnology (USA); donkey anti-rat Cy3 from Jackson Immunoresearch (UK), goat anti-rabbit Alexa Fluor® 488 from Thermo Fisher Scientific (RRID AB_143165; A11008, Molecular Probes, USA). FURA-2AM, pluronic acid F-127, Lipofectamine™ 2000 (11668027), Opti-MEM medium and small interfering RNA (siRNA) targeting TAS2R14 (s27144), TAS2R39 (s48942) and scramble siRNA (4390843) were purchased in Thermo Fisher Scientific (USA).

A stock solution of each bitter compound was prepared in dimethyl sulfoxide (DMSO), and freshly dissolved in Tyrode´s solution or culture medium before the experiments, where the DMSO final concentration did not exceed 0.20%.

4.2.2. Microarray data analysis

Since TAS2Rs expression in human CP has not been investigated before, we performed an initial search in transcriptomic data available of human CP in order to exploit this hypothesis. For that, microarray data related to human CP transcriptomics was obtained from a genomics data repository (GEO – Gene Expression Omnibus). An *in silico* analysis on TAS2Rs expression in human CP was performed with data retrieved from the expression profile of human CP epithelium of seven male healthy donors (51-73 years old) (accession number: GSE49974, [31]), and from another one containing the expression profile of the human CP cell line HIBCPP (accession number: GSE42870, [32]). Briefly, we searched for TAS2Rs genes in the two databases, and the mean values of TAS2Rs expression were calculated for all the available human CP samples (N=7), and HIBCPP cells (N=3). Validation of these data was further processed by IHC, in human CP sections, and by Reverse Transcription-Polymerase Chain Reaction (RT-PCR), immunofluorescence and Western blot, in the human CP cell line HIBCPP.

4.2.3. Immunohistochemistry

Cases for IHC study were obtained from the Institute of Neuropathology Brain Bank (HUB-ICO-IDIBELL Biobank) following the guidelines of the Spanish legislation on this matter (Real Decreto 1716/2011) and the approval of the local ethics committee of the Bellvitge University Hospital-IDIBELL. CP samples were fixed in buffered formalin for no less than 3 weeks and then embedded in paraffin. These were from four males aged 52, 62, 67 and 69, and one woman 81 years old. The neuropathological study of the brain disclosed no associated neurodegenerative and vascular alterations excepting early stages of neurofibrillary tangle degeneration (Braak stage I-II) and small blood vessel disease in older cases.

Paraffin-embedded human CP slices from men and women were pretreated with Trilogy™ (Cell Marque™, Millipore Sigma, Portugal) which combines deparaffinization, rehydration and unmasking, in accordance with manufacture recommendations. After washing with Tris-buffered saline containing 0.1% of Tween 20 (TBS-T), endogenous peroxidases activity were blocked with 3% H_2O_2 for 10 min at RT. Slices were then washed twice with TBS-T. Next, slices were incubated for 1h at RT with the following primary antibodies: rabbit TAS2R4 (1:500), TAS2R5 (1:500), TAS2R10 (1:300), TAS2R14 (1:100) or TAS2R39 (1:300). Slices were washed twice with TBS-T and treated with HiDef Detection™ HRP Polymer System (Cell Marque™, Millipore Sigma, Portugal). First, HiDef Detection™ Amplifier was applied in the human CP slices for 10 min RT, washed twice with TBS-T, followed by HiDef Detection™ HRP Polymer Detector also for 10 min at RT. After slices washing with TBS-T, immunoreactivity was detected with diaminobenzidine (DAB) for 10 min, RT. Slices were washed twice with TBS-T. Next, tissue sections were stained with Hematoxylin for 3 min RT to allow nuclei visualization. Negative control slices were treated under the same conditions without primary antibody. After dehydration, the slices were mounted and the images were acquired in a Zeiss Primo Star microscope (Carl Zeiss, Germany) using a magnification of 40x.

4.2.4. Cell Culture

Experiments were performed using the Human epithelial CP papilloma (HIBCPP) cell line derived from a human malignant CP papilloma [33]. HIBCPP cells were cultured in Dulbecco's Modified Eagle Medium: nutrient mixture F-12 (DMEM/F12, Pan-Biotech, Germany) supplemented with 5 µg/mL insulin (Sigma-Aldrich, Merck, Portugal), 4 mM L-glutamine, 100 U/mL penicillin, 100 µg/mL streptomycin and 10% (v/v) fetal bovine

serum (FBS). For all studies here described, HIBCPP cells were used between passage 26 and 33.

4.2.5. RT-PCR

To validate TAS2Rs expression in human CP, total RNA was isolated from HIBCPP cells using TRI Reagent (Sigma-Aldrich, Merck, Portugal) following the manufacturer's instructions. After treatment with DNAse I (Sigma-Aldrich, Merck, Portugal), 500 ng of total RNA was reverse transcribed using a M-MLV Reverse Transcriptase (NZYTech, Ltd., Portugal). For the RT-PCR, cDNA was amplified by KAPA2G Fast ReadyMix PCR Kit (Sigma-Aldrich, Merck, Portugal) and specific primers targeting 21 TAS2R (Table 1) in a final volume of 25 µL. Specific primer design for TAS2R43, 45 and 46 was not possible due to high homology shared between these receptors. Also, TAS2R30/47 was not detected in the microarrays data thus its expression was not analyzed. For the remaining TAS2Rs, every set of RT-PCR included a control without cDNA, and a cDNA synthesis control (absence of reverse transcriptase). The RT-PCR protocols comprised a 15s denaturation at 95ºC, 15s annealing period at 58-60ºC, and 30s to 1 min extension at 72ºC, for 40 cycles. PCR products were analyzed by electrophoresis on 1 or 1.5% agarose gels, visualized by GreenSafe staining (NZYTech, Ltd., Portugal) and detected using UVITEC transilluminator (UVitec Cambridge). In addition, PCR products were purified, and Sanger sequenced by Stabvida (Portugal).

Table 4. 1. Primer sequences.

Gene	Primer Fw (5´-3')	Primer Rv (5´-3')	Amplicon size (bp)
TAS2R3	ATCAGGGCTGCCTAATTGCT	GTCCTGTAGTCTTGAGCCAGG	1035
TAS2R4	TGCTTCGGTTATTCTATTTCTCTGC	CCTGGAGAGTAAAGGGTGGC	823
TAS2R5	ACTACCAGGGGATCTGACCTC	CCGAGCACACACTGTCTTCC	937
TAS2R8	TGTTCAGTCCTGCAGATAACATC	GCATTCTGACAAATGTCTGCC	897
TAS2R10	GCTACGTGTAGTGGAAGGCA	TGCAGTACCCTCAAAGAGGC	876
TAS2R13	GCTAGGGCTCAGCAGAGAAAT	GGCAAGTCCAAACTTCCCTAAT	1607
TAS2R14	TGGGTGGTGTCATAAAGAGCAT	CTGAGGGCTCCCCATCTTTG	924
TAS2R39	TCTGCGATCCTGCAGAAAGT	GATGAAGTCGAAGCTGAAGCC	930
TAS2R40	TCTTGGCGCAGAAACCTGAA	TTCCAGTCACAGAGTCTGCC	1015
TAS2R41	GCAGCGAATGGCTTCATTGT	AACAGGAGCTGCGAGAACAC	833
TAS2R44	TTTTTCCAGTGTGGTAGTGGTTCT	GATGAAGGCTTCTCTCCTTTCACC	900
TAS2R48	GAACAAGTGTTACTAAGCCTGC	CTTCTTTCACTCAGCGTGTCA	952
TAS2R50	ACAACCAGTGATATTAGGCTTGC	TCAGGTCTTTTACTCAGCACCT	963
GAPDH	ATGGGGAAGGTGAAGGTCG	GGGGTCATTGATGGCAACAATA	108

Fw-forward; Rv-reverse.

4.2.6. Immunocytochemistry

The taste transduction machinery components were also analyzed by immunocytochemistry. HIBCPP cells were cultured in 12 well plate with glass coverslips for 5-6 days. Then, cells were washed three times with phosphate-buffered saline (PBS), fixed with 4% paraformaldehyde (PFA) at room temperature for 10 min, permeabilized and blocked for 1h with PBS containing 0.2% Triton X-100 and 3% bovine serum albumin (BSA). After that, cells were incubated overnight at 4ºC with the following primary antibodies: rabbit TAS2R4 (1:300), TAS2R5 (1:300), TAS2R10 (1:300), TAS2R14 (1:300), TAS2R39 (1:300), GNAT3 (1:100), PLCβ2 (1:100) or TRPM5 (1:500). Next, cells were washed and incubated with secondary antibody goat anti-rabbit Alexa Fluor® 488 (1:1000) at room temperature for 1h. Nuclei were stained with Hoechst 33342 (1:1000) for 10 min, and coverslips were placed on glass slides using fluorescence mounting medium (Dako, USA). Images were then acquired on a LSM710 confocal laser scanning microscope (Carl Zeiss, Germany) at a 63x magnification.

4.2.7. Western blot

Protein expression of the taste machinery components was analyzed by Western blotting (WB). The bitter receptors TAS2R4, TAS2R5, TAS2R14 and TAS2R39 were also analyzed

based on the following criteria: 1) expression validated by RT-PCR; 2) number and therapeutic relevance of known ligands; 3) primary antibodies commercially available, suitable for both WB and immunofluorescence techniques; 4) previous validation of primary antibodies.

WB was performed with protein extracts obtained from HIBCPP cells using ice-cold RIPA lysis buffer (NaCl 150mM, NP-40 1%, sodium deoxycholate 0.5%, SDS 0.1%, Tris 50 mM). Total protein content was measured using Pierce BCA Protein Assay Kit (Thermo Fisher Scientific, USA) according to the manufacturer's recommendations. Samples were separated by SDS-PAGE using 8-12.5% gels and were electrically transferred to polyvinylidene difluoride (PVDF) membranes (Millipore, Merck, Portugal). Blots were blocked for 1h at room temperature with TBS containing 5% skimmed milk powder. Then blots were incubated overnight with primary rabbit antibodies to TAS2R4 (1:1000), TAS2R5 (1:1500), TAS2R14 (1:500), TAS2R39 (1:500), GNAT3 (1:100), PLCβ2 (1:100), TRPM5 (1:500). Moreover, GNAT3, TRPM5 and PLCβ2 primary antibodies specificity was assessed through parallel incubation with the respective peptides. After this, blots were washed at room temperature with TBS-T before incubation for 1h with HRP-conjugated goat anti-rabbit secondary antibody (1:40 000). Blots were washed, and antibody binding was detected using the ECL substrate (ClarityTM Western ECL Substrate, Bio-Rad, Portugal) according to the manufacturer's instructions. Images of blots were captured with the ChemiDoc MP Imaging system (Bio-Rad). Additionally, expression of TAS2R4, TAS2R5, TAS2R14 and TAS2R39 was normalized with β-actin. For that, blots were incubated during 1h at room temperature with mouse anti- β-actin (1:20 000) before incubation for 1h with HRP-conjugated goat anti-mouse secondary antibody (1:40 000). After blotting, images were acquired, and protein bands were quantified using the Image Lab software (Bio-Rad).

4.2.8. Single Cell Calcium Imaging

4.2.8.1. MTT assay

Before Ca^{2+} imaging experiments, the cytotoxicity of the selected bitter compounds was assessed in HIBCPP cells by the 3-(4,5-dimethylthiazol-2-yl)-2,5-diphenyltetrazolium bromide (MTT) assay. Briefly, 2 x10^4 cells were seeded in a 96-well plate and 24h before incubation, the culture medium was replaced by serum-free medium. Cells were incubated for 24h with chloramphenicol (0.125-1.5 mM), haloperidol (25-200 μM), quercetin (25-200 μM) or vehicle (DMSO ≤ 0.2%) diluted in culture medium. Then, culture medium was removed, cells were washed twice with PBS and incubated with 50 μl of MTT solution (5 mg/mL in PBS), for approximately 3h at 37 °C in a humidified

atmosphere containing 5% CO_2. Untreated cells and ethanol 70% treated cells were used as negative and positive controls, respectively. Following MTT incubation, formazan crystals were dissolved in DMSO for 30 minutes, and absorbance was read at 570 nm in a microplate spectrophotometer xMark™ (Bio-Rad). HIBCPP cell viability was expressed as a percentage relative to the absorbance determined in the negative control cells.

4.2.8.2. Single Cell Ca^{2+} Imaging

Once the cytotoxic profile of bitter compounds in HIBCPP cells had been established we proceeded with Ca^{2+} imaging assays. Briefly, HIBCPP cells were seeded in μ-slide 8 well ibiTreat (Ibidi, Germany) and changes in intracellular calcium levels were measured after stimulation of cells with confluency about 60-70%. HIBCPP cells were loaded with 5 μM of FURA-2 AM and 0.02% pluronic acid F-127 in HIBCPP culture medium for 1h. Next, cells were washed twice with Tyrode's solution (NaCl 140 mM, KCl 5 mM, $MgCl_2$ 1.0 mM, $CaCl_2$ 2 mM, Na-pyruvate 10 mM, glucose 10 mM, HEPES 10 mM, $NaHCO_3$ 5mM, pH 7.4) and loaded with Tyrode's for 30 min. After that, dose-response experiments were performed with chloramphenicol, haloperidol and quercetin. The μ-slide plates were placed on an inverted fluorescence microscope (Axio Imager A1, Carl Zeiss). Stock solution of each bitter compound was freshly prepared in Tyrode´s solution before the experiments. The stimulus was applied manually with a micropipette after baseline was recorded. The intracellular calcium levels were evaluated by quantifying the ratio of the fluorescence emitted at 520 nm following alternate excitation at 340 nm and 380 nm, using a Lambda DG4 apparatus (Sutter Instruments, Novato) and a 520 nm bandpass filter (Carl Zeiss) under a 40x objective (Carl Zeiss) with an AxioVision camera and software (Carl Zeiss). Data was processed using the Fiji software (MediaWiki). Changes in fluorescence ratio ($F=F_{340}/F_{380}$) were measured in at least 20 cells, in three or more independent experiments. Response intensity, or intracellular calcium variation, ($\Delta F/F_0$), was calculated in the following way: $\Delta F/F_0=(F-F_0)/F_0$, where F_0 corresponds to fluorescence ratio average at baseline (2 min acquisition before stimulus) and F correspond to maximum peak of fluorescence ratio evoked by the stimulus applied to the cells.

4.2.9. TAS2R14 and TAS2R39 knockdown

The specific activation of TAS2R14 by haloperidol or quercetin, and of TAS2R39 by chloramphenicol was assessed by calcium imaging assays in HIBCPP cells after TAS2R14 or TAS2R39 knockdown with specific siRNAs. Briefly, HIBCPP cells were transfected for

72h with a mixture of siRNA targeting TAS2R14 (siRNA TAS2R14) or TAS2R39 (siRNA TAS2R39) and Lipofectamine™ 2000 in Opti-MEM medium, following the manufacturer's instructions. A scramble siRNA was also used as negative control for TAS2R14 or TAS2R39 specific targeting. After transfection, calcium imaging assays were carried out as described in the previous section (2.8.2.) with chloramphenicol (500 μM), haloperidol (50 μM) and quercetin (50 μM) stimuli.

4.2.10. Statistical analysis

Statistical analysis and comparison was performed using GraphPad Prism 7 software. Statistical significance was determined by one-way analysis of variance (ANOVA) followed by Bonferroni´s post hoc test. Results are reported as mean ± SEM and data were considered statistically significant at a value of $p<0.05$.

4.3. Results

4.3.1. Taste transduction signalling is present in human CP

There are 25 members of the bitter taste receptor gene family in humans [13,14]. In this work we intended to analyze their expression profile in human CP. Therefore, our first approach consisted in investigating the presence of TAS2Rs in human CP microarrays (tissue and HIBCPP cells), in GEO repository databases (Table 2). In human CP tissue, almost all the 25 TAS2Rs, except for TAS2R10, 30/47 and 40, were detected. In HIBCPP cells, 15 TAS2Rs were detected, including TAS2R10 and 40. Notably, expression levels of TAS2Rs in both databases are very similar for these receptors.

In order to validate the data obtained from human CP microarrays studies, we evaluated the expression of bitter taste receptors in human CP sections collected from men and women. All the four TAS2Rs selected to immunohistochemistry were detected: TAS2R4, TAS2R5, TAS2R14 and TAS2R39 in the epithelial cells of both men and women CP samples (Figure 4.1.). The receptor TAS2R10 was not detected in human CP samples, which is in accordance with microarray data (Figure 4.1.). Notably, TAS2R4, TAS2R5 and TAS2R39 seem to have higher levels of expression in the human CP of women than men (Figure 4.1.).

Table 4. 2. TAS2R expression in human CP transcriptome databases available in the GEO (Gene Expression Omnibus) repository of human CP samples and HIBCPP cells, and validation of TAS2Rs expression in HIBCPP cells by RT-PCR.

	Human CP samples (GSE49974)	HIBCPP cells (GSE42870)	HIBCPP cells RT-PCR
TAS2R1	●●	●●	-
TAS2R3	●●	●●	+
TAS2R4	●●	●●	+
TAS2R5	●●	-	+
TAS2R7	●●●	●●	-
TAS2R8	●●	●●	+
TAS2R9	●●	●●	-
TAS2R10	-	●●	+
TAS2R13	●●	●●	+
TAS2R14	●●	●●	+
TAS2R16	●●	●●	-
TAS2R20/49	●●	-	na
TAS2R30/47	-	-	na
TAS2R38	●●	●●	-
TAS2R39	●●	●●	+
TAS2R40	-	●●	+
TAS2R41	●●	●●	+
TAS2R42	●●	-	-
TAS2R43	●●	-	na
TAS2R44	●●●	-	+
TAS2R45	●●	-	na
TAS2R46	●●	-	-
TAS2R48	●●	-	+
TAS2R50	●●●	●●	+
TAS2R60	●●	-	-
Expression levels	**0-4** **4-8** **>8**	● ●● ●●●	

CP-choroid plexus; HIBCPP-human choroid plexus papilloma cells; "-"– absence/not detected; "+" – detected; na – not analyzed.

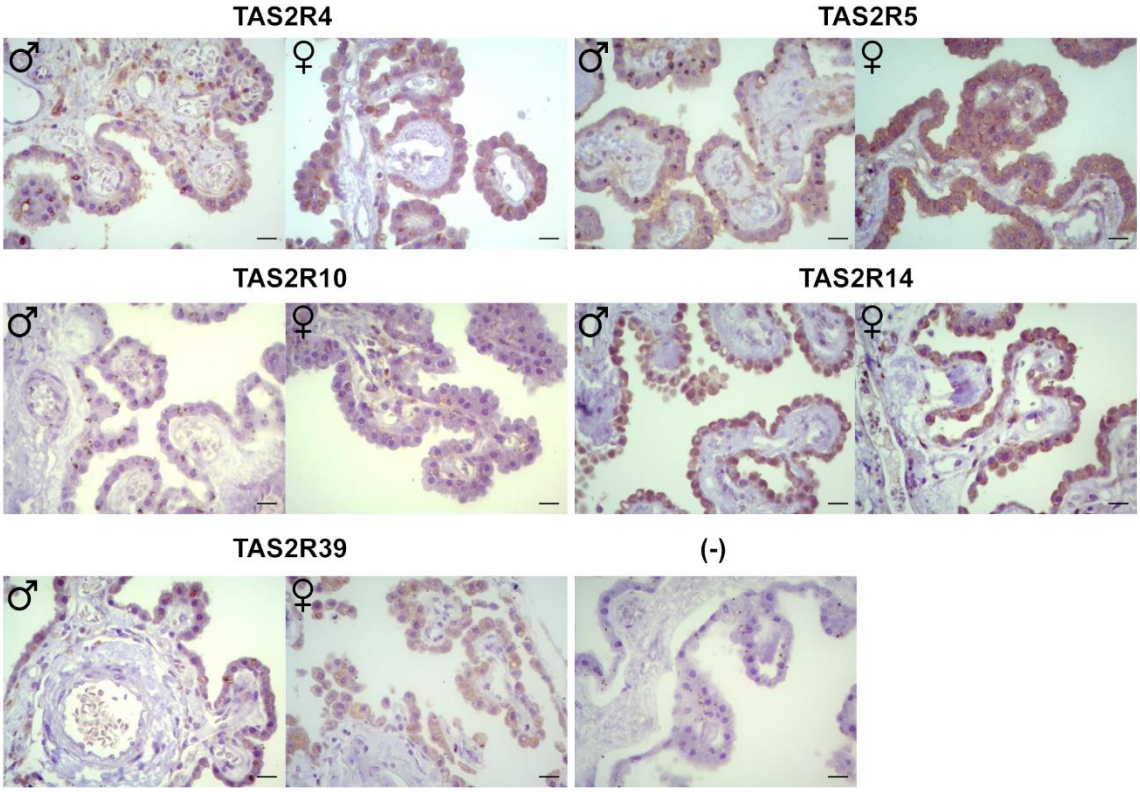

Figure 4. 1. Representative images showing the immunolocalization of taste receptors in human CP slices of men (♂) and women (♀). Bitter taste receptors TAS2R4, TAS2R5, TAS2R14 and TAS2R39 but not TAS2R10 were detected in human CP of men and women. Immunohistochemistry was performed using DAB and Hematoxylin. (-) negative control. Scale bar - 10 μm.

4.3.2. HIBCPP cells express 13 different TAS2Rs

The expression of bitter taste receptors in HIBCPP cells was also validated by RT-PCR using specific primers (Table 4.1). The results demonstrated the mRNA expression of 13 TAS2Rs (3, 4, 5, 8, 10, 13, 14, 39, 40, 41, 44, 48 and 50) (Table 4.2 and Figure 4.2). No mRNA was detected for TAS2R1, 7, 9, 16 and 38, although microarrays data indicate they are expressed in human CP tissue and HIBCPP cells. Also, TAS2R42 which was only detected in CP tissue was not detected by RT-PCR in HIBCPP cells. On the other hand, TAS2R5, 44 and 48 that have not been detected by cDNA microarrays in HIBCPP cells reveal valid transcripts by RT-PCR assay (Figure 4.2). TAS2R20/49, 43 and 45 mRNA expression was not analyzed due three different factors: data was not registered in HIBCPP cells microarrays; the design of specific primers failed due to the great homology between them; and no ligands are known for TAS2R45. Based on data retrieved from the transcriptome databases of human CP samples and HIBCPP cells and on our analysis on the expression of bitter taste receptors, it is important to highlight that TAS2R 3, 4, 5, 8,

13, 14, 39, 41, 44, 48 and 50 (Table 4.2, shaded) were detected by these three different approaches.

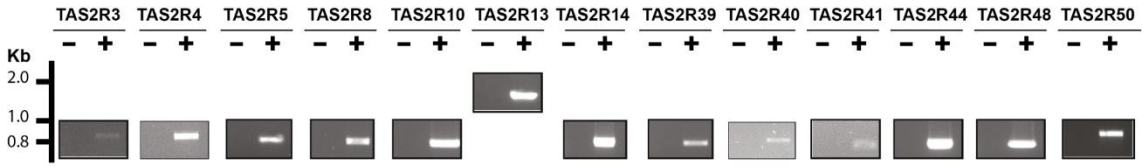

Figure 4. 2. mRNA expression profile of bitter taste receptors in HIBCPP cells. RT-PCR was performed with cDNA synthetized from HIBCPP cells RNA in the presence (+) or absence (-) of reverse transcriptase. The identities of the amplified products were confirmed by Sanger sequencing. Kb – Kilobase.

4.3.3. The key components of the taste signalling machinery are expressed in HIBCPP cells

The taste transduction machinery consists of taste receptors and downstream effector proteins like GNAT3, PLCβ2, and TRPM5. Thus, we assessed these taste-related proteins and the same four bitter taste receptors in protein extracts of HIBCPP cells by immunofluorescence and WB (Figure 4.3. and 4.4.) using available antibodies, previously validated [7,21]. Taste receptors TAS2R4, TAS2R5 and TAS2R39 were detected in the cytoplasm and plasma cell membrane, while TAS2R14 was located exclusively at the plasma membrane of HIBCPP cells (Figure 4.3.). GNAT3, PLCβ2, and TRPM5 were found in the cytoplasm of HIBCPP cells. Unexpectedly, GNAT3 was also detected in the nucleus (Figure 4.3.), although in our previous work in rat CP, we observed GNAT3 localization in the cytoplasm and plasma membrane [7]. Protein detection was reduced by pre-incubation of the antibodies with the respective peptides (Figure 4.3.).

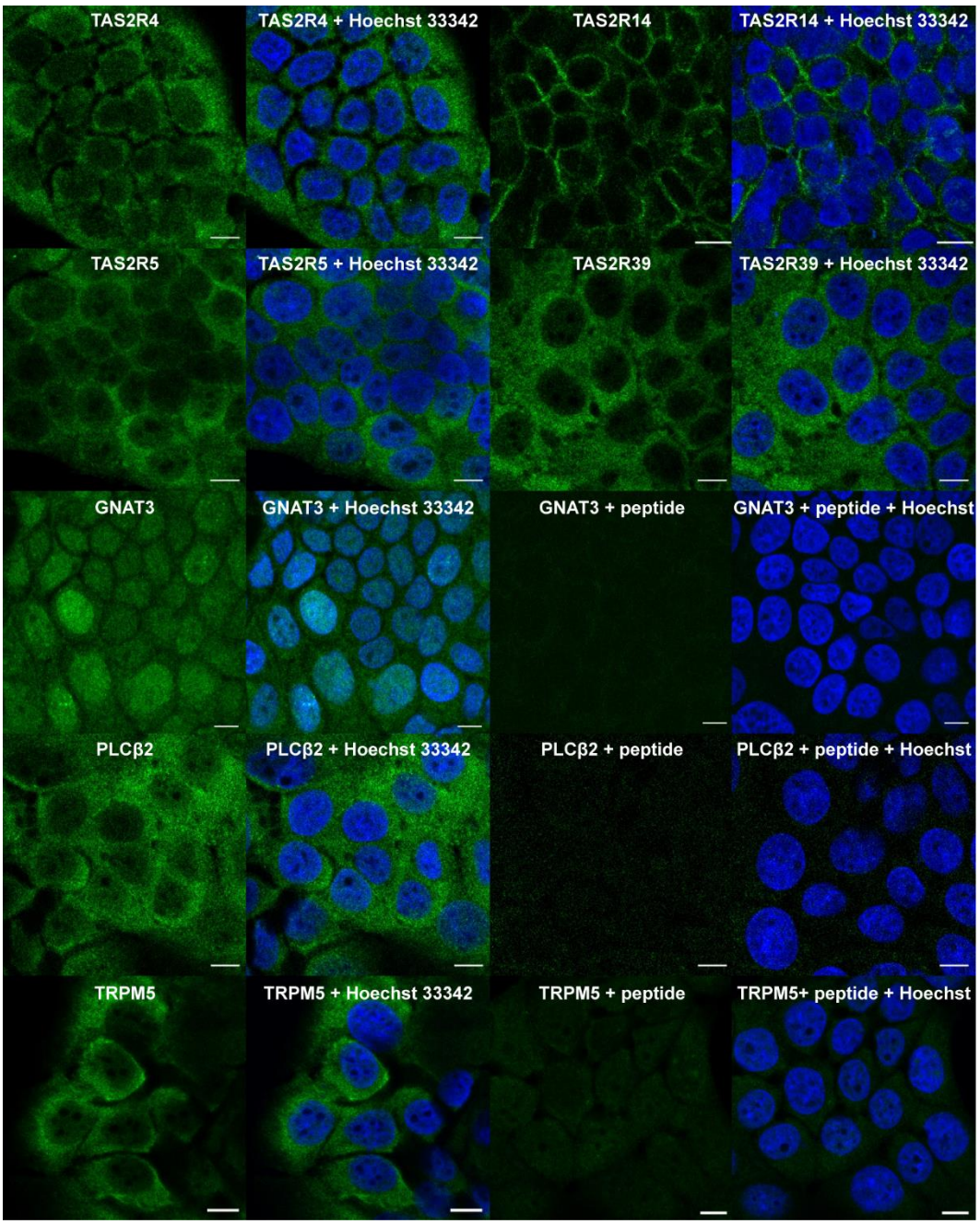

Figure 4. 3. Immunofluorescence detection of bitter taste receptors and taste signalling pathway effector proteins in HIBCPP cells. Confocal images of bitter taste receptors TAS2R4, TAS2R5, TAS2R14, TAS2R39 and downstream effectors GNAT3, PLCb2 and TRPM5 expression in HIBCPP cells (green). Nuclei were stained with Hoechst 33,423 (blue). Scale bar – 10 μm.

Moreover, expression of TAS2R4, TAS2R5, TAS2R14 and TAS2R39, and of downstream effectors GNAT3, PLCβ2, and TRPM5 was also detected by WB (Figure 4.4.). All these taste-related proteins were detected at the expected size except for TAS2R14, showing a molecular weight of approximately 20 kDa, instead of 36 kDa as reported by the antibody manufacturer. Once again, pre-incubation of the antibodies of the downstream effector proteins GNAT3, PLCβ2, and TRPM5 with the respective peptides, abolished the signal obtained in WB demonstrating antibody specificity (Figure 4.4.). Regarding TAS2R4, a

previous study in human airway epithelial cells validated the antibody used in our experiments [34], and also TAS2R14 and TAS2R39 antibodies were previously used in human A549 cells [21].

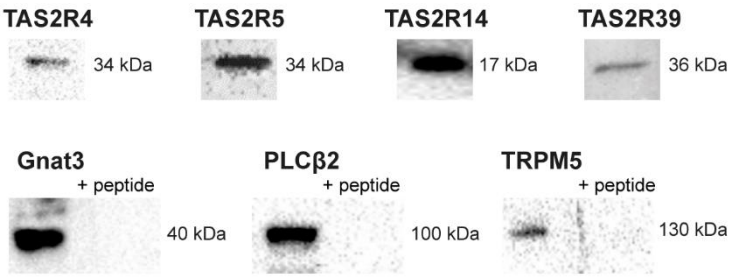

Figure 4. 4. Taste receptors and taste signalling pathway effector proteins are expressed in HIBCPP cells. WB detection of bitter taste receptors TAS2R4, TAS2R5, TAS2R14 and TAS2R39, and of taste machinery components GNAT3, PLCb2 and TRPM5 in HIBCPP protein extracts. kDa – kilo Dalton; WB – Western blot.

In addition, we analyzed TAS2Rs relative expression in HIBCPP cells. Of the four bitter receptors studied, TAS2R14 presented the higher protein levels followed by TAS2R4, TAS2R5 and TAS2R39, with the last two presenting very similar levels (Figure 4.5.).

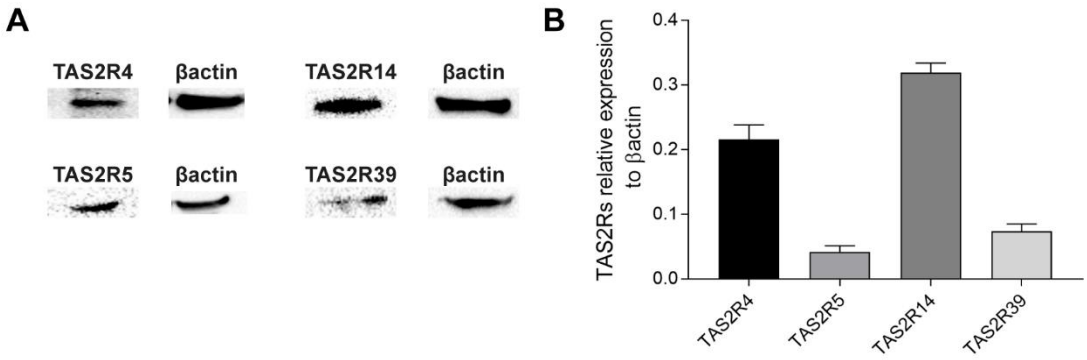

Figure 4. 5. Bitter taste receptors relative expression to β-actin. (A) Detection of the bitter receptors TAS2R4, TAS2R5, TAS2R14 and TAS2R39, and β-actin in HIBCPP by WB. (B) Quantification of TAS2R4, TAS2R5, TAS2R14 and TAS2R39 protein levels in HIBCPP by WB and normalized to β-actin levels. Among the TAS2Rs analyzed, TAS2R14 presented the higher protein levels followed by TAS2R4. Graphs indicates the mean ± SEM (N ≥ 3, independent cultures). WB – Western blot.

4.3.4. Chloramphenicol, haloperidol and quercetin elicited calcium responses in HIBCPP cells

After confirming bitter taste receptors expression in HIBCPP cells, their functionality was analyzed by stimulating these cells with three bitter agonists: chloramphenicol, haloperidol and quercetin. Beforehand, the viability of HIBCPP cells was assessed for 24h with the selected bitter compounds (Figure 4.6 A-C). We found that concentrations above 1 mM of chloramphenicol, 100 μM of haloperidol and quercetin reduced HIBCPP cells viability (Figure 4.6 A-C). Next, we proceeded to calcium functional studies using

concentrations of ligands that would not affect cell viability. Therefore, we analyzed HIBCPP calcium responses to chloramphenicol (0.125-0.5 mM), haloperidol (10-100 μM) and quercetin (10-100 μM) stimuli by calcium imaging experiments (Figure 4.6 D-F). For each compound, calcium imaging assays were carried out in the presence of vehicles and compared to untreated cells to establish that calcium variations observed were not related to vehicle concentration (data not shown). Moreover, calcium variations were collected during 2 min before the stimuli to obtain a baseline (F) that was used to normalize the responses obtained with the compounds. Additionally, only assays showing a uniform baseline were evaluated. Chloramphenicol and haloperidol elicited calcium responses in a dose-dependent manner (Figure 4.6.D, F). Chloramphenicol at 0.5 mM (ΔF/F= 0.405 ± 0.072), but not at 0.125 (ΔF/F= 0.206 ± 0.028) or 0.250 mM (ΔF/F= 0.260 ± 0.024), triggered a significant increase in intracellular calcium levels in HIBCPP cells (Figure 4.6.D). Cells treated with 50 or 100 μM of haloperidol showed higher calcium levels (ΔF/F= 0.738 ± 0.010 and 0.845 ± 0.061) in comparison with vehicle treated cells (ΔF/F= 0.1076 ± 0.003). Lower concentrations of haloperidol, 10 μM (ΔF/F= 0.319 ± 0.033) and 25 μM (ΔF/F= 0.334 ± 0.079), did not provoke significant calcium responses (Figure 4.6.E). Quercetin stimuli at all concentrations tested 10, 50 and 100 μM (ΔF/F= 0.397 ± 0.026, 0.323 ± 0.041 and 0.597 ± 0.062) increased intracellular calcium levels in comparison to vehicle treated cells (ΔF/F= 0.104 ± 0.004) (Figure 4.6.F).

4.3.5. Chloramphenicol and quercetin responses in HIBCPP cells are mediated by TAS2R39 and TAS2R14

In calcium imaging experiments we observed dose-responses of HIBCPP cells to chloramphenicol, haloperidol and quercetin. It has been reported that chloramphenicol binds TAS2R1, 8, 10, 39, 41, 43, and 46 [27], haloperidol binds TAS2R10 and 14 [27] and quercetin binds TAS2R14 [35]. Thus, these bitter compounds are all TAS2R14 and/or TAS2R39 ligands. Therefore, we explored the specific activation of TAS2R14 and/or TAS2R39 by performing calcium assays in HIBCPP cells after TAS2R14 or TAS2R39 knockdown. HIBCPP cells responses to chloramphenicol (500 μM), after TAS2R39 silencing, showed decreased calcium levels of 72.89 ± 11.21 % in comparison to untreated, 42.73 ± 11.21 % to mock-, or 60.79 ± 10.23 % to scramble siRNA-transfected cells (Figure 4.6.G). On the other hand, haloperidol (50 μM) responses, after TAS2R14 silencing, did not reveal alterations in comparison with untreated, mock- or scramble siRNA-transfected cells (Figure 4.6.H). At last, the HIBCPP cell responses to quercetin (50 μM) after TAS2R14 knockdown, decreased 56.53 ± 9.41 % in comparison to

untreated, 37.57 ± 10.24 % to mock- or 48.29 ± 10.24 % to scramble siRNA-transfected cells (Figure 4.6.I). Additionally, no significant differences were observed between control conditions (untreated, mock-, or scramble siRNA-transfected cells) in calcium imaging assays with any of these compounds.

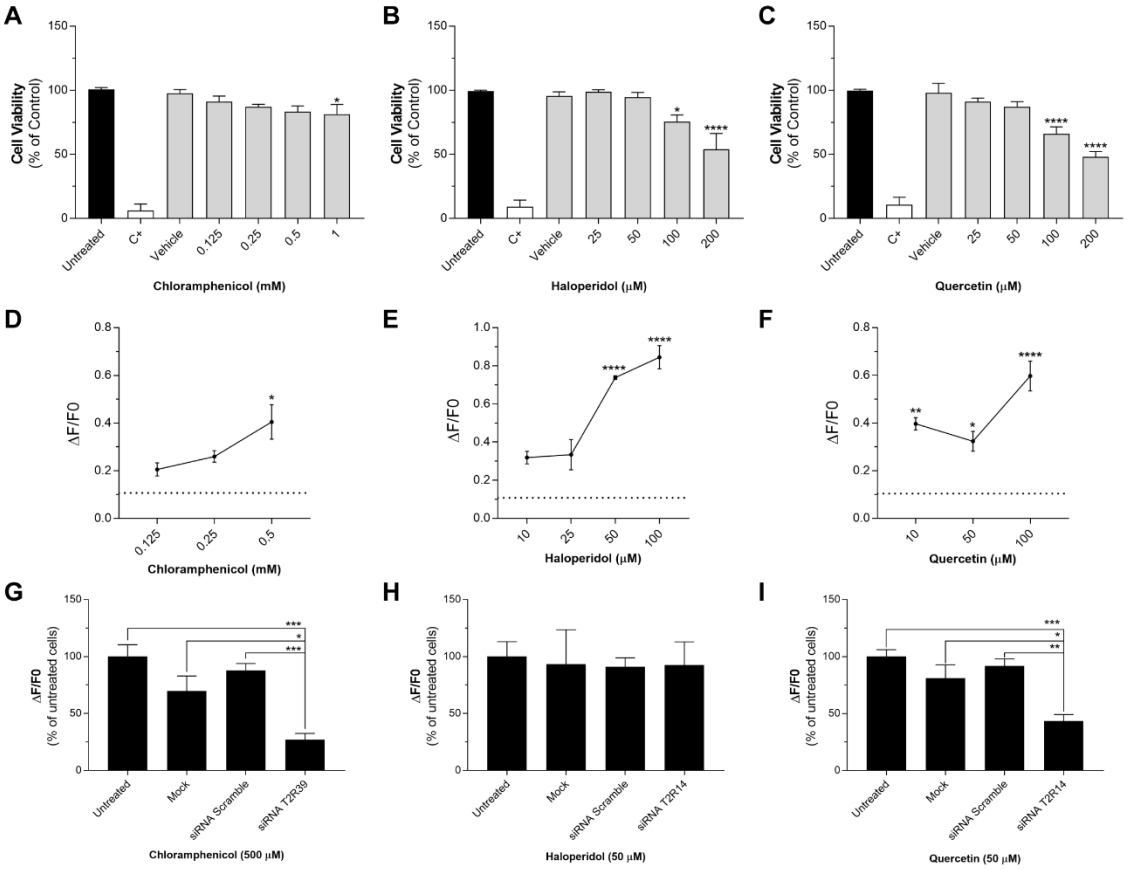

Figure 4. 6. Bitter taste signalling pathway is functional in human CP epithelial cells. (A) Bitter compounds cytotoxicity in HIBCPP cells was assessed by MTT assay. HIBCPP cells were treated for 24 h with different concentrations of chloramphenicol, haloperidol and quercetin. Bar graphs represent mean ± SEM [N ≥ 3; *p < 0.05, ***p < 0.001, ****P < 0.0001 vs untreated cells; One-way ANOVA followed by Bonferroni's post hoc test]. Cells treated with vehicle (DMSO ≤ 0.2%) do not show alterations in cellular viability. C+ positive control. (B) Calcium dose response curves of HIBCPP cells to different concentrations of chloramphenicol (0.125–0.5 mM), haloperidol (10–100 mM) and quercetin (10–100 mM). Dot line – calcium levels measured in cells with vehicle only (DMSO ≤ 0.2%). (C) Calcium responses to chloramphenicol, haloperidol and quercetin in transfected HIBCPP cells with TAS2R14 or TAS2R39 siRNAs. Intracellular calcium levels were measured in HIBCPP cells transfected or mock-transfected for 72 h with TAS2R14 or TAS2R39 siRNA, or a scramble siRNA, after chloramphenicol (0.5 mM), haloperidol (50 mM) or quercetin (50 mM) stimuli. Response intensity was measured: (ΔF/F0) = ((F340-F380)-F0)/F0, where F0 corresponds to fluorescence ratio average of a 2 min baseline and F corresponds to maximum peak of fluorescence ratio evoked by stimuli. Graphs indicate the mean ± SEM (N ≥ 4, independent cultures; *p < 0.05, **p < 0.01, ***p < 0.001, ****p < 0.0001; One-way ANOVA followed by Bonferroni's post hoc test). There were no significant differences between untreated cells and mock or scramble siRNA-transfected cells.

4.4. Discussion

A functional taste signalling pathway has been previously reported in mouse [19] and rat CP [7]. Since the CP has a crucial role in the maintenance of brain homeostasis as an

important interface between the blood and the CSF, the taste transduction pathway in the CP suggests a likely mechanism to survey both blood and CSF composition. To date, taste signalling or TAS2Rs presence in human CP epithelial cells have not been confirmed. In this study, we aimed to address this question to evaluate whether these receptors may be associated with the capacity of the human CP to monitor the blood and the CSF and respond to alterations in their composition. The *in silico* analysis of human CP microarray data available in the GEO database provided strong evidences that several TAS2Rs mRNAs are present in human CP tissue [31], and in the human CP cell line HIBCPP [32]. In our study, we validated and confirmed the mRNA expression of thirteen TAS2Rs in the HIBCPP cells. Of these, eleven were also detected in human CP tissue microarrays data including TAS2R4, TAS2R5, TAS2R14 and TAS2R39 whose expression was confirmed in men and women CP sections. Interestingly, TAS2R4, TAS2R5 and TAS2R39 seem to present higher levels in women CP sections in comparison to men, indicating that TAS2Rs expression and their function might be different between men and women. In accordance, previous studies in rat CP showed that the sex hormone background regulates the taste signalling pathway [36,37].

The downstream effector proteins GNAT3, PLCβ2 and TRPM5 are important components of the taste signalling pathway. Therefore, their expression was analyzed and confirmed in HIBCPP cells, reinforcing the presence and functionality of this pathway in the human CP. Moreover, our findings not only confirm the presence of the bitter taste signalling machinery in the human CP but also suggest that these receptors might be activated by circulating compounds in the bloodstream and/or in the CSF. Among the bitter taste receptors studied, TAS2R14 and TAS2R4 presented considerably higher protein levels in comparison with TAS2R5 and TAS2R39. Interestingly, TAS2R14 is the one TAS2R with more known ligands (150) [38,39]. In addition, some of the bitter agonists that bind TAS2R14 have neuroactive effects such as the phenolic compound resveratrol [40], the flavonoids quercetin [35] and epigallocatechin gallate [41], or the anti-psychotic drug haloperidol [27], suggesting an important role of TAS2R14 in the cells/tissue where it is expressed. Actually, in the human upper airways, TAS2R14 seem to mediate anti-inflammatory responses to flavones [21]. However, the function of this and other TAS2Rs remain to be elucidated despite their presence in many tissues. Along with TAS2R14, also TAS2R39 has a wide range of ligands (84) such as flavonoids and other compounds [38,39], while the remaining TAS2Rs whose expression was confirmed, only bind specific ligands. However, the importance of these receptors should not be neglected since some of their ligands had shown neuroprotective actions. This is the case of dapsone, a ligand of TAS2R4 [27], that seem to be effective to prevent seizures

when combined with diazepam [42]. Interestingly, other ligands had shown antitumoral properties such as arborescin [43] that binds TAS2R4 [27] and parthenolide [44], a TAS2R4 and TAS2R8 ligand [27]. Additionally, arborescin and parthenolide are also TAS2R14 agonists [27]. Another interesting bitter ligand is andrographolide that binds TAS2R30/47, TAS2R46 and TAS2R50 [27] and seems to be a promising drug against several CNS disorders such as AD and PD [45]. Of these three receptors, only TAS2R50 expression was confirmed in HIBCPP cells.

To ascertain that the bitter taste signalling pathway is functional and responsive in HIBCPP cells, single cell calcium imaging experiments were conducted with some bitter agonists: chloramphenicol, that binds TAS2R1, 8, 10, 39, 41, 43, and 46 [27], haloperidol that binds TAS2R10 and TAS2R14 [27] and quercetin that only binds TAS2R14 [35].Importantly, of these, TAS2R8, TAS2R10, TAS2R13, TAS2R14, TAS2R39 and TAS2R41 expression was found in HIBCPP cells. Our results showed intracellular calcium dose-dependent responses to chloramphenicol and haloperidol in HIBCPP cells. Moreover, chloramphenicol and quercetin responses seem to be mediated by TAS2R39 and TAS2R14 activation, respectively, since knockdown of these receptors induced a massive decrease in calcium responses. Therefore, these results support that the bitter taste signalling pathway is functional in human CP epithelial cells.

In summary, the expression and function of the bitter taste signalling pathway were analyzed in an *in vitro* model of the human CP, showing that this model is suitable for future studies on the function of these receptors, as these cells also contain the downstream effector molecules and respond to bitter compounds. Moreover, the bitter taste receptors TAS2R4, TAS2R5, TAS2R14 and TAS2R39, present in both human CP tissue and in HIBCPP cells, might become activated by circulating compounds, such as therapeutic drugs or components of our diet like flavonoids. Thus, the effect of TAS2Rs activation by therapeutic compounds or flavonoids should be assessed to investigate the intracellular cascades triggered by TAS2R activation.

4.5. References

[1] Z.B. Redzic, M.B. Segal, The structure of the choroid plexus and the physiology of the choroid plexus epithelium, Adv. Drug Deliv. Rev. 56 (2004) 1695–1716. doi:10.1016/j.addr.2004.07.005.

[2] C.R.A. Santos, A.C. Duarte, T. Quintela, J. Tomás, T. Albuquerque, F. Marques, J.A. Palha, I. Gonçalves, The choroid plexus as a sex hormone target: Functional implications, Front. Neuroendocrinol. 44 (2017) 103–121. doi:10.1016/j.yfrne.2016.12.002.

[3] J.F. Ghersi-Egea, N. Strazielle, M. Catala, V. Silva-Vargas, F. Doetsch, B. Engelhardt, Molecular anatomy and functions of the choroidal blood-cerebrospinal fluid barrier in health and disease, Acta Neuropathol. 135 (2018) 337–361. doi:10.1007/s00401-018-1807-1.

[4] N. Strazielle, J.-F. Ghersi-Egea, Potential Pathways for CNS Drug Delivery Across the Blood-Cerebrospinal Fluid Barrier, Curr. Pharm. Des. 22 (2016) 5463–5476. doi:10.2174/1381612822666160726112115.

[5] C. Johanson, N. Johanson, Merging Transport Data for Choroid Plexus with Blood-Brain Barrier to Model CNS Homeostasis and Disease More Effectively, CNS Neurol. Disord. - Drug Targets. 15 (2016) 1151–1180. doi:10.2174/1871527315666160915120727.

[6] Q. Wang, Z. Zuo, Impact of transporters and enzymes from blood–cerebrospinal fluid barrier and brain parenchyma on CNS drug uptake, Expert Opin. Drug Metab. Toxicol. 14 (2018) 961–972. doi:10.1080/17425255.2018.1513493.

[7] J. Tomás, C.R.A. Santos, T. Quintela, I. Gonçalves, "Tasting" the cerebrospinal fluid: Another function of the choroid plexus?, Neuroscience. 320 (2016) 160–171. doi:10.1016/j.neuroscience.2016.01.057.

[8] I. Gonçalves, P.C. Hubbard, J. Tomás, T. Quintela, G. Tavares, S. Caria, D. Barreiros, R.A. Santos, ' Smelling ' the cerebrospinal fluid : olfactory signalling molecules are expressed in and mediate chemosensory signalling from the choroid plexus, FEBS J. 283 (2016) 1748–1766. doi:10.1111/febs.13700.

[9] T.-I. Jeon, Y.-K. Seo, T.F. Osborne, Gut bitter taste receptor signalling induces ABCB1 through a mechanism involving CCK, Biochem. J. 438 (2011) 33–37. doi:10.1042/bj20110009.

[10] M.M. Gaida, C. Mayer, U. Dapunt, S. Stegmaier, P. Schirmacher, G.H. Wabnitz, G.M. Hänsch, Expression of the bitter receptor T2R38 in pancreatic cancer: localization in lipid droplets and activation by a bacteria-derived quorum-sensing molecule, Oncotarget. 7 (2016) 12623–12632. doi:10.18632/oncotarget.7206.

[11] G. Nelson, M.A. Hoon, J. Chandrashekar, Y. Zhang, N.J.P. Ryba, C.S. Zuker, Mammalian Sweet Taste Receptors, Cell. 106 (2001) 381–390. doi:10.1016/S0092-8674(01)00451-2.

[12] G. Nelson, J. Chandrashekar, M.A. Hoon, L. Feng, G. Zhao, N.J.P. Ryba, C.S. Zuker, An amino-acid taste receptor, Nature. 416 (2002) 199–202. doi:10.1038/n416031a.

[13] E. Adler, M.A. Hoon, K.L. Mueller, J. Chandrashekar, N.J.P. Ryba, C.S. Zuker, A novel family of mammalian taste receptors, Cell. 100 (2000) 693–702. doi:10.1016/S0092-8674(00)80705-9.

[14] J. Chandrashekar, K.L. Mueller, M.A. Hoon, E. Adler, L. Feng, W. Guo, C.S. Zuker, N.J. Ryba, T2Rs function as bitter taste receptors, Cell. 100 (2000) 703–711. doi:10.1016/s0092-8674(00)80706-0.

[15] J. Chandrashekar, M.A. Hoon, N.J. Ryba, C.S. Zuker, The receptors and cells for mammalian taste, Nature. 444 (2006) 288–294. doi:10.1038/nature05401.

[16] N. Chaudhari, S.D. Roper, The cell biology of taste, J. Cell Biol. 190 (2010) 285–296. doi:10.1083/jcb.201003144.

[17] N.M. Dalesio, S.F. Barreto Ortiz, J.L. Pluznick, D.E. Berkowitz, Olfactory, Taste, and Photo Sensory Receptors in Non-sensory Organs: It Just Makes Sense, Front. Physiol. 9 (2018) 1673–1691. doi:10.3389/fphys.2018.01673.

[18] S.J. Lee, I. Depoortere, H. Hatt, Therapeutic potential of ectopic olfactory and taste receptors, Nat. Rev. Drug Discov. 18 (2019) 116–138. doi:10.1038/s41573-018-0002-3.

[19] X. Ren, L. Zhou, R. Terwilliger, S.S. Newton, I.E. de Araujo, Sweet taste signalling functions as a hypothalamic glucose sensor, Front. Integr. Neurosci. 3 (2009) 1–15. doi:10.3389/neuro.07.012.2009.

[20] A.A. Clark, S.B. Liggett, S.D. Munger, Extraoral bitter taste receptors as mediators of off-target drug effects, FASEB J. 26 (2012) 4827–4831. doi:10.1096/fj.12-215087.

[21] B.M. Hariri, D.B. McMahon, B. Chen, J.R. Freund, C.J. Mansfield, L.J. Doghramji, N.D. Adappa, J.N. Palmer, D.W. Kennedy, D.R. Reed, P. Jiang, R.J. Lee, Flavones modulate respiratory epithelial innate immunity: Anti-inflammatory effects and activation of the T2R14 receptor, J. Biol. Chem. 292 (2017) 8484–8497. doi:10.1074/jbc.M116.771949.

[22] Y. Wang, A. Wang, M. Zhang, H. Zeng, Y. Lu, L. Liu, J. Li, L. Deng, Artesunate attenuates airway resistance in vivo and relaxes airway smooth muscle cells in vitro via bitter taste receptor-dependent calcium signalling, Exp. Physiol. 104 (2019) 231–243. doi:10.1113/EP086824.

[23] Y. Seo, Y.S. Kim, K.E. Lee, T.H. Park, Y. Kim, Anti-cancer stemness and anti-invasive activity of bitter taste receptors, TAS2R8 and TAS2R10, in human neuroblastoma cells, PLoS One. 12 (2017) 1–20. doi:10.1371/journal.pone.0176851.

[24] A.A. Clark, C.D. Dotson, A.E.T. Elson, A. Voigt, U. Boehm, W. Meyerhof, N.I. Steinle, S.D. Munger, TAS2R bitter taste receptors regulate thyroid function, FASEB J. 29 (2015) 164–172. doi:10.1096/fj.14-262246.

[25] A. Luddi, L. Governini, D. Wilmskötter, T. Gudermann, I. Boekhoff, P. Piomboni, Taste Receptors: New Players in Sperm Biology, Int. J. Mol. Sci. 20 (2019) 967–987. doi:10.3390/ijms20040967.

[26] A. Malki, J. Fiedler, K. Fricke, I. Ballweg, M.W. Pfaffl, D. Krautwurst, Class I odorant receptors, TAS1R and TAS2R taste receptors, are markers for subpopulations of circulating leukocytes, J. Leukoc. Biol. 97 (2015) 533–545. doi:10.1189/jlb.2a0714-331rr.

[27] W. Meyerhof, C. Batram, C. Kuhn, A. Brockhoff, E. Chudoba, B. Bufe, G. Appendino, M. Behrens, The molecular receptive ranges of human TAS2R bitter taste receptors, Chem. Senses. 35 (2009) 157–170. doi:10.1093/chemse/bjp092.

[28] A. Di Pizio, M.Y. Niv, Promiscuity and selectivity of bitter molecules and their receptors, Bioorganic Med. Chem. 23 (2015) 4082–4091. doi:10.1016/j.bmc.2015.04.025.

[29] C. Schwerk, T. Papandreou, D. Schuhmann, L. Nickol, J. Borkowski, U. Steinmann, N. Quednau, C. Stump, C. Weiss, J. Berger, H. Wolburg, H. Claus, U. Vogel, H. Ishikawa, T. Tenenbaum, H. Schroten, Polar invasion and translocation of neisseria meningitidis and streptococcus suis in a novel human model of the blood-cerebrospinal fluid barrier, PLoS One. 7 (2012) e30069. doi:10.1371/journal.pone.0030069.

[30] A. Bernd, M. Ott, H. Ishikawa, H. Schroten, C. Schwerk, G. Fricker, Characterization of efflux transport proteins of the human choroid plexus papilloma cell line HIBCPP, a functional in vitro model of the blood-cerebrospinal fluid barrier, Pharm. Res. 32 (2015) 2973–2982. doi:10.1007/s11095-015-1679-1.

[31] S.F. Janssen, S.J.F. Van Der Spek, J.B. Ten Brink, A.H.W. Essing, T.G.M.F. Gorgels, P.J. Van Der Spek, N.M. Jansonius, A.A.B. Bergen, Gene expression and functional annotation of the human and mouse choroid plexus epithelium, PLoS One. 8 (2013). doi:10.1371/journal.pone.0083345.

[32] J. Borkowski, L. Li, U. Steinmann, N. Quednau, C. Stump-Guthier, C. Weiss, P. Findeisen, N. Gretz, H. Ishikawa, T. Tenenbaum, H. Schroten, C. Schwerk, Neisseria meningitidis elicits a pro-inflammatory response involving IκBζ in a human blood-cerebrospinal fluid barrier model, J. Neuroinflammation. 11 (2014) 1–18. doi:10.1186/s12974-014-0163-x.

[33] I. Ishiwata, C. Ishiwata, E. Ishiwata, Y. Sato, K. Kiguchi, T. Tachibana, H. Hashimoto, H. Ishikawa, Establishment and characterization of a human malignant choroids plexus papilloma cell line (HIBCPP), Hum Cell. 18 (2005) 67–72. doi:10.1111/j.1749-0774.2005.tb00059.x.

[34] A.S. Shah, B.S. Yehuda, T.O. Moninger, J.N. Kline, M.J. Welsh, Motile cilia of human airway epithelia are chemosensory, Science (80-.). 325 (2009) 1131–1134. doi:10.1126/science.1173869.

[35] A. Levit, S. Nowak, M. Peters, A. Wiener, W. Meyerhof, M. Behrens, M.Y. Niv, The bitter pill : clinical drugs that activate the human bitter taste receptor TAS2R14, FASEB J. 27 (2014) 1181–1197. doi:10.1096/fj.13-242594.

[36] T. Quintela, I. Goncalves, L.C. Carreto, M.A. Santos, H. Marcelino, F.M. Patriarca, C.R. Santos, Analysis of the effects of sex hormone background on the rat choroid plexus transcriptome by cDNA microarrays, PLoS One. 8 (2013) e60199. doi:10.1371/journal.pone.0060199.

[37] J. Tomás, C.R.A. Santos, A.C. Duarte, M. Maltez, T. Quintela, M.C. Lemos, I. Gonçalves, Bitter taste signalling mediated by Tas2r144 is down-regulated by 17β-estradiol and progesterone in the rat choroid plexus, Mol. Cell. Endocrinol. 495 (2019) 110521. doi:10.1016/j.mce.2019.110521.

[38] A. Dagan-Wiener, A. Di Pizio, I. Nissim, M.S. Bahia, N. Dubovski, E. Margulis, M.Y. Niv, Bitterdb: Taste ligands and receptors database in 2019, Nucleic Acids Res. 47 (2019) D1179–D1185. doi:10.1093/nar/gky974.

[39] A. Wiener, M. Shudler, A. Levit, M.Y. Niv, BitterDB: a database of bitter compounds., Nucleic Acids Res. 40 (2012) D413-9. doi:10.1093/nar/gkr755.

[40] W.S.U. Roland, H. Gruppen, M. Driesse, G. Smit, J.-P. Vincken, L. Van Buren, R.J. Gouka, Bitter taste receptor activation by flavonoids and isoflavonoids: Modeled structural requirements for activation of hTAS2R14 and hTAS2R39, J. Agric. Food Chem. 61 (2013) 10454–10466. doi:10.1021/jf403387p.

[41] T. Yamazaki, M. Narukawa, M. Mochizuki, T. Watanabe, Activation of the hTAS2R14 Human Bitter-Taste Receptor by (–) -Epigallocatechin Gallate and (–) - Epicatechin Gallate, Biosci. Biotechnol. Biochem. 8451 (2014) 1753–1756. doi:10.1271/bbb.130329.

[42] C. Ríos, A.C. Farfán-briseño, J. Manjarrez-marmolejo, J. Franco-pérez, M. Méndez-armenta, C. Nava-ruiz, Efficacy of dapsone administered alone or in combination with diazepam to inhibit status epilepticus in rats, Brain Res. 1708 (2019) 181–187. doi:10.1016/j.brainres.2018.12.017.

[43] A. Martins, R. Mignon, M. Bastos, D. Batista, N.R. Neng, J.M.F. Nogueira, C. Vizetto-duarte, L. Custódio, J. Varela, A.P. Rauter, In vitro Antitumoral Activity of Compounds Isolated from Artemisia gorgonum Webb, Phytother Res. 1334 (2014) 1329–1334. doi:10.1002/ptr.5133.

[44] Z. Yu, Y. Chen, S. Wang, P. Li, G. Zhou, Y. Yuan, Inhibition of NF-κB results in anti-glioma activity and reduces temozolomide-induced chemoresistance by down-regulating MGMT gene expression, Cancer Lett. 428 (2018) 77–89. doi:10.1016/j.canlet.2018.04.033.

[45] J. Lu, Y. Ma, J. Wu, H. Huang, X. Wang, Z. Chen, A review for the neuroprotective effects of andrographolide in the central nervous system, Biomed. Pharmacother. 117 (2019) 109078. doi:10.1016/j.biopha.2019.109078.

[46] A. Jaggupilli, N. Singh, J. Upadhyaya, A.S. Sikarwar, M. Arakawa, S. Dakshinamurti, R.P. Bhullar, K. Duan, P. Chelikani, Analysis of the expression of human bitter taste receptors in extraoral tissues, Mol. Cell. Biochem. 426 (2017) 137–147. doi:10.1007/s11010-016-2902-z.

Chapter 5

Research Work 2
The bitter taste receptor TAS2R14 regulates resveratrol transport across the human blood-cerebrospinal fluid barrier

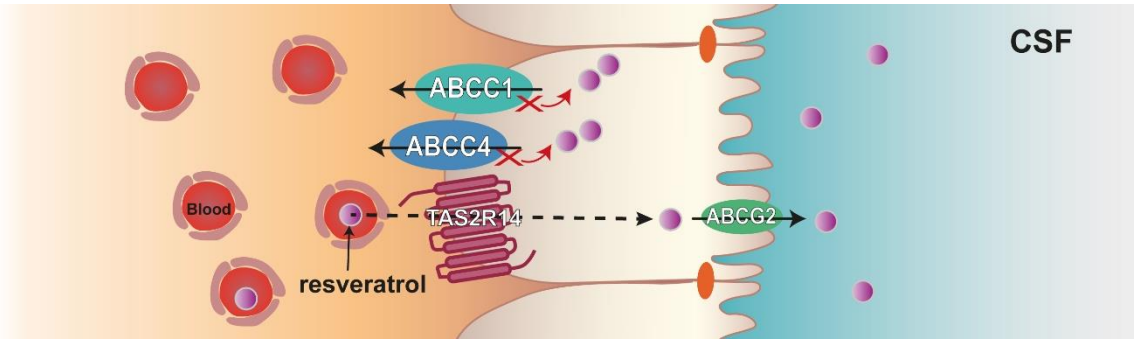

This chapter corresponds to the original research article:
Duarte AC, Rosado T, Costa AR, Santos J, Gallardo E, Quintela T, Ishikawa H, Schwerk C, Schroten H, Gonçalves I, Santos CRA (2020). The bitter taste receptor TAS2R14 regulates resveratrol transport across the human blood-cerebrospinal fluid barrier, Biochemical Pharmacology, https://doi.org/10.1016/j.bcp.2020.113954

5.1. Abstract

The regulation of transport mechanisms at brain barriers must be thoroughly understood, so that novel strategies for improving drug delivery to the brain can be designed. The blood-cerebrospinal fluid barrier (BCSFB) established by the choroid plexus (CP) epithelial cells has been poorly studied in this regard despite its relevance for the protection to the central nervous system (CNS).

This study assessed the role of bitter taste receptors (TAS2Rs), TAS2R14 and TAS2R39, in the transport of neuroactive compounds across CP epithelial cells using an *in vitro* model of the human BCSFB. Both receptors are expressed in human CP cells and known to bind resveratrol. First, Ca^{2+} imaging assays demonstrated that resveratrol specifically activates the TAS2R14 receptor, but not TAS2R39, in these human CP epithelial cells. Then, we proceeded with permeation studies that showed resveratrol can cross the human BCSFB, from the blood to the CSF side and that TAS2R14 knockdown decreased the transport of resveratrol across these cells. Conversely, inhibition of efflux transporters ABCC1, ABCC4 or ABCG2 also restrained the transport of resveratrol across these cells. Interestingly, resveratrol upregulated the expression of ABCG2 located at the apical membrane of the cells via TAS2R14, whereas ABCC1 and ABCC4 at the basolateral membrane of the cells were not affected. Altogether, our study demonstrates that the BCSFB is a gateway for resveratrol entrance into the CNS and that the receptor TAS2R14 regulates its transport by regulating the action of efflux transporters at CP epithelial cells.

Keywords:
Blood-cerebrospinal fluid barrier, chemical surveillance, bitter taste receptors, resveratrol, ABC transporters

5.2. Introduction

Brain barriers are fundamentally the gatekeepers of the CNS. There are two major brain barriers: the BBB constituted by the endothelial cells of brain capillaries, and the BCSFB established by the CP epithelial cells in the ventricles of the brain [1]. The BCSFB stands as a unique interface between the blood and the CSF regulating the molecular trafficking between the two fluids, thus promoting homeostatic balance and ensuring proper CNS function [2]. This strict regulation is guaranteed by the presence of influx and efflux transporters that control the entrance and exit of many substances into and out of the CNS, and by detoxifying enzymes that reduce the toxicity of many compounds in transit [2–4]. Efflux mechanisms at the BCSFB depend mainly on ABC transporters that are expressed at the basolateral membrane (blood facing) of CP epithelial cells such as ABCC1/Mrp1 and ABCC4/Mrp4, or at the apical membrane (CSF facing) such as ABCG2/Bcrp and ABCB1/P-gp [2,5]. ABCB1 is highly expressed in the BBB, but has very low expression in the CP [6]. ABC transporters are of great interest, since they are responsible for the resistance to many chemotherapies, thus interfering with the CNS delivery of anticancer drugs, such as doxorubicin (ABCB1, ABCC2, ABCC3, ABCG2), methotrexate (ABCB1, ABCC1, ABCC2, ABCC4, ABCG2), temozolomide (ABCB1, ABCG2) and paclitaxel (ABCB1, ABCC1) [7,8]. However, how the function of ABC transporters is regulated at the BCSFB remains unclear despite its importance for drug delivery to the CNS.

Bitter taste receptors (TR2) belong to the GPCR family. In humans, 25 TAS2Rs enable the identification of a wide range of bitter compounds [9,10]. Upon ligand-binding TAS2Rs trigger the activation of the GNAT3, and thus PLCβ2 that induces the production of IP3. IP3 elicits an increase in intracellular Ca^{2+} levels, that, on taste buds, activates the TRPM5 causing cell depolarization [11,12]. Besides the oral cavity, the taste signalling pathway is widespread in several barrier tissues: airways [13,14], gastrointestinal tract [15–18], kidney [19,20], testis [21,22], skin [23,24], not only in humans but also in mouse [25] and rat CP [26], where they regulate several biological processes in response to alterations in the composition of body fluids. For example, bronchoconstriction and bronchodilation, release of gut hormones (e.g. ghrelin, leptin, cholecystokinin), and regulation of sperm chemotaxis (reviewed in [27]). Interestingly, activation of TAS2R38 in Caco-2 cells by a bitter agonist (phenylthiocarbamide) increased ABCB1 expression and its efflux activity, but not ABCC1 or ABCG2 expression. Moreover, TAS2R38 knockdown prevented ABCB1 upregulation [17]. This suggests that TAS2Rs might regulate biomolecular transport by modulating the expression and activation of ABC

transporters. Our previous findings of TAS2Rs in the CP epithelial cells and the data available demonstrating expression and activity of taste receptors in extra-oral tissues suggest that, at the CP, these receptors might function as chemical sensors of blood and CSF composition and be involved in the control of the traffic of chemical compounds across this brain barrier.

TAS2R14 and TAS2R39 bind various compounds [24,28,29] and are expressed in several tissues [14,24,30–32] including human CP samples and in HIBCPP cells, an *in vitro* model of the human BCSFB where their functional relevance remains unknown. In this study, we proposed that TAS2Rs, more specifically TAS2R14 and/or TAS2R39 could mediate the entrance of molecules from circulation into the CSF. To explore this hypothesis, we used the HIBCPP cell line to carry out functional Ca^{2+} imaging studies using resveratrol, a ligand of these two receptors that is also a neuroactive compound and a flavonoid well documented for their antioxidant, anti-inflammatory, anti-bacterial and anticarcinogenic properties. We found that, in HIBCPP cells, resveratrol specifically activates TAS2R14. Permeation studies showed that resveratrol can cross the human CP epithelial cells and, interestingly, TAS2R14 knockdown decreased resveratrol efflux at the apical membrane. Additionally, inhibition of ABCC1, ABCC4 and ABCG2 transporters decreased the efflux and increased accumulation of resveratrol inside the cells. Altogether, the present study provides strong evidence for an important role of TAS2R signalling at the human BCSFB regarding the passage of resveratrol, from the bloodstream into the CSF and the CNS.

5.3. Materials and Methods

5.3.1. Reagents

Resveratrol was obtained from TCI Europe N.V. (Japan), 3-(4,5-dimethylthiazol-2-yl)-2,5-diphenyltetrazolium bromide (MTT) from GERBU Biotechnik GmbH (Germany), fluorescein-methotrexate (FL-MTX) from Biotium (USA), reversan, and lucifer yellow from Sigma-Aldrich (Portugal), Ko143 from Tebu-bio and Ceefourin 1 from Tocris (UK). The primary antibodies, previously validated, rabbit TAS2R14 (RRID AB_2556261; PA5-39710), TAS2R39 (RRID AB_2556262; PA5-39711), mouse occludin Alexa Fluor® 594 conjugated (RRID AB_2532186; 331594) were obtained from Fisher Thermo Scientific (USA); and mouse β-actin (A1978) from Sigma-Aldrich (Portugal). Secondary antibodies goat anti-rabbit HRP-conjugated (sc-2004) and goat anti-mouse HRP-conjugated (sc-2005) were purchased from Santa Cruz Biotechnology (USA); donkey anti-rat Cy3 from Jackson Immunoresearch (UK), goat anti-rabbit Alexa Fluor® 488 from Thermo Fisher

Scientific (RRID AB_143165; A11008, Molecular Probes, USA). Hoechst 33342 (I34406), FURA-2 AM (F1221), pluronic acid F-127, Lipofectamine™ 2000 (11668027), Opti-MEM medium and small interfering RNA (siRNA) targeting TAS2R14 (s27144), TAS2R39 (s48942), scramble siRNA (4390843) and PowerUp™ SYBR™ Green were purchased from Thermo Fisher Scientific (USA). Acetonitrile analytical grade was purchased from Enzymatic, deionised (DI) water was obtained from a Milli-Q System (Millipore) and glacial acetic acid from Fisher Scientific UK.
A stock solution of resveratrol was prepared in dimethyl sulfoxide (DMSO), and freshly dissolved in Tyrode´s solution, culture medium or Krebs Ringer buffer (KRB) before the experiments, where the DMSO final concentration did not exceed 0.25%.

5.3.2. Establishment of Human epithelial CP papilloma Cell Culture

Human epithelial CP papilloma (HIBCPP) cells derived from a human malignant CP papilloma [33], were cultured, as previously reported [34], in DMEM/F12 (Pan-Biotech, Germany) supplemented with 5 µg/mL insulin (Sigma-Aldrich, Portugal), 4 mM L-glutamine, 100 U/mL penicillin, 100 ug/mL streptomycin and 10% (v/v) FBS. For all studies described here HIBCPP cells were used between passage 26 and 34.

5.3.3. Assessment of the responses of Human epithelial CP papilloma to neuroactive compounds by Ca^{2+} imaging

The response of HIBCPP cells to resveratrol was evaluated by Ca^{2+} imaging experiments. This bitter compound was selected considering its ability to bind TAS2R14 and/or TAS2R39, present in CP epithelial cells, and its potential therapeutic application in neurologic diseases.

5.3.4. Assessment of the cytotoxicity of resveratrol in HIBCPP cells

Before Ca^{2+} imaging experiments, the cytotoxicity of resveratrol was assessed in HIBCPP cells by the MTT assay. Briefly, 2 x10^4 cells were seeded in a 96-well plate and 24h before incubation, the culture medium was replaced by serum-free medium. Cells were incubated for 24h with resveratrol (50-250 µM), or vehicle (DMSO ≤ 0.25%) diluted in culture medium. Then, culture medium was removed, cells were washed twice with PBS and incubated with 50 µl of MTT solution (5 mg/mL in PBS), for approximately 3h at 37 °C in a humidified atmosphere containing 5% CO_2. Untreated cells and ethanol 70% treated cells were used as negative and positive controls, respectively. Following MTT incubation, formazan crystals were dissolved in DMSO for 30 minutes, and absorbance

was read at 570 nm in a microplate spectrophotometer xMark™ (Bio-Rad). HIBCPP cell viability was expressed as a percentage relative to the absorbance determined in the negative control cells.

5.3.5. Single Cell Ca^{2+} Imaging

Once the cytotoxic profile of resveratrol in HIBCPP cells had been established we proceeded with Ca^{2+} imaging assays. First, we performed a dose-response experiment with resveratrol (25-250 μM) or vehicle only (DMSO ≤ 0.25%).

Ca^{2+} imaging assays were performed as described before [35]. HIBCPP cells were seeded in μ-slide 8 well ibiTreat (Ibidi, Germany) and 72h after transfection, cells were loaded with 5 μM of FURA-2 AM and 0.02% pluronic acid F-127 in culture medium for 1h. Next, cells were washed twice with Tyrode's solution (NaCl 140 mM, KCl 5 mM, $MgCl_2$ 1.0 mM, $CaCl_2$ 2 mM, Na-pyruvate 10 mM, glucose 10 mM, HEPES 10 mM, $NaHCO_3$ 5 mM, pH 7.4) and loaded with Tyrode's for 30 minutes before acquisition. The μ-slide plates were placed on an inverted fluorescence microscope (Axio Imager A1, Carl Zeiss, Germany). Resveratrol stimulus was applied manually with a micropipette, and cells Ca^{2+} response was evaluated by quantifying the ratio of the fluorescence emitted at 520 nm following alternate excitation at 340 nm and 380 nm, using a Lambda DG4 apparatus (Sutter Instruments, Novato, CA) and a 520 nm bandpass filter (Carl Zeiss) under a 40x objective (Carl Zeiss) with an AxioVision camera and software (Carl Zeiss). Data was processed using the Fiji software (MediaWiki). Changes in fluorescence ratio ($F=F_{340}/F_{380}$) were measured in at least 20 cells, in four or more independent experiments. Response intensity, or intracellular Ca^{2+} variation, ($\Delta F/F_0$), was calculated in the following way: $\Delta F/F_0=(F-F_0)/F_0$, where F_0 corresponds to the fluorescence ratio average of baseline (2 minutes acquisition before stimuli) and F correspond to the maximum peak of fluorescence ratio evoked by stimuli.

5.3.6. TAS2R14 and TAS2R39 knockdown

Then, TAS2R14 and/or TAS2R39 specific activation by resveratrol (50 μM) was also assessed by Ca^{2+} imaging experiments in HIBCPP cells after silencing TAS2R14 or TAS2R39 expression.

HIBCPP cells were transfected with a mixture of siRNA targeting TAS2R14 (siRNA TAS2R14) or TAS2R39 (siRNA TAS2R39) and Lipofectamine™ 2000 in Opti-MEM medium, following the manufacturer's instructions. A scramble siRNA was also used as negative control for TAS2R14 or TAS2R39 specific targeting. Transfection conditions

were optimized using different timeframes (24, 48 and 72h), siRNA and transfection agent concentrations (data not shown). TAS2R14 and TAS2R39 expression were then analyzed by Western blot (WB) and immunofluorescence in mock- and siRNAs-transfected cells.

5.3.6.1. Western blot

Protein expression of the TAS2R14 and TAS2R39 was analyzed in protein extracts obtained from HIBCPP cells, after transfection, using ice-cold RIPA lysis buffer (NaCl 150mM, NP-40 1%, sodium deoxycholate 0.5%, SDS 0.1%, Tris 50 mM). Total protein content was measured using Pierce BCA Protein Assay Kit (Thermo Fisher Scientific, USA) according to the manufacturer's recommendations. Samples were separated by SDS-PAGE using a 12.5% gel and were electrically transferred to polyvinylidene difluoride (PVDF) membranes (Millipore, Merck). Blots were blocked for 1h at room temperature (RT) with Tris-buffered saline (TBS) containing 5% skimmed milk powder. Then blots were incubated overnight with primary rabbit antibodies to TAS2R14 (1:500) or TAS2R39 (1:500), and 1h RT with mouse anti-β-actin (1:20 000). After this, membranes were washed at RT with TBS containing 0.1% of Tween (TBS-T) before incubation for 1h with HRP-conjugated goat anti-rabbit or goat anti-mouse (1:40 000) secondary antibodies. Blots were washed, and antibody binding was detected using the ECL substrate (ClarityTM Western ECL Substrate, Bio-Rad, USA) according to the manufacturer's instructions. Images of blots were captured with the ChemiDoc MP Imaging system (Bio-Rad) and protein bands were quantified using the Image Lab software (Bio-Rad).

5.3.6.2. Immunofluorescence

Immunostaining of TAS2R14 and TAS2R39 in HIBCPP cells was also carried out after transfection. HIBCPP cells were cultured in 12 well plates with glass coverslips for 5-6 days. Then, cells were washed three times with phosphate-buffered saline (PBS), fixed with 4% paraformaldehyde (PFA) at RT for 10 min, permeabilized and blocked for 1h with PBS containing 0.2% Triton X-100 and 3% bovine serum albumin (BSA). Then cells were incubated overnight at 4°C with the rabbit primary antibodies TAS2R14 (1:300) and TAS2R39 (1:300). Next, cells were washed and incubated with secondary antibody goat anti-rabbit Alexa Fluor® 488 (1:1000) at RT for 1h. Nuclei were stained with Hoechst 33342 (1:1000) for 10 min, and coverslips were placed on glass slides using fluorescence mounting medium (Dako, Germany). Images were then acquired on a

LSM710 confocal laser scanning microscope (Carl Zeiss) at a 63x magnification. Fluorescence images from at least three different experiments were processed using Zen software (Carl Zeiss). For all conditions, five to six regions of interest (ROIs) were captured, and the staining intensity of fluorescence was quantified.
After WB and immunofluorescence assays, the optimal transfection conditions established were the following: 10 nM of siRNA (TAS2R14, TAS2R39 and scramble) for 72h. These conditions were applied in Ca^{2+} imaging and permeation studies.

5.3.7. Assessment of the role of TAS2R14 in the flow of resveratrol across the BCSFB

5.3.7.1. Cell culture in inserts and assessment of paracellular permeability

To determine if TAS2R14 regulates resveratrol flow across the BCSFB, we had to set up a proper model of the BCSFB using HIBCPP cells. For that, HIBCPP cells were plated in culture inserts (pore diameter 0.4 μm, 0.33 cm^2; VWR, Portugal), as described previously [34,35]. Briefly, HIBCPP cells were seeded in the upper chamber at a density of 1.5 $x10^5$ in culture inserts, in culture medium containing 10% of FBS. Culture medium was added to the lower chamber only two days after seeding. Paracellular permeability of HIBCPP layers was monitored through transepithelial electrical resistance (TEER) measurement, using an Epithelial-volt-ohm-meter (EVOM, World Precision Instrument, USA), every day from culture day 3, and culture medium was maintained with 1% FBS from day 4 onwards. TEER values of blank inserts (without cells) were used as control values and subtracted to calculate the final TEER (Ω**.** cm^2).
In addition to TEER measurement, the paracellular flux of lucifer yellow was determined at the 8th day of cell culture. Briefly, culture inserts were transferred to a new plate, washed and incubated in KRB for 30 minutes, at 37 ºC in a humidified atmosphere containing 5% CO_2. Next, lucifer yellow (50 μM) dissolved in KRB was applied to the apical chamber of inserts, and only KRB was added to the basolateral chamber. After an incubation period of 60 minutes at 37 ºC, samples of apical and basolateral chambers were collected, and lucifer yellow concentration was measured with a SpectraMax Gemini spectrofluorometer (Molecular Devices) at excitation/emission wavelengths of 398 nm/518 nm. The % of lucifer yellow in the basolateral chamber was calculated to estimate cell layer integrity. The establishment of HIBCPP layers under the culture conditions described before was also analyzed by occludin staining to visualise tight junctions (described in the next section).

5.3.7.2. Subcellular localization of TAS2R14

Before assessing if TAS2R14 regulates the flow of resveratrol across the BCSFB, it was important to determine the TAS2R localization in the membrane of these cells. The localization of TAS2R14, whether in the basolateral or in the apical membrane was assessed by double staining with the ABCC1 transporter, that locates to the basolateral membrane of CP epithelial cells [5], or with the tight junction occludin that localizes between cells close to the apical membrane [34]. Briefly, HIBCPP cells were grown in culture filter inserts for 8 days and then washed with PBS, fixed with 4% PFA at RT for 10 min, permeabilized and blocked for 1 hour with PBS containing 0.2% Triton X-100 and 3% BSA. Next, cell inserts were cut out and transferred to a coverslip and cells were incubated with rabbit anti-TAS2R14 (1:300) combined with rat anti-ABCC1 (1:100) overnight at 4ºC. After that, cells were washed several times and incubated with secondary antibodies goat anti-rabbit Alexa Fluor® 488 (1:1000) and donkey anti-rat Cy3 (1:800) or mouse anti-occludin Alexa Fluor® 594 conjugated at RT for 1h. After wash, nuclei were stained with Hoechst 33342 (1:1000) for 10 minutes. For each condition, fluorescence z-stack images (0.5 μm thickness) were acquired with a confocal LSM 710 Zeiss microscope using a 63x objective (Carl Zeiss, Germany). Image processing was conducted with Zen software (Carl Zeiss) and representative images, from at least 3 different experiments, were selected for graphical presentation. Optical slice view was constructed from fluorescence samples and subcellular localization of TAS2R14 was compared to ABCC1 or occludin expression at the basolateral or apical membrane, respectively.

5.3.7.3. Resveratrol permeation studies

HIBCPP cells were seeded in culture inserts as previously described, and experiments were performed at the 8th day of culture at full-confluence, assessed following the protocol described in 5.3.7.1. First, the passage of resveratrol across HIBCPP cells was assessed at different time points (0, 2 and 3h) after incubation of cells with resveratrol. Briefly, culture medium was removed from the apical and basolateral chambers, cells were washed three times with KRB and allowed to equilibrate in this buffer for 30 minutes at 37ºC, 5% CO_2. Next, resveratrol (50 μM) in KRB was added to the basolateral chamber of culture inserts and only KRB was added to the apical side. After 0, 2 and 3h the media in the basolateral and apical chambers was collected, and samples were stored at -20 ºC for analysis of resveratrol levels by high-performance liquid chromatography (HPLC).

Then, the role of TAS2R14 in resveratrol transport was evaluated. For that, permeation assays were carried out as described above in mock-, siRNA scramble- or siRNA TAS2R14-transfected HIBCPP cells for 72h. Resveratrol (50 μM) in KRB was added to the basolateral side and samples from both chambers were collected after 3h for resveratrol measurement by HPLC.

5.3.7.4. Measurement of resveratrol by HPLC

A high-performance liquid chromatography system (HPLC) 1290 Infinity with a binary pump 1290 VL from Agilent Technologies (Soquimica, Lisboa, Portugal) was set to perform the chromatographic analysis coupled to diode array detection (DAD) carried with a 1290 DAD detector (Soquimica, Lisboa, Portugal). The chosen wavelength to detect resveratrol was 306 nm. Separation was achieved with a Zorbax Eclipse plus C18 (1.8 μm, 2.1 × 50 mm i.d.) analytical column from Agilent Technologies (Soquimica, Lisboa, Portugal) with a guard column Zorbax Ecliple pluc C18 (1.8 μm, 2.1 × 5 mm i.d.) also from Agilent Technologies (Soquimica, Lisboa, Portugal). The HPLC-DAD worked on isocratic mode with a mobile phase composed by deionized water: acetonitrile: glacial acetic acid (66:33.9:0.1). Mobile phase rate was 0.5 mL/min and sampler and column temperatures were set to 4 and 35 °C, respectively. Chromatographic runtime was 5 min. The analysis was carried out according to the Food and Drug Administration guidelines.

5.3.7.5. Effect of TAS2R14 activation on ABC transporters

Based on the initial hypothesis, a way by which taste receptors might control cell trafficking of their ligands, could be through the regulation of ABC transporters. To test this hypothesis, we first analysed the role of basolateral ABC transporters ABCC1 and ABCC4 and apical transporter ABCG2 in resveratrol transport across the BCSFB.
The functionality of ABC transporters in HIBCPP cells was assessed by analysing the cell accumulation of its known substrates ABCC1 - Calcein AM (0.1 μM), ABCC4 - FL-MTX (2 μM) and ABCG2 - Hoechst 33342 (1 μM). For that, cells were seeded in culture inserts to assess ABCC1 and ABCC4 function due to their basolateral localization, or in 96-well plates with a density of 3.2 x10^4 cells/well to analyse ABCG2 as described before [5], as this transporter is located at the apical membrane of cells. At the 8th day of culture, cells were washed three times with KRB and preincubated for 1h at 37 °C, with or without their inhibitors; ABCC1 - reversan (10 μM), ABCC4 - ceefourin 1 (5 μM) or ABCG2 - Ko143 (100 nM). Next, cells were incubated with the substrates in the presence or absence of inhibitors for 2h at 37 °C. Finally, cells were washed with ice-cold KRB and

lysed with 1% Triton X-100 in KRB for 30 minutes at 37 ºC. Calcein AM, FL-MTX and Hoechst 33342 accumulation in HIBCPP cells was analysed in a SpectraMax Gemini spectrofluorometer (Molecular Devices) at excitation/emission wavelengths of 490 nm/520 nm, 490 nm/520 nm and 350 nm/480 nm, respectively.
Then, the role of TAS2R14 and ABCC1, ABCC4 and ABCG2 in resveratrol transport was evaluated. For that, permeation assays were carried out as described above in mock-, siRNA scramble- or siRNA TAS2R14-transfected HIBCPP cells for 72h. Another group of cells was pre-incubated with or without ABCs inhibitors, reversan (10 μM), ceefourin 1 (5 μM) and Ko143 (100 nM) for 1h at 37 ºC. In all experiments, resveratrol (50 μM) in KRB was added to the basolateral side and samples of both chambers were collected after 3h.

5.3.8. Effect of TAS2R14 activation on the expression and function of ABC transporters

Besides ABC transporters function on resveratrol transport across the BCSFB, also TAS2R14 role in ABC transporters expression and function was analysed in HIBCPP cells. For that, at the end of the experiments performed in the previous section (2.4.5.), mock-, siRNA scramble- and siRNA TAS2R14-transfected cells in culture inserts were collected in TripleXtractor (Grisp Research Solutions, Portugal) for subsequent RNA extraction and ABC transporters expression analysis by real time RT-PCR. Moreover, ABC transporters function was evaluated through the analysis of their substrate's accumulation in mock-, siRNA scramble- and siRNA TAS2R14-transfected cells as described below at the section 5.3.8.1.

5.3.8.1. Analysis of the expression of ABC transporters by Real time RT-PCR

Real time RT-PCR (RT-qPCR) was used to analyse the expression of ABC transporters (ABCC1, ABCC4 and ABCG2) after TAS2R14 activation by resveratrol. Total RNA was isolated from HIBCPP cells using TripleXtractor following the manufacturer's instructions, and 500 ng of total RNA was reverse transcribed using a M-MLV Reverse Transcriptase (NZYTech, Ltd., Portugal). RT-qPCR reactions were carried out using 1 μL of cDNA synthesized in a 10 μL reaction mixture containing PowerUp™ SYBR™ Green and specific primers (Table 1) [5]. Glyceraldehyde-3-phosphate dehydrogenase (GAPDH) was used as endogenous control. RT-qPCR was carried out in a 96-well plate (Thermo Fisher Scientific, USA) and amplification conditions used were 50 ºC for 2

minutes, 95 ºC for 2 minutes, and 40 cycles of 95 ºC for 15 seconds, 60 ºC for 15 seconds and 72 ºC for 1 minute. Fluorescence was measured after each cycle and displayed graphically (iCycles iQ Real-time detection System Software, Bio-Rad). The software determined the quantification cycle (Ct) values for each sample. Data collected from RT-qPCR experiments and ABCC1, ABCC4 and ABCG2 relative expression was analysed using the formula $2^{-(\Delta\Delta Ct)}$ [36].

Table 5. 1. Primer sequences used in real-time RT-qPCR.

Gene	Primer Fw (5' – 3')	Primer Rv (5' – 3')	AT
ABCC1	CGACATGACCGAGGCTACATT	AGCAGACGATCCACAGCAAAA	60 ºC
ABCC4	TGTGGCTTTGAACACAGCGTA	CCAGCACACTGAACGTGATAA	
ABCG2	ACGAACGGATTAACAGGGTCA	CTCCAGACACACCACGGAT	
GAPDH	ATGGGGAAGGTGAAGGTCG	GGGGTCATTGATGGCAACAATA	

Fw – forward; Rv – reverse; T – temperature.

5.3.8.2. Analysis of the role of TAS2R14 on the function of ABC transporters

The role of TAS2R14 activation in the functionality of ABC transporters in HIBCPP cells was assessed by analysing the cell accumulation of its known substrates ABCC1 - Calcein AM (0.1 μM), ABCC4 - FL-MTX (2 μM) and ABCG2 - Hoechst 33342 (1 μM) in mock-, siRNA scramble- and siRNA TAS2R14 transfected cells. ABCC1 and ABCC4 function was assessed using culture inserts and ABCG2 in 96-well plates, as described in the section 5.3.7.5. Therefore, at the 8th day of culture, cells in the culture inserts and in the 96-well plates were washed three times with KRB and allowed to equilibrate for 30 minutes at 37 ºC. Next, cells were incubated with the ABC substrates (Calcein AM, FL-MTX and Hoechst 33342) for 3h at 37 ºC, with or without resveratrol. Then, the cells were washed with ice-cold KRB and lysed with 1% Triton X-100 in KRB for 30 minutes at 37 ºC. Calcein AM, FL-MTX and Hoechst 33342 accumulation in HIBCPP cells was analysed in a SpectraMax Gemini spectrofluorometer (Molecular Devices) at excitation/emission wavelengths of 490 nm/520 nm, 490 nm/520 nm and 350 nm/480 nm, respectively.

5.3.9. Statistical analysis

Statistical analysis and comparison were performed using GraphPad Prism 7 software. Statistical significance of differences between two groups was determined by the student *t-test*, and for more than two groups it was used the one-way or two-way analysis of

variance (ANOVA) followed by Bonferroni´s post hoc test. Results are reported as mean ± SEM and data were considered statistically significant at a value of $p<0.05$.

5.4. Results

5.4.1. Resveratrol elicited Ca^{2+} responses in HIBCPP cells via TAS2R14 activation

The activation of TAS2R14 and TAS2R39 in HIBCPP cells by resveratrol was evaluated by Ca^{2+} imaging. Prior to Ca^{2+} imaging assays, resveratrol cytotoxicity in HIBCPP cells was assessed by the MTT assay (Figure 5.1.A). Resveratrol (Figure 5.1.A) for all the concentrations tested no significant differences in cell viability were noticed in comparison with untreated or vehicle-only treated cells after 24h of incubation.

Once the toxicity profile of this bitter compound was assessed, we proceeded to functional studies. As mentioned before, TAS2Rs activation upon ligand-binding triggers a cascade that leads to increased intracellular Ca^{2+} levels. Therefore, we analyzed the HIBCPP responses to resveratrol (25-250 μM) stimuli by Ca^{2+} imaging experiments (Figure 5.1.B). Ca^{2+} imaging assays were carried out in the presence of vehicle and compared to untreated cells to establish that Ca^{2+} responses observed were not related to vehicle concentration (data not shown). Moreover, Ca^{2+} variations were collected during 2 min before the stimuli to obtain a baseline (F0) that was used to normalize the responses obtained with the compounds. Only assays showing a uniform baseline, meaning without significant Ca^{2+} changes were analyzed. Resveratrol (Figure 5.1.B) elicited Ca^{2+} responses in a dose-dependent manner. HIBCPP cells treated with resveratrol stimuli above 50 μM showed a massive increase of Ca^{2+} levels ($\Delta F/F0= 0.961 \pm 0.094$) in comparison with vehicle treated cells ($\Delta F/F0= 0.1035 \pm 0.004$) (Figure 5.1.B).

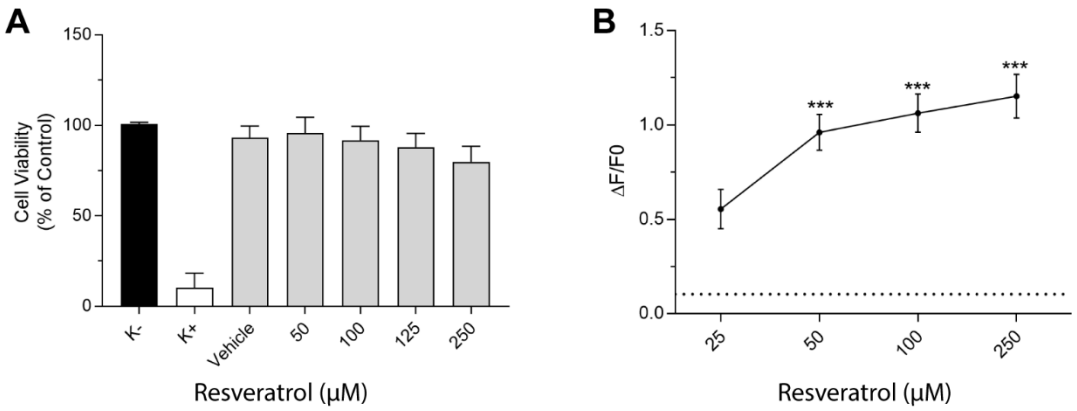

Figure 5. 1. Resveratrol elicited Ca2+ responses in HIBCPP cells. (A) The cytotoxicity of resveratrol was assessed in HIBCPP cells by the MTT assay. HIBCPP cells were treated for 24 h with different concentrations of resveratrol. Bar graphs represent mean ± SEM (N ≥ 3). Vehicle - cells treated with ≤ 0.25% DMSO. K+ - positive control. (B) Ca2+ dose–response curves obtained in HIBCPP cells in response to different concentrations of resveratrol (25–250 μM). Dot line – calcium levels measured in cells in response to vehicle DMSO ≤ 0.25%. Average response intensity, or intracellular Ca2+ variations were measured: (ΔF/F0) = ((F340-F380)-F0)/F0, where F0 corresponds to fluorescence ratio of a 2 min baseline and F corresponds to the maximum peak of fluorescence ratio evoked by stimuli. Results are presented as the mean ± SEM (N ≥ 4, independent experiments; ***p < 0.001; One-way ANOVA followed by Bonferroni's post hoc test).

Next, we investigated whether the Ca^{2+} response observed was dependent on TAS2R14 or TAS2R39 activation. Previous studies showed that resveratrol binds TAS2R14 and TAS2R39 [37]. Therefore, specific activation of TAS2R14 and/or TAS2R39 by resveratrol was evaluated in Ca^{2+} imaging studies in HIBCPP cells after TAS2R14 or TAS2R39 siRNA silencing.

TAS2R14 and TAS2R39 silencing was achieved by transfecting HIBCPP cells for 72h with 10 nM of specific TAS2R14 or TAS2R39 siRNAs, respectively. Knockdown efficiency was assessed by WB and immunofluorescence experiments in mock- and siRNAs-transfected cells (Figure 5.2.). The protein expression of TAS2R14 and TAS2R39 decreased significantly in WB (Figure 5.2.A) and in immunofluorescent assays (Figure 5.2.B) in comparison with mock- and siRNA scramble-transfected cells. In addition, no significant differences were observed between mock-transfected cells and TAS2R14 or TAS2R39 siRNAs alone, or scramble siRNA-transfected cells. These optimized silencing conditions were then applied in Ca^{2+} imaging assays. A similar effect of resveratrol was observed in untreated, mock- and siRNA scramble-transfected cells (Figure 5.2.C). On the other hand, TAS2R14 knockdown resulted in a decreased response to resveratrol in comparison to controls: 39.36 ± 12.19 % vs untreated, 39.27 ± 11.49 % vs mock- and 39.06 ± 12.19 % vs siRNA scramble-transfected cells (Figure 5.2.). TAS2R39 knockdown, however, had no significant effect in the Ca^{2+} response to resveratrol in HIBCPP cells. Additionally, no significant differences were observed between control conditions (untreated, mock-, or scramble siRNA-transfected cells) in Ca^{2+} imaging assays.

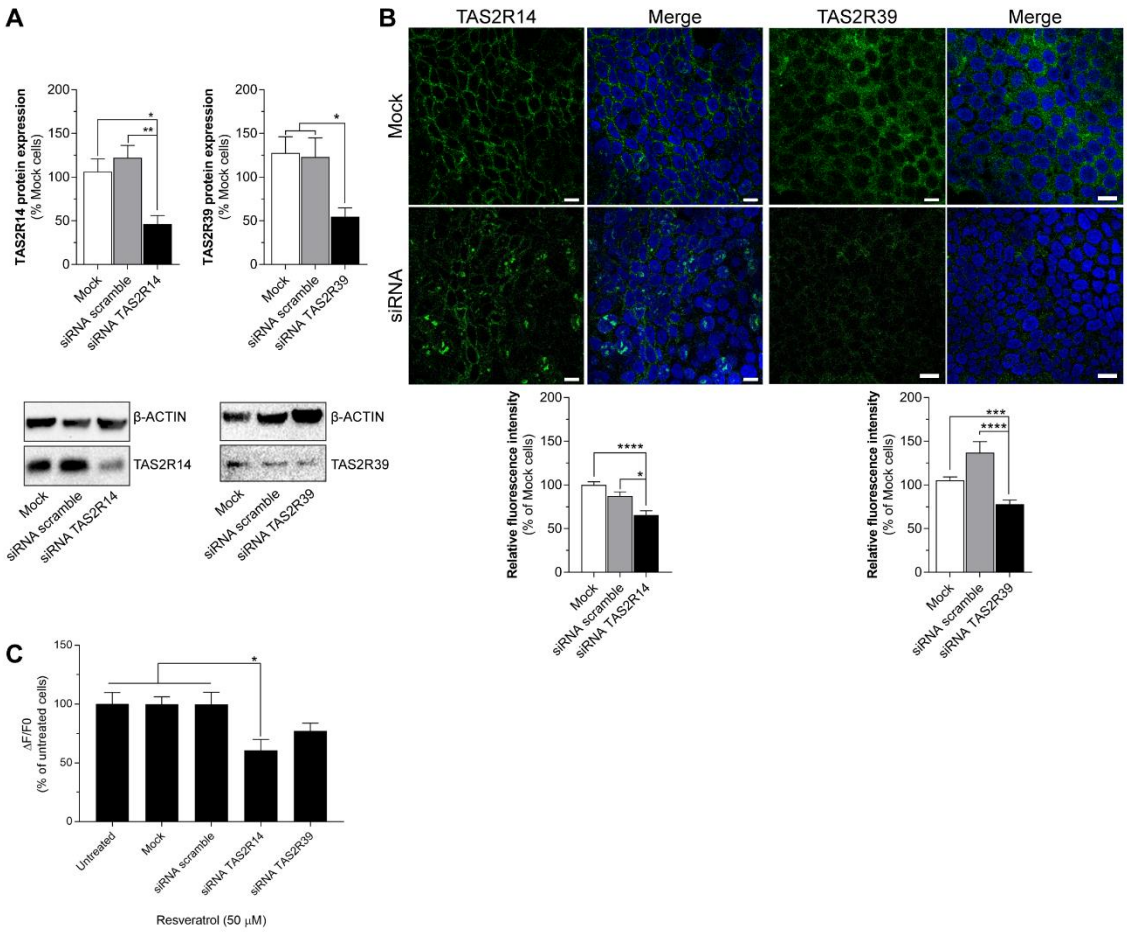

Figure 5. 2. Ca^{2+} responses of HIBCPP cells to resveratrol is dependent on TAS2R14 expression. (A) WB analysis of TAS2R14 and TAS2R39 expression following siRNA transfection (72 h) in HIBCPP cells. Protein levels of both TAS2R14 and TAS2R39 decreased in siRNA TAS2R14- and siRNA TAS2R39-transfected cells in comparison with mock- and siRNA scramble-transfected cells. β-actin served as loading control. (B) Immunofluorescence analysis of TAS2R14 and TAS2R39 expression after siRNA transfection. HIBCPP cells immunoreactive to antibodies TAS2R14 and TAS2R39, after nuclei staining with Hoechst 33423 were observed and images obtained in confocal microscope. Quantification of TAS2R14 or TAS2R39 expression (green fluorescence) was performed in different regions of interest (ROIs) of images obtained from three independent experiments. Fluorescence intensity decreased in siRNA TAS2R14- and siRNA TAS2R39-transfected cells in comparison to mock- and siRNA scramble-transfected cells. Scale bar – 10 μm. Graph bars indicates the mean ± SEM (N ≥ 3, independent cultures; *p < 0.05, **p < 0.01, ****p < 0.0001; One-way ANOVA followed by Bonferroni's post hoc test). (C) Ca^{2+} responses to resveratrol stimulus in HIBCPP cells transfected with TAS2R14 or TAS2R39 siRNAs. Intracellular Ca2+ levels were measured in HIBCPP cells transfected or mock-transfected for 72 h with TAS2R14 or TAS2R39 siRNA, or with scramble siRNA, after resveratrol (50 μM) stimulus. Graph bars indicate the mean ± SEM (N ≥ 4, independent cultures; *p < 0.05; One-way ANOVA followed by Bonferroni's post hoc test). For all the experiments, there were no significant differences between untreated cells and mock- or scramble siRNA-transfected cells.

5.4.2. TAS2R14 localizes in the basolateral membrane of HIBCPP cells

Ca^{2+} imaging assays showed that TAS2R14 is activated by resveratrol in HIBCPP cells. Thus, we tested whether this interaction occurs in the basolateral or apical membrane of HIBCPP cells, by determining the subcellular localization of this bitter taste receptor. These studies were performed after establishment of HIBCPP cell layers cultured in permeable filter culture inserts (pore 0.4 μm) mimicking BCSFB features, as previously

described [5,34,35]. Barrier properties were evaluated through the measurement of TEER, evaluation of lucifer yellow flux and analysis of the expression of the tight junction protein occludin (Figure 5.3.).

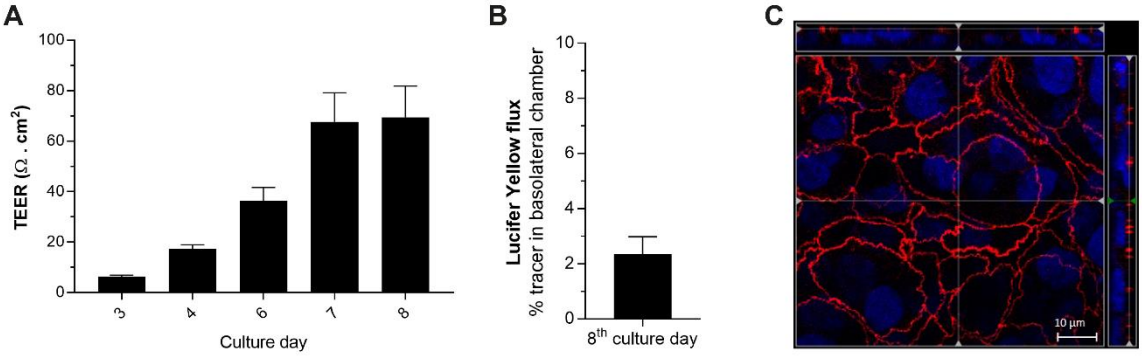

Figure 5. 3. Establishment of a barrier of HIBCPP cells. The barrier properties of HIBCPP cells were evaluated through the measuring of the parameters: (A) TEER values were measured in HIBCPP culture from the 3rd to 8th day of culture. TEER values increased along culture time reaching maximum levels on 7 or 8th day of culture. (B) Paracellular permeability was evaluated analysing the Lucifer yellow flux through the HIBCPP cells' barrier at the 8th day of culture. After incubating HIBCPP cells with Lucifer yellow for 1 h, low paracellular flux was observed with only 2.029 ± 0.625% of the tracer being detected in the basolateral chamber. (C) The formation of tight junctions and polarization of HIBCPP cells was also analysed by occludin staining, that showed a continuous pattern of apical localization. Together, this data indicates a high tightness of the HIBCPP layers, mimicking the BCSFB.

Then, the subcellular localization of TAS2R14 was analyzed by confocal microscopy, comparing to the basolateral localization of the ABCC1 transporter (Figure 5.4.A) and to the apical thigh junction occludin (Figure 5.4.B) [5]. Double staining of TAS2R14 (Figure 5.4Ai) and ABCC1 (Figure 5.4Aii) in HIBCPP cells showed an overlap in the expression of both proteins (Figure 5.4Aiii). On the other hand, TAS2R14 co-staining with occludin did not provide evidences of existing co-localization (Figure 5.4Bii). Indeed, occludin staining (Figure 5.4Biii) was not observed in the same z-plane as TAS2R14 (Figure 5.4Bi).

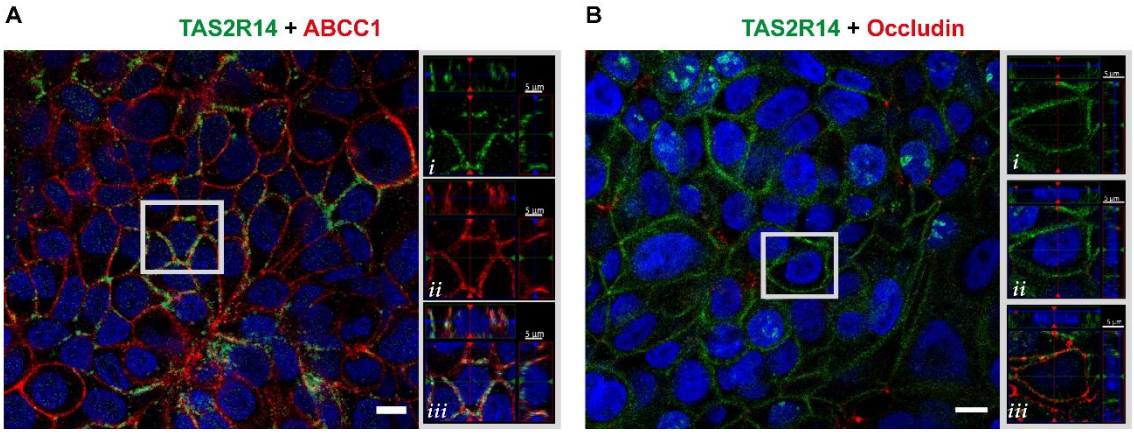

Figure 5. 4. TAS2R14 localizes at the basolateral membrane of HIBCPP cells. Subcellular localization of TAS2R14 in the basolateral or apical membrane of HIBCPP cells was analysed by confocal microscopy. HIBCPP cells were stained with rabbit polyclonal antibody to TAS2R14 (green) followed by a rat polyclonal antibody to ABCC1 (red) (A) or a monoclonal antibody to occludin (red) (B). Nuclei were stained with Hoechst 33423 (blue). At the same z-stack plane, TAS2R14 expression (Ai) overlaps with ABCC1 (Aii)

indicating a basolateral localization of TAS2R14 (Aiii). Contrarily, double staining with TAS2R14 and occludin does not show colocalization. In the same z-stack plane of TAS2R14 expression (Bi) and when merging both signals (Bii), occludin expression is not observed. However, in a different z-stack plane (more apical) occludin staining becomes evident but does not merge with TAS2R14 (Eiii). Scale bar – 10 μm.

5.4.3. The permeability of HIBCPP cells to resveratrol is dependent on TAS2R14 activation at the basolateral membrane

The knowledge regarding resveratrol ability to cross brain barriers and to permeate the brain is still scarce, despite its therapeutic potential. We further explored whether the human BCSFB could be a gateway for resveratrol into the CNS and what are the mechanisms underlying its trafficking across HIBCPP cells. In fact, subcellular localization of TAS2R14 expression at the basolateral membrane of HIBCPP cells gave further support to the hypothesis that this receptor could be involved in the passage of resveratrol from the bloodstream into the CSF. To address this possibility, resveratrol permeation studies were performed in this *in vitro* BCSFB model, to evaluate if TAS2R14 silencing would affect the ability of resveratrol to cross the barrier from the basolateral to the apical side (Figure 5.5.A). Permeation assays with resveratrol were carried out at three different time-points (0, 2 and 3h) adding resveratrol at 50 μM to the basolateral chamber, and then, collecting samples from the apical and basolateral chambers to measure resveratrol levels by HPLC. At time 0h, resveratrol was not detected at the apical chamber of culture inserts. After 2h and 3h, resveratrol was already detectable in the apical chamber, providing evidence that it was able to cross the barrier formed by HIBCPP cells (Figure 5.5.B). Additionally, resveratrol levels in the apical chamber after 3h (13.43 ± 0.87 μM) were two times higher than after 2h (6.40 ± 1.05 μM) (Figure 5.5.B). Furthermore, the total levels of resveratrol in both chambers after the experiment were also evaluated (Figure 5.5.C). No significant differences in total resveratrol levels were found between 2h (33.76 ± 2.37 nmol) and 3h (33.52 ± 1.40 nmol) of incubation (Figure 5.5.C). However, in comparison with the initial levels of resveratrol (50 μM or 50 nmol), there was some retention of this compound in cells or culture inserts.

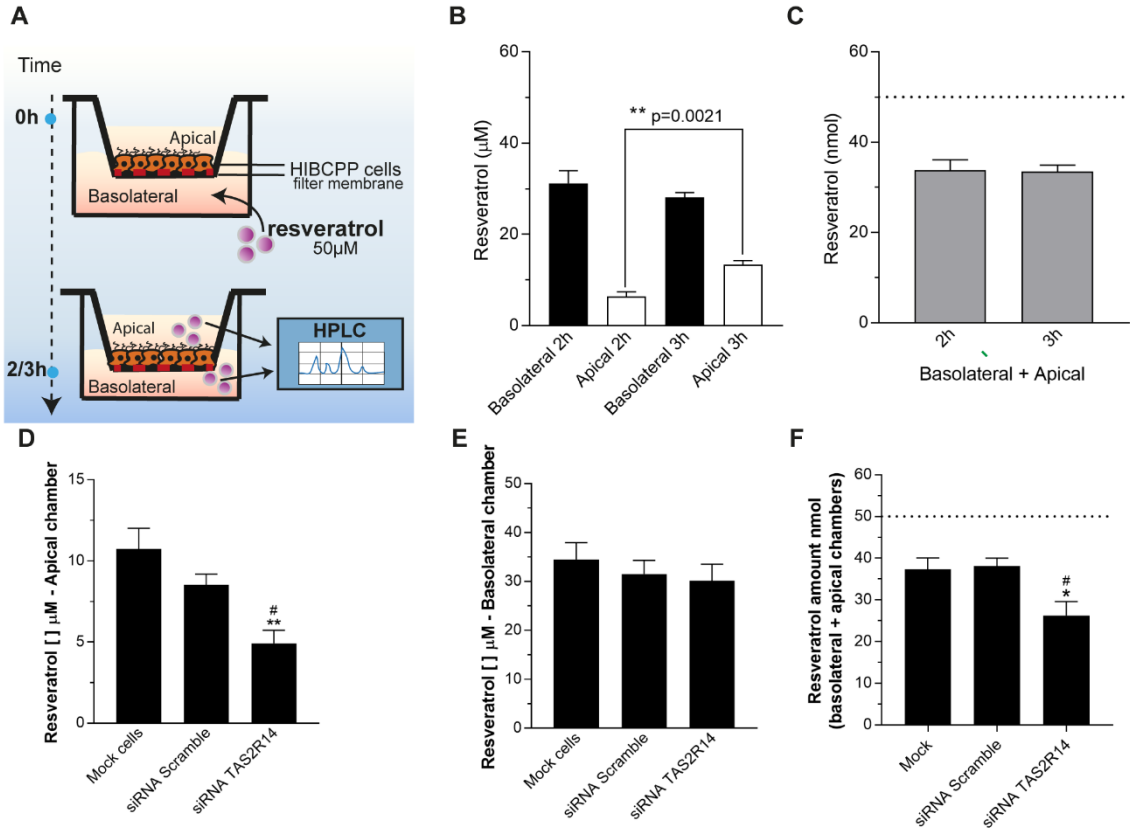

Figure 5. 5. Resveratrol transport across HIBCPP cells depends on TAS2R14 expression. (A) Schematic presentation of the experimental setup for resveratrol permeation assays in HIBCPP cells. At the 7-8th day of culture, resveratrol (50 µM) was added to the basolateral chamber, and after 2 h or 3 h the medium in the basolateral and apical chambers were collected, and resveratrol levels analyzed by HPLC. In addition, resveratrol was also measured after TAS2R14 knockdown by siRNA transfection. (B) Accumulation of resveratrol in the apical chamber occurred in a time dependent manner (**p = 0.0021). Graph bars indicate the mean ± SEM (N = 3, **p < 0.01; Student T-test unpaired). (C) Resveratrol accumulation/retention in HIBCPP cells or culture inserts membrane was low and did not depend on incubation time. Resveratrol accumulation on the apical side decreased in TAS2R14 knockdown cells (D) but did not change in the basolateral side (E). (F) The sum of resveratrol in both compartments was reduced in TAS2R14 silenced cells. Graphs indicate the mean ± SEM (N > =5; *p < 0.05, **p < 0.01 vs mock-transfected cells; #p < 0.05 vs siRNA scramble-transfected cells; One-way ANOVA followed by Bonferroni's post hoc test).

As resveratrol is a TAS2R14 ligand, we evaluated the possible involvement of TAS2R14 in the passage of resveratrol across the BCSFB. Thus, we silenced TAS2R14, as described before, and compared resveratrol transport of controls (mock- and siRNA scramble-transfected cells) with cells silenced for TAS2R14. Silencing of TAS2R14 resulted in a reduction in resveratrol accumulation of 5.83 µM (57.33 ± 14.03%) and 3.60 µM (42.12 ± 14.46%) in the apical chamber in comparison with mock- and siRNA scramble-transfected cells, respectively (Figure 5.5.D). No differences were observed in resveratrol levels at the basolateral chamber (Figure 5.5.E). Additionally, we compared the total levels of resveratrol in the apical and basolateral chambers to assess resveratrol accumulation in cells during the assays with TAS2R14 knockdown (Figure 5.5.F). After 3h of incubation with resveratrol (50 nmol), our results show that total levels of resveratrol detected in both chambers in mock-transfected cells were 39.54 ± 2.73 nmol

(Figure 5.5.F), indicating low accumulation of resveratrol by HIBCPP cells. However, the levels of resveratrol found, after silencing TAS2R14, in the basolateral chamber and apical chambers decreased to 28.36 ± 3.30 nmol suggesting increased cellular accumulation of resveratrol by HIBCPP cells.

5.4.4.ABCC1, ABCC4 and ABCG2 modulate resveratrol transport in HIBCPP cells

Our observation of resveratrol accumulation at the apical side raised the possibility that this could be occurring by facilitated transport via the action of ABC transporters. Thus, we analysed the functionality of ABCC1, ABCC4 and ABCG2 in HIBCPP cells. Specific inhibitors of each transporter were selected, and inhibition of their function was analysed by measuring the cellular accumulation of known ABCC1, ABCC4 and ABCG2 substrates (Figure 5.6.). We used the following ABCC1, ABCC4 and ABCG2 substrates: Calcein AM (0.1 μM), FL-MTX (2 μM) and Hoechst 33342 (1 μM), respectively. Our results showed Calcein AM accumulation in HIBCPP cells in the presence of the ABCC1 inhibitor reversan (10 μM) (Figure 5.6.A), as well as FL-MTX in the presence of Ceefourin 1 (5 μM), a specific inhibitor of ABCC4 (Figure 5.6.B). Moreover, Hoechst 33342 accumulation in HIBCPP cells also increased significantly after incubation with the ABCG2 inhibitor Ko143 at 100 nM (Figure 5.6.C). Therefore, these results indicate that inhibition of ABCC1, ABCC4 and ABCG2 was achieved at each of the conditions used.

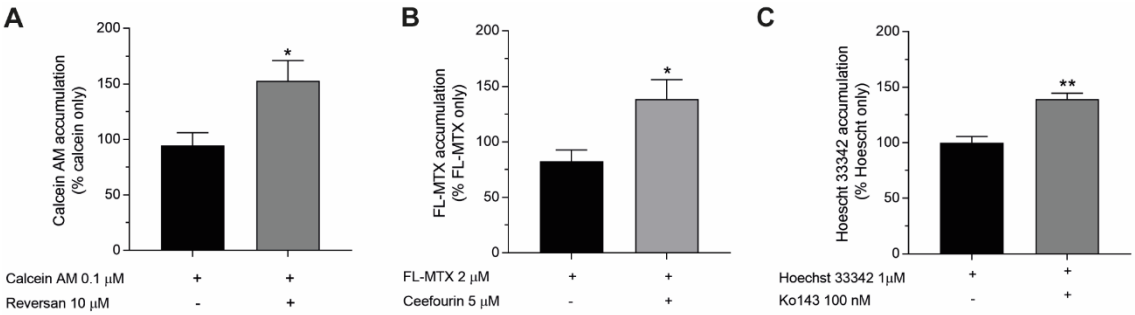

Figure 5. 6. Evaluation of ABCC1, ABCC4 and ABCG2 function in HIBCPP cells. The cellular accumulation of specific substrates for ABCC1, Calcein AM (0.1 μM) (A), ABCC4, FL-MTX (2 μM) (B) and ABCG2, Hoechst 33342 (1 μM) (C) was evaluated after 2 h of incubation, in the presence (+) or absence (-) of specific inhibitors reversan-ABCC1 (10 μM), Ceefourin 1-ABCC4 (5 μM) and Ko143-ABCG2 (100 nM). Graph bars indicate the mean ± SEM (N ≥ 3; *p < 0.05, **p < 0.01; Student T-test unpaired). FL- fluorescein, MTX – methotrexate.

Then, we explored whether ABC transporters are involved in resveratrol transport across HIBCPP cells, also with the same type of permeation studies in HIBCPP cells. Prior to incubation with resveratrol for 3h, a pre-treatment of 1h was performed with each ABC inhibitor (ABCC1 - reversan, ABCC4 - ceefourin 1 or ABCG2 - Ko143) by adding each one to basolateral and apical chambers (Figure 5.7.A). In the presence of each ABC inhibitor

resveratrol levels decreased in both the apical (Figure 5.7.B) and basolateral (Figure 5.7.C) chambers. In the apical chamber resveratrol accumulation decreased: 6.34 µM (69.95 ± 14.35%) with reversan, 7.45 µM (74.03 ± 15.42%) with Ceefourin 1 and 7.04 µM (62.94 ± 14.35%) with Ko143 in comparison with control cells (Figure 5.7.B). In the donor (basolateral) chamber, Ceefourin 1 reduced resveratrol levels by 22.84 µM (58.81 ± 9.52%) when compared with control cells. Further, in the basolateral side, reversan and Ko143 reduced resveratrol levels by 11.82 µM (37.12 ± 9.52%) and 13.52 µM (34.81 ± 8.83%) in comparison to control cells, respectively (Figure 5.7.C). Additionally, inhibition of ABCC1, ABCC4 or ABCG2 also decreased total levels of resveratrol (apical + basolateral), which corresponded to 26.69 ± 3.28, 13.90 ± 2.41 or 24.64 ± 2.29 nmol, respectively, in comparison to 39.55 ± 3.10 µM of resveratrol found in controls (Figure 5.7.D). The enhancement of cellular accumulation of resveratrol after inhibition of ABCC1, ABCC4 and ABCG2 suggest that all these transporters are involved in resveratrol efflux in CP epithelial cells.

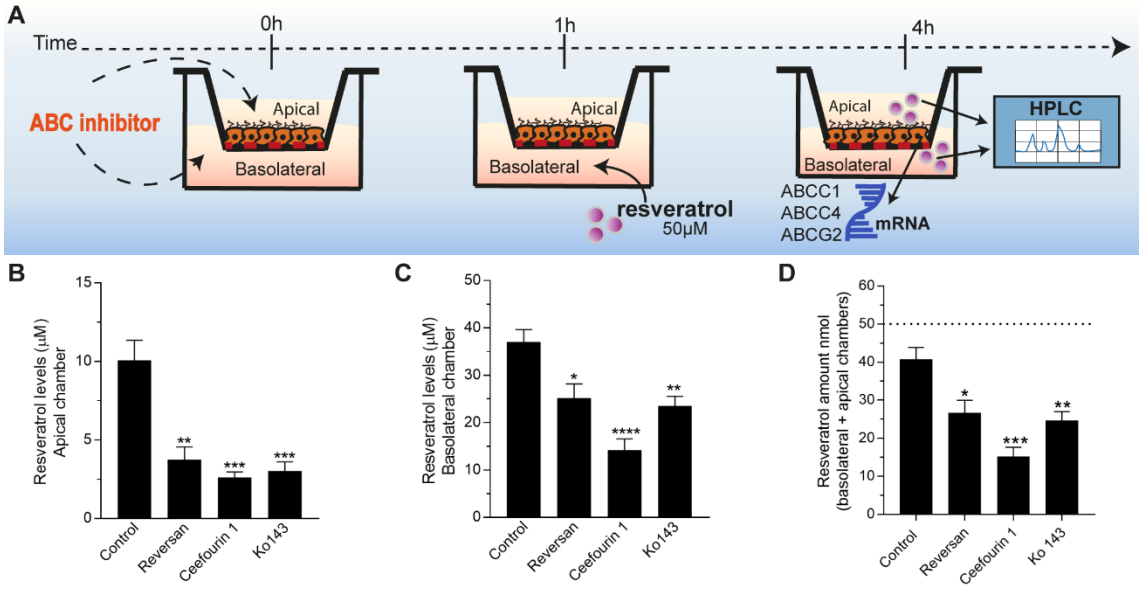

Figure 5. 7. ABCC1, ABCC4 and ABCG2 participate in resveratrol transport across HIBCPP cells. (A) Schematic presentation of the setup of resveratrol permeation assays in HIBCPP. HIBCPP cells were pre-treated for 1 h with or without ABC specific inhibitors: reversan-ABCC1 (10 µM), Ceefourin 1-ABCC4 (5 µM) and Ko143-ABCG2 (100 nM) (added to both chambers), followed by an incubation for 3 h with resveratrol (50 µM). After the permeation experiments, resveratrol levels were evaluated in apical (B), basolateral (C) and both chambers (D). In the presence of each ABC inhibitor, resveratrol levels decreased in the apical and/or basolateral chambers. Graphs indicate the mean ± SEM (N > =5; *p < 0.05, **p < 0.01, ***p < 0.001, ****p < 0.0001 vs control; One-way ANOVA followed by Bonferroni's post hoc test).

5.4.5. Resveratrol modulates ABCC1, ABCC4 and ABCG2 expression, an effect dependent on TAS2R14 expression

Permeation assays indicated that TAS2R14 regulates resveratrol transport across HIBCPP cells as resveratrol accumulation at the apical chamber decreased in TAS2R14 knockdown cells. Resveratrol levels at the apical chamber also decreased after ABCC1, ABCC4 and ABCG2 inhibition. This suggested a possible role of TAS2R14 and/or resveratrol in modulating the expression of these ABCs and their function. To further understand the mechanisms involved in this transport, we investigated the effects of TAS2R14 knockdown and resveratrol on the expression of ABCC1, ABCC4 and ABCG2.
We observed that TAS2R14 knockdown by itself did not change ABCC1 expression, unless siRNA TAS2R14-transfected cells were incubated with resveratrol treatment (50 μM). In this situation ABCC1 expression decreased 51.96 ± 14.65 %, while no differences were observed in mock- or siRNA scramble-transfected cells (Figure 5.8.A). Silencing TAS2R14 increased ABCC4 expression in comparison with mock- and siRNA scramble-transfected cells (Figure 5.8.B) in the absence of resveratrol, however resveratrol treatment in TAS2R14 knockdown cells decreased ABCC4 expression, reversing the effect observed in siRNA TAS2R14-transfected cells without resveratrol treatment (Figure 5.8.B). On the other hand, resveratrol increased ABCG2 expression in mock- and siRNA scramble-transfected cells, but not in siRNA TAS2R14-transfected cells (Figure 5.8.C), suggesting that the resveratrol induction of ABCG2 expression is dependent of TAS2R14 activation.

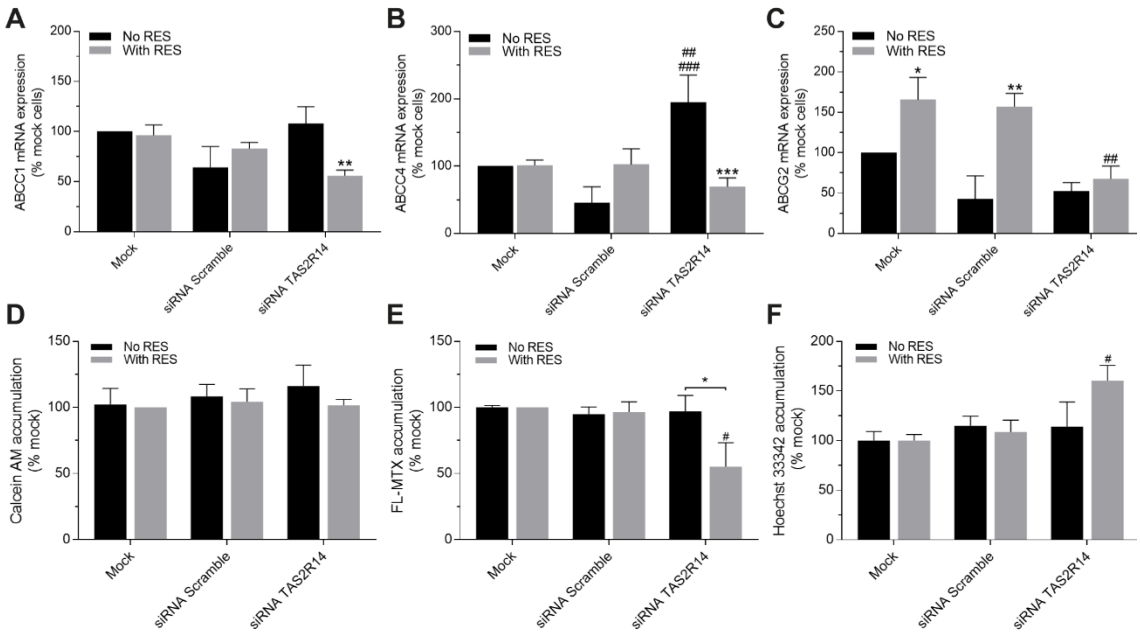

Figure 5. 8. Resveratrol modulates ABCG2 expression and function by a mechanism dependent of TAS2R14 expression. ABCC1 (A), ABCC4 (B) and ABCG2 (C) expression was analyzed by RT-qPCR in mock- and siRNA scramble/TAS2R14-transfected cells in the presence or absence of resveratrol (50 μM). Additionally, also accumulation of ABC's substrates Calcein AM-ABCC1 (0.1 μM), FL-MTX-ABCC4 (2 μM) and Hoechst 33342-ABCG2 (1 μM) was analysed in mock-, siRNA scramble- and siRNA TAS2R14-transfected HIBCPP cells in the presence or absence of resveratrol (50 μM) for 3 h. Graphs indicate the mean ± SEM (N > =3; *p < 0.05, **p < 0.01, ***p < 0.001 vs cells without resveratrol; #p < 0.05, ##p < 0.01, ###p < 0.001 vs mock- and siRNA scramble-transfected cells; Two-way ANOVA followed by Bonferroni's post hoc test). RES – resveratrol.

5.4.6. Resveratrol modulates ABCC4 and ABCG2 efflux activity, an effect dependent of TAS2R14 expression

In our previous experiments we observed that the effects of resveratrol on the expression of ABCC1, ABCC4 and ABCG2 in HIBCPP cells were modulated by TAS2R14, raising the hypothesis that the effect of resveratrol on the activity of these transporters could also be mediated by this receptor. Thus, we explored the effects of resveratrol on the function of ABCC1, ABCC4 and ABCG2 efflux activity by analysing the cellular accumulation of Calcein AM, Fl-MTX and Hoechst 33342 in mock-, siRNA scramble- and siRNA TAS2R14-transfected HIBCPP cells. Regarding ABCC1 activity, Calcein AM accumulation in HIBCPP cells was similar for all the conditions tested, and therefore neither resveratrol or TAS2R14 seem to affect ABCC1 efflux of Calcein AM (Figure 5.8.D). Conversely, Fl-MTX accumulation in HIBCPP cells decreased in siRNA TAS2R14-transfected HIBCPP cells treated with resveratrol in comparison with mock- (44.83 ± 15.58 %) and scramble-transfected cells (41.14 ± 15.58 %) treated with resveratrol, but also with untreated siRNA TAS2R14-transfected cells (41.88 ± 13.49 %) (Figure 5.8.E). Concerning Hoechst 33342, ABCG2 substrate, its accumulation increased in siRNA TAS2R14-transfected cells treated with resveratrol in comparison with mock- (60.44 ±

19.6 %) and siRNA scramble-transfected cells (51.87 ± 18.15 %) also treated with resveratrol (Figure 5.8.F). Therefore, our results indicate that resveratrol modulates ABCC4 and ABCG2 activity in HIBCPP cells dependently of TAS2R14 expression, but not ABCC1 activity.

5.5. Discussion

The BCSFB at the CP performs a critical role in the CNS homeostasis by regulating the molecular exchanges between the bloodstream and the CSF. The mechanisms operating at the BCSFB that are responsible for the maintenance of a homeostatic environment comprise several influx and efflux transporters, as well as detoxifying enzymes [2]. Upstream regulators of these transporters, however, are still poorly studied. Previously, we have identified several taste receptors in the rat CP [26]. The TR2, a class of taste receptors specialised in the detection of bitter compounds, are expressed in a wide range of extra-oral organs and tissues and can be activated by several natural or synthetic compounds [32,38,42,43]. Despite the growing evidence of TR2 roles in non-gustatory tissues, in the CP, functions of TR2 remain to be elucidated. In the present study, we proposed that a function of TAS2Rs could be that of upstream regulators of efflux transporters expressed at the human CP epithelial cells. To explore this hypothesis, we analysed the function of TAS2R14 and TAS2R39, previously reported in human CP samples and in the HIBCPP cell line to be activated by several ligands . Next, we evaluated their response to resveratrol that elicited an increase in intracellular Ca^{2+} in these cells. Based on the stronger stimulus exerted by resveratrol on these cells and on the indication that TAS2R14 mediated the response of these cells to resveratrol, we further explored the role of this receptor in the transport of resveratrol across the human CP epithelial cells. The interest in exploring the transport of resveratrol across the human CP epithelial cells was also raised by its intrinsic properties.

Resveratrol is a natural polyphenol that has been extensively studied regarding its potential as a therapeutic agent. It might be an important co-adjuvant in AD treatment by reducing oxidative stress and counteracting Aβ toxicity. Additionally, resveratrol co-administration with L-DOPA, that is used in Parkinson's disease treatment, enhanced the anti-inflammatory effects of L-DOPA [44]. Furthermore, resveratrol also has anticancer effects (reviewed in [45,46]). In glioblastoma cells, combination of resveratrol and the anticancer drug paclitaxel showed a synergic interaction improving the anticancer effects of paclitaxel [47]. Despite all the evidences of neuroprotective effects of resveratrol, its low bioavailability is still a great limitation to its successful use as co-adjuvant in the therapy of neurologic diseases [48–51]. Thus, it is critical to explore the

mechanisms associated with its transport into the CNS. Previous studies demonstrated that resveratrol reaches the brain of rodents [49] and humans [50], probably by crossing the BBB. However, these evidences were only based on resveratrol detection, at low levels, in the brain, which indeed indicates that resveratrol must be able to cross brain barriers.

Interestingly, the CP was identified as one of the principal sites for resveratrol binding on the brain through quantitative autoradiographic studies, suggesting that the CP might play an important role in resveratrol uptake into the brain [52]. However, since the report by Han and colleagues [52] back in 2006, no further studies approached this subject. The binding of resveratrol by TAS2Rs was previously described by Roland and colleagues [37] in a study conducted to analyse the ability of several phenolic compounds, such as flavonoids and isoflavones, to activate TAS2R14 and TAS2R39 in the human HEK293 cell line. Interestingly, resveratrol was able to bind both TAS2R14 and TAS2R39 [37]. Considering these data, we investigated TAS2R14 and TAS2R39 activation by resveratrol, in HIBCPP cells, and observed that resveratrol induced intracellular Ca^{2+} responses in a dose-dependent manner. Moreover, we observed that this response was dependent on TAS2R14 activation, but not on the activation of TAS2R39, suggesting that TAS2R14 binds resveratrol in human CP epithelial cells rather than TAS2R39. The preferential binding of resveratrol to TAS2R14 instead of TAS2R39 might be explained by differences in the concentration of resveratrol required to activate each receptor, and/or on the basal levels of each receptor in this cell model. Actually, in our previous analysis regarding TAS2Rs expression profile in this *in vitro* model of the human BCSFB we detected TAS2R14 and TAS2R39 expression, where TAS2R14 expression was three times higher than TAS2R39. Moreover, Roland and colleagues [37] reported that resveratrol has a threshold value of 16 μM for TAS2R14, and of 63 μM for TAS2R39, in HEK293 cells. Since we analyzed TAS2R14 and TAS2R39 activation by resveratrol at the concentration of 50 μM in Ca^{2+} assays, which is below the threshold value reported to TAS2R39, our results seem to be in accordance to those previous observations.

Our data in culture inserts show that resveratrol crosses HIBCPP cells, from the basolateral to the apical side. Supporting the hypothesis that resveratrol might enter the CNS at the BCSFB and not exclusively at the BBB as previously thought. After confirming the ability of resveratrol to cross human CP epithelial cells, we explored the putative role of TAS2R14 in resveratrol transport, and we found that silencing TAS2R14 the resveratrol levels decreased at the apical side. At this stage, our results indicated that the

presence of TAS2R14 at the BCSFB plays an essential role in enabling the access of resveratrol to the CSF.

Another important issue to disclose is the transport of resveratrol mechanisms at the BCSFB. Despite the few data related to resveratrol transport and metabolism in the CNS, it was already known that passive diffusion and facilitated transport are possible routes of entry of resveratrol across CP cells [56]. More than a decade ago, resveratrol was described as a substrate of ABCG2 [57]. Subsequently, ABCC2 and ABCG2 were also implicated in the transport of resveratrol in the intestine [58–60] and kidney [61]. On the other hand, resveratrol seems to regulate some ABC transporters expression and function [62], although this function is dependent of the tissue analysed. In rat kidney, resveratrol upregulated ABCG2 [61], but in Caco-2 cells downregulated ABCB1, ABCC1, ABCG2 [63] and ABCC2 [64,65]. Consequently, resveratrol can enhance the delivery of therapeutic compounds that are substrates of ABC transporters, such as doxorubicin [63–66] and MTX [61,65]. In our study we focused on resveratrol transporters that are expressed in CP epithelial cells. We found that inhibition of ABCC1, ABCC4 and ABCG2, whose expression and function was previously demonstrated at the HIBCPP cells [5], decreased both basolateral and apical accumulation of resveratrol thus confirming their implication in enabling resveratrol across CP cells. As mentioned before, resveratrol itself might have an impact on the overall function and expression of its transporters [61,63,65–68]. To address this possibility, we evaluated resveratrol effects in the expression of ABCC1, ABCC4 and ABCG2 in controls and siRNA TAS2R14-transfected cells. Interestingly, resveratrol only upregulated the expression of ABCG2, but this effect was reverted after TAS2R14 knockdown, suggesting an upregulation of ABCG2 mediated by TAS2R14. Resveratrol had no effect on the expression of ABCC1 or ABCC4. However, reduced ABCC1 expression was observed in TAS2R14 knockout cells but only upon resveratrol treatment. In opposition, ABCC4 expression was higher in TAS2R14 knockout cells than in controls. Concurrently the effect of resveratrol on the function of these three transporters was observed in ABCC4 and ABCG2. When TAS2R14 was silenced, resveratrol lead to a decreased accumulation of FL-MTX, ABCC4 substrate, and increased accumulation of the ABCG2 subtract Hoechst 33342 in HIBCPP cells, demonstrating that resveratrol affects the expression and the function of its transporters. In the literature, ABCG2 is the transporter most often implicated in resveratrol transport. Resveratrol and other polyphenols decreased ABCG2 transport capacity and activity resulting in increased cellular accumulation of known ABCG2 substrates [67]. Regarding resveratrol effects on ABCG2 expression levels, El-Sheik and colleagues [61] reported an upregulation in rat kidney after resveratrol administration, which is in

accordance with our results. In opposition, in Caco-2 cells, a cell line derived from the intestine, resveratrol treatment decreased the mRNA expression of ABCB1, ABCC1 and ABCG2 [63]. ABCG2 is commonly associated with the resistance to cancer therapies, since many chemotherapeutic agents are known substrates of this transporter [69]. In the BBB, ABCG2 localizes at the luminal side of endothelial cells which faces to the bloodstream, where it restrains the access of the chemotherapeutic drugs to the CNS [69,70]. In the BCSFB, ABCG2 localizes at the apical membrane of CP epithelial cells facing the CSF [71,72]. Therefore, ABCG2 expression at the human CP epithelial cells should facilitate the transport of substances from blood to the CSF [73]. Our results showing that resveratrol enhanced ABCG2 expression in CP epithelial cells indicate that this compound might increase the efflux of anti-cancer drugs into the CSF, probably by TAS2R14 activation.

ABCC1 and ABCC4 are both expressed in the basolateral membrane of CP epithelial cells, where they impair noxious substances to reach the CNS and extrude endogenous metabolic waste products from the CSF to the blood [2]. Noteworthy, ABCC1 has been linked to the clearance of Aβ peptide [74,75]. Concerning ABCC4 function in the CP epithelial cells, it has been reported that mice lacking ABCC4 expression showed increased brain and CSF accumulation of the chemotherapeutic drug topotecan [76]. Thus, all the transporters analysed in our study play an important role in the ability or inability of certain molecules, such as chemotherapeutic drugs, to reach the CNS, but also in the clearance of noxious compounds, such as Aβ. Therefore, the regulation control of ABCC1, ABCC4 and ABCG2 expression and of their activity would have serious impact in the CNS function. Overall, our data showed that resveratrol interacts with transporters at the human CP epithelial cells, as observed before in other tissues, and the expression of TAS2R14 seems to be critical for resveratrol effects on ABC transporters observed in CP epithelial cells.

5.6. References

[1] A.G. de Boer, P.J. Gaillard, Drug targeting to the brain, Annu. Rev. Pharmacol. Toxicol. (2007) 323–355. doi:10.1146/annurev.pharmtox.47.120505.105237.

[2] J.F. Ghersi-Egea, N. Strazielle, M. Catala, V. Silva-Vargas, F. Doetsch, B. Engelhardt, Molecular anatomy and functions of the choroidal blood-cerebrospinal fluid barrier in health and disease, Acta Neuropathol. 135 (2018) 337–361. doi:10.1007/s00401-018-1807-1.

[3] C.R.A. Santos, A.C. Duarte, T. Quintela, J. Tomás, T. Albuquerque, F. Marques, J.A. Palha, I. Gonçalves, The choroid plexus as a sex hormone target: Functional implications, Front. Neuroendocrinol. 44 (2017) 103–121. doi:10.1016/j.yfrne.2016.12.002.

[4] N. Strazielle, J.-F. Ghersi-Egea, Potential Pathways for CNS Drug Delivery Across the Blood-Cerebrospinal Fluid Barrier, Curr. Pharm. Des. 22 (2016) 5463–5476. doi:10.2174/1381612822666160726112115.

[5] A. Bernd, M. Ott, H. Ishikawa, H. Schroten, C. Schwerk, G. Fricker, Characterization of efflux transport proteins of the human choroid plexus papilloma cell line HIBCPP, a functional in vitro model of the blood-cerebrospinal fluid barrier, Pharm. Res. 32 (2015) 2973–2982. doi:10.1007/s11095-015-1679-1.

[6] S. Gazzin, N. Strazielle, C. Schmitt, M. Fevre-Montange, J.D. Ostrow, C. Tiribelli, J.F. Ghersi-Egea, Differential expression of the multidrug resistance-related proteins ABCb1 and ABCc1 between blood-brain interfaces, J. Comp. Neurol. 510 (2008) 497–507. doi:10.1002/cne.21808.

[7] Z. Chen, T. Shi, L. Zhang, P. Zhu, M. Deng, C. Huang, T. Hu, L. Jiang, J. Li, Mammalian drug efflux transporters of the ATP binding cassette (ABC) family in multidrug resistance: A review of the past decade, Cancer Lett. 370 (2016) 153–164. doi:10.1016/j.canlet.2015.10.010.

[8] J. Wijaya, Y. Fukuda, J.D. Schuetz, Obstacles to brain tumor therapy: Key ABC transporters, Int. J. Mol. Sci. 18 (2017). doi:10.3390/ijms18122544.

[9] E. Adler, M.A. Hoon, K.L. Mueller, J. Chandrashekar, N.J.P. Ryba, C.S. Zuker, A novel family of mammalian taste receptors, Cell. 100 (2000) 693–702. doi:10.1016/S0092-8674(00)80705-9.

[10] J. Chandrashekar, K.L. Mueller, M.A. Hoon, E. Adler, L. Feng, W. Guo, C.S. Zuker, N.J. Ryba, T2Rs function as bitter taste receptors, Cell. 100 (2000) 703–711. doi:10.1016/s0092-8674(00)80706-0.

[11] J. Chandrashekar, M.A. Hoon, N.J. Ryba, C.S. Zuker, The receptors and cells for mammalian taste, Nature. 444 (2006) 288–294. doi:10.1038/nature05401.

[12] N. Chaudhari, S.D. Roper, The cell biology of taste, J. Cell Biol. 190 (2010) 285–296. doi:10.1083/jcb.201003144.

[13] A.S. Shah, B.S. Yehuda, T.O. Moninger, J.N. Kline, M.J. Welsh, Motile cilia of human airway epithelia are chemosensory, Science (80-.). 325 (2009) 1131–1134. doi:10.1126/science.1173869.

[14] B.M. Hariri, D.B. McMahon, B. Chen, J.R. Freund, C.J. Mansfield, L.J. Doghramji, N.D. Adappa, J.N. Palmer, D.W. Kennedy, D.R. Reed, P. Jiang, R.J. Lee, Flavones modulate respiratory epithelial innate immunity: Anti-inflammatory effects and activation of the T2R14 receptor, J. Biol. Chem. 292 (2017) 8484–8497. doi:10.1074/jbc.M116.771949.

[15] Q. Wang, K.I. Liszt, E. Deloose, E. Canovai, T. Thijs, R. Farré, L.J. Ceulemans, M. Lannoo, J. Tack, I. Depoortere, Obesity alters adrenergic and chemosensory signalling pathways that regulate ghrelin secretion in the human gut, FASEB J. 33 (2019) 4907–4920. doi:10.1096/fj.201801661RR.

[16] X.-C. Luo, Z.-H. Chen, J.-B. Xue, D.-X. Zhao, C. Lu, Y.-H. Li, S.-M. Li, Y.-W. Du, Q. Liu, P. Wang, M. Liu, L. Huang, Infection by the parasitic helminth Trichinella spiralis activates a Tas2r-

mediated signalling pathway in intestinal tuft cells , Proc. Natl. Acad. Sci. 116 (2019) 5564–5569. doi:10.1073/pnas.1812901116.

[17] T.-I. Jeon, Y.-K. Seo, T.F. Osborne, Gut bitter taste receptor signalling induces ABCB1 through a mechanism involving CCK, Biochem. J. 438 (2011) 33–37. doi:10.1042/bj20110009.

[18] S.V. Wu, N. Rozengurt, M. Yang, S.H. Young, J. Sinnett-Smith, E. Rozengurt, Expression of bitter taste receptors of the T2R family in the gastrointestinal tract and enteroendocrine STC-1 cells., Proc. Natl. Acad. Sci. U. S. A. 99 (2002) 2392–7. doi:10.1073/pnas.042617699.

[19] X. Liu, F. Gu, L. Jiang, F. Chen, F. Li, Expression of bitter taste receptor Tas2r105 in mouse kidney, Biochem. Biophys. Res. Commun. 458 (2015) 733–738. doi:10.1016/j.bbrc.2015.01.089.

[20] J. Liang, F. Chen, F. Gu, X. Liu, F. Li, D. Du, Expression and functional activity of bitter taste receptors in primary renal tubular epithelial cells and M-1 cells, Mol. Cell. Biochem. 428 (2017) 193–202. doi:10.1007/s11010-016-2929-1.

[21] F. Li, M. Zhou, Depletion of bitter taste transduction leads to massive spermatid loss in transgenic mice, Mol. Hum. Reprod. 18 (2012) 289–297. doi:10.1093/molehr/gas005.

[22] J. Xu, J. Cao, N. Iguchi, D. Riethmacher, L. Huang, Functional characterization of bitter-taste receptors expressed in mammalian testis, Mol. Hum. Reprod. 19 (2013) 17–28. doi:10.1093/molehr/gas040.

[23] U. Wölfle, F.A. Elsholz, A. Kersten, B. Haarhaus, W.E. Müller, C.M. Schempp, Expression and functional activity of the bitter taste receptors TAS2R1 and TAS2R38 in human keratinocytes., Skin Pharmacol. Physiol. 28 (2015) 137–46. doi:10.1159/000367631.

[24] L. Shaw, C. Mansfield, L. Colquitt, C. Lin, J. Ferreira, J. Emmetsberger, D.R. Reed, Personalized expression of bitter “taste” receptors in human skin, PLoS One. 13 (2018) 1–18. doi:10.1371/journal.pone.0205322.

[25] X. Ren, L. Zhou, R. Terwilliger, S.S. Newton, I.E. de Araujo, Sweet taste signalling functions as a hypothalamic glucose sensor, Front. Integr. Neurosci. 3 (2009) 1–15. doi:10.3389/neuro.07.012.2009.

[26] J. Tomás, C.R.A. Santos, T. Quintela, I. Gonçalves, “Tasting” the cerebrospinal fluid: Another function of the choroid plexus?, Neuroscience. 320 (2016) 160–171. doi:10.1016/j.neuroscience.2016.01.057.

[27] S.J. Lee, I. Depoortere, H. Hatt, Therapeutic potential of ectopic olfactory and taste receptors, Nat. Rev. Drug Discov. 18 (2019) 116–138. doi:10.1038/s41573-018-0002-3.

[28] A. Dagan-Wiener, A. Di Pizio, I. Nissim, M.S. Bahia, N. Dubovski, E. Margulis, M.Y. Niv, Bitterdb: Taste ligands and receptors database in 2019, Nucleic Acids Res. 47 (2019) D1179–D1185. doi:10.1093/nar/gky974.

[29] A. Wiener, M. Shudler, A. Levit, M.Y. Niv, BitterDB: a database of bitter compounds., Nucleic Acids Res. 40 (2012) D413-9. doi:10.1093/nar/gkr755.

[30] L.T.P. Martin, M.W. Nachtigal, T. Selman, E. Nguyen, J. Salsman, G. Dellaire, D.J. Dupré, Bitter taste receptors are expressed in human epithelial ovarian and prostate cancers cells and noscapine stimulation impacts cell survival, Mol. Cell. Biochem. 454 (2019) 203–214. doi:10.1007/s11010-018-3464-z.

[31] S. Grassin-Delyle, C. Abrial, S. Fayad-Kobeissi, M. Brollo, C. Faisy, J.C. Alvarez, E. Naline, P. Devillier, The expression and relaxant effect of bitter taste receptors in human bronchi, Respir. Res. 14 (2013) 1–14. doi:10.1186/1465-9921-14-134.

[32] A. Jaggupilli, N. Singh, J. Upadhyaya, A.S. Sikarwar, M. Arakawa, S. Dakshinamurti, R.P. Bhullar, K. Duan, P. Chelikani, Analysis of the expression of human bitter taste receptors in extraoral tissues, Mol. Cell. Biochem. 426 (2017) 137–147. doi:10.1007/s11010-016-2902-z.

[33] I. Ishiwata, C. Ishiwata, E. Ishiwata, Y. Sato, K. Kiguchi, T. Tachibana, H. Hashimoto, H. Ishikawa, Establishment and characterization of a human malignant choroids plexus papilloma cell line (HIBCPP), Hum Cell. 18 (2005) 67–72. doi:10.1111/j.1749-0774.2005.tb00059.x.

[34] C. Schwerk, T. Papandreou, D. Schuhmann, L. Nickol, J. Borkowski, U. Steinmann, N. Quednau, C. Stump, C. Weiss, J. Berger, H. Wolburg, H. Claus, U. Vogel, H. Ishikawa, T. Tenenbaum, H. Schroten, Polar invasion and translocation of neisseria meningitidis and streptococcus suis in a novel human model of the blood-cerebrospinal fluid barrier, PLoS One. 7 (2012) e30069. doi:10.1371/journal.pone.0030069.

[35] I. Gonçalves, T. Quintela, A.C. Duarte, P. Hubbard, C. Schwerk, A.C. Belin, J. Toma, R.A. Santos, Experimental Tools to Study the Regulation and Function of the Choroid Plexus., in: Barichello T. Blood-Brain Barrier. Neuromethods, Humana Press, New York, NY, 2018.

[36] M.W. Pfaffl, A new mathematical model for relative quantification in real-time RT-PCR., Nucleic Acids Res. 29 (2001) 2002–2007. doi:10.1093/nar/29.9.e45.

[37] W.S.U. Roland, H. Gruppen, M. Driesse, G. Smit, J.-P. Vincken, L. Van Buren, R.J. Gouka, Bitter taste receptor activation by flavonoids and isoflavonoids: Modeled structural requirements for activation of hTAS2R14 and hTAS2R39, J. Agric. Food Chem. 61 (2013) 10454–10466. doi:10.1021/jf403387p.

[38] W. Meyerhof, C. Batram, C. Kuhn, A. Brockhoff, E. Chudoba, B. Bufe, G. Appendino, M. Behrens, The molecular receptive ranges of human TAS2R bitter taste receptors, Chem. Senses. 35 (2009) 157–170. doi:10.1093/chemse/bjp092.

[39] A. Levit, S. Nowak, M. Peters, A. Wiener, W. Meyerhof, M. Behrens, M.Y. Niv, The bitter pill : clinical drugs that activate the human bitter taste receptor TAS2R14, FASEB J. 27 (2014) 1181–1197. doi:10.1096/fj.13-242594.

[40] T. Yamazaki, M. Narukawa, M. Mochizuki, T. Watanabe, Activation of the hTAS2R14 Human Bitter-Taste Receptor by (–) -Epigallocatechin Gallate and (–) - Epicatechin Gallate, Biosci. Biotechnol. Biochem. 8451 (2014) 1753–1756. doi:10.1271/bbb.130329.

[41] M. Narukawa, C. Noga, Y. Ueno, T. Sato, T. Misaka, T. Watanabe, Evaluation of the bitterness of green tea catechins by a cell-based assay with the human bitter taste receptor hTAS2R39, Biochem. Biophys. Res. Commun. 405 (2011) 620–625. doi:10.1016/j.bbrc.2011.01.079.

[42] A. Di Pizio, M.Y. Niv, Promiscuity and selectivity of bitter molecules and their receptors, Bioorganic Med. Chem. 23 (2015) 4082–4091. doi:10.1016/j.bmc.2015.04.025.

[43] A. Jaggupilli, R. Howard, J.D. Upadhyaya, R.P. Bhullar, P. Chelikani, Bitter taste receptors: Novel insights into the biochemistry and pharmacology, Int. J. Biochem. Cell Biol. 77 (2016) 184–196. doi:10.1016/j.biocel.2016.03.005.

[44] Q. Liu, D. Zhu, P. Jiang, X. Tang, Q. Lang, Q. Yu, S. Zhang, Y. Che, X. Feng, Resveratrol synergizes with low doses of L-DOPA to improve MPTP-induced Parkinson disease in mice, Behav. Brain Res. 367 (2019) 10–18. doi:10.1016/j.bbr.2019.03.043.

[45] I. Lejri, A. Agapouda, A. Grimm, A. Eckert, Mitochondria- and Oxidative Stress-Targeting Substances in Cognitive Decline-Related Disorders: From Molecular Mechanisms to Clinical Evidence, Oxid. Med. Cell. Longev. 2019 (2019) 1–26. doi:10.1155/2019/9695412.

[46] R. Hornedo-Ortega, A.B. Cerezo, R.M. de Pablos, S. Krisa, T. Richard, M.C. García-Parrilla, A.M. Troncoso, Phenolic Compounds Characteristic of the Mediterranean Diet in Mitigating Microglia-Mediated Neuroinflammation, Front. Cell. Neurosci. 12 (2018) 1–20. doi:10.3389/fncel.2018.00373.

[47] Y. Öztürk, C. Günaydın, F. Yalçın, M. Nazıroğlu, N. Braidy, Resveratrol enhances apoptotic and oxidant effects of paclitaxel through TRPM2 channel activation in DBTRG glioblastoma cells, Oxid. Med. Cell. Longev. 2019 (2019). doi:10.1155/2019/4619865.

[48] M. Asensi, I. Medina, A. Ortega, J. Carretero, M.C. Baño, E. Obrador, J.M. Estrela, Inhibition of cancer growth by resveratrol is related to its low bioavailability, Free Radic. Biol. Med. 33 (2002) 387–398. doi:10.1016/s0891-5849(02)00911-5.

[49] Q. Wang, J. Xu, G.E. Rottinghaus, A. Simonyi, D. Lubahn, G.Y. Sun, A.Y. Sun, Resveratrol protects against global cerebral ischemic injury in gerbils, Brain Res. 958 (2002) 439–447. doi:10.1016/s0006-8993(02)03543-6.

[50] R.S. Turner, R.G. Thomas, S. Craft, C.H. van Dyck, J. Mintzer, B.A. Reynolds, J.B. Brewer, R.A. Rissman, R. Raman, P.S. Aisen, A randomized, double-blind, placebo-controlled trial of resveratrol for Alzheimer disease, Neurology. 85 (2015) 1383–1391. doi:10.1212/wnl.0000000000002035.

[51] X.H. Shu, L.L. Wang, H. Li, X. Song, S. Shi, J.Y. Gu, M.L. Wu, X.Y. Chen, Q.Y. Kong, J. Liu, Diffusion Efficiency and Bioavailability of Resveratrol Administered to Rat Brain by Different Routes: Therapeutic Implications, Neurotherapeutics. 12 (2015) 491–501. doi:10.1007/s13311-014-0334-6.

[52] Y.-S. Han, S. Bastianetto, Y. Dumont, R. Quirion, Specific Plasma Membrane Binding Sites for Polyphenols, Including Resveratrol, in the Rat Brain, J. Pharmacol. Exp. Ther. 318 (2006) 238–245. doi:10.1124/jpet.106.102319.

[53] N. Khan, H. Mukhtar, Tea polyphenols in promotion of human health, Nutrients. 11 (2019) 39–54. doi:10.3390/nu11010039.

[54] P. Maher, The Potential of Flavonoids for the Treatment of Neurodegenerative Diseases, Int. J. Mol. Sci. 20 (2019) 3056–3074. doi:10.3390/ijms20123056.

[55] C. Bo, B. Stefano, M. Mirko, P. Marisa, T. Massimiliano, G. Simone, C. Antonio, C. Barbara, K. Benjamin, K. Paul, Z.-R. Raul, L. Nicole Hidalgo, A.-L. Cristina, R. Patrizia, Systematic Review on Polyphenol Intake and Health Outcomes: Is there Sufficient Evidence to Define a Health-Promoting Polyphenol-Rich Dietary Pattern?, Nutrients. 11 (2019) 1355–1409. doi:10.3390/nu11061355.

[56] J.M. Smoliga, O. Blanchard, Enhancing the delivery of resveratrol in humans: If low bioavailability is the problem, what is the solution?, Molecules. 19 (2014) 17154–17172. doi:10.3390/molecules191117154.

[57] P. Breedveld, D. Pluim, G. Cipriani, F. Dahlhaus, M.A.J. van Eijndhoven, C.J.F. de Wolf, A. Kuil, J.H. Beijnen, G.L. Scheffer, G. Jansen, P. Borst, J.H.M. Schellens, The Effect of Low pH on Breast Cancer Resistance Protein (ABCG2)-Mediated Transport of Methotrexate, 7-Hydroxymethotrexate, Methotrexate Diglutamate, Folic Acid, Mitoxantrone, Topotecan, and Resveratrol in In Vitro Drug Transport Models, Mol. Pharmacol. 71 (2007) 240–249. doi:10.1124/mol.106.028167.properties.

[58] I. Alfaras, M. Pérez, M.E. Juan, G. Merino, J.G. Prieto, J.M. Planas, A.I. Álvarez, Involvement of breast cancer resistance protein (BCRP1/ABCG2) in the bioavailability and tissue distribution of trans- resveratrol in knockout mice, J. Agric. Food Chem. 58 (2010) 4523–4528. doi:10.1021/jf9042858.

[59] M.E. Juan, E. González-Pons, J.M. Planas, Multidrug Resistance Proteins Restrain the Intestinal Absorption of trans-Resveratrol in Rats, J. Nutr. 140 (2010) 489–495. doi:10.3945/jn.109.114959.

[60] J.M. Planas, I. Alfaras, H. Colom, M.E. Juan, The bioavailability and distribution of trans-resveratrol are constrained by ABC transporters, Arch. Biochem. Biophys. 527 (2012) 67–73. doi:10.1016/j.abb.2012.06.004.

[61] A.A.K. El-Sheikh, M.A. Morsy, A.Y. Al-Taher, Protective mechanisms of resveratrol against methotrexate-induced renal damage may involve BCRP/ABCG2, Fundam. Clin. Pharmacol. 30 (2016) 406–418. doi:10.1111/fcp.12205.

[62] Y. Li, J. Revalde, J.W. Paxton, The effects of dietary and herbal phytochemicals on drug transporters, Adv. Drug Deliv. Rev. 116 (2017) 45–62. doi:10.1016/j.addr.2016.09.004.

[63] M.Z. El-Readi, S.Y. Eid, A.A. Abdelghany, H.S. Al-Amoudi, T. Efferth, M. Wink, Resveratrol mediated cancer cell apoptosis, and modulation of multidrug resistance proteins and metabolic enzymes, Phytomedicine. 55 (2019) 269–281. doi:10.1016/j.phymed.2018.06.046.

[64] Y. Jia, Z. Liu, X. Huo, C. Wang, Q. Meng, Q. Liu, H. Sun, P. Sun, X. Yang, X. Shu, K. Liu, Enhancement effect of resveratrol on the intestinal absorption of bestatin by regulating PEPT1, MDR1 and MRP2 in vivo and in vitro, Int. J. Pharm. 495 (2015) 588–598. doi:10.1016/j.ijpharm.2015.09.042.

[65] Y. Jia, Z. Liu, C. Wang, Q. Meng, X. Huo, Q. Liu, H. Sun, P. Sun, X. Yang, X. Ma, K. Liu, P-gp, MRP2 and OAT1/OAT3 mediate the drug-drug interaction between resveratrol and methotrexate, Toxicol. Appl. Pharmacol. 306 (2016) 27–35. doi:10.1016/j.taap.2016.06.030.

[66] F. Huang, X.N. Wu, J. Chen, W.X. Wang, Z.F. Lu, Resveratrol reverses multidrug resistance in human breast cancer doxorubicin-resistant cells, Exp. Ther. Med. 7 (2014) 1611–1616. doi:10.3892/etm.2014.1662.

[67] H.C. Cooray, T. Janvilisri, H.W. Van Veen, S.B. Hladky, M.A. Barrand, Interaction of the breast cancer resistance protein with plant polyphenols, Biochem. Biophys. Res. Commun. 317 (2004) 269–275. doi:10.1016/j.bbrc.2004.03.040.

[68] R. Zhang, M. Lu, Z. Zhang, X. Tian, S. Wang, D. Lv, Resveratrol reverses P-glycoprotein-mediated multidrug resistance of U2OS/ADR cells by suppressing the activation of the NF-κB and p38 MAPK signalling pathways, Oncol. Lett. 12 (2016) 4147–4154. doi:10.3892/ol.2016.5136.

[69] A. Basseville, M.D. Hall, C.H. Chau, R.W. Robey, M. Gottesman, W.D. Figg, S.E. Bates, The ABCG2 Multidrug Transporter, in: G. A. (Ed.), ABC Transp. - 40 Years, Springer, Cham, 2016: pp. 195–226. doi:10.1007/978-3-319-23476-2.

[70] H.C. Cooray, C.G. Blackmore, L. Maskell, M.A. Barrand, Localisation of breast cancer resistance protein in microvessel endothelium of human brain, Neuroreport. 13 (2002) 2059–2063. doi:10.1097/00001756-200211150-00014.

[71] S. Halwachs, C. Lakoma, I. Schafer, P. Seibel, W. Honscha, The Antiepileptic Drugs Phenobarbital and Carbamazepine Reduce Transport of Methotrexate in Rat Choroid Plexus by Down-Regulation of the Reduced Folate Carrier, Mol. Pharmacol. 80 (2011) 621–629. doi:10.1124/mol.111.072421.

[72] L.M. Roberts, D.S. Black, C. Raman, K. Woodford, M. Zhou, J.E. Haggerty, A.T. Yan, S.E. Cwirla, K.K. Grindstaff, Subcellular localization of transporters along the rat blood-brain barrier and blood-cerebral-spinal fluid barrier by in vivo biotinylation, Neuroscience. 155 (2008) 423–438. doi:10.1016/j.neuroscience.2008.06.015.

[73] M. Grube, P. Hagen, G. Jedlitschky, Neurosteroid transport in the brain: Role of ABC and SLC transporters, Front. Pharmacol. 9 (2018) 1–9. doi:10.3389/fphar.2018.00354.

[74] J. Hofrichter, M. Krohn, T. Schumacher, C. Lange, B. Feistel, B. Walbroel, H.-J. Heinze, S. Crockett, T.F. Sharbel, J. Pahnke, Reduced Alzheimer's disease pathology by St. John's wort treatment is independent of hyperforin and facilitated by ABCC1 and microglia activation in mice, Curr Alzheimer Res. 10 (2013) 1057–1069. doi:10.2174/15672050113106660171.

[75] M. Krohn, C. Lange, J. Hofrichter, K. Scheffler, J. Stenzel, J. Steffen, T. Schumacher, T. Bruning, A.S. Plath, F. Alfen, A. Schmidt, F. Winter, K. Rateitschak, A. Wree, J. Gsponer, L.C. Walker, J. Pahnke, Cerebral amyloid-beta proteostasis is regulated by the membrane transport protein ABCC1 in mice, J Clin Invest. 121 (2011) 3924–3931. doi:10.1172/JCI57867.

[76] M. Leggas, M. Adachi, G.L. Scheffer, D. Sun, P. Wielinga, G. Du, K.E. Mercer, Y. Zhuang, J.C. Panetta, B. Johnston, R.J. Scheper, C.F. Stewart, J.D. Schuetz, Mrp4 Confers Resistance to Topotecan and Protects the Brain from Chemotherapy, Mol. Cell. Biol. 24 (2004) 7612–7621. doi:10.1128/mcb.24.17.7612-7621.2004.

Chapter 6

Concluding Remarks and Future Trends

6.1. Concluding Remarks

Despite all the efforts, brain drug delivery is still a great challenge mostly because most drugs have a limited capacity to cross brain barriers to reach the CNS. Although it is known that the efflux transporters at brain barriers play a critical role in this selective permeability, the upstream mechanisms that control these transporters are still poorly understood.

In the last years, several reports indicate that some bitter compounds display uncountable health beneficial effects including neuroprotective and anti-tumoral activities, underscoring their potential as candidates to treat CNS disorders. However, the low bioavailability of bitter compounds' in the brain is an obstacle to their therapeutic application. Interestingly, bitter compounds bind to TR2 in a wide range of organs and tissues triggering cellular responses related with different biological processes, which seem to be organ and tissue specific.

Recently, our research group reported that there are functional TRs in the rat CP, including TR2, and the downstream effectors of the taste signalling pathway. Thus, as a starting point for this thesis it was hypothesized that TR2 in the CP could act as upstream regulators of transport and detoxification systems harbored at the BCSFB. Taking this into account, this thesis intended to characterize the expression and function of TAS2Rs in the human BCSFB.

In the first original article presented in this thesis (Bitter taste receptors profiling in the human blood-cerebrospinal fluid barrier) the mRNA expression of 13 TAS2Rs was confirmed. Among them, TAS2R4, TAS2R5, TAS2R14 and TAS2R39 were chosen for protein analysis, which confirmed their presence in CP sections from men and women and in HIBCPP cells. Additionally, the expression of the expression of downstream effector proteins GNAT3, PLCβ2 and TRPM5 was also detected in HIBCPP cells, providing strong evidence that the bitter taste signalling is present in human BCSFB. Interestingly, the TAS2R with higher protein levels in HIBCPP cells, the TAS2R14, is also the one with more known ligands. This receptor can interact with phenolic compounds, flavonoids, and several therapeutic drugs. TAS2R39 is the second TAS2R member with more known ligands, sharing several of them with TAS2R14. On the other hand, TAS2R4 and TAS2R5 are activated by a more restrict number of ligands. Despite this, all these four TAS2Rs interact with compounds that show neuroactive properties. For example, resveratrol and epigallocatechin gallate bind to TAS2R14 and TAS2 R39; haloperidol and

quercetin bind to TAS2R14; arborescin and dapsone bind to TAS2R4; epicatechin binds to TAS2R4 and 5; and parthenolide binds to TAS2R4 and TAS2R14 among other TAS2Rs.

Taking this into account, some of these bitter compounds (chloramphenicol, haloperidol, and quercetin) were selected to analyze the functionality of bitter taste signaling in HIBCPP cells. The obtained results showed that all these compounds can elicited calcium responses in HIBCPP cells. Moreover, it was also demonstrated that chloramphenicol and quercetin specifically activate TAS2R39 and TAS2R14, respectively.

This work demonstrated for the first time that human CP epithelial cells express key members of the taste signalling pathway, the TAS2Rs and downstream effector proteins. Moreover, the HIBCPP cell line can be used as a reliable *in vitro* model of the BCSFB to investigate TAS2Rs functions. Until now, the bitter taste signalling had been only reported in mouse and rat CP [1,2]. Moreover, it is worth noticing that despite some homology, the TR2 in human and rodents differ in number and amino acids composition. There are 25 TR2 in humans and 34 in rodents. Given the potential of TAS2Rs as potential therapeutic targets, it is of major importance to study these receptors in human models.

The preliminary screening for TAS2Rs on the HIBCPP cells indicated that the TAS2Rs can modulate cellular responses. Such data suggest that the TAS2Rs in the BCSFB might be targeted by many therapeutic drugs for the treatment of CNS diseases, and thus TAS2Rs might regulate the access of these chemicals to the brain. Otherwise, as observed in other non-gustatory organs, TAS2Rs at the human CP may also play an important role in the regulation of downstream cellular events triggered by their cognate bitter ligands.

Resveratrol is probably the most studied bitter compound and shows a remarkable therapeutic potential in brain disorders. Several studies show that resveratrol improves cognitive and memory performance and decreases Aβ levels in AD mouse models [3,4]. In addition, resveratrol has also therapeutic potential to treat stroke. This has been demonstrated in different *in vivo* studies where resveratrol administration decreased the damaged area and cell apoptosis, and increased angiogenesis [5–8]. Anti-cancer activity of resveratrol in brain tumors such as glioblastoma as also been demonstrated [9,10]. However, little is known about its transport across brain barriers.

Therefore, in the second original article (The bitter taste receptor TAS2R14 regulates resveratrol transport across the human blood-cerebrospinal fluid barrier) we aimed to

explore the role of TAS2Rs in the transport of resveratrol across the human BCSFB. Firstly, we demonstrated that TAS2R14 is activated by resveratrol in HIBCPP cells using calcium functional assays. Then, we showed that TAS2R14 is localized in the basolateral membrane of HIBCPP cells what suggests that it senses compounds that are present in the bloodstream, which is the case of resveratrol, that upon ingestion or other forms of administration circulates in the blood stream. However, as resveratrol also appears in the CSF, we hypothesized that TAS2R14 could control its transport from the periphery to the brain. Accordingly, permeation studies confirmed resveratrol transport across HIBCPP cells from the basolateral to the apical side, and importantly, this transport depended on TAS2R14 expression.

In addition, previous studies reported resveratrol as a substrate of some ABC transporters which are also expressed in human CP epithelial cells. As already discussed, ABC transporters play a critical role in the human BCSFB for brain homeostasis, allowing the clearance of deleterious compounds such as Aβ by ABCC1, but also restrain the brain delivery of certain chemicals and drugs, including the chemotherapeutic topecan that is effluxed by ABCC4 in CP epithelial cells. In our work, we found that resveratrol transport across HIBCPP cells is mediated by ABCC1 and ABCC4 in the basolateral membrane, and by ABCG2 at the apical membrane. Moreover, resveratrol increased ABCG2 expression and activity via TAS2R14, a transporter commonly associated to drug resistance.

Thus, in this second original article we confirmed that resveratrol is transported into the brain, through the human BCSFB via ABC transporters, whose expression and activity is modulated by TAS2R14 activation.

Over the last years, the neuroactive potential of resveratrol has been demonstrated by several studies. However, the translation of resveratrol-based therapies to the treatment of CNS disorders has been hindered because resveratrol transport mechanisms across the brain barriers remained unclear. Therefore, our findings showed that resveratrol crosses the human BCSFB and accumulates in the CSF, which supports the application of these type of therapies providing more insights in the drug interaction with the brain barriers. Moreover, we provide for the first-time evidences of TAS2Rs functions, particularly of TAS2R14, in the human BCSFB. The expression of TAS2R14 in human CP epithelial cells allowed the transport of resveratrol across the human BCSFB and mediated resveratrol effects in the expression and activity of ABCG2, an important efflux transporter.

Overall, the results presented in this doctoral thesis demonstrate that TAS2Rs are expressed in the human BCSFB and that TAS2R14 acts as an upstream regulator of the activity of efflux transporters in this barrier. Moreover, we expect that the work here presented can be useful in the future to understand the interaction of other promising molecules for CNS therapies with the BCSFB, and thus improve their uptake to the brain.

6.2. Future Trends

Beyond the scientific advances achieved with the experimental work carried out in this thesis, several new avenues for disentangling the complexity of chemical sensing at brain barriers, and many novel research questions were put forward:

What are the effects of resveratrol in CP epithelial cells and what is the role of TAS2R14 in the process?

The CP perform multiple functions that are critical for CNS homeostasis, which might be impaired in aging and in some diseases, such as AD. Since resveratrol presents neuroactive effects, it would be interesting to analyze if resveratrol is able to regulate CP epithelial cells functions beyond the regulation of its own transporters. In order to analyze that, the transcriptome of HIBCPP cells upon TAS2R14 activation by resveratrol would disclose potential pathways regulated by resveratrol in the human CP cells.

Also, resveratrol seems to contribute to decrease Aβ deposition, which is known to accumulate in the CP epithelial cells contributing to CP dysfunction. Therefore, it would be important to assess if resveratrol is able to protect CP epithelial cells from Aβ-induced toxicity that usually is associated with increased oxidative stress and loss of barrier integrity at the BCSFB. The role of TAS2R14 as a regulator of resveratrol effects should thus be also assessed in this context.

As mentioned before, ABCC1 in the CP is associated with Aβ clearance. Interestingly, in the second original paper present, we observed that ABCC1 mediates resveratrol transport across the human BCSFB, and in turn resveratrol downregulated ABCC1 expression in siRNA TAS2R14-transfected HIBCPP cells. Thus, it seems important to investigate this interaction between ABCC1 and resveratrol concerning Aβ clearance and toxicity in the human CP.

Does TAS2R14 activation by resveratrol facilitate brain drug delivery?

TAS2R14 activation by resveratrol regulates the expression and activity of ABC transporters. Therefore, this indicates that the permeability of the BCSFB is altered in the presence of resveratrol. Thus, it would be interesting to combine resveratrol with other compounds, such as chemotherapeutic drugs or others, and analyze the transport of these across the BCSFB.

What other functions do TAS2Rs play in the human CP?

We hypothesized that TAS2Rs regulate transport and detoxifying mechanisms at the human BCSFB. Although we have demonstrated that TAS2Rs, particularly TAS2R14, affects ABC transporters activity in human CP epithelial cells, in the future it would be interesting to analyze also the role of TAS2R14 and other TAS2Rs in detoxifying processes.

This work shows that thirteen TAS2Rs are expressed in HIBCPP cells, which can be activated by several compounds with biological activity, such as flavonoids (e.g. epigallocatechin gallate, quercetin, kaempferol) and the alkaloid parthenolide. Most flavonoids bind TAS2R14 and/or TAS2R39, both functional at HIBCPP cells as we showed in the first original article presented in this doctoral thesis. On the other hand, parthenolide has been extensively reported as a promising anti-cancer molecule and binds TAS2R1, 4, 8, 10, 14, 44, 46. Therefore, evaluating the potential of these known TAS2R ligands and other bitter compounds to activate TAS2Rs in the human CP epithelial cells, and determining the cellular responses elicited upon ligand binding might unveil other functions of these receptors in the human BCSFB.

Overall, our results indicate that the bitter taste signalling has important roles at the BCSFB, which might be critical for CNS homeostasis. Moreover, we characterized the HIBCPP cells as a proper *in vitro* model of the BCSFB to study TAS2Rs functions. Despite the relevance of these achievements, we are far from a complete understanding of TAS2Rs role in the human BCSFB. Rather, we pioneered the study of important components of the chemical surveillance system at brain barriers and expect that future studies will contribute to unveil more about bitter taste signalling in the human BCSFB, and its impact in health and disease.

The BCSFB and the BBB are the two main brain interfaces between the blood and the CSF or the interstitial fluid, respectively. Moreover, both comprise a chemical surveillance system that allow the clearance of brain metabolic waste but impose

chemoresistance which compromise the treatment of many CNS disorders. Considering our findings in the human BCSFB, it is possible that also the BBB presents a functional bitter taste signalling that would be able to perceive chemical variations in the blood and in the interstitial fluid and respond accordingly. Interestingly, transcriptomic analysis of BBB (GSE45171) also shows the expression of TR2 [11,12]. Thus, in the future, the analysis of bitter taste signalling in the human BBB is of utmost importance considering our findings in the human BCSFB. Of paramount interest, this knowledge might contribute to disclose the regulation of transport and detoxifying mechanisms at the BBB, which are still poorly understood subjects.

6.3. References

[1] J. Tomás, C.R.A. Santos, T. Quintela, I. Gonçalves, "Tasting" the cerebrospinal fluid: Another function of the choroid plexus?, Neuroscience. 320 (2016) 160–171. doi:10.1016/j.neuroscience.2016.01.057.

[2] X. Ren, L. Zhou, R. Terwilliger, S.S. Newton, I.E. de Araujo, Sweet taste signaling functions as a hypothalamic glucose sensor, Front. Integr. Neurosci. 3 (2009) 1–15. doi:10.3389/neuro.07.012.2009.

[3] R. Corpas, C. Griñán-Ferré, E. Rodríguez-Farré, M. Pallàs, C. Sanfeliu, Resveratrol Induces Brain Resilience Against Alzheimer Neurodegeneration Through Proteostasis Enhancement, Mol. Neurobiol. 56 (2019) 1502–1516. doi:10.1007/s12035-018-1157-y.

[4] Y. Qi, L. Shang, Z. Liao, H. Su, H. Jing, B. Wu, K. Bi, Y. Jia, Intracerebroventricular injection of resveratrol ameliorated Aβ-induced learning and cognitive decline in mice, Metab. Brain Dis. 34 (2019) 257–266. doi:10.1007/s11011-018-0348-6.

[5] N. Aziz, I. Iezhitsa, R. Agarwal, A. Kadir, R. Fatmawati, A. Abd. Latiff, N.M. Ismail, Neuroprotection by trans-resveratrol against collagenase-induced neurological and neurobehavioural deficits in rats involves adenosine A1 receptors, Neurol. Res. 42 (2020) 189–208. doi:10.1080/01616412.2020.1716470.

[6] F. Bonsack, C.H. Alleyne, S. Sukumari-Ramesh, Resveratrol attenuates neurodegeneration and improves neurological outcomes after intracerebral hemorrhage in mice, Front. Cell. Neurosci. 11 (2017) 1–9. doi:10.3389/fncel.2017.00228.

[7] C.H. Lin, C.J.B. Nicol, Y.C. Cheng, C. Yen, Y.S. Wang, M.C. Chiang, Neuroprotective effects of resveratrol against oxygen glucose deprivation induced mitochondrial dysfunction by activation of AMPK in SH-SY5Y cells with 3D gelatin scaffold, Brain Res. 1726 (2020) 146492. doi:10.1016/j.brainres.2019.146492.

[8] D.M. Hermann, A. Zechariah, B. Kaltwasser, B. Bosche, A.B. Caglayan, E. Kilic, T.R. Doeppner, Sustained neurological recovery induced by resveratrol is associated with

angioneurogenesis rather than neuroprotection after focal cerebral ischemia, Neurobiol. Dis. 83 (2015) 16–25. doi:10.1016/j.nbd.2015.08.018.

[9] Y. Song, Y. Chen, Y. Li, X. Lyu, J. Cui, Y. Cheng, T. Zheng, L. Zhao, G. Zhao, Resveratrol Suppresses Epithelial-Mesenchymal Transition in GBM by Regulating Smad-Dependent Signaling, Biomed Res. Int. 2019 (2019). doi:10.1155/2019/1321973.

[10] Y. Yang, J. Cui, F. Xue, A.M. Overstreet, Y. Zhan, D. Shan, H. Li, H. Li, Y. Wang, M. Zhang, C. Yu, Z.Q.D. Xu, Resveratrol Represses Pokemon Expression in Human Glioma Cells, Mol. Neurobiol. 53 (2016) 1266–1278. doi:10.1007/s12035-014-9081-2.

[11] C.R.A. Santos, A.C. Duarte, A.R. Costa, J. Tomás, T. Quintela, I. Gonçalves, The senses of the choroid plexus, Prog. Neurobiol. 182 (2019) 101680. doi:10.1016/j.pneurobio.2019.101680.

[12] R. Cecchelli, S. Aday, E. Sevin, C. Almeida, M. Culot, L. Dehouck, C. Coisne, B. Engelhardt, M.P. Dehouck, L. Ferreira, A stable and reproducible human blood-brain barrier model derived from hematopoietic stem cells, PLoS One. 9 (2014). doi:10.1371/journal.pone.0099733.